COUPLING GEOTHERMAL HEATING WITH BTEX BIOREMEDIATION IN THE SUBSURFACE

GURPREET KAUR

A DISSERTATION SUBMITTED
TO THE FACULTY OF GRADUATE STUDIES
IN PARTIAL FULFILLMENT OF THE REQUIREMENTS
FOR THE DEGREE OF
DOCTOR OF PHILOSOPHY

GRADUATE PROGRAM IN CIVIL ENGINEERING
YORK UNIVERSITY
TORONTO, ONTARIO

January 2026

ABSTRACT

There has been a worldwide interest in renewable energy technologies as a means of reducing reliance on fossil fuels, mitigating the effects of climate change, and reducing greenhouse gas emissions. One such technology is geothermal heating, where the constant subsurface temperature is used to cool or heat building interiors via heat pumps. In Canada, the use of geothermal heat pumps (GHPs) has become a popular option for heating and cooling buildings. It is anticipated that, in the near term, most large buildings will incorporate GHPs as part of their climate control strategy. However, little is known about the environmental impacts of geothermal heating on the subsurface environment. The present thesis examined the effect of geothermal heating on groundwater flow and remediation efforts, whereby the heat generated by geothermal systems may aid in addressing urban pollution. "Geothermal remediation" could leverage the subsurface heating resulting from geothermal systems to accelerate biodegradation of certain petroleum-based pollutants at brownfield sites, while providing building(s) with sustainable heating and cooling. This idea coincides with the rising momentum towards sustainable and green remediation in Europe and the United States. To ensure that Geothermal remediation is achievable, the effect of heat on bioremediation needs to be examined. This research investigated the heat effects on the bioremediation potential of pure culture and consortia and their potential for (Benzene, Toluene, Ethylbenzene and Xylene(s)) BTEX degradation as a pollutant.

In the present thesis, soil microorganisms with the potential to degrade BTEX were isolated using an enrichment method from soil samples collected at different depths from geothermal boreholes. The microbes were screened and optimized for BTEX degradation at three different temperatures (15, 28 and 40 °C). The bacterial strains *Microbacterium esteraromaticum* and *Bacillus infantis* exhibited the highest degradation compared to other isolated strains and the reference strain, *Pseudomonas putida*. All four BTEX compounds were metabolized 2 times faster at 28 °C and 40 °C. Metabolomics data showed that BTEX was metabolized entirely to acetaldehyde and carbon dioxide by these selected strains. The catechol 1,2-dioxygenases, catechol 2,3-dioxygenases, and toluene monooxygenase enzyme activity confirmed the *tol* and *tod* degradation pathways. Furthermore, the present work offers new insights into the responses of soil microbial communities to electron acceptors under anoxic conditions, indicating that

intrinsic microorganisms can be successfully stimulated for *in-situ* bioremediation (ISB) with electron acceptors as a supplement. The investigation revealed a maximum BTEX biodegradation of 57% by *B. infantis* under sulfate reduction and overall, 98% by *M. esteraromaticum* in combined nitrate and sulfate reduction. To understand the soil matrix influence and to mimic geothermal heating effects, small-scale soil batch experiments and continuous soil column experiments with cyclic temperature were performed. The results revealed that cyclic temperature of 5 °C to 40 °C (shallow low enthalpy geothermal temperature range) enhanced the BTEX biodegradation by 2-fold in silty loam soil (> 80%) in comparison to constant aquifer temperature (12 °C) (40%). Finally, a metagenomics study was performed on soil samples from different depths at three temperatures (15, 28, and 40 °C) to provide insight into how geothermal heat could impact the soil microbiome and its effect on bioremediation activities. Potential known strains for BTEX biodegradation such as *Pseudomonas, Arthrobacter, Bacillus,* as well as some novel strains such as *Microbacterium, Janthinobacterium, Methylotenera,* were found to be dominant at 28 °C and 40 °C. Since microbial abundance and diversity decreased drastically at 15 °C; these findings showed the potential of geothermal heating as a sustainable heat source for ISB of pollutants.

Capsule: GHPs can be used as a heat source for bioremediation, known as Geothermal remediation, which can enhance microbial activity and alter the properties of pollutants, making them more bioavailable for bioremediation in a sustainable manner.

Keywords: Bioremediation, BTEX, Geothermal remediation, Geothermal heat pumps, Groundwater, Microbes, Renewable resources, Soil

DECLARATION

I, **Gurpreet Kaur,** hereby declare that this thesis, entitled *"***Coupling Geothermal Heating with BTEX Bioremediation in the Subsurface***"*, is the result of my own independent research carried out in Civil Engineering at Lassonde School of Engineering at York University under the supervision of **Prof. Satinder Kaur Brar** and **Prof. Magdalena Krol**. Except where otherwise stated, this thesis contains no material previously published or written by another person, nor material which has been accepted for the award of any other degree or diploma at any university or other institution of higher learning.

Any work, ideas, or quotations from the publications of other authors, collaborators, or sources have been duly acknowledged and referenced in the text and in the list of references. This thesis is submitted in partial fulfillment of the requirements for the degree of Doctor of Philosophy at York University.

Gurpreet Kaur

30 September, 2025

DEDICATION

Dedicated to all those who believe in the power of knowledge and persistence.

ACKNOWLEDGEMENTS

First and foremost, I am deeply grateful to **Almighty God** for granting me the strength, wisdom, and perseverance to complete this doctoral journey. Without His blessings and guidance, none of this would have been possible.

I would like to express my sincere gratitude to my supervisor, **Prof. Satinder Kaur Brar** and **Prof. Magdalena Krol**, for their invaluable guidance, patience, and continuous encouragement throughout this research. Their expertise, constructive feedback, and support have been instrumental in shaping this thesis and in helping me grow as a researcher.

I am also indebted to the members of my thesis advisory committee, **Dr. Kamelia Atefi Monfared** and **Dr. Sara Magdouli**, for their insightful comments, critical suggestions, and constant encouragement, which have significantly enriched this work. I would also like to thank my internal examiner**, Dr. Siu Ning (Sunny) Leung** and my external examiner, **Dr. Bipro Ranjan Dhar,** for their time, effort and for playing an important role in accomplishing this process.

My heartfelt thanks go to the faculty and staff of Lassonde School of Engineering at **York University** for their academic and administrative support. I am especially grateful to **Ms. Sindy Mahal,** for her administrative support at each stage and **Mr. Kunjan Rupakheti,** for helping me with gaining a lot of knowledge about soil experiments with his practical assistance and kindness.

I am fortunate to have been surrounded by wonderful colleagues and friends in the Inzymes and Iwater group. Our discussions, collaborations, and shared experiences have made this journey not only productive but also enjoyable. In particular, I would like to thank **Dr. Rahul Saini, Pratishtha Khurana, Dr. Carlos Saul Osorio-Gonzalez, Dr. Reema Kumar**, **Dr. Harman Gill, Kamalpreet Kaur, Arunjot Kaur** for their encouragement, advice, and companionship to make this journey smoother.

On a deeply personal note, I would like to express my everlasting gratitude to my family. To my late father, **S. Hardeep Singh,** who always believed in the power of education and whose

greatest dream was to see his children achieve academic success - I dedicate this to you. Though you are not here to witness this moment, your vision and values have guided me every step of the way.

To my mother, my strength, **Mrs. Sukhwant Kaur** who turned that dream into reality with countless sacrifices, boundless love, and unwavering strength - this achievement belongs to you as much as it does to me. Your resilience and dedication to our education have been my greatest source of inspiration.

To my **brothers and sister**, thank you for your constant encouragement, support, and belief in me. You have been my pillars of strength through both the challenges and successes of this journey. I am equally grateful to my extended family members, whose love, prayers, and encouragement have carried me forward.

To all who contributed academically, emotionally, and spiritually to this journey, I offer my deepest gratitude. Finally, I dedicate this work to all those who inspired my pursuit of knowledge and stood by me during this academic endeavour.

To all who have contributed, directly or indirectly, to this work, I extend my heartfelt thanks.

Gurpreet Kaur

TABLE OF CONTENTS

LIST OF TABLES

LIST OF FIGURES

GRAPHICAL ABSTRACT

Coupling Geothermal Heating with BTEX Bioremediation in the Subsurface

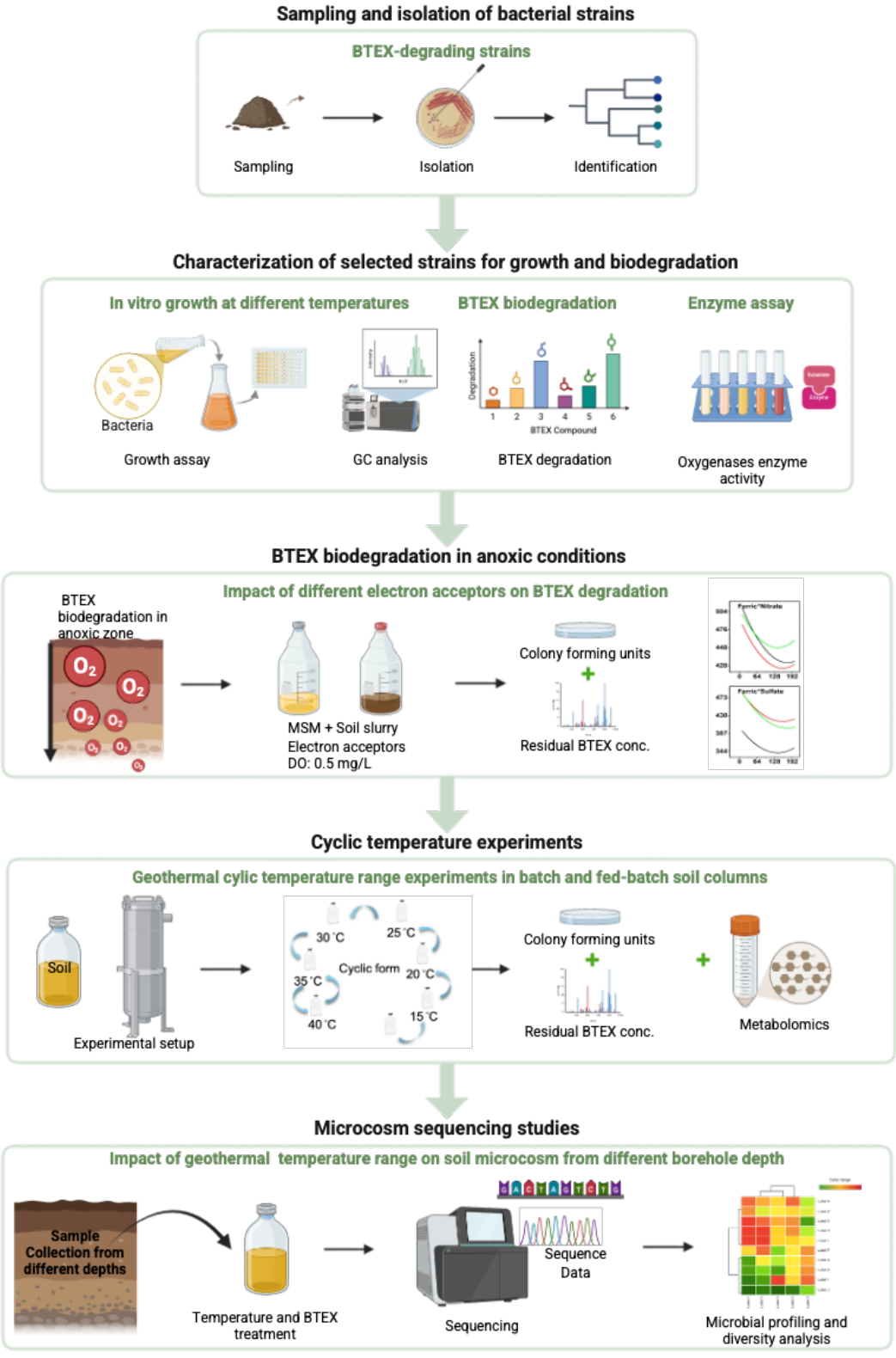

LIST OF PUBLICATIONS

- Gurpreet Kaur, Magdalena Krol, and Satinder Kaur Brar (2021**). Geothermal heating: Is it a boon or a bane for bioremediation?** *Environmental Pollution*, *287*, 117609. **IF: 8.07** (Published 2021).
- Gurpreet Kaur, Guneet Kaur, Magdalena Krol, and Satinder Kaur Brar (2022). **Unravelling the mystery of subsurface microorganisms in bioremediation.** *Current research in Biotechnology*. **IF: 9.1** (Published 2022).
- Gurpreet Kaur, Joanna Lecka, Magdalena Krol, and Satinder Kaur Brar (202**3**). **Novel BTEX-degrading strains from subsurface soil: Isolation, Identification and Growth Evaluation.** *Environmental Pollution*. **IF: 8.9** (Published).
- Gurpreet Kaur, Satyam Verma, Magdalena Krol, and Satinder Kaur Brar (2024**). Analysis of benzene, toluene, ethylbenzene, xylene(s) biodegradation under anoxic conditions using response surface methodology.** *International Biodeterioration & Biodegradation.* **IF: 4.1** (Published, 2024).
- Gurpreet Kaur, Magdalena Krol, and Satinder Kaur Brar (2025**). Investigation of geothermal heating impacts on soil microbiome communities along with the borehole depth by 16S rRNA sequencing.** *Current research in Biotechnology***. IF: 5.6** (Submitted, 2025).
- Gurpreet Kaur, Magdalena Krol, and Satinder Kaur Brar (2025**). Biodegradation of BTEX in soil columns under the cyclic fluctuation of temperature due to geothermal heating.** *Environmental Pollution.* **IF: 8.5** (Submitted, 2025).

Outside of thesis

- Gurpreet Kaur, Satinder Kaur Brar (2021). **Feedstocks and pretreatment techniques for 3G bioethanol production.** Chapter 13 in book " Liquid biofuels: Bioethanol", Volume Editors: Carlos R Soccol, Gonçalo Pereira, Claude Gille and Luciana Vandenberghe. Springer (Accepted 2021).
- Kamalpreet Kaur Brar, Gurpreet Kaur, Sara Magdouli, Satinder Kaur Brar, Carlos Ricardo Soccol (2021). **Lipid production using agricultural residues.** Chapter 11 in book "Microbial Lipids – Processes, Products, and Innovations - Bioproduction for foods, nutraceuticals and biofuels", Volume Editors: Carlos R Soccol, Ashok Pandey, Julio Carvalho, RD Tyagi. Elsevier (Accepted 2021).

- Mohammad Hossein Karimi Darvanjooghi, Shiva Akhtarian, Gurpreet Kaur, Zeinab Ganji, Sara Magdouli, Satinder Kaur Brar, Rama Pulicharla (2022). **Nanomaterials: A Double-edged Sword as Pollution Busters or Pollutants?** Chapter 2 in book "Nanoparticles as Sustainable Environmental Remediation Agents", Volume Editors: Konstantinos Simeonidis and Stefanos Mourdikoudis. Royal Society of Chemistry (Published 2023).
- Pratishtha Khurana, Xuhan Shu, Gurpreet Kaur, Rama Pulicharla, Pratik Kumar, Satinder Kaur Brar (2025). **Long-chain perfluoro carboxylic acids in landfill leachate: Extraction, detection and biodegradation.** *Journal of Environmental Management*. (Published 2025).
- Waseem Raja, Ubhat Ali, Gurpreet Kaur, Agnieszka Cuprys, Guneet Kaur, Satinder Kaur Brar, Pratik Kumar (2025). **Decentralized Modular Electrochemical Technologies for Advanced Wastewater Treatment: A Comprehensive Review of Advanced Oxidation and Reduction Processes, Bioelectrochemical Systems, and Photocatalysis.** Journal of Hazardous, Toxic, and Radioactive Waste. (Published 2025).

LIST OF CONFERENCES

- Gurpreet Kaur, Magdalena Krol, Satinder Kaur Brar (2022). **Coupling of Geothermal Heating with Bioremediation for Enhanced Degradation of BTEX from Subsurface.** Canadian Geothermal Students' Day, August 22-23, 2022, University of Alberta, Edmonton, **Canada**.
- Gurpreet Kaur, Ginelle Aziz, Magdalena Krol, Satinder Kaur Brar (2023). **Potential of microbes towards decontamination of harmful pollutants in the subsurface.** World Water Day Celebrations and CAWQ, March 20-21, 2023, York University, Toronto, **Canada**.
- Gurpreet Kaur, Magdalena Krol, Satinder Kaur Brar (2023). **Analysis of geothermal heating effects on BTEX biodegradation using novel bacterial strains isolated from borehole soil.** International In-situ Thermal Treatment (i2t2) Symposium, May 17-18, 2023, Banff Centre, Calgary, **Canada.**
- Gurpreet Kaur, Magdalena Krol, Satinder Kaur Brar (2024). **Analyzing the role of geothermal heating on bacterial community through metagenomics approaches.** 59th Central Canadian Symposium on Water Quality Research. April 9, 2024, Western University, London, **Canada**.
- Gurpreet Kaur, Ginelle Aziz, Magdalena Krol, Satinder Kaur Brar (2024). **Coupling geothermal heating with bioremediation for enhanced degradation of BTEX from subsurface.** IWA World Water Day Congress and Exhibition, August 11-15, 2024, Toronto Metropolitan Centre, Toronto, **Canada**.
- Gurpreet Kaur, Magdalena Krol, Satinder Kaur Brar (2025). **Investigation of geothermal heating impacts on BTEX biodegradation in soil under cyclic fluctuating temperature.** 60th Central Canadian Symposium on Water Quality Research. February 29, 2025, Toronto Metropolitan University, Toronto, **Canada**.
- Gurpreet Kaur, Ginelle Aziz, Magdalena Krol, Satinder Kaur Brar (2025). **Geothermal remediation: Coupling of geothermal heating with bioremediation for enhanced BTEX degradation.** GAC-MAC-IAH-CNC 2025 Conference, May 11-14, 2025, University of Ottawa, Ottawa, **Canada**.

LIST OF ABBREVIATIONS

ASTM: American society for test and materials

ATES: Aquifer thermal energy storage

BHE: Borehole heat exchangers

BTES: Borehole thermal energy storage

BTEX: Benzene, Toluene, Ethylbenzene, and Xylene

B. infantis: Bacillus infantis

CEC: Cation exchange capacity

CHC: Chlorinated hydrocarbons

COP: Coefficient of performance

CVOC: Chlorinated volatile organic compound

DHC: *Dehalococcoides*

DNA: Deoxyribonucleic acid

DNAPLS: Dense non-aqueous phase liquids

DTS: Distributed temperature sensing

EPA: Environmental protection agency

EPS: Extracellular polysaccharides

ESB: *Ex-situ* bioremediation

FID: Flame ionization detector

GC-MS: Gas chromatography-Mass spectrometry

GEMs: Genetically engineered microorganisms

GHG: Greenhouse gases

GHPs: Geothermal heat pumps

GSHP: Ground-source heat pumps

GW: Groundwater

HM: Heavy metal

ICP-OES: Inductively coupled plasma-optical emission spectroscopy

ISB: *In-situ* bioremediation

LCA: Life Cycle Assessment

LNAPLS: Light non-aqueous phase liquids

MSM: Mineral salt media

M. esteraromaticum: Microbacterium esteraromaticum

NB: Nutrient broth

NSF: Nitrate-sulfate-ferric

OD: Optical density

PAH: Polyaromatic hydrocarbon

PCE: Perchloroethylene

ppb: Parts per billion

ppm: parts per million

RNA: Ribonucleic acid

TCE: Trichloroethylene

TSB: Tryptic soy broth

VAC: Volatile aromatic compounds

VC: Vinyl chloride

GLOSSARY

- **Aerobic Biodegradation**: Breakdown of contaminants in the presence of oxygen.
- **Anaerobic Biodegradation**: Breakdown of contaminants in oxygen-deficient environments, using alternative electron acceptors such as nitrate, sulfate, or CO_2.
- **Aquifer Thermal Energy Storage (ATES)**: Technology that uses aquifers for storing and recovering thermal energy.
- **Aquifer:** The naturally occurring formations that store groundwater
- **Bacteria:** Single-celled living prokaryotic microorganisms
- **Bioaugmentation**: The addition of exogenous microorganisms to contaminated environments to accelerate biodegradation.
- **Bioavailability**: The fraction of a contaminant that is accessible to microorganisms for degradation.
- **Bioremediation**: A process that uses microorganisms (bacteria, fungi, archaea) to degrade pollutants.
- **Biostimulation**: The addition of nutrients or electron acceptors to enhance *in-situ* biodegradation.
- **Biosurfactants**: Surface-active compounds produced by microbes that increase contaminant solubility and bioavailability.
- **Borehole Thermal Energy Storage (BTES)**: Seasonal storage of heat in underground boreholes for later recovery.
- **BTEX**: A group of volatile aromatic hydrocarbons common in petroleum contamination.
- **Geothermal Heat Pumps (GHPs)**: Systems that exploit stable subsurface temperatures to provide heating and cooling to buildings.
- **Geothermal Remediation**: The integration of geothermal heating with bioremediation, using subsurface heat to enhance microbial degradation of pollutants.
- **Groundwater:** Fresh water present underground in saturated soil layers.
- **Koc (Organic Carbon Partition Coefficient)**: A measure of contaminant sorption to soil organic matter.
- **Microbial Consortia**: Groups of different microbial species that work together.
- **Natural Attenuation**: The natural breakdown of contaminants through microbial activity, chemical processes, or dilution without engineered intervention.

- **Psychrophiles / Mesophiles / Thermophiles**: Microorganisms classified by temperature ranges for optimal growth: <15 °C, 15–45 °C, and 45–75 °C, respectively.
- **Q10 Rule**: Empirical rule that microbial activity approximately doubles for every 10 °C increase in temperature.
- **Redox Conditions**: The balance of oxidizing and reducing processes in soil or groundwater that influences contaminant degradation pathways.
- **Sequencing:** Process to identify the logical order of building blocks in DNA or RNA to identify organism.
- **Soil:** It is a mixture of minerals, organic matter, air, water and microorganisms.
- **Sorption/Desorption**: The reversible process of contaminants binding to (sorption) or releasing from (desorption) soil particles.

CHAPTER 1: INTRODUCTION

Introduction

Two major environmental issues currently facing the world are energy demand and environmental pollution resulting from increased globalization and population growth. The increasing global demand for energy has intensified interest in renewable energy technologies, aiming to reduce reliance on fossil fuels and mitigate greenhouse gas emissions. Firstly, for energy demands, which are utilized in various forms, heating and cooling of buildings account for approximately 50-60% of the total energy demand in Canada (Casasso & Sethi, 2019). To obtain this energy sustainably, renewable energy sources are needed. Among these, geothermal heating has gained momentum due to its capacity to provide stable and sustainable heating and cooling through the use of geothermal heat pumps (GHPs). GHPs inject and extract heat from the shallow subsurface (Beyer et al., 2016; Garnier et al., 2011), resulting in cooling and heating of buildings, respectively. These pumps are cost-effective and publicly accepted for heating purposes; however, the effect of operating GHP on the subsurface, groundwater, and bioremediation is not well studied. Secondly, environmental pollution from hydrocarbons, particularly BTEX (benzene, toluene, ethylbenzene, and xylene), remains a persistent concern in groundwater and soil (Garnier et al., 2011; Sommer et al., 2013). Bioremediation, which employs natural or engineered microorganisms to degrade pollutants, is a cost-effective and environmentally friendly alternative to physical and chemical remediation methods (Fleuchaus et al., 2018; Koshlaf & Ball, 2017; Yuniati, 2018), however it can sometimes not be as reliable or efficient as more energy intensive methods.

The major issue associated with natural degradation is that microorganisms in the subsurface may proliferate at a slower rate because of unsuitable conditions in the subsurface for growth and metabolic activity (Iqbal, 2003). Lower temperature is one of the main factors that limit their metabolic activity towards the degradation of pollutants, since subsurface temperatures are typically in the order of 10 – 15 ºC. In addition to microbes, the properties of the pollutants also limit the rate of bioremediation. As in the ground, the pollutants are present in different phases, limiting their bioavailability for degradation by microbes (Sanscartier et al., 2011; Sanscartier et al., 2009; Walworth et al., 2001). The effect of temperature on microbial activity is known to be a positive stimulator; however, this is not studied in detail with respect to subsurface bioremediation, especially when heat is used from GHP (i.e. cyclical). The emerging

concept of Geothermal remediation explores the synergistic integration of geothermal heating and bioremediation, where subsurface heating enhances microbial degradation of petroleum-based pollutants such as BTEX. Hence, in this thesis, we aim to examine the role of heat injected by GHPs on the bioremediation of our model contaminants (BTEX) and other subsurface properties, to see if a positive association between GHP and bioremediation can be demonstrated that is sustainable and cost-effective.

Other researchers have explored the effect of geothermal heating on bioremediation. Studies claimed that warming up of subsurface during the cooling mode of GHPs, can help to improve the decontamination of pollutants like dichloroethylene, benzene, vinyl chloride by microorganisms (Beyer et al., 2016; Garnier et al., 2011; Moradi et al., 2018; Ni et al., 2016, 2020; Roohidehkordi & Krol, 2021a; Sommer, 2015), while others show many challenges to this method, for instance; well clogging, microbial colonization, mineral dissolution, geochemical changes in aquifer especially for open-loop systems (Bezelgues et al., 2010; Bonte et al., 2011; Jesußek et al., 2013). However, experimental validation of the effect of GHPs on BTEX bioremediation has not been reported. BTEX are monoaromatic hydrocarbons, commonly found in the subsurface and groundwater at concentrations in the mg/L range, whereas the maximum acceptable concentrations are in the ug/L range. Exposure to elevated BTEX concentrations can lead to severe chronic health concerns. Addressing BTEX contamination is particularly important, as more than nine million Canadians rely on groundwater as their sole drinking water source. Therefore, this research examined the advantages and disadvantages associated with using geothermal heating for bioremediation by investigating, for the very first time to the best of our knowledge, the effect of cyclic low-enthalpy heat on BTEX biodegradation. Overall, the thesis focused on the results of laboratory experiments to summarize whether coupling geothermal shallow energy with BTEX bioremediation could be a sustainable and eco-friendly (advantage) approach towards site remediation, or if the negative impacts outweigh the associated benefits (disadvantage).

This thesis is structured into six chapters that explore the application of geothermal heating and microbial bioremediation to remediate BTEX contamination in subsurface environments. The experimental work was conducted with four research objectives. Chapter 1 serves as the introduction, outlining the research context, stating the problem, and emphasizing the

importance of geothermal energy and biodegradation. Chapter 2 is a review of the literature, which critically examines BTEX contamination, microbial remediation, and problems with bioremediation, while introducing geothermal heating as a sustainable option. It also presents critical studies to identify knowledge gaps that underpin this study. This review integrates two complementary perspectives: (1) the role of microbial ecology, diversity, and function in subsurface biodegradation (Graphical review, Kaur et al., 2022), and (2) the role of geothermal heating and shallow geothermal systems on subsurface environments and pollutant degradation (Critical review, Kaur et al., 2021). Together, these provide a foundation for evaluating the potential of geothermal heating as a sustainable tool to enhance BTEX bioremediation. Chapter 3 introduces the research hypotheses, four objectives, and the novel link between subsurface thermal dynamics and microbial activity as shown in Figure 1.1. Chapter 4 outlines the methodology employed in experimental work for each specific objective, for instance, for isolating and characterizing BTEX-degrading strains, utilizing response surface methodology for optimizing anoxic degradation, conducting bench-scale GHP simulations for cyclic heating, and employing 16S rRNA sequencing for microbial community analysis. Chapter 5 presents and discusses the results corresponding to each objective, focusing on microbial performance, degradation kinetics, system response to thermal cycling, and community-level changes along borehole depth. Finally, Chapter 6 summarizes the main findings, discusses geothermal–biological coupling's scientific and practical implications, and recommendations for future research.

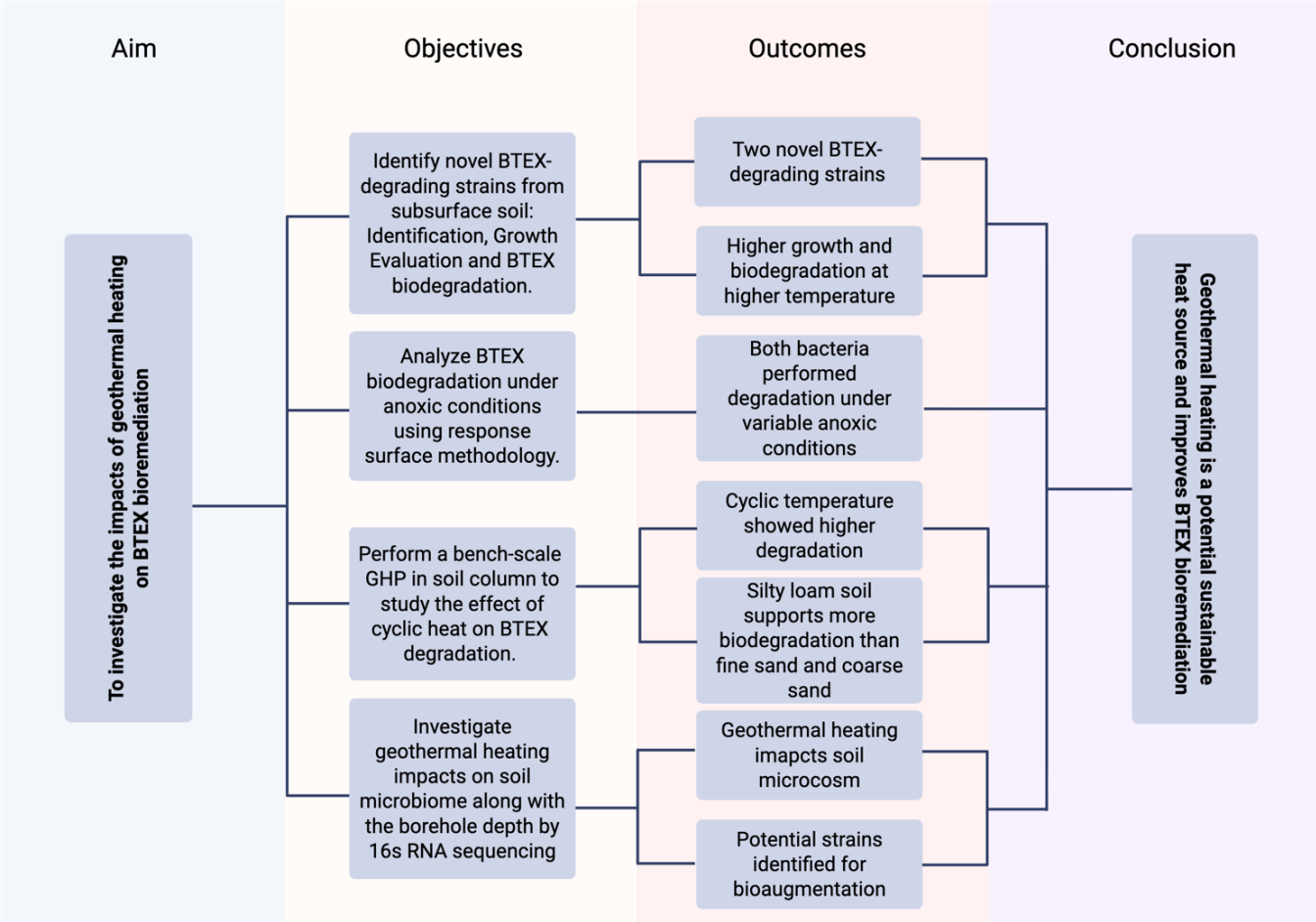

Figure 1.1: Thesis outline showing research objectives and the outcomes.

CHAPTER 2: REVIEW OF LITERATURE

Published as a Critical Review entitled **"Geothermal heating: Is it a boon or bane for bioremediation?" with** DOI: https://doi.org/10.1016/j.envpol.2021.117609 and as a Graphical Review entitled "**Unraveling the mystery of subsurface microorganisms in bioremediation**" with DOI: https://doi.org/10.1016/j.crbiot.2022.07.001. The references have been updated in this section since its publication.

2. Introduction

In this energy-demanding world, the rate of energy consumption for the welfare of human beings has increased rapidly. Among the various energy utility processes, the heating and cooling of infrastructure consume approximately 50-60% of the total energy consumption (Casasso & Sethi, 2019). Typically, the energy demand has been fulfilled using fossil fuels; however, the drawbacks, including limited resources, high greenhouse gas emissions, and high cost, have resulted in sustainable sources like air, wind and subsurface to become more prevalent (Moradi et al., 2018). One of the applicable and eco-friendly approaches is to use shallow subsurface for the storage and extraction of heat, which can be used for heating and cooling of interiors, according to the season, without much external energy consumption and low climate effects. This is done using geothermal heat pumps (GHPs).

In addition to the demands for natural and renewable energy sources such as geothermal, the requirement for appropriate treatment for removal and decontamination/degradation of pollutants created by the growing population has become a necessity for regulatory authorities. Furthermore, the industrial and technical development of different sectors has led to an increase in the amount, complexity, and toxicity of waste. The inadequate disposal of these wastes has resulted in environmental pollution, resulting in water and soil contamination, which is one of the major challenges faced by the world (Giovanella et al., 2020). These pollutants can include various mutagenic and carcinogenic pollutants like BTEX, chlorinated volatile organic compounds (CVOC), and petroleum hydrocarbons, among others, making them an environmental and public health concern (Garnier et al., 2011; Sommer et al., 2013).

Typically, under natural conditions, the rate of contaminant degradation is slow, hence contaminated sites have a high potential for environmental impact and therefore typically require appropriate removal or treatment of the contaminants (Iqbal et al., 2007). There are various ways to battle pollution and to date, various physical, chemical and biological treatments have been implemented to remediate contaminated environments and to protect soil and water quality (Fleuchaus et al., 2018; Koshlaf & Ball, 2017; Yuniati, 2018). Some aggressive treatments boast that land can be restored to its natural state quickly; however, ample drawbacks are associated with these rapid methods, including high cost, high energy

consumption, soil excavation and groundwater extraction (H. I. Gomes et al., 2013; Koul & Taak, 2018; Kuppusamy et al., 2016). They can also be labor-intensive, limiting their utilization. More gradual remediation methods can avoid these shortcomings if the site conditions allow for less rapid measures to be implemented. Among these technologies, bioremediation has garnered significant attention in recent decades due to its effectiveness and low-cost application (Castro et al., 2019; Giovanella et al., 2020).

Bioremediation is the ability to degrade pollutants with the help of natural microbes present in soil and groundwater. If bioremediation occurs within the site, then it is referred to as *in-situ* bioremediation (ISB) and if the polluted material is taken out for treatment, then it is called *ex-situ* bioremediation (ESB) (Carberry & Wik, 2001; Hatzinger et al., 2002; Kensa, 2011; Wadgaonkar et al., 2019). The natural rate of bioremediation can be quite slow, generally taking years to completely degrade the pollutants (Iqbal, 2003). Studies have shown that multiple factors, including subsurface temperature, soil moisture content, pollutant concentration, contaminant compositions, sediment type, interaction among the contaminants, and type of microorganisms control the nature and extent of microbial metabolism in the presence of most contaminants. Alteration to these parameters can affect the rate of bioremediation and therefore, they need to be considered when developing a successful bioremediation strategy for elimination of a particular contaminant (Giovanella et al., 2020; Moradi et al., 2018). In addition, a single approach may not result in the bioremediation of various contaminants (if the site contains multiple pollutants) and therefore a combination of techniques may be required (National Research Council, 1993).

Over the past decade, various articles and reviews have been published, focusing on the methods to improve ISB. For instance, bioremediation can be augmented with archaea or bacterial cultures to speed up the rate of contaminant degradation, referred to as bioaugmentation (Adams et al., 2015; Major et al., 2002; Naeimi et al., 2021; Sarkar et al., 2017; Varjani & Upasani, 2019), nutrients can be added (biostimulation) (Adams et al., 2015; Ape et al., 2019; A. Roy et al., 2018; Tyagi et al., 2011), or hydrophobic and hydrophilic compounds (biosurfactants) can be injected to increase the bioavailability of hydrocarbons (Decesaro et al., 2017; Gidudu & Chirwa, 2021; V. G. Martins et al., 2009; Prakash et al., 2020). In addition, numerous field and real bioaugmentation studies have been conducted using commercial

microbes, genetically modified microbes or enriched culture of microbes (Plangklang & Reungsang, 2011; Thompson et al., 2005; Tsutsumi et al., 2000); as well as biostimulation using N and P fertilizers, manure, oleophilic fertilizer, and inorganic mineral nutrients. These nutrients were injected into wells at contaminated sites using battery operated pumps and recirculated using an extraction well while monitoring wells monitored the process (Garcia-Blanco et al., 2007; W. Liu et al., 2010; Sanscartier et al., 2009; Yabusaki et al., 2007). In some cases, the microbial culture, nutrients or biosurfactants were first mixed with soil from the desired site in a concrete mixer and then recirculated to the field (Szulc et al., 2014). Likewise, biosurfactants have been injected into oil-contaminated areas to make pollutants more bioavailable to microbes (Bai et al., 1997; Szulc et al., 2014; Whang et al., 2008).

The addition of cold-adapted enzymes has also been studied to enhance biodegradation in cold climates (Adams et al., 2015; Miri et al., 2019; Salwoom et al., 2019). Similarly, the addition of heat up to a favorable level for native microbes can enhance the biodegradation rate (Sanscartier et al., 2011; Sanscartier et al., 2009; Walworth et al., 2001), because increased temperature corresponds to a decrease in adsorption of pollutants (therefore making them available for degradation), increases bioavailability, microbial growth, and elevated metabolic activity.

Traditionally, heat has been introduced into the subsurface to increase the contaminant removal rate using various remediation methods, such as electrical resistance heating (Buettner & Daily, 1995; Krol et al., 2011; Truex et al., 2009), radiofrequency techniques (Huon et al., 2012), steam enhanced extraction and thermal conduction heating (Heron et al., 2009; Kingston et al., 2014). These techniques can be used to warm up the subsurface which leads to contaminant volatilization and helps in their removal (Azadpour-Keeley et al., 2004; Barba et al., 2018; Farber et al., 2019). However, the mobilization of volatilized contaminants in the subsurface relies on soil permeability, porosity, contaminant vapour pressure, and soil-vapor extraction rate. Typically, higher permeability soils result in lower capillary pressures that need to be overcome for mobilization to occur (Huang, 2021; Krol et al., 2011; Molnár et al., 2019; Wang et al., 2020).

These technologies can be very effective in remediating contaminated lands, nevertheless, multiple disadvantages like high energy demand, significant set-up, and site disruption make

them an unfavorable option for some remediation sites (Moradi et al., 2018). Therefore, other, less intrusive technologies have been used by many, including bioremediation coupled with thermal treatment (Agrawal et al., 2019; I. Hassan et al., 2016; I. A. Hassan et al., 2019; Moradi et al., 2018). An alternative approach over conventional heating technologies is to use geothermal heat pumps to apply heat to the subsurface, as it is a renewable energy source. However, the question remains if this type of approach could be done effectively and cost-efficiently. Hence, in this research, the role of geothermal heating on BTEX bioremediation has been studied at the laboratory scale.

2.1 Background: Overview of subsurface and groundwater pollution

The subsurface is a major component of the Earth, playing a versatile role in the ecosystem. It contains groundwater that can be found within the pore space of porous media and rock fractures. Groundwater accounts for approximately 30% of the freshwater found on Earth and serves a potable source for drinking water, and is used in agriculture and industry (Canada, 2007). As such, the availability, quality, and sustainability of groundwater are important considerations for future generations. In Canada, approximately one-third of the population relies on groundwater as their sole water source. This figure varies from province to province; for example, people in New Brunswick and Prince Edward Island depend on groundwater for domestic use at rates of around 64% and 100%, respectively (Canada, 2007). Since groundwater is an unseen resource, groundwater contamination often goes unnoticed for extended periods. Any addition of undesirable substances caused by anthropogenic activities is known as contamination. Contamination can occur from both point (underground storage leakage, chemical spills, landfills, and leaking septic tanks) and non-point (road salt, industrial waste, and infiltration of pesticides and fertilizers) sources. Point sources are more localized and often readily identified due to their high concentrations, while non-point sources sometimes remain undetected (Xepapadeas, 2011).

Groundwater contamination can be difficult to clean up, as the contaminants can spread far beyond the site of original contamination or sink deep into the subsurface. If an aquifer gets contaminated, then it usually becomes unsuitable for use unless it is remediated. Many individual cases of contamination have been investigated, such as Ville Mercier in Quebec; the highway de-icing salt problem in Nova Scotia; industrial effluents in Elmira, Ontario; various

pesticides in the Prairie provinces; industrial contamination in Vancouver, British Columbia. In many cases, contamination is recognized only after groundwater users have been exposed to potential health risks and the cost of cleaning up contaminated water supplies in Canada can be expensive (Environment and Climate Change, 2007).

Contamination sites are reportedly increasing in Canada, primarily due to the growing number of toxic compounds used in industry and agriculture (Environment and Climate Change, 2007). It has been predicted that in the next few decades, more contaminated aquifers will be discovered, new contaminants will be identified, and more contaminated groundwater will be discharged into wetlands, streams and lakes. Once an aquifer is contaminated, it may be unusable for decades. The residence time can be anywhere from two weeks to 10,000 years. Hence, preventive measures are required, along with a proper remediation strategy and management practices, to protect groundwater (Environment and Climate Change, 2007).

2.1.1 Statistical overview of subsurface pollution in Canada

In Canada, thousands of contaminated sites have been identified that require economical and effective treatment without any additional harm to our environment. The Treasury Board of Canada Secretariat has identified close to 23,000 federal contaminated sites, where 3,855 of these are still active, and where remedial action is, or may be, required. Among these sites, 2,945 have groundwater contamination (Figure 2.1a), and 578 (20%) of those sites were located in Ontario (Figure 2.1b). Contaminants come mostly from anthropogenic sources. The most common source of contamination is leakage of underground storage tanks and piping, which were widely installed during the 1950s and 1960s to store petroleum products. They were made of steel without any corrosion protection, and hence, they have become corroded. Up to half of them leaked within 15 years of installation, and over the past two decades, leaks of petroleum products have increased significantly.

Contaminated sites can be contaminated with different contaminants such as heavy metals, polyaromatic hydrocarbons (PAHs), chlorinated hydrocarbons, and BTEX, which are all regarded as priority pollutants by the National Classification System of the Canadian Council of Ministers of Environment (Figure 2.1b). Some sites are difficult to remediate due to the chemical nature of the contaminants or due to site conditions. Therefore, continuous efforts are

made by researchers and regulators to develop new and innovative remediation treatments. The goal is to find affordable and effective remediation options that restore the subsurface to regulation standards.

a.

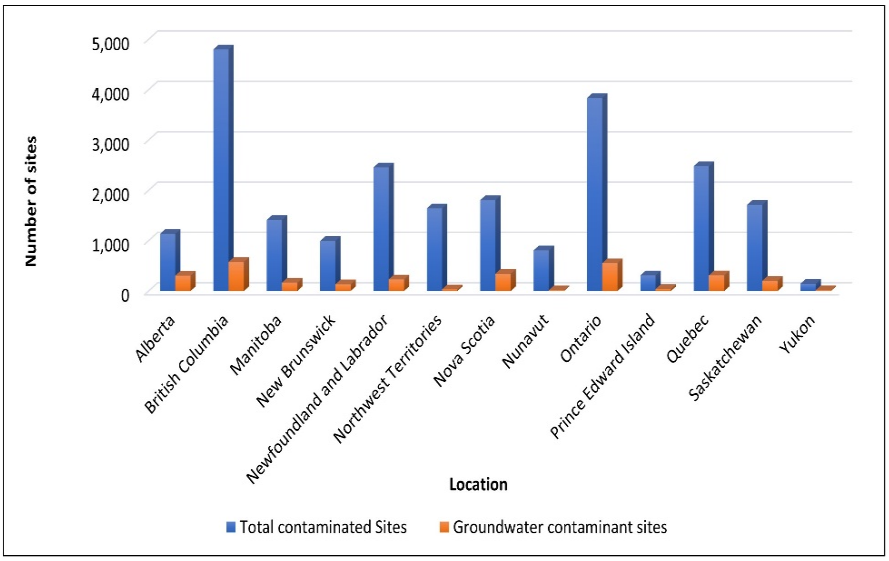

b.

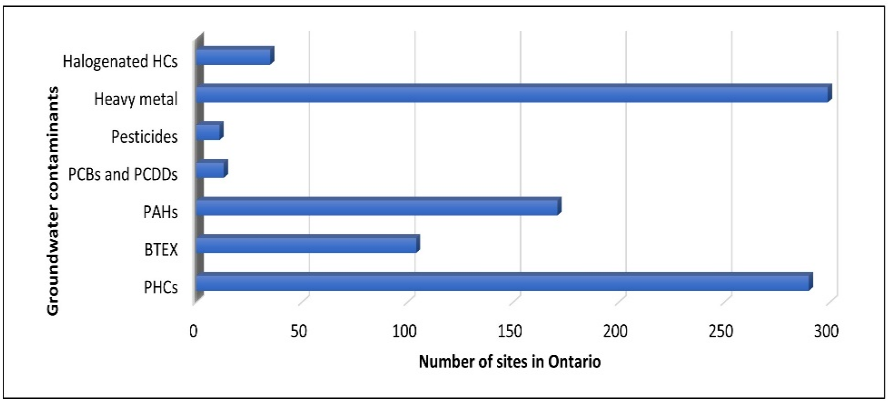

Figure 2.1: Summary of various contaminated sites in Canada (2020), with contaminants drawn mostly from anthropogenic sources, showing: (a) Total contaminated sites (23,546) and groundwater contaminated sites in different provinces and territories of Canada, (b) Number of groundwater contaminated sites in Ontario, by contaminant type. (Retrieved from the Federal Treasury Board of Canada Secretariat).

2.1.2 Common pollutants: BTEX

Benzene, toluene, ethylbenzene, and xylenes, collectively known as BTEX, are light non-aqueous phase liquids (LNAPLs) that are major pollutants in the environment. BTEX is used

in the processing of petroleum products and during the production of cosmetic products, pharmaceutical products, and consumer goods, including paint, ink, rubber, and adhesives (Martins et al., 2016). BTEX is released to the atmosphere by fossil fuel combustion, evaporation while gas filling, and accidental spillage. Subsurface contamination occurs mainly through underground storage tank leakage, spillage, oil transportation pipeline leakage, and improper disposal of industrial solvents containing BTEX. When BTEX is found in higher quantities in the environment, it can lead to several adverse effects on human health, for instance, respiratory disorders, kidney, liver and lung problems, central nervous system depression, and more. Benzene is reported to be cancerous (Bolden et al., 2015) and has also been found in cord blood through transplacental migration, leading to several prenatal disorders (Dowty et al., 1976). One study found that BTEX has hormonal effects and could lead to endocrine-disrupting properties even at exposure below ambient levels set by the U.S. Environmental Protection Agency (Bolden et al., 2015). The Canadian federal guidelines for maximum acceptable concentrations of these pollutants in drinking water are 0.005 mg/L, 0.06 mg/L, 0.14 mg/L, and 0.09 mg/L for BTEX, respectively (Health Canada, 2025). As BTEX has several hazardous impacts, BTEX-contaminated sites are receiving more public attention; therefore, researchers have focused on finding viable remediation technologies (Khodaei et al., 2017a; Y. Meng & Li, 2025; Seagren & Becker, 2002).

Chemically, these compounds are monoaromatic hydrocarbons, consisting of one hexagonal ring with alkyl groups. They are LNAPLs with limited water solubility. Since the density is lower than that of water they are frequently found as an organic layer on top of the water table. Moreover, they are volatile compounds, which means they can evaporate easily into the air and are found in all three different phases: air, water, and soil. Common properties of BTEX are listed in Table 2.1, which are needed when planning and designing a remediation approach. Due to these properties, contaminated sites have BTEX in groundwater, soil, and void space, according to the partition coefficient and contaminant amount. Additionally, BTEX can undergo transformation and biodegradation, depending on the type of microbes, oxygen, and electron acceptors present in the subsurface, as further explained in sections 2.2.2 and 2.2.3.

Table 2.1: Physical and chemical properties of BTEX

Common name (IUPAC)	Chemical structure	Molecular weight (g/mol)	Log Kow	Henry Constant	Vapor pressure (mmHg)	Density (g/mL)	Solubility (mg/L)	MCL (mg/L)
Benzene		78.1	2.13	0.228	76	0.88	1750	0.005
Toluene	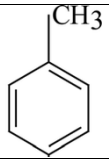	92.1	2.73	0.272	22	0.87	526	0.06
Ethylbenzene	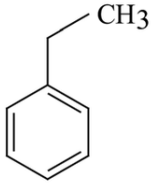	106.2	4.34	0.323	7	0.87	169	0.14
o-Xylene	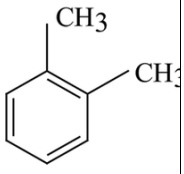	106.2	3.12	0.213	5	0.86	178	-
p-Xylene	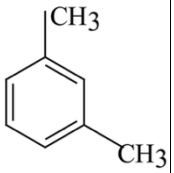	106.2	3.20	0.301	6	0.86	161	-
m-Xylene	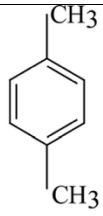	106.2	3.15	0.314	6.5	0.86	185	-
Total Xylene	-	-	-	-	-	-	-	0.09

IUPAC: International Union of Pure and Applied Chemistry; MCL: Maximum Contaminant Level

2.2 Bioremediation Principles

Microorganisms play a vital function in different applications for better human health and environment protection; for instance, microbes have roles in digestion, immunity generation, photosynthesis, bioremediation, essential elements' cycle, and waste decomposition. In addition, they have been used extensively to remove potential contaminants from the environment, especially after the introduction of proper regulation to protect soil and groundwater in the 1970s. More recently, intrinsic microbes present in the ground are being explored widely to investigate their role in the bioremediation of pollutants.

The deterioration of groundwater sources has led to an increased interest in the investigation of subsurface microbiology and microbes' role in pollutant removal. Bioremediation of contaminated sites by indigenous microorganisms, known as natural attenuation, is an attractive option as it can provide good contaminant removal at a low cost. The rate of natural pollutant removal can be stimulated by bioaugmentation, biostimulation and genetic engineering of the subsurface microflora. The background knowledge of native microbes regarding their activity and distribution in the subsurface is essential for the successful stimulation of microbes at a contaminated site to degrade specific pollutants and to evaluate the interaction among intrinsic and extrinsic microbes for enhanced bioremediation (Amend & Teske, 2005; Aulenta et al., 2021).

Additional motivation to investigate subsurface microbiology is the potential of undiscovered reservoirs of microbes for bioproduct production and other biotechnological applications. Moreover, the development of sequencing and metagenomic analysis allows the recovery and discovery of new microbial strains from deep terrestrial habitats without culturing them (Griebler & Lueders, 2009a).

Microbes have been studied for their role in bioremediation for a long time and in various applications, as such there is significant knowledge of microbes and how to utilize them for environmental protection and human benefits. The oldest approach used to study microbes is culturing them in synthetic media in artificial conditions in a laboratory and analyze their ability to degrade pollutants (Carini, 2019). However, this approach is limited to only culturable microbes, whereas our environment has an abundance of microbes, which are unable to grow in artificial conditions, though they have been important drivers for major biogeochemical

processes (Carini, 2019). To study such unculturable microbes, techniques like sequencing, and metagenomics are widely used to estimate genetic diversity, and microbial activity (Kadnikov et al., 2020). However, with the further development in technologies, techniques like community-level physiological profiling, proteomics, metabolomics, metabonomics, and microbial profiling have helped to understand the complete metabolic pathways and functional diversity of microbes, which is a fundament step in exploring the biodegradation processes in the subsurface (Z. Zhou et al., 2022).

2.2.1 Microbes present in the subsurface: their potential and interactions

An abundant number of microbes ranging from prokaryotes to eukaryotes are present in the subsurface and their role in bioremediation and their biochemical activity has been reviewed by several studies (Hazen, 2018; Lawniczak et al., 2020; Leung et al., 2019; Long et al., 2016; Quintella et al., 2019). Microbial type and abundance depend on various factors such as soil type, soil depth, oxygen presence, and temperature. With an increase in soil depth, the temperature and pressure gradually increase and the amount of biomass decreases, as shown in Figure 2.2. In addition, the type of porous media also affects microbe proliferation, for example, more microorganisms will be present in sandy soil than in clays due to sand's larger pores (Meyer et al., 2022). Likewise, the presence of oxygen will dictate what type of microbe is present in the subsurface: aerobic or anaerobic. These microbes have been studied in various reports for their role and fate in the subsurface, however, the interaction among these microbial consortia is not well studied. Although these subsurface microbes broadly belong to bacteria, archaea, fungi, and viruses species, bacteria are most prominently found and have a major role in the biodegradation of the pollutants and biogeochemical cycle in the subsurface (Griebler & Lueders, 2009a; Meckenstock et al., 2015).

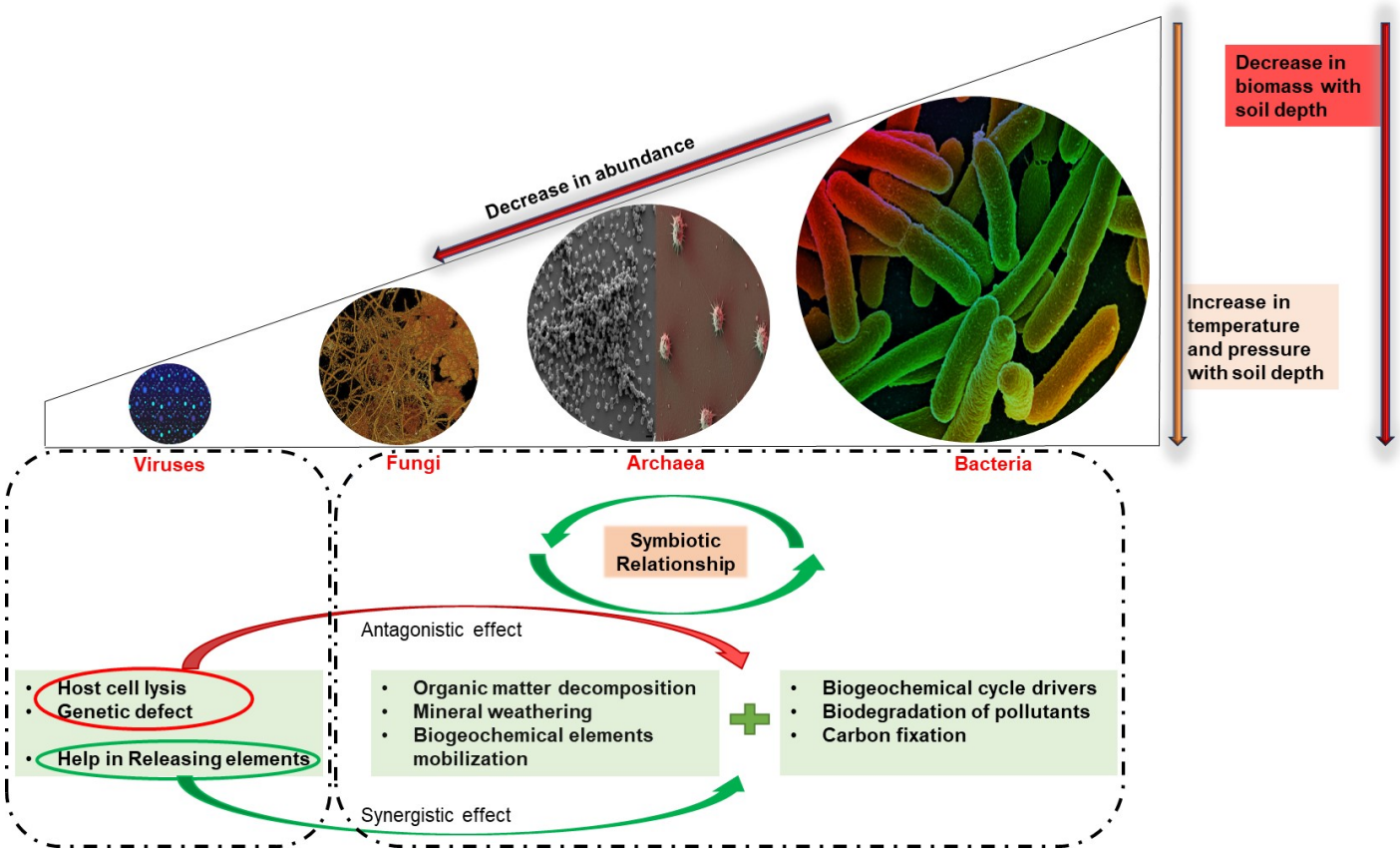

Figure 2.2: A general interaction among various microbial communities. The circle size roughly represents the relative size of these groups in the subsurface, where bacteria, archaea and fungi work in a symbiotic relationship towards the biogeochemical cycle and bioremediation while viruses have dual effects. The lysis of host cells leads to a decrease in host cell count, while the same time they release essential elements into the subsurface which are used for by the other microbial communities for their energy requirement and growth.

Microorganisms act as key players in the biogeochemical processes occurring in the shallow subsurface during bioremediation. The biogeochemical cycle is a fundamental pathway in an ecological system that is entirely dependent on the microbial community, soil minerals, and the pollutants present in the subsurface (Canadell et al., 2021; Falkowski et al., 2008). As the biogeochemical cycle relies on microbial diversity, it has co-evolved with specific metabolic and functional pathways. Figure 2.3 shows an overall interaction of subsurface components with the flow of atmospheric gases and the movement of various elements.

Figure 2.3b shows the detailed carbon, sulfur and nitrogen cycles that occur in the ecosystems. In these cycles, bacteria and archaea are the biggest contributors (Hug, Baker, Anantharaman, Brown, Probst, Castelle, Butterfield, Hernsdorf, Amano, Ise, et al., 2016), while deep-inhabiting fungi work in a symbiotic relationship with the prokaryotes helping to provide essential minerals through mineral decomposition and mobilization (Figure 2.2). Viruses generally have a dual role as a predator and regulator in the biogeochemical cycles and microbial ecology. They help to release essential elements in the ecosystem (Tran & Anantharaman, 2021). However, they affect microbial growth through three main approaches which include biogeochemical cycle modification by disturbing the microbial loop through the lysis of host cells, altering the diversity and number of their microbial hosts, and producing mutation in the genetic material of the host cell. The last approach has the potential to fundamentally change the course of evolution in their microbial hosts (Anderson et al., 2011).

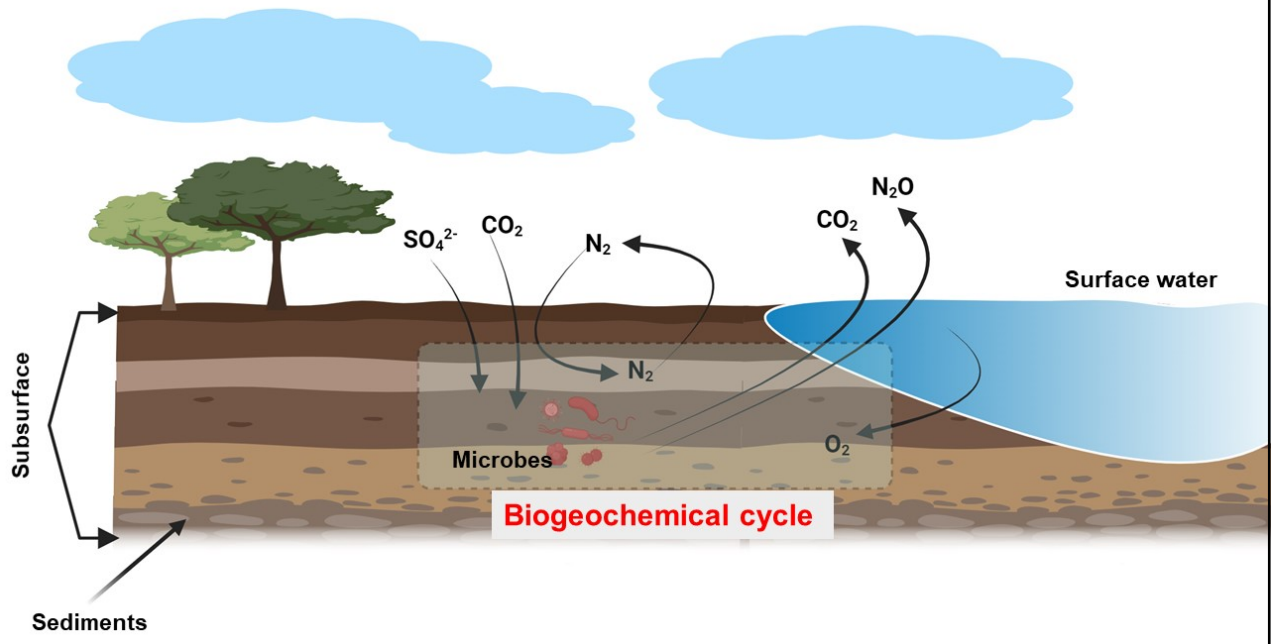

a. **Overview of biogeochemical cycle**

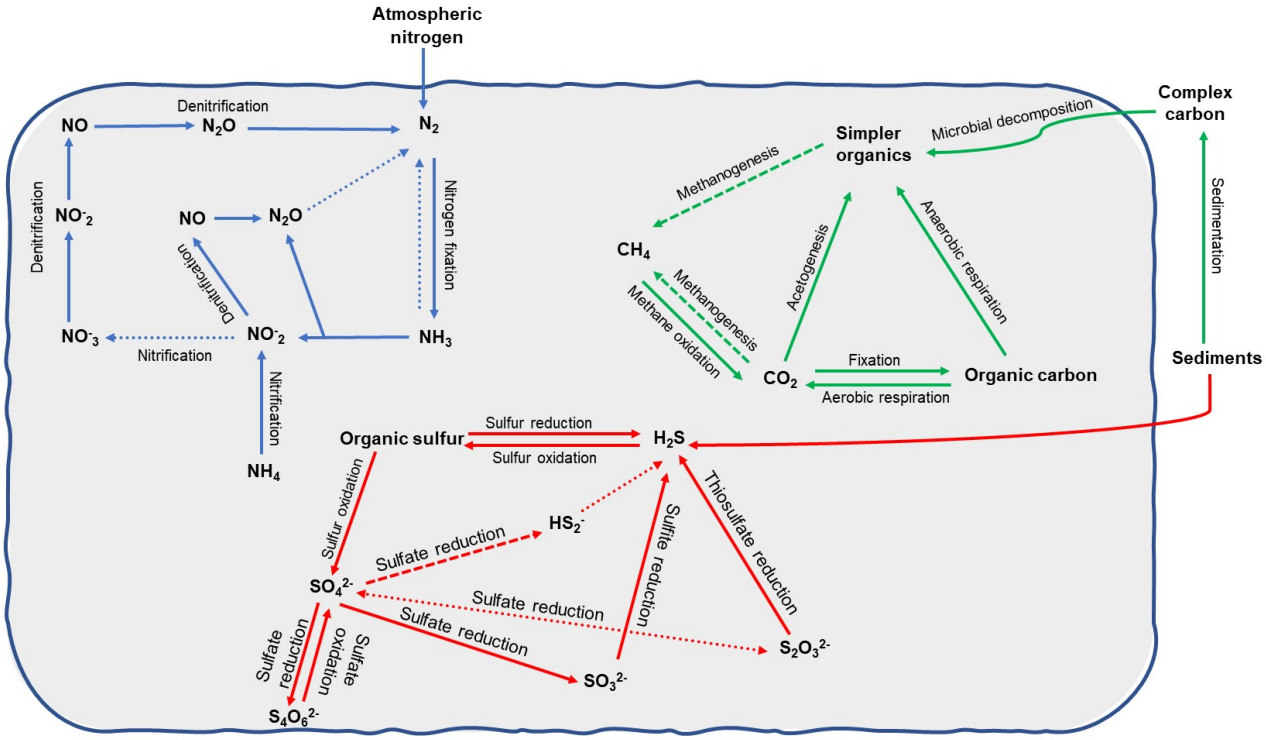

b. **Detailed nitrogen, sulfur, and carbon cycle**

Figure 2.3: A schematic representation of the overall biogeochemical cycle in the subsurface performed by the microbes. The microbes shown are taken as a consortium and the direction of the arrows shows the flow of different chemicals, ions, and energy within the microbial cell and within the outer environment. Figure 2.3b shows a detailed carbon, nitrogen, and sulfur cycle. The distinct colors symbolize different element cycles: red, blue, and green represent sulfur, nitrogen, and carbon cycle, respectively. The solid arrows represent the metabolic processes performed by both archaea and bacteria, while the dashed and dotted arrows show the processes performed only by archaea and bacteria respectively.

Furthermore, based on respiration and metabolic pathways, metagenomic analysis explored the main metabolic groups of microorganisms as shown in Figure 2.4 (Matsushita et al., 2020). Most of the microbial community in the subsurface is composed of anaerobic heterotrophic microbes that have a fermentation-based metabolism. These microbes encode enzymes that can reduce nitrite, nitrate, Fe (III), thiosulfate, tetrathionate, polysulfides, etc. Such metabolic groups mostly comprise *Firmicutes, Chloroflexi, Bacteroidetes, Proteobacteria, Armatimonadetes, Actinobacteria, Spirochaetes, Aminicenantes*, and less abundant species of many more phyla. Some of these anaerobic microbes have the ability for autotrophic carbon fixation by using the Wood–Ljungdahl pathway as shown in Figure 2.3. These microbes can also generate acetate and hydrogen which are consumed by sulfate reducers and methanogens as an energy source. Sulfate reducers typically develop in sulfate-rich environments while methanogens grow in the conditions having low sulfate. In syntrophic associations with anaerobic microbes and methanogens, fermentative species such as *Firmicutes* and *Deltaproteobacteria* oxidize the organic pollutants with low-molecular-weight for biodegradation in oxygen-deficient sites. Such anaerobic environments are beneficial for fermentative microbes, sulfate reducers, and methanogens for consuming their metabolic products (Matsushita et al., 2020; Qiao et al., 2019).

Along with anaerobic microbes, the other metabolic group comprises aerobic heterotrophs. The aerobic heterotrophs and methanogens have mutually unique growth and environmental conditions, which shows the heterogeneity of conditions in the subsurface. The expected delivery of aerobic microbes and oxygen from surface to subsurface is via meteoric recharge

waters. The zones of entry of waters into the aquifer become a favorable and advantageous environment for the growth and proliferation of aerobic microbes and sulfide oxidation producing sulfate ions. The respiratory versatile bacteria that can use oxygen as well as sulfate for their respiration, could successfully proliferate at the oxy-anoxic boundaries in unconfined aquifers and recharge zones (Kadnikov et al., 2020).

2.2.2 Role of Microbes in Biodegradation

As microbes have a versatile role in the subsurface biogeochemical processes, likewise they have the potential to consume and degrade pollutants. However, the biodegradation rate depends on the microbes, pollutants, and surrounding conditions. There are numerous subsurface contaminated sites, and these sites are home to microbes with unique metabolic capabilities, such as prokaryotes, that can survive and use the organic chemicals that would be fatal to higher multicellular organisms. These intrinsic microbes present in the subsurface have been explored for their role in bioremediation (Kumar Gupta, 2020; Lawniczak et al., 2020; Leung et al., 2019; Mishra et al., 2022). However, the mechanism used by the microbes to utilize pollutants and to convert them to non-toxic compounds varies by the types of pollutants, their amount, soil type, and the host microbes, which still needs more investigation. The central biodegradation pathway of the contaminant is divided into anaerobic and aerobic degradation relying on the type of electron acceptors (pollutants) present at the contaminated site as shown in Figure 2.4. As subsurface environments are mostly anaerobic with low oxygen amounts, the microorganisms can also use substitute electron acceptors such as nitrate, manganese, iron, sulfate, and rarely carbon dioxide for their metabolism respiration (Gou et al., 2020; Witthayaphirom et al., 2020). Microbes in the subsurface are adapted to such conditions and are metabolically flexible as conditions change over time in and around the contaminant plumes.

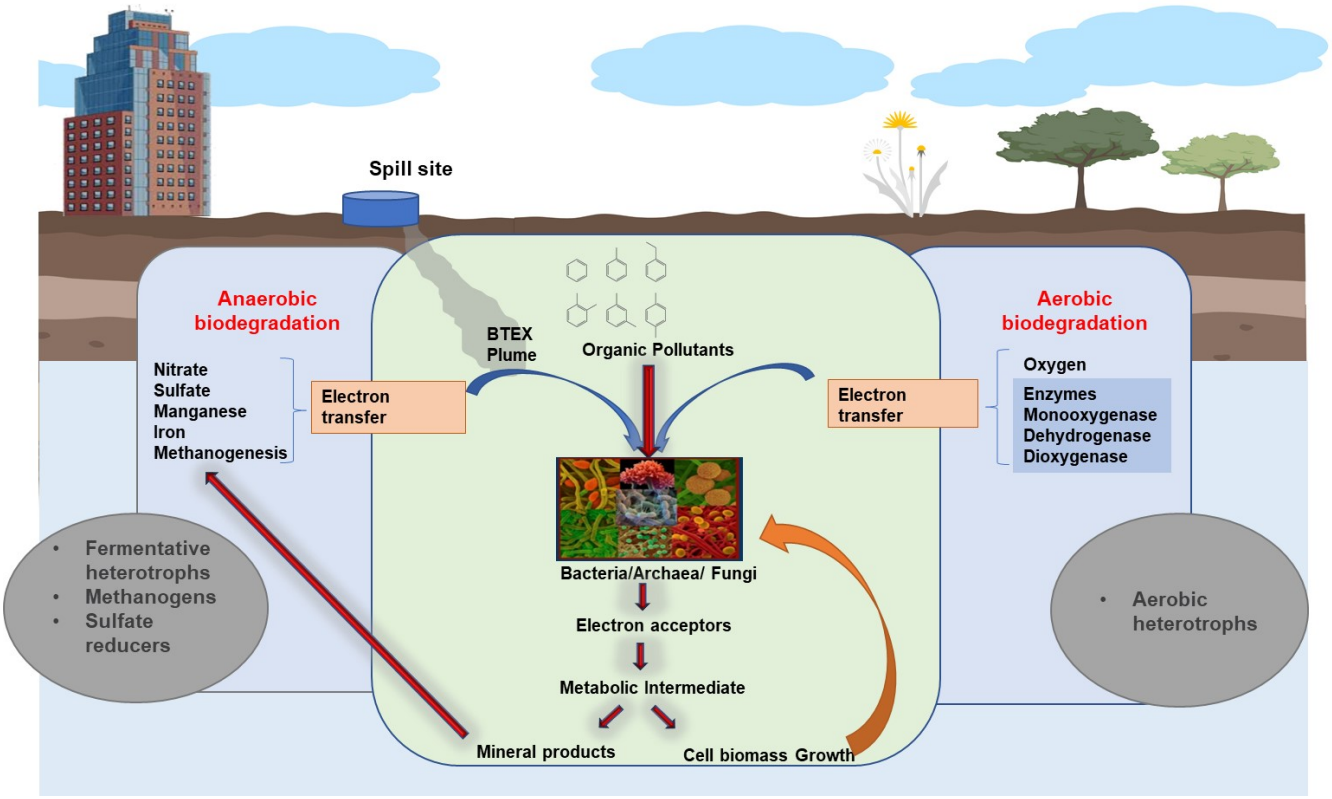

Figure 2.4: An overall representation of aerobic and anaerobic biodegradation mechanisms. In aerobic conditions, the only electron donor is oxygen which is used by aerobic heterotrophs for aerobic biodegradation respiration. The remaining degradation is performed by anaerobic pathways using non-oxygenic ions with the help of anaerobic heterotrophs. BTEX is considered a model pollutant in this study while the different phenomena of pollutant behavior discussed in this paper apply to a wide range of hydrocarbon pollutants.

The subsurface contaminant plumes exhibit a sequential and anticipated degradation process designated as the redox zonation effect. The aerobic and nitrate-reducers recruit rapidly on the leading edge of a new contamination plume, followed by manganese-reducing, iron (III)-reducing, sulfate-reducing, and finally methanogenic microbes for the biodegradation of pollutants by using them as electron donors as shown in Figure 2.5. In point source spills, an increase among the native microbes occurs because of the rapid seepage of carbon substrates, however, the metabolically flexible microbes persist even after substrate utilization (Meckenstock et al., 2015).

2.2.3 Fate and transport:

As mentioned previously, the subsurface has a diverse range of microbes with the potential to degrade several pollutants, but the bioavailability and biodegradation are influenced by the transport mechanism of pollutants as well as microbes. The pollutants found in the groundwater and soil are present in separate phases depending on the type of pollutant and subsurface conditions. These phases include the gas phase, aqueous phase, organic phase, and soil phase as shown in Figure 2.5. The pollutant partitioning affects the rate of biodegradation by the microbes, so it is important to understand how microbes behave in the subsurface and their transport mechanism. The interaction among themselves, with porous media, and their transport in the subsurface, represents a significant challenge and is an open area for continuing research.

It is hypothesized that along with microbial-driven degradation processes other transport mechanisms like volatilization, dissolution, and sorption are involved in many pollutant removal mechanisms in the subsurface as shown in Figure 2.5. The movement of microbes and contaminant depends on various physical, chemical, and biological parameters. The colloid filtration theory (CFT) and Derjaguin-Landau-Verwey-Overbeek (DLVO) theory have been widely used for the transport mechanism of colloid particles (organic pollutants, nanoparticles and microbes) (Afrooz et al., 2018; Molnar et al., 2019; Oudega et al., 2021). As the microbes lie within the size range of 1 nm to 100 nm, like colloids, these theories are useful to predict microbe transport in the subsurface and to understand fluid influence. In the subsurface, colloids and microbes can be subject to different mechanisms like aggregation, blocking, detachment, and biofilm formation, although advection and dispersion are the major key mechanisms for pollutant and microbes transport as shown in Figure 2.6 (Ginn et al., 2002; Kumar Gupta, 2020; Oudega et al., 2021). Microbes that produce extracellular polysaccharides tend to form a biofilm on porous media and are hence not transported as easily via traditional mechanisms. Biofilm formation restricts microbe movement due to attachment, which is a disadvantage from a transport perspective but can be a positive stimulator for enhanced biodegradation (Mishra et al., 2022).

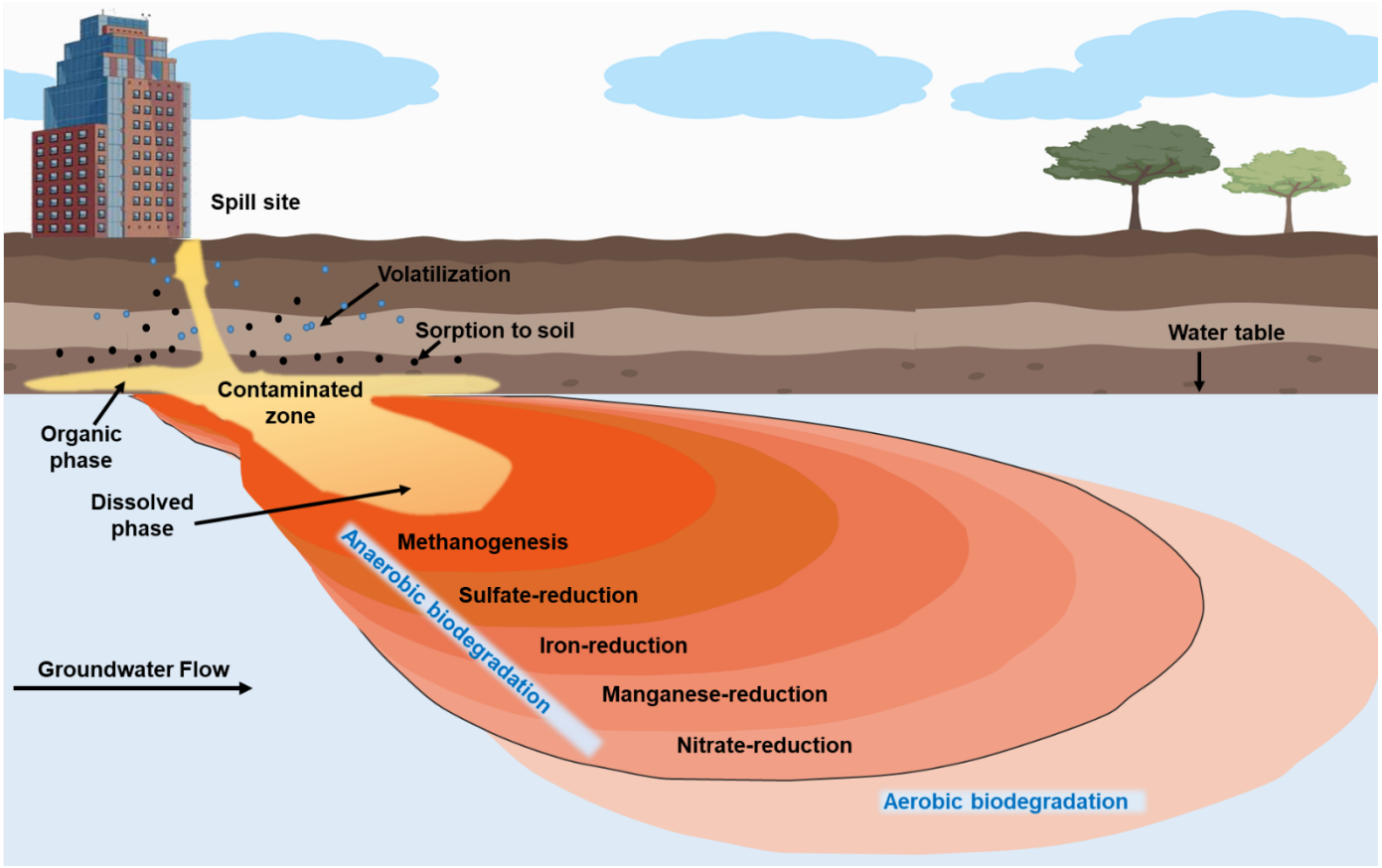

Figure 2.5: Fate of organic pollutants and resulting contaminated plume in the subsurface. This figure shows the transport of pollutants through the porous media, where pollutants separate into four different phases: gas phase (volatilization), solid phase (sorption), aqueous phase (dissolution), and organic phase (undissolved phase). The dissolved contaminated plume is degraded by different mechanisms using different electron donors by microbes in a sequential process. Blue and black dots represent the gas and solid BTEX phases, respectively.

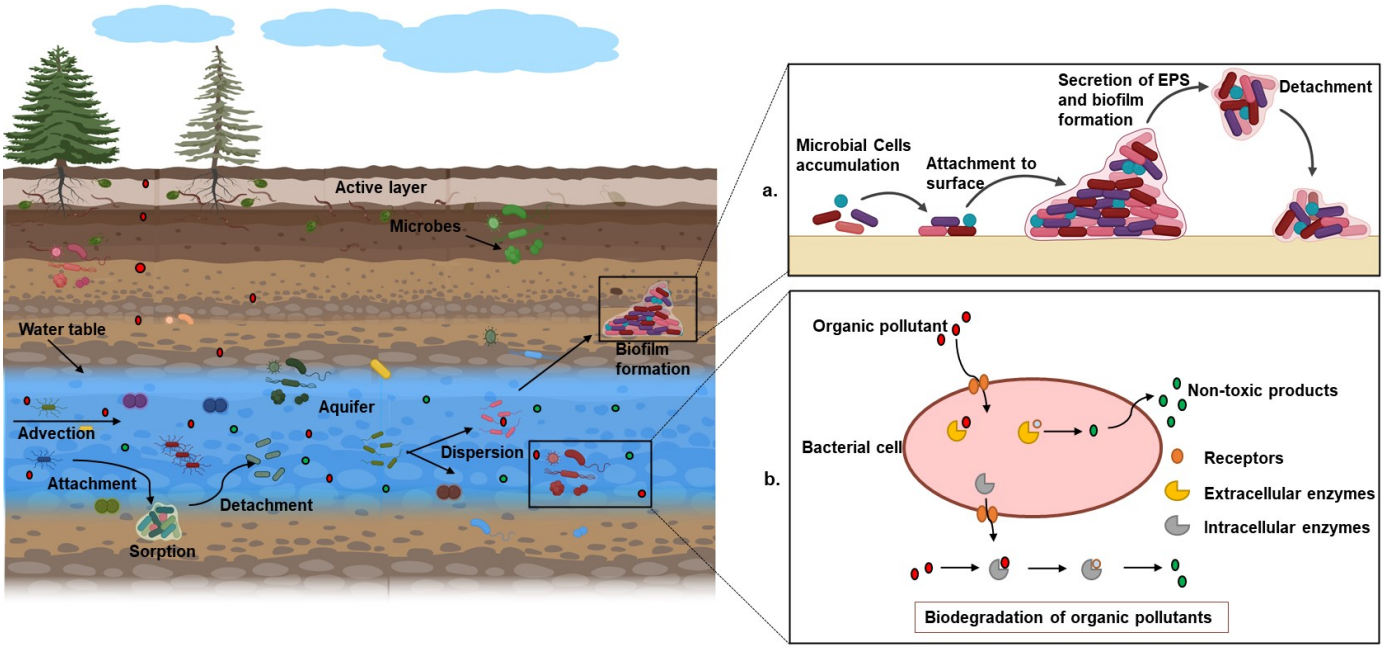

Figure 2.6: Different transport mechanisms (advection, dispersion, sorption) of microbes in the subsurface. This figure shows the fate and transport routes of microbes as well as pollutants in the subsurface. Part a describes the process for biofilm formation on the soil particle - microbes secrete extracellular polysaccharides (EPS) that help microbes to form biofilms, and part b highlights the intracellular and extracellular degradation of pollutants, where toxic pollutant molecules are degraded to non-toxic products through a series of chemical reactions catalyzed by specific enzymes in different metabolic pathways of the microbes.

Lastly, exploring the native microorganisms of the subsurface by metagenomics and metabolic profiling is helpful to understand the actual abundance of different species at a particular site and the interaction among different species respectively, which in turn help to design a proper remediation approach and to estimate approximate removal time for a contaminated site (Kadnikov et al., 2020; Z. Zhou et al., 2022). The background knowledge of microbes helps to design specific approaches for enhanced ISB. For example, while applying extrinsic microbes to a contaminant site for bioaugmentation, understanding intrinsic microbes is important to eliminate the chances of competitive inhibition between intrinsic and extrinsic microbes (Tyagi et al., 2011).

Likewise, biostimulation can be performed depending on the growth requirement of native microbes for specific nutrients and other physiological factors for their optimized growth such as temperature (Tyagi et al., 2011). Furthermore, genetic engineering approaches for enhanced bioremediation can only be implemented if we have the microbial profiling knowledge of the contaminated site, to minimize the chances of resistant microbes and other environmental issues (Hollander, 2018).

To conclude, microbes are a versatile part of the subsurface, helping to maintain regular biogeochemical processes that transfer essential elements, thereby ensuring the continuity of the ecosystem. Likewise, their unique properties to thrive in unfavourable subsurface conditions, adapt to such conditions, and be able to consume pollutants make microbes a powerful tool to remediate polluted sites. It has been demonstrated that microbial communities can thrive in both aerobic and anaerobic conditions, and their metabolic pathways depend on the electron acceptors available. Transport behaviour and degradation kinetics-based experiments also demonstrate the complexity of biodegradation, as surrounding physicochemical parameters play a crucial role in their movement and degradation pattern. Hence, the interactions among microbes, with pollutants, as well as the effects of physicochemical parameters, are a significant topic of research that influences the mechanisms of microbial metabolism. By understanding these mechanisms, bioremediation can be enhanced, and subsurface pollution can be remediated sustainably. Hence, in this research, temperature is considered an important parameter for microbial growth, pollutant transport behaviour, and biodegradation, and the influence of temperature changes has been studied using BTEX as a model pollutant.

2.3 Thermally enhanced bioremediation

Bioremediation relies on native microbes to convert environmental contaminants into less toxic forms via a cascade of biochemical conversions (Carberry & Wik, 2001; Kensa, 2011). ISB can help treat brownfield sites, and is considered to be economical, but requires a remediation strategy specific to the subsurface environment. The process of bioremediation depends on various environmental conditions that could affect microbial growth and activity, and the application often involves the manipulation of these parameters to allow microbial growth and encourage contaminant degradation. Various parameters like waste composition, native

microbial consortium, soil type, water content, pollutant interactions, adsorption kinetics, degradation kinetics, as well as subsurface temperature regulate bioremediation (Boopathy, 2000; National Research Council, 1993). The occurrence of various pollutants in the subsurface can complicate adsorption behavior, as well as biological processes. These interactions between compounds can be a concern for soil remediation as it can result in conversion of chemicals or a change their physicochemical property, such as bioavailability to living organisms, solubility, and binding status (Ye et al., 2017; Yong, 2000).

Therefore, before approving ISB at a contaminated site, the EPA requests that important environmental factors like pH, soil moisture, oxygen, contaminant concentration, and redox potential fall within a certain approved range (Moradi et al., 2018).

Along with other parameters, temperature is a crucial factor for microbial growth which influences the rate of biodegradation. Increasing temperature up to mesophilic and thermophilic range (20 – 60 °C) could generally enhance the biodegradation rates of hydrocarbons (Koshlaf & Ball, 2017; Song et al., 1990; Walworth et al., 2001; Westlake et al., 2011; Yuniati, 2018), but this method is typically not considered to be energy and cost-effective because the heat is obtained from conventional sources like the burning of fossil fuels, which ultimately leads to an increase in cost and pollution. In addition, such conventional technologies can be limited or often not feasible or practical for remote areas (Miri et al., 2019).

Most studies show a positive effect of temperature, although the heat is supplied through conventional methods rather than geothermal heat. Therefore, it is hypothesized that the heat from GHPs could also be a positive stimulator for bioremediation with the added benefit of having the heating energy come from a sustainable source. Several studies have examined the combination of geothermal energy and bioremediation and concluded that geothermal heating had a positive effect on microbial activity and on the degradation rate of pollutants (Attard et al., 2020; Garnier et al., 2011; Iqbal et al., 2007; Ni et al., 2015, 2020; Moradi et al., 2018; Sommer, 2013, 2015). This section discusses various studies done on how heat can influence bioremediation and the possible role GHPs can play in polluted sites.

2.4 Geothermal heat pumps

The gap between energy consumption and production is growing, so renewable energy resources are gaining attention to attain sustainable development (Moradi et al., 2018). In addition, global warming and environmental pollution are major challenges faced globally. One way to address both concerns is to use renewable energy sources such as low-grade shallow geothermal energy as energy sources for remediation. As building heating and cooling loads represents about 40% of the world's energy (Casasso & Sethi, 2019), using geothermal heating can reduce the demand for fossil fuels (Garrido Schneider et al., 2016; Nejat et al., 2015; Ni et al., 2020). Several studies have shown that in comparison to conventional energy resources, geothermal heat pumps (GHPs) can achieve 40 − 70% energy savings and can reduce carbon dioxide emissions by 40 – 60% worldwide (Curtis et al., 2005; Fleuchaus et al., 2018; Hoekstra et al., 2020; Pellegrini et al., 2019). The following section reviews the various types of heat pumps available to assess which system may be more suitable for Geothermal remediation.

GHPs, also known as ground-source heat pumps (GSHP), use the subsurface to inject and extract energy, otherwise known as an energy sink and source, respectively. The temperature of the subsurface is constant throughout the year because the seasonal temperature variations of the atmosphere only affect the upper few meters of the subsurface. This affected zone is termed as "zone of seasonal fluctuations" (Banks, 2012) or "neutral zone" (Majorowicz et al., 2009). This is because the thermal conductivity of soil and rocks is modest and therefore solar radiation penetrates to a limited distance. The zone of seasonal fluctuation in Canada is reported to be around 20 m below the ground surface (Majorowicz et al., 2009).

Below this zone of seasonal fluctuations, the temperature of the subsurface is reported to be constant and is approximately equal to the mean annual surface temperature (Banks, 2012). This means that the subsurface temperature is lower than the summer atmospheric temperature and higher than the ambient winter temperature as shown in Figure 2.7. The subsurface has a modest thermal conductivity and high thermal storage capacity (Banks, 2012; Raymond & Therrien, 2014). These properties are useful for GHP systems where the subsurface acts as a sink in the summer and allows for thermal extraction in winter (Banks, 2012).

However, at some point, the geothermal gradient of the earth influences the subsurface temperature therefore a GHP system has to be placed below the zone of seasonal fluctuation

and above the geothermal gradient effect (Banks, 2012; Bryś et al., 2020). The geothermal gradient is defined as a gradual increase of temperature from the interior of the earth (Arndt, 2011). In southern Canada, the geothermal gradient is measured to be as 0.01 °C m^{-1} at 50 – 100 m depth, 0.012 °C m^{-1} at 100 – 150 m, 0.014 °C m^{-1} at 150 – 200 m and 0.016 °C m^{-1} at 200 – 250 m depth (Majorowicz et al. 2009; Banks, 2012). Given this, typically vertical GHPs are located up to a depth of around 50-200 m below ground surface (Casasso & Sethi, 2019), where, depending on latitude, ground temperatures range from 7 °C (45 °F) to 21 °C (75 °F) (Wolf, 1982). GHPs take advantage of this constant temperature by exchanging heat with the earth through a borehole heat exchanger (K. S. Lee, 2010; Sagia et al., 2012).

The efficiency of GHPs is evaluated using the coefficient of performance (COP). The COP is the ratio of heat delivered or heat injected (H) to the amount of electricity consumed (E).

$$COP = H/E \qquad (2.1)$$

In general terms, for an ideal heat pump, the COP value should be between 3 and 4 (Banks, 2012). For Canada, the heating COP of GHPs with less than 35 kW power capacity must have a minimum value of 3. The reduction of greenhouse gas emissions with heat pumps depends on the COP and GHG emission factors of the electrical grid (Ni et al., 2020).

GHPs installations are entirely borehole-based systems, however, engineers and developers are looking at ways to integrate GHPs within building foundations, as a means for providing heating and cooling to buildings. For example, geothermal piles, (otherwise called energy geostructures, energy foundations or thermo-active ground structures) (Bourne-Webb et al., 2016; Laloui & Loria, 2019) are gaining interest because they use existing structures such as pile foundations that support the structure, and combine it with GHP technology which can reduce the overall building costs (Brandl, 2006; Laloui & Loria, 2019).

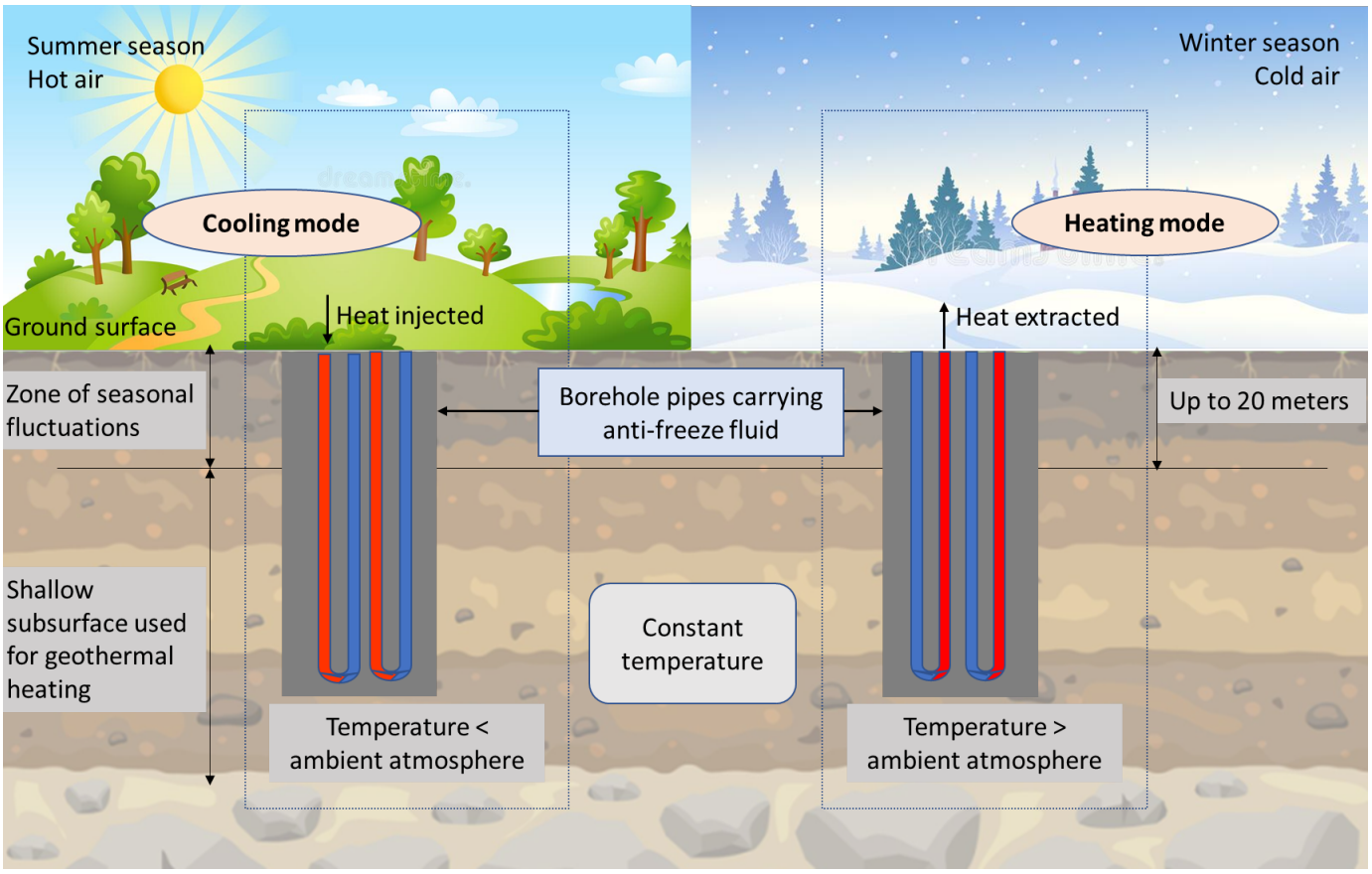

Figure 2.7: How do GHPs work.

2.4.1 GHP types

Heat pumps are categorized into two main types: air-source (80.1%) and ground-source (16.4%) according to the European heat pump association (Casasso & Sethi, 2019). Air-source heat pumps are more often used due to simple and cheaper installations, while GHPs require underground pipes and ground heat exchangers or wells. However, GHPs have a higher COP and lower noise pollution compared to air-source pumps, making them more convenient and efficient (Caird et al., 2012). A geothermal cooling and heating system which capitalizes on constant temperature, consists of three main components: the heat-pump unit, the liquid heat-exchange medium, and the air-delivery system (Al-Khoury et al., 2005; Steiger & Kees, 1981). Ground source or geothermal heat pumps are further divided into two sub-categories as shown in Figure 2.8 and described in the following subsection.

2.4.1.1 Closed-loop systems

These systems exchange heat with the ground through the circulation of a heat carrier fluid that flows within a closed-loop pipe. These are also known as ground source heat pumps or earth-coupled heat pumps. The pipes that make up an earth loop are usually made of polyethylene and can be buried under the ground horizontally or vertically, depending on the characteristics of the site. Closed-loop systems can be installed in three configurations: shallow horizontal heat exchanger, in which horizontal pipes are installed at very small depths; vertical boreholes or borehole heat exchangers (BHEs), which are installed having a depth range of 50 – 200 m and diameter of 15 – 20 cm; and a closed pond loop system where the pipes are put into a pond (Casasso et al., 2020; Casasso & Sethi, 2019). If the geology allows, borehole thermal energy storage (BTES) units can be used. BTES uses the ground to store the energy which can be later extracted to heat buildings. BTES differ from GHPs since GHPs don't rely on the storage of heat but rather assume that the heat will be dissipated with time (Earth Energy Systems in Ontario | Ontario.Ca, 2013).

2.4.1.2 Open-loop systems

In open-loop systems, a well is drilled into an aquifer and water is directly exchanged. Water is pumped out through an extraction well and then the water is returned to the same aquifer, through reinjection (Al-Khoury et al., 2005). These are commonly known as groundwater heat pumps (GWHPs) and aquifer thermal energy storage (ATES) systems. Similar to BTES, ATES differ from GWHPs since they rely on the storage of heat (Earth Energy Systems in Ontario | Ontario.Ca, 2013).

The feasibility of GWHPs relies on the groundwater chemistry including the degree of hardness, mineralization, which can cause clogging or corrosion of the heat exchanger. Some suggest that in the case of soft water with low minerals, heat pumps could be operated directly but in the case of hard water, the use of an intermediate heat exchanger is suggested to simplify maintenance (Banks, 2012; Rafferty, 2004).

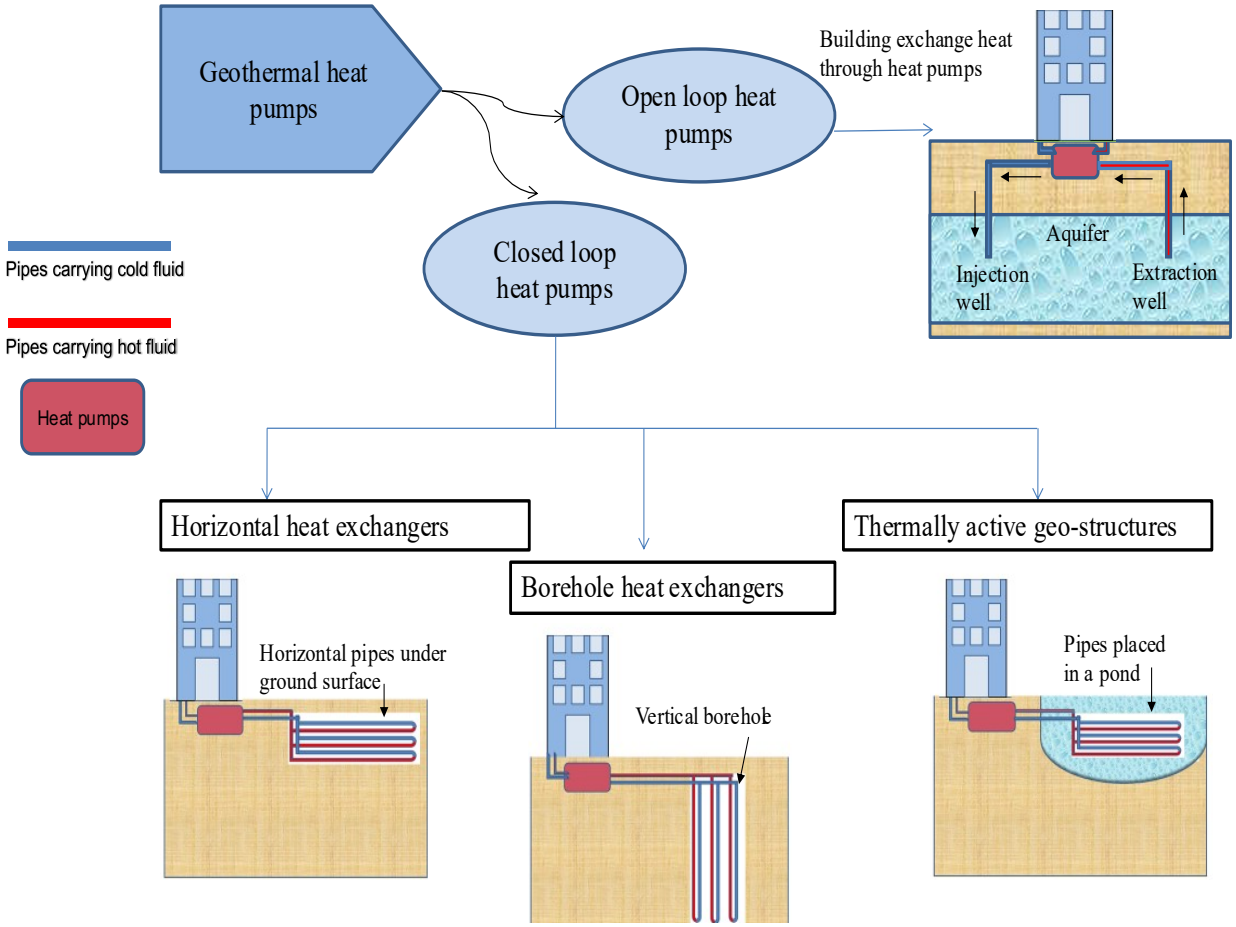

Figure 2.8: Different types of geothermal heat pumps.

2.4.2 Environmental impacts of GHP

Over the years, GHP installations have become more popular because of their low heating cost and low greenhouse gas emission compared to fossil fuels (Ni et al., 2020). Furthermore, several governments are encouraging their citizens to conserve energy and to make infrastructures more energy efficient. An example of this is the LEED program in Canada. This encourages the use of green energy technologies such as GHPs in large building designs. Although overall positive, the large-scale use of GHPs worldwide can lead to various environmental impacts on its surroundings.

Although not common, some negative environmental impacts can occur during the installation and working of closed-loop BHEs. For example, pipe leakage from BHEs can lead to anti-freeze such as propylene glycol release into the subsurface and result in well contamination; similarly defective borehole filling can cause distribution of contaminants from one aquifer to another (Casasso & Sethi, 2019).

A more likely impact is the alteration of subsurface temperatures resulting from the propagation of thermal plumes from the long-term or unbalanced operation of GHPs, which could raise the temperature of subsurface up to 70 °C (Jesußek et al., 2013). Thermal plumes may affect the performance of GHPs, especially GSHPs which rely on the dissipation of subsurface temperatures (Casasso & Sethi, 2015). The literature on thermal alteration and its effects on the surrounding subsurface has been reported in large numbers (Barla et al., 2018; Beyer et al., 2016; García-Gil et al., 2016; Herbert et al., 2013; Moradi et al., 2018; Piga et al., 2017; Pophillat et al., 2020).

The temperature change induced by GHPs could affect groundwater flow due to the changes in water viscosity and density. For instance, the formation of density-driven flows might change the direction of groundwater flow if thermal plumes reach high enough temperatures (Bonte et al., 2011; Daemi & Krol, 2019; Griebler et al., 2016; Krol, Mumford, et al., 2011; Krol et al., 2014). The altered subsurface temperature could also impact the transport of contaminants and reaction kinetics (Beyer et al., 2016; Sleep & McClure, 2001a; Zuurbier et al., 2013).

For open-loop systems, the re-injection of water into the same aquifer can change the groundwater flow pattern up to a distance of several kilometers (Bonte et al., 2013). The groundwater chemistry can also change due to the mixing of different groundwater types, which might result in well clogging due to mineral precipitation at higher temperatures (Bonte et al., 2013).

Considering the possible impacts and conflicts associated with GHPs, some European countries have issued regulations restricting the use of GHPs in various areas and specifying operating temperature, the minimum distance between adjacent pumps and the size of thermal plumes to minimize environmental impacts (Casasso & Sethi, 2015, 2019).

2.4.3 Modelling of GHPs

To evaluate the effects of a GHP system on the subsurface, to optimize its performance, and limit its environmental impacts, computer modelling is often used. A comprehensive literature review on existing simulation models of GHP systems has been done by Beyer et al. (2016); Carotenuto et al. (2016); and Piga et al. (2017). These modelling methods can be categorized into two main types of analytical methods and numerical modelling. Analytical methods have simple physical meanings and are easy to understand and apply (Lee, 2010), but are incapable of modeling complicated geometries and boundary conditions. On the other hand, numerical models are used for many field applications of GHP systems. They are also used to address the potential interference between adjacent GWHP systems and their environmental impacts in urban areas (Barla et al., 2018; Bonte et al., 2011; Herbert et al., 2013; Moradi et al., 2018; Pophillat et al., 2020). Analytical or numerical models can be further categorized into two groups that simulate either heat conduction outside the borehole or heat transfer inside the borehole.

Various models have been used to evaluate the thermal load of GHPs and temperature distribution in the field including FEFLOW (Daemi and Krol, 2019; Dehkordi & Schincariol, 2014), GEMS3D (Luo et al., 2019; Naicker & Rees, 2010; Rees & He, 2013) MODFLOW (Alberti et al., 2012; Casasso & Sethi, 2015), COMSOL (Gultekin et al., 2016; Lazzari et al., 2010; Sagia et al., 2012) and GLHEPRO (Hong et al., 2019; Staiti & Angelotti, 2015). Computer simulations are a good way to optimize design, examine the effect of various parameters and evaluate the impacts of GHP operation on the environment. The detailed discussion about the key finding of these modelling studies with context to biodegradation has been explained in section 2.6.1 and 2.6.2.

2.5 Influence of thermal energy on bioremediation

The basic principles of “Geothermal remediation”, also regarded as “bio-thermo-remediation” and “thermal enhancement” (Garnier et al., 2011), relies on higher temperatures to effect degradation kinetics as well as contaminant transport properties such as advection, diffusion and sorption as described in Table 2.2 (Krol et al., 2011, 2014; Beyer et al., 2016; Dehkordi et al., 2014; Diao et al., 2004; Sleep and McClure., 2001). As shown in Figure 2.10, temperature plays a crucial role in facilitating biodegradation due to the temperature preference of microorganisms for proliferation, so the elevated temperature also helps to stimulate the activity

of mesophilic and thermophilic microorganism (Iqbal et al., 2007; Hubert et al., 2009) and have great potential towards ISB (Perfumo et al., 2007; Castro et al., 2019; Freedman et al., 2012). A brief comparison between the role of thermophiles and mesophiles in the biodegradation of the major pollutants is given in section 2.7.

Temperature, in general, is an important factor for living cells. Low temperature can cause severe damage to the cellular function of microbes through the disintegration of cell structure, solidifying membrane fluidity, disruption of macromolecular interactions (Wang et al., 2017; Welander, 2005), and thereby affecting solute diffusion rates and enzyme kinetics. While very high temperatures are just as disruptive to some organisms due to a decrease in moisture content of soil (Alster et al., 2020; Hallsworth, 2018). In addition, heated subsurface temperatures have been shown to double microbial growth rate for every increase of 10 °C according to the Q10 rule stated by Van't Hoff (1884). Similarly, storage of high-temperature water (>25 °C) and/or net heating of the subsurface could further increase degradation rates (Moradi et al., 2018). For contaminated sites, this could be quite beneficial. For example, a study by Sanscartier et al. (2009) showed that bioremediation of petroleum hydrocarbon contaminated soil was enhanced by raising the temperature only 5 °C, using a heated and humidified biopile system. Three biopiles, constructed with an initial concentration of PHC, 11,000 mg/kg dry weight of soil, significantly reduced to 300 mg/kg dry weight after 10 months of operation in Kingston, Canada (Sanscartier, et al., 2009). Similarly, Perfumo et al. (2007) showed that an increase in temperature and the existence of thermophilic and mesophilic bacteria remarkably accelerated the rate of degradation of hexadecane-contaminated soil. In this experimental work, the hexadecane polluted soil microcosms were augmented with nutrients like nitrogen, phosphorus and potassium, thermophile *Geobacillus thermoleovorans* and biosurfactant rhamnolipid, leading to the removal of 42% hexadecane at 18 °C and up to 90% at 60 °C (Perfumo et al., 2007).

Most microorganisms have a specific temperature range for optimum growth and degradation activity (Moradi et al., 2018). Psychrophilic microorganisms exist and proliferate below 15 °C, mesophilic bacteria survive at the temperature range of 15 °C to 45 °C whereas thermophilic bacteria thrive at high temperatures, ranging from 45 °C to 75 °C. It has been claimed that psychrophile microorganisms can perform hydrocarbon biodegradation even at a temperature

as low as -6 °C. However, the rate of degradation is not comparable to mesophilic and thermophilic microorganisms. The rate constants for BTEX biodegradation at some cold sites in Alberta, Canada, are in the range of 0.001 to 0.005 per day, and the half-life of BTEX components is estimated at 1 to 2 years, while the values of rate constants at warmer sites in the United States are higher (Van Stempvoort & Biggar, 2008). Research into mesophilic and thermophilic bacteria comes from wastewater engineering and environmental microbiology, where both of these microorganisms are used to degrade organic wastes at temperatures ranges from 20 °C to 60 °C (Alisawi, 2020; Duncan et al., 2017; Fang et al., 2006).

Table 2.2: Effect of temperature on different bioremediation parameters

Parameter studied	**Temperature range**	**Sediment type**	**Influence on studied parameter**	**Reference**
Respiration rate and bacterial activity	0 – 45 °C	Agricultural and humus soil	Respiration rate increased for whole temperature range Bacterial activity increased up to 30 °C	(Pietikäinen et al., 2005)
Respiration rate	5 – 50 °C	Soil from cold-temperate, mid-temperate, warm-temperate, subtropical, and tropical forests	Increased for all soil types with optimum temperature range of 38.5 to 46.0 °C	(Y. Liu et al., 2018)
Heterotrophic respiration rates and microbial metabolic activity	-2 – 40 °C	Soil from tundra, boreal forest, temperate forest, temperate grassland, and tropical forest soils	Microbial activity and respiration rate increased over the whole range of temperature for all soil types	(Johnston & Sibly, 2018)
Cadmium desorption	20 – 7 °C	Goethite	Decreased from 71% to 31% when temperature increased from 20 to 70 °C	(Mustafa et al., 2006)
Sorption of hydrophobic organic compounds	0.5 – 40 °C	Activated Carbon	With an increase of 40 °C temperature, sorption rate decreased by 10%	(Pikaar et al., 2006)

Dissolution of immobile DNAPL, * biodegradation kinetics, and desorption from soil micropores	15 – 40 °C	Aquifer sediments	94% overall reduction of DNAPL in effluent at 35 °C Biodegradation rate also increased but at lower initial biomass concentration	(Kosegi et al., 2000)
Sorption of toluene, perchloroethylene, and naphthalene	22 – 92 °C	Silty gravel-till aquifer material	Decrease in sorption coefficients for all compounds when temperature increased from 22 – 92 °C	(Sleep & McClure, 2001)
Mineral dissolution, precipitation, and microbial redox processes	10 – 70 °C	Aquifer sediment and tap water	Redox process shifted from nitrate and iron (III) reducing conditions at 25 and 40 °C to sulphate reducing conditions at 70 °C. Organic carbon release at three times higher rate from the sediment at 70 °C	(Jesußek et al., 2013)

DNAPL*- Dense non aqueous phase liquid

The rate of contaminant decomposition during bioremediation relies on contaminant uptake, metabolism, and the rate of mass transfer to the cell (Boopathy, 2000). The relationship between temperature and microbial activity is usually investigated by measuring soil respiration rates (Pietikäinen et al., 2005), such as the study by Liu et al. (2018), shown in Figure 2.9. Carbon dioxide is an indicator of microbial respiration, so the amount of carbon dioxide in unsaturated soil systems is strongly linked to microbial activity and seasonal fluctuations in temperature (Hendry et al., 1999). It has been reported that the highest and lowest concentration of soil

carbon dioxide is observed during summer months and winter months respectively, indicating that temperature stimulates microbial activity. Likewise, carbon dioxide concentrations typically decrease with depth in the summer and increase in the winter, due to shallow vertical temperature profiles (Hendry et al., 1999). Therefore, artificially heating the soil and groundwater could improve the efficiency of bioremediation in comparison to natural attenuation. Previous studies confirmed the effect of temperature on microbial respiration, while Lin et al. (2017) went further and concluded that elevated soil temperature results in increased soil respiration as well as carbon and nitrogen consumption. The experiments included soil samples that were incubated at 15, 20 and 35 °C, and the bacterial community was examined by soil analysis and pyrosequencing.

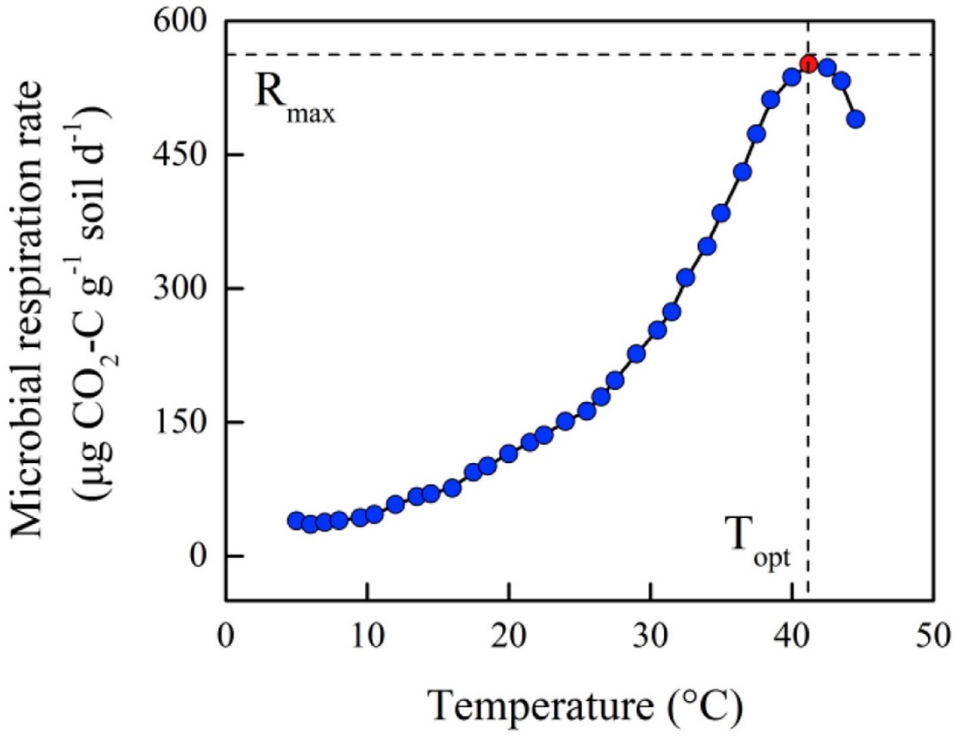

Figure 2.9: Relation between temperature and microbial growth in soil (Taken from Liu et al., 2018 with copyright permission obtained from Elsevier).

Temperature also affects the adsorption/desorption process which further influences the bioavailability of pollutants to the microorganisms. Contaminants adsorbed onto the soil or aquifer organic matter will be less bioavailable for biodegradation (Si-Zhong et al., 2009). However, adsorption of organic compounds decreases with rising temperature, making the

pollutants more bioavailable (Iqbal, 2003). Sleep & McClure (2001) studied the effect of temperature on the adsorption of some organic contaminants onto soil by a series of column experiments. They concluded that sorption coefficients for toluene, perchloroethylene (PCE) and naphthalene concentrations reduced by 35%, 40% and 60% respectively, with increased temperature from 22 to 92 °C. Ngueleu et al. (2018) also found that the sorption coefficient for benzene and naphthalene decreased with increasing temperature.

Andrade et al. investigated the potential of thermally enhanced bioremediation in naphthalene-contaminated soil at various temperatures (28, 38, 48, and 58 °C). The study analyzed microbial activity, biomass, metabolic quotient, bacterial count, and phytotoxicity in lettuce seeds at 0, 15, and 30 days of contamination. The temperature range of 28 to 38 °C stimulated microbial growth, regardless of naphthalene concentration, indicating that temperatures below 40 °C are promising for thermal bioremediation applications (Andrade et al., 2025).

Furthermore, along with enhancing microbial activity and decreasing sorption rates, elevated temperatures can also affect the contaminant transport properties. Raised temperatures lead to a decrease in contaminant viscosity, increases its solubility and diffusivity, which can favor ISB (Garnier et al., 2011). A study by (Kosegi et al., 2000) demonstrated using a mathematical model that an increase in temperature from 15 °C to 35 °C at a DNAPL (dense non-aqueous phase liquid) contaminated site could reduce effluent concentrations by 94% and in comparison to ambient conditions, thermally enhanced bioremediation can reduce clean-up time by 70%.

In the case of GHPs, temperature increase in the subsurface can be measured by using thermocouples installed in the field which record the inlet and outlet borehole temperature by converting the thermal energy into electrical energy (Cimmino & Bernier, 2015; Hepbasli & Akdemir, 2004; Yu et al., 2020) and distributed temperature sensing (DTS) with fiber optic cable can also use in some cases to monitor the subsurface temperature of subsurface (Sommer et al., 2014; Vogt et al., 2010). Alternatively, numerical models can be used to interpolate or predict subsurface temperatures, as explained in section 2.4.3. The heat transfer rate depends on the thermal load of the building, as well as the subsurface parameters such as soil density, porosity, thermal conductivity, groundwater velocity, and specific heat capacity of the subsurface. As expected, higher building thermal loads can result in bigger thermal plumes (Daemi & Krol, 2019; Gultekin et al., 2016).

However, it should be noted that an increase in temperature could also have some negative impacts on contaminated sites. In particular, it can lead to a decrease in viscosity and increase in diffusion which can lead to increased contaminant transport. This can be particularly concerning if the groundwater velocities are high (Krol et al., 2011, 2014; Beyer et al., 2016; Casasso & Sethi, 2019; Sleep & McClure, 2001b, 2001a). Therefore, the application of temperature-stimulated ISB has to be at sites where the site is well characterized, and the source of the contaminant is finite (Roohidehkordi & Krol, 2021a).

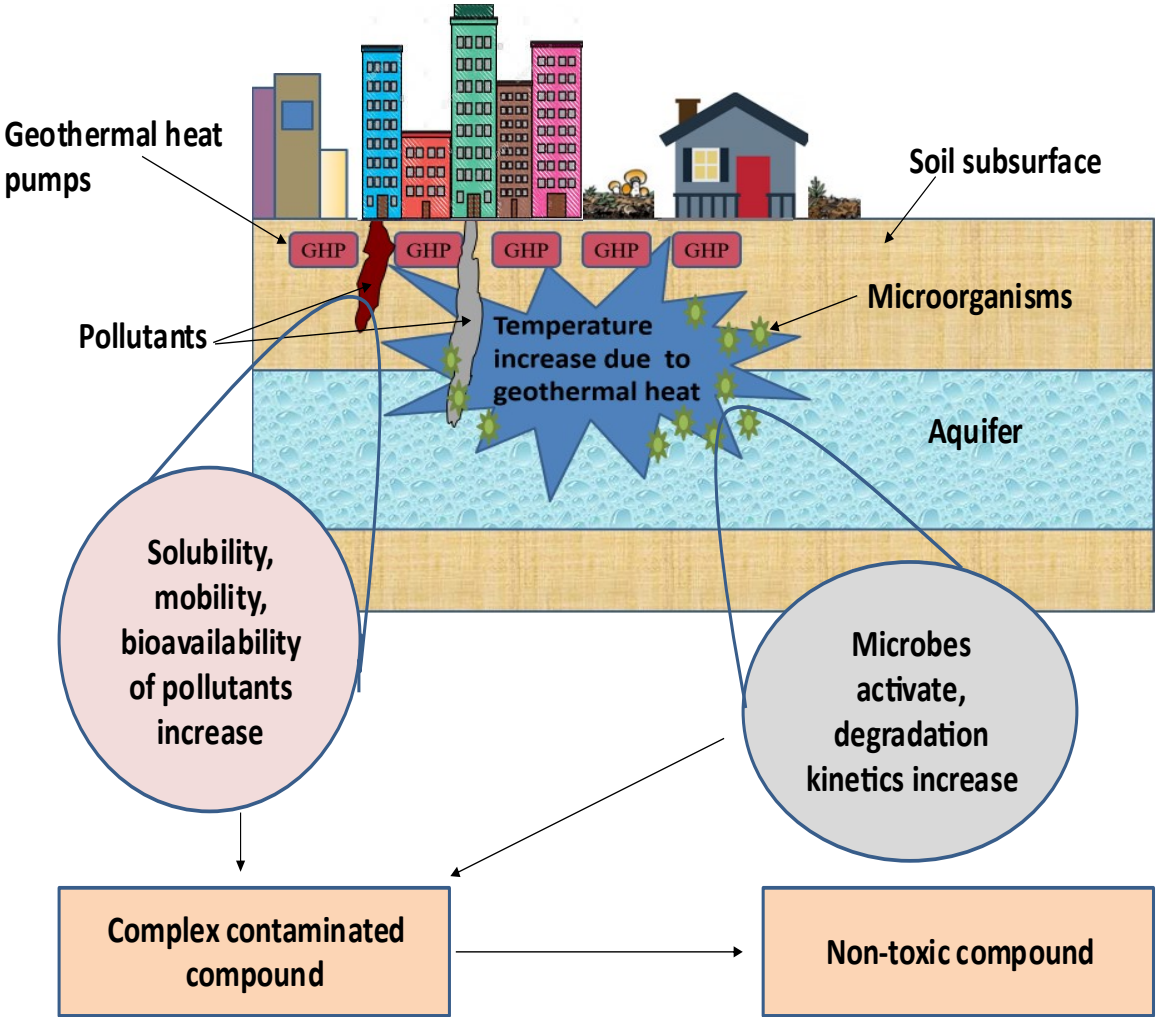

Figure 2.10: Factors responsible for Geothermal bioremediation.

2.6 Role of GHPs in bioremediation

The use of renewable energy like wind, solar, or geothermal energy has been proposed to provide heat for thermally enhanced bioremediation systems as a cost-effective remediation method (Rossman et al., 2006). Although solar and wind energy is found in abundance, these energy sources are not available throughout the year especially in northern countries where solar energy may be unavailable in the winter (Boyle, 2004; K. Li et al., 2015). However, geothermal energy is applicable anywhere depending on the type of installation and building thermal load. In particular, GHPs and geostructures could be used in urban settings, such as brownfield sites.

Reuse and redevelopment of brownfield sites is an efficient way of utilizing existing infrastructures to promote sustainable urban development. However, any potential health risk needs to be addressed since brownfields are contaminated with different compounds including petroleum products. Since these contaminants are susceptible to thermal treatment, employment of GHPs at these sites might be a promising way to help in the cleanup of such areas while using renewable energy to heat and cool buildings, as shown by (Garnier et al., 2011; Moradi et al., 2018; Ni et al., 2016, 2020; Roohidehkordi & Krol, 2021a; Sommer, 2015). Garnier et al. (2011) has reviewed the importance of geothermal heating in bioremediation and suggest that it has potential to degrade organic pollutants up to 90% such as VOCs, volatile organo-halogenated compounds, and some dicyclic aromatic hydrocarbons which are among the priority pollutants. This study also concluded that the increase in aquifer temperature during Geothermal remediation assists in the reduction of treatment time, energy consumption, treatment cost and groundwater quality. Numerous laboratory-scale experiments were conducted using columns packed with aquifer sediments at different operating temperatures to study the impact of temperature alteration on water quality during GHP operation, and no major negative effects were observed under normal operating temperatures (Bonte et al., 2011; García-Gil et al., 2016; Garrido Schneider et al., 2016; Griebler & Lueders, 2009b). However, field and modelling studies have shown that some disadvantages do exist depending on the type of installation and environmental conditions.

2.6.1 Impact of open-loop pumps on bioremediation

In open-loop heat pumps, the water injected back into the aquifer has different temperatures and sometimes characterises, than the ambient groundwater. Typically, the injected water

temperature is higher in the summer and lower in winter and this temperature change may influence the aquifer's environment and consequently, the associated ecosystems.

Monitoring of the first ATES system and contaminated groundwater bioremediation combination (known as Sanergy) in the Netherland shows that the biological activity had significantly improved. The concentration of *Dehalococcoides ethenogenes* (a mesophilic dechlorinating bacteria) increased 1,000 fold and an enzyme VC-reductase increased to 100 - 1,000 fold (Sommer, 2015; Sommer et al., 2013). This indicates that biological performance in terms of decontamination was improved. Additionally, results of carbon isotope analysis showed that the contaminant concentration of chlorinated hydrocarbons (CHC) and vinyl chloride (VC) reduced significantly (Sommer et al., 2013). The analysis of geochemical parameters of ATES also showed significant change in pH, electrical conductivity, redox potential, and groundwater concentrations of ions and metals such as nickel, chromium and copper due to circulating waters (Choi et al., 2020; Park et al., 2015; Sommer et al., 2013).

A study by Ni et al. (2020) investigated the impact of ATES system on groundwater contaminated with CVOCs for the sustainable re-development of urban brownfield sites. A comparison study between the combined ATES−ISB and individual conventional heating and cooling method plus ISB (CHC+ISB) was done by using the Life Cycle Assessment (LCA) model. The observation of the study shows that ATES−ISB causes smaller environmental impacts in contrast to CHC+ISB. For instance, CHC+ISB used twice as much water and energy while emitting CO_2, SO_2, $PM_{2.5}$ at double the rate than that of the ATES−ISB system; CHC +ISB also led to 40% more eutrophication effect with consumption of 30% more natural abiotic resources (Ni et al., 2020). The performance of ATES-ISB and CHC+ISB was analyzed for 30 years, where ATES was continuously fed with a biological medium containing sodium lactate and dechlorinating bacteria by reductive dechlorination. The authors concluded that the amount of CVOCs removed by ATES-ISB in 30 years, would be removed by bioremediation alone (CHC+ISB) in 390 years. However, the amount of energy produced by ATES in 30 years was the same as of the CHC. From such observations, it can be concluded that ATES outperforms ISB and does not affect the working efficiency of ATES heat pumps.

A study by Garnier et al. (2011) on Geothermal remediation at a site contaminated with polyaromatic hydrocarbons PAH, volatile aromatic compounds (VAC), volatile organic

hydrocarbons (VOHC) and hydrocarbon oil, also showed that the rate of the microbial activity was enhanced due to ATES operation. The microbial activity was observed by two approaches: the *Dehydrogenase* activity approach and the carbon source utilization profile at a laboratory scale. The results concluded that with an increase in temperature, both the activity of enzyme *Dehydrogenase* and carbon utilization rate were increased. In this field study, more than 80% of organic compounds degraded over the 5 year period (Garnier et al., 2011).

Some studies revealed that alteration of subsurface temperatures during ATES operation affected the groundwater quality, microbial consortium and mineral desorption (Bonte et al., 2011; Griebler et al., 2016; Jesußek et al., 2013). In the Netherlands, Bonte et al. (2011) conducted a case study to investigate the effect of ATES on public drinking water well located 570 m away. The data collected revealed a change in groundwater quality as well as the presence of fecal microbes.

The elevated temperature resulting from ATES may also affect the mobility of heavy metals and trace element concentrations. In a laboratory study, the impact of different temperatures (5, 11, 25 and 60 °C) on aquifer sediments where geothermal heating was occurring was examined. The increased temperature led to increased mobility of heavy metal (arsenic), and other trace elements such as phosphorus, silicon, potassium, boron and dissolved organic carbon (Bonte et al., 2013) (Figure 2.10). Similarly, a column-based experiment with aquifer sediment was performed to study the effect of temperature on mineral desorption and reaction kinetics at 10, 25, 40 and 70 °C (Jesußek et al., 2013). The findings concluded that microbial activity was shifted from nitrate reducing to sulphate reducing conditions with increasing temperature but at 70 °C, cation desorption, organic carbon release, sulphate reduction and release of metals were observed (Jesußek et al., 2013). Such alteration in aquifer quality would make it unusable for drinking purposes.

Furthermore, issues like redox fluctuations, biological and chemical clogging of wells due to injected water into an aquifer may limit the sustainability of ATES and the rate of bioremediation. Well clogging in particular, is a challenging issue associated with GWHPs and ATES. Clogging can occur due to chemical, physical or biological processes and can lead to a gradual reduction in permeability of the well screen or gravel filling zone, resulting in an inability to achieve efficient recharge. There are numerous studies and literature regarding the

mechanism and factors that lead to clogging (García-Gil et al., 2016; X. Liu et al., 2017; Pavelic et al., 2008; W. Song et al., 2020).

Complex hydrogeochemical reactions account for 10% of all clogging and result in the accumulation of sediment and chemical precipitation, when groundwater get concentrated with minerals because of recirculating water (recharging), (Bouwer, 2002). (García-Gil et al., 2016) used a transient reactive transport model to simulate chemical clogging and dissolution subsidence processes in a GWHP system located in an alluvial aquifer. Results showed that the spatial soil permeability changes with precipitation-dissolution reactions over time and that a reduction in hydraulic conductivity forces re-injected water to flow downwards, thereby increasing the dissolution of evaporitic bedrock and producing subsidence that can ultimately result in a dramatic collapse of the injection well infrastructure.

Biological clogging can also occur when nutrient conditions are suitable for native microorganisms to breed and multiply rapidly near the well resulting in a formation of a biofilm (Flemming & Wingender, 2010). It is estimated that biological clogging can cause a reduction in aquifer permeability by 2–4 folds of magnitude and lead to a decrease in porosity and saturated hydraulic conductivity (Fernández Escalante, 2015). However, microbial biomass can also control contaminant migration by sorbing hydrophobic organic molecules or by changing hydraulic conductivity of soil (Fernández Escalante, 2015; Song et al., 2020; Yarwood et al., 2006).

Ni et al. (2016) investigated the effect of redox changes by simulating lactate and nitrate addition as a substrate on dechlorination and activity of *Dehalococcoides* in a column study. The addition of lactate enhanced the dechlorination of *cis*-DCE, while nitrate addition ceased the process. Similarly, in his second experiment, the effect of lactate addition on chemical and biological well clogging was observed. Biostimulation with lactate in ATES, resulted in no biological clogging while it helped to counter with chemical clogging caused by iron precipitate (Ni et al., 2018). Thus, proper monitoring of ATES combined with bioremediation is required to control geochemical aquifer parameters to ensure proper operation.

(Zuurbier et al., 2013) studied the impact of low-temperature seasonal ATES systems on groundwater contaminated with chlorinated solvents observed various negative impacts like increased spreading and mobilization of contaminants and enhanced dissolution from the pure

product. Whereas numerous researchers favor the hypothesis that dilution, mixing of water qualities and temperature changes may have a positive effect on ISB (Hartog et al., 2013; Sommer et al., 2013; Zuurbier et al., 2013). As such, there is still debate on the use of ATES in bioremediation sites and further investigation is still required.

Simulation studies also showed that GHPs can help in reducing the concentrations of organic contaminants of emerging concern. A study by Pujades et al. (2023) simulated the effect of thermal plumes on the degradation of carbamazepine and diclofenac in an aquifer. The extent of removal depended strongly on system design, flow rates, injection and production well distance, and duration of operation. Some contaminants (e.g., carbamazepine) respond more strongly to temperature increases than others (e.g., diclofenac) (Pujades et al., 2023). Likewise, a study on the effect of ATES on dichlorination of trichloroethene from contaminated aquifer sediment showed promising results for reductive dichlorination and microbial community development, as reported by (Bin Hudari et al., 2025). Therefore, geothermal heating could be a potential heat source for enhanced bioremediation when the subsurface temperature increases moderately to around 30 °C.

2.6.2 Impact of closed-loop pumps on bioremediation

Unlike open-loop systems, closed-loop does not have any water injected into the subsurface, rather the thermal energy is transferred to the subsurface using conductive flow from several closely spaced boreholes. Typically, closed-loop systems are installed below the groundwater table (i.e., vertical GHPs), however, they can also be installed horizontally in the unsaturated zone.

Similar to ATES systems, the heat stored during the BTES cooling mode might aid in the degradation of contaminants present in the subsurface. Moradi et al. (2018) studied Geothermal remediation coupled with BTES using a numerical model. The results of the study suggested that linking these two systems provides a sustainable way to achieve desired temperature-moisture distribution in soil that can be beneficial for optimum microbial activity. The study focused on modeling the bioremediation process in the unsaturated zone and a Van't Hoff-Arrhenius equation was used to calculate the microbial activity with changing temperature. The results showed that microbial activity doubled with a 10 °C rise in subsurface temperature (Moradi et al., 2018).

A study by Ni et al. (2015) demonstrated the role of both BTES and ATES in *in-situ* degradation of *cis*-DCE (*cis*-dichloroethene) in comparison to natural attenuation at a constant temperature of 10ºC. Both systems were operated at 25ºC and 5ºC for warm and cool wells, respectively. For ATES, the effect of circulating liquid and changing temperature drove the change in contaminant removal, while for BTES, only the effect of changing temperature was observed on the rate of *cis*-DCE dechlorination by using Dehalococcoides as inoculum. The overall reductive dechlorination or removal efficiency of ATES and BTES was 13 times and 8.6 higher, respectively than natural attenuation. The rate of thermally enhanced bioremediation was most effective in the warm ATES well due to a combination of perfect temperature range and biomass growth (Ni et al., 2015).

A simulation study to analyse the effect of thermal plumes generated from boreholes on Trichloroethylene (TCE) decontamination, suggested a localized increase in groundwater velocity, decrease in viscosity and increase in solubility of TCE making it more bioavailable to microbes. Also, the rate of microbial activity was increased, which led to enhanced TCE biodegradation rate by reductive dichlorination (Beyer et al., 2016).

A numerical study by Daemi & Krol (2019) showed the effect of vertical GSHP system in three different Canadian cities. The model simulated a hypothetical GSHP and evaluated the effect of building thermal load on the development of subsurface thermal plumes. The study concluded that the size of thermal plumes generated depends on the climate (thermal load) and a ten-year simulation result showed that the size and temperature of thermal plumes were directly proportional to the thermal load.

Yadav et al. (2022) performed a one-dimensional soil column study at different soil-water temperatures (4 °C, 20 °C, 28 °C, and 36 °C) using automatic temperature-controlled baths for NAPL biodegradation. Results showed that at high soil-water temperatures (28 °C and 36 °C), toluene dissolution and biodegradation rates were higher. The biodegradation rate was reported to be two times higher at elevated temperatures: 0.002 mg L/h, 0.008 mg L/h, 0.012 mg L/h, and 0.015 mg L/h at soil-water temperature levels of 4 °C, 20 °C, 28 °C, and 36 °C, respectively. It suggests that accelerated temperature plays a key role in microbial actions and could significantly enhance the biodegradation rate of NAPL in the subsurface system (B. K. Yadav & Gupta, 2022).

Lastly, a simulation study of 10 years of GHP operation was conducted by Roohidenhkordi & Krol (2021b) in the Canadian environment to assess their geo-environmental impacts in contaminated sites using FEFLOW. Results compared the heat transport and benzene concentration with variable biodegradation kinetics to the constant temperature of 10 °C (no GHPs). Benzene was degraded to a remarkable level, from 0.306 to 0.011 mg/L (96%), after one year of GHP operation. This study also showed that Geothermal remediation is only effective at sites with a well-defined mass source. The application of GHPs at a continuous source or NAPL site would lead to the cyclical reduction of mass but not to a complete decline (Roohidehkordi & Krol, 2021b).

As seen from this review, open-loop systems (ATES) outperform closed-loop systems (BTES and GSHPs) in remediation efficiency. However, more negative impacts of ATES on water geochemistry due to the re-injection of water into the subsurface have been reported.

2.7 Role of thermophiles in bioremediation

Mesophilic bacteria can survive at typical GHP temperature ranges (15 °C to 45 °C), therefore, they are the most common bacteria to become “activated” when the subsurface is heated. However, in some cases, subsurface temperatures have been observed to go higher than 45 °C (Jesußek et al., 2013), especially with ATES and BTES systems where the heat is stored. In these environments, thermophilic bacteria would thrive.

Thermophiles belong to extremophilic organisms having the capacity to thrive at high temperatures (i.e., more than 50 °C). It is reported that thermophiles are present everywhere despite the different environmental conditions (even in low-temperature climates). However, their activity is limited under sub-optimum conditions. If the optimum temperature is provided, they proliferate at a faster rate (Hubert et al., 2009). Therefore, providing heat to the subsurface could help to activate endogenous thermophiles to enhance bioremediation. It has been shown by some that thermophiles play a dominant role in biodegradation in comparison to mesophiles and psychrophiles as they can survive under harsh conditions, exhibit higher growth rates, have higher stability and are capable of degrading recalcitrant pollutants (Sawle & Ghosh, 2011).

For instance, bioleaching can extract metals from metal-contaminated wastes, sludges, and sediments. In bioleaching, given the exothermic nature of the biological processes, only

thermophiles can survive. Likewise, in radionuclide decay, thermophilic microorganisms have been reported for nuclear waste treatment (Castro et al., 2019).

Numerous researchers have examined the role of *Geobacillus*, *Anoxybacillus*, *Thermus* and *Thermococcus* in the biosorption of different metals such as Cd, Cu, Ni, Zn and Mn (Chatterjee et al., 2010). Chatterjee et al. (2010) reported the potential of thermophiles in the bioremediation of industrial effluents by applying *Geobacillus thermodenitrificans* (MTCC 8341) cells to industrial effluent, resulting in the removal of 44% of Fe^{3+}, 39% of Cr^{3+}, 35% of Cd^{2+} and 18% of Pb^{2+}.

Besides metal recovery, thermophiles have been reported to biodegrade hydrocarbons and textile dyes. In the study reported by Guevara-Luna et al. (2018), the biotransformation of benzo[a]pyrene into an intermediate innocuous compound corresponding to phthalic acid, was performed by the thermophilic bacterium, *Bacillus licheniformis* M2-7.

Boyd & Barkay (2012) have cited that mercury (Hg)-resistance system originated in the thermophiles that inhabit early geothermal areas and high Hg content areas, because thermophilic genera like *Sulfolobus*, *Thermus*, and *Aquificae*, belonging to hot spring environments present simpler versions of the *mer* operon. Similarly, Freedman et al. (2012) studied two hyper-thermophilic bacteria isolated from a hot spring environment that lack the homologous genes of the operon mer (MerR) regulator. Advantageously, such species are independent of Hg presence in the environment, hence they can be a good tool in the bioremediation of Hg-contaminated environments (Freedman et al., 2012).

Such studies have proved the potential of thermophiles towards Geothermal remediation. Since some GHP operation have exhibited high thermophilic temperatures (i.e. greater than 50 °C) (Jesußek et al., 2013), the operation of GHPs at elevated temperature could activate thermophiles in the subsurface leading to higher degradation rates. Furthermore, if endogenous microbes do not have degradation properties, sites could be bioaugmented with exogenous thermophiles to achieve complete bioremediation.

2.8 Role of engineered bacteria in bioremediation

A recent development in the field of genetic engineering provides a novel opportunity to construct genetically engineered microorganisms (GEMs) which have bioremediation potential

in heated environments (S. Kumar et al., 2013; Pieper & Reineke, 2000; Sayler & Ripp, 2000). Bioremediation of aromatic hydrocarbons by GEMs has already been reported by several authors (Ang et al., 2005; T. C. Zhang et al., 2017).

For field applications of GEMs for enhanced bioremediation, knowledge about site pollutants is essential as different microbes will react with different compounds. Depending upon the pollutant, the native or commercial microbes can be modified genetically by employing metabolic techniques or biomolecular engineering. Methods such as rational designing and directed evolution have evolved to enhance the activity of microbes or metabolites towards degradation (Kumar et al., 2013; Singh et al., 2008). For instance, Huang et al. (2015) cloned a heat-resistant gene (i.e. arsenite methyltransferase) into *Bacillus subtilis* for the enhanced bioremediation of arsenic-contaminated organic waste. The GEM converted inorganic arsenic into dimethyl arsenate and trimethyl arsenate within 48 hours. Similarly, the laccase gene was transferred from *Thermus thermophilus* and an enzyme was obtained that had a high tolerance to NaCl, with an optimum temperature of 90°C and able to decolorize the textile dyes (Liu et al., 2015).

For successful ISB of contaminated sites using GEMs, detailed information of microbiological and ecological background, genes responsible for biodegradation, biochemical mechanisms and engineering designs would be required (Pieper & Reineke, 2000; Singh et al., 2011). Ni et al. (2016) studied the effect of bioaugmentation by injecting mobile DHC (*Dehalococcoides*) on coupled ATES and bioremediation of CVOCs, and the result showed a positive effect on overall degradation. Likewise, GEMs can be applied for the bioaugmentation of Geothermal remediation. To the best of our knowledge, there is still no literature available on the coupling of these three technologies: geothermal heating, bioremediation enhanced by GEMs. This means there is room for investigation in this field, where microbes are modified with genes so that they are capable of decomposing subsurface pollutants both in the heating and cooling mode of GHP operation, while thermophiles (or mesophiles) work only in cooling mode. Nevertheless, the environmental impact and biosafety regarding the release of GEMs in the environment for ISB still needs to be investigated.

2.9 Conclusions

A significant amount of research has demonstrated the quantitative relationships between thermal energy and bioremediation. It is now well understood that there is a correlation between thermal energy, the activity of microorganisms, and the biodegradation of dissolved pollutants. The addition of heat to the subsurface has traditionally been done using high energy-high temperature methods based on conventional fossil fuel technologies. Although effective, these technologies may not be needed to enhance bioremediation since they can add too much heat (which is not conducive for bacterial grown), increase the cost of remediation substantially and contribute to global warming. As such, there has been a rise in low temperature bioaugmentation using renewable energy sources such as geothermal heat pumps. GHPs are cheaper to operate and can provide heating and cooling to buildings while the resulting heat could help to enhance bioremediation and clean up contaminated areas. Moreover, as seen through the various studies reviewed herein, bioremediation is a complex phenomenon, controlled by multiple parameters including temperature. The effect of temperature on parameters such as sorption, volatility, contaminant transport, bioavailability and metabolic rates can favor biodegradation to a certain extent. However, bioremediation is also very site specific and greatly depends on the type of pollutant as well as the native microbes present, therefore site investigation is a crucial step that is required for Geothermal remediation of brownfield sites.

This review has highlighted the advantages and disadvantages of "Geothermal remediation" for the decontamination of pollutants by non-carbon energy sources. Based on the reviewed literature, GHPs may be effective for bioremediation, with open-loop systems having higher degradation potential than closed-loops systems but with higher chance of water quality deterioration. However, to date there are still unknowns about the environmental impacts of geothermal heating on the subsurface environment, especially using field-scale studies. In particular, the influence of geothermal heating on the biodegradation of monoaromatic hydrocarbons such as BTEX has not been experimentally validated, and the response of soil microbial communities to cyclic low-enthalpy thermal conditions remains poorly understood. This knowledge gap is critical, given the persistence, toxicity, and widespread occurrence of BTEX in soil and groundwater systems.

Accordingly, this thesis specifically focused on BTEX as a priority contaminant and investigated the role of soil microorganisms in mediating BTEX removal under cyclic geothermal heating conditions. By adopting a cyclic rather than constant thermal regime, this research introduces a novel and more realistic representation of shallow geothermal operation. The findings presented herein establish a clear rationale for the specific experimental objectives detailed in the following chapter and contribute new insight into the feasibility of coupling geothermal shallow energy systems with microbial BTEX bioremediation.

The major benefits related to coupled GHP and bioremediation, or Geothermal remediation are:

- Easily implemented in urban areas (e.g., under building foundations), and remote locations,
- Except for the initial GHP installation costs, the operating costs are considerably cheaper than conventional thermal remediation systems,
- Open-loop systems are effective for bioremediation, however groundwater mixing, and quality is an issue that needs to be monitored,
- Closed-loop systems increase bioremediation but are not as efficient in remediation compared to open-loop systems,
- Geothermal remediation is eco-friendly as it links bioremediation with a clean and renewable energy supply,
- After achieving the remediation goals, the system can still be used to provide heating and cooling without any additional investment or modification.

CHAPTER 3: RESEARCH OBJECTIVES

3.1 Research problems

This research addresses two major environmental issues currently facing the world, namely energy demand and pollution resulting from increased globalization and population growth. Researchers are continually finding alternatives to minimize these effects.

1. BTEX are volatile aromatic hydrocarbons that constitute a significant fraction of petroleum-derived products such as gasoline, crude oil, and industrial solvents. Their high solubility and mobility in groundwater make BTEX compounds persistent environmental pollutants, particularly in subsurface and aquifer systems impacted by fuel leakage, spills, or improper waste disposal. Benzene, a known human carcinogen, and its analogues toluene, ethylbenzene, and xylenes exhibit acute and chronic toxicity toward aquatic and terrestrial organisms, leading to mutagenic, neurotoxic, and hematological effects (Bolden et al., 2015; Y. Meng & Li, 2025). In anaerobic subsurface environments, BTEX degradation is often limited due to oxygen depletion and the slow adaptation of native microbial communities to alternative electron acceptors. Consequently, BTEX contamination poses a long-term risk to soil and groundwater quality, necessitating innovative remediation strategies that enhance biodegradation under anoxic or thermally influenced subsurface conditions (Y. Meng & Li, 2025). Understanding the complex interplay between microbial metabolism, temperature gradients, and electron acceptor availability is therefore critical for developing sustainable bioremediation approaches for BTEX-impacted environments.
2. Microorganisms play a crucial role in biogeochemical processes in the shallow subsurface, thereby facilitating bioremediation. Estimation of genetic diversity, microbial activity, and their metabolic functions are the most effective methods for exploring biodegradation processes in the subsurface. Several techniques, including community-level physiological profiling, sequencing, metagenomics, enzyme assays, and culture-based methods, are employed to investigate the metabolic potential, functional diversity, and genetic diversity of native microbial communities (Amend & Teske, 2005; Griebler & Lueders, 2009a). These studies help to understand the metabolic pathways and biodegradation patterns in the subsurface; however, interspecies microbial interactions and their transport mechanisms in porous media, particularly in relation to bioremediation of subsurface pollutants, are still not well understood. Despite the advanced characterization methods for microbes, multiple crucial knowledge gaps of the

dynamic subsurface microbial community remain unraveled. A detailed understanding of subsurface microbial interactions, mineral-metal-microbial correlation, transport mechanisms, and degradation pathways will help in the optimization and design of ISB in the future. There is a need for a detailed exploration of these fundamental microbial processes to gain a deeper understanding of microbial dynamics, facilitating the development of advanced bioremediation processes that are sustainable.

3. The major issue associated with natural degradation is that microorganisms in the subsurface may proliferate at a slow rate because of unsuitable conditions for growth and metabolic activity. Lower temperature is one of the main factors which limit their metabolic activity towards the degradation of pollutants (Boopathy, 2000; Koshlaf & Ball, 2017). In addition to microbes, the properties of the pollutants also limit the rate of bioremediation. As in the ground, the pollutants are present in different phases, limiting their bioavailability for degradation by microbes. The increasing temperature could be a positive stimulator for enhancing the bioremediation rate, and this heat can be provided to the surface using GHP sustainably without any additional cost (Moradi et al., 2018).
4. For energy demands, which are utilized in various forms, the heating and cooling of interiors contribute majorly to the total energy demand in Canada. To obtain this energy sustainably from renewable sources, geothermal heat pumps are used to inject and extract heat from the shallow subsurface (Casasso & Sethi, 2019; Pophillat et al., 2020). These pumps are cost-effective and widely accepted for heating purposes; however, fluctuations in subsurface temperature geothermal cycles could severely affect subsurface geochemical parameters, as explained in the chapter 2. The effect of operating GHP on the subsurface could be positive or negative towards pollution mitigation and bioremediation, but it has not been well studied. Hence, it is of primary importance to understand the impacts of geothermal heating on the subsurface, in order to continue using geothermal heating as demand grows faster.
5. Lastly, the effect of temperature on microbial activity is known to be a positive stimulator (Iqbal, 2003; Koshlaf & Ball, 2017); however, the effect on subsurface bioremediation is not well studied, especially when GHP heat is used. Hence, in this research, we aim to examine the role of heat injected by GHP in the bioremediation of our model contaminants (BTEX) and other subsurface properties, to see if a positive association between GHP and bioremediation can be established.

3.2 Research originality

Experimental validation of geothermal heating impacts on BTEX bioremediation in the subsurface.

3.3 *Research hypotheses and objectives*

***3.3.1 Research gap 1*:** Although soil microorganisms are known to contribute to BTEX degradation, their temperature-dependent biodegradation kinetics under geothermal-relevant conditions remain poorly understood.

Hypothesis 1: The intrinsic microbes present in the subsurface have the potential to degrade several pollutants by using them as a substrate for their energy source and food through their metabolic pathways and converting them to non-toxic products. Thus, we need to explore the capability of intrinsic microbes to serve as a sustainable bioremediation option. Moreover, temperature is a limiting factor for the growth of microbes, and it also affects the properties of pollutants and porous media, which could affect the rate of bioremediation. Hence, we analyzed the biodegradation of BTEX at temperatures ranging from 10 to 40 °C.

***Objective 1*:** Identify novel BTEX-degrading strains from subsurface soil: Isolation, Identification and Growth Evaluation.

1.1 Isolation and screening of BTEX-degrading microbes.

1.2 Degradation of BTEX by isolated microbes at different temperatures.

3.3.2 Research gap 2: The BTEX biodegradation potential of *B. infantis* and *M. esteraromaticum*, particularly under varying redox conditions and alternative electron acceptors, has not been previously reported.

Hypothesis 2: Microbes use different electron acceptors for biodegradation processes, whereas subsurface environments are mostly anoxic. The dissolved oxygen is rapidly consumed by microorganisms near contamination plumes, making the environment anoxic. Some microorganisms switch the metabolic mechanism and start using other electron acceptors like nitrate, sulfate etc. Hence, it is crucial to comprehend the response of microbes to various electron acceptors.

Objective 2: Analyze BTEX biodegradation under anoxic conditions using response surface methodology.

3.3.3 Research gap 3: While optimum growth temperature enhances biodegradation, the effects of cyclic temperature of geothermal heating on BTEX biodegradation in different soil types have not been experimentally evaluated.

Hypothesis 3: GHP dissipates the heat into the subsurface as a thermal plume, generating a thermal gradient around the borehole. Hence, we designed the bench-scale experiment to simulate real subsurface conditions and cumulatively study the effect of all factors (soil porosity, heat dissipation, adsorption, etc.) that could influence the rate of biodegradation of BTEX.

Objective 3: Perform a bench-scale GHP system in a bioreactor to study the effect of cyclic heat on BTEX biodegradation.

3.3.4 Research gap 4: The influence of depth-dependent soil microbial community structure on BTEX biodegradation, and how geothermal-induced temperature changes affect microbial diversity across different subsurface depths, remains largely unexplored.

Hypothesis 4: The heat injected into the subsurface by GHP could affect the behaviour and existence of microbes present in the subsurface throughout the boreholes, which are important to consider during biodegradation studies.

Objective 4: Investigate geothermal heating impacts on soil microbiome communities along with the borehole depth by 16S rRNA sequencing.

CHAPTER 4: METHODOLOGY

4.1 Chemicals and growth media

BTEX compounds were procured from Fisher Scientific (Mississauga, ON, Canada) at a high grade, with >97% purity. The salts used for the growth media preparation (mineral salt media (MSM), tryptic soy broth (TSB), tryptic soy agar (TSA)) and other chemicals were obtained from Sigma-Aldrich (Mississauga, ON, Canada) and Fisher Scientific (Mississauga, ON, Canada) and were of analytical and microbiological grade.

For the enrichment of selective BTEX-degrading strains and degradation analysis, MSM was used, as it contains a high concentration of essential inorganic salts with no carbon source. BTEX was used in the experiment as a carbon source for the selective isolation of bacteria that degrade BTEX. The composition of MSM was 1.8 g K_2HPO_4, 4.0 g NH_4Cl, and 0.01 g $FeSO_4$. $7H_2O$, 0.1 g NaCl, 0.2 g $MgSO_4.7H_2O$, and 3 g yeast extract per 1 liter of distilled water (Miri et al., 2021). All salts, except iron sulfate, were added to distilled water, and the pH was balanced to 7±0.5 with 1M HCl and 1M NaOH. The media was heat sterilized at 121±1 °C using an autoclave. The iron sulfate salt was prepared separately in distilled water, sterilized by a 0.2 micron filter separately, and added to the MSM media during the experimental setup.

For inoculum preparation, TSB, a highly nutritious media that contain all essential nutrients for microbial growth, was used. TSB media was prepared by dissolving 30 g of tryptic soy powder in 1 L of distilled water and steam sterilized with an autoclave. The solidified agar media TSA for Petri plates was prepared by adding 1.5% agar in TSB media.

Soil samples were collected from three different depths (3.0, 42.6, and 73.2 m) of two boreholes from a planned GSHP site located in Toronto, ON. The boreholes were dug to install a geothermal heat pump system, but these wells were not operational at the time of sampling, nor was the site contaminated. The soil samples were collected in November 2020, with an average outdoor ambient temperature of 10 °C. The drilled soil was packed in Ziploc polybags and stored in cold storage box. These soil samples are used for bacterial isolation in objective 1 and for soil microbiome studies by 16S rRNA sequencing in objective 4.

For objectives 2 and 3, soil samples used in soil slurry and soil column experiments were collected from a site in Toronto. The soil was always dry and steam-sterilized by autoclave prior

to experimental setups. The physicochemical soil properties were analyzed before the experiments.

Objective 1: Identify novel BTEX-degrading strains from subsurface soil: Isolation, Identification and Growth Evaluation.

4.2 Soil sample characterization

4.2.1 Physical parameters analysis: The collected soil samples were analyzed for their physical characteristics, including moisture content, plastic limit, liquid limit, and grain size distribution, in accordance with the standard ASTM protocol (*Appendix A*).

4.2.2 Physicochemical analysis: The physiochemical parameters such as cation exchange capacity (CEC) and heavy metals (HM) were analyzed as per the protocol mentioned in *Appendix A*. Briefly, the CEC was performed by the ammonium acetate method and analysed by UV-visible spectrophotometer (GENESYS 50, Thermo Scientific). HM analysis was done by nitric acid digestion followed by detection using inductively coupled plasma-optical emission spectroscopy (ICP-OES) (*Agilent* 5110 ICP-OES Dual View). Nitrate and sulfate content of the soil was measured with Ion chromatography (Dionex Integrion HPIC, Thermo Fisher Scientific) and iron was analyzed by Inductively coupled plasma-optical emission spectroscopy (Agilent 5110 ICP-OES Dual View*).*

4.3 Isolation of BTEX-tolerant bacteria

Bacteria were isolated from the borehole soil samples and used to investigate the effect of geothermal heating on bioremediation at a laboratory scale. To accomplish the isolation of the strains, an enrichment media was used. About 20 mL MSM was supplemented with 0.5 g of soil and 100 mg/L BTEX (in a 1:1:1:1 ratio) as the sole carbon source in crimp-sealed serum bottles and incubated in a shaker incubator (INFORS HT) at 28±1 °C and 200 rpm. Each week the culture was sub-cultured into fresh MSM media with a higher concentration of BTEX (200 mg/L). This was done for four weeks. Afterward, the culture was spread onto TSA agar plates using the spread plate technique and incubated at 28±1 °C in a static incubator to culture the tolerant bacteria. After incubation, 48 single morphologically distinct colonies were picked up

and streaked twice on fresh agar plates to collect pure strains. The results of spreading and streaking are illustrated in *Appendix B* (Figure B1, B2 and B3). From the 48 isolated tolerant bacteria, a total of 12 isolates (two from each soil sample) with higher growth and degradation ability were selected. The single pure colony was then inoculated in TSB media for 24 hours and used for the preparation of a glycerol stock for long-term storage at -80±1 °C and future experiments.

4.4 Bacterial identification

To identify the isolated strains, genomic DNA was isolated using a DNA extraction kit (Miniprep kit from Zymo Research, New England) from an overnight grown culture of all isolates with O.D. of 2 x 10^8 cells/mL. The purity and concentration of extracted DNA were analyzed by Nanodrop Spectrophotometer (Thermo Scientific, USA) (Table B1), and the extracted DNA was amplified for 16S rRNA using universal primers 27F (5′-AGAGTTTGATCCTGGCTCAG-3′), 1492R (5′-GGTTACCTTGTTACGACTT-3′) by polymerase chain reaction (PCR). Using the same primers, sanger sequencing was performed, and the resultant sequence of each isolate was aligned with the five highest similar (>97%) 16S rRNA from bacterial and archaea databases using Blastn from NCBI (National Center for Biotechnology Information) to identify the strains. The phylogenetic tree of the identified sequence was generated with the five most similar strains in MEGA 7 (Molecular evolutionary genetics analysis) software using the bootstrap method (S. Kumar et al., 2018).

4.5 Growth kinetics

Inoculum preparation: For primary culture, the bacteria were grown in liquid TSB media, by inoculating with a single pure colony from an agar plate. After 24 hours, the optical density of the culture was observed, and at a cell concentration of 2 × 10^^{8} cells/mL, the cells were pelleted down using a centrifuge (21,475 × *g* for 5 minutes at 4 °C). The supernatant was discarded, and the pellet was washed twice with distilled water using the same conditions for centrifugation. Finally, the pellet was suspended in distilled water and used as inoculum for batch culture experiments.

Screening for the growth and degradation analysis: The collected 48 strains were pre-screened based on their growth in MSM and 12 strains, which show good growth in liquid media were further selected for a specific screening. To observe the growth kinetics of the isolated strains, first, all 12 strains were screened based on growth in different growth media such as MSM, and MSM supplemented with glucose (0.2%) and yeast extract (0.3%). MSM media was supplemented with these nutrients as there was the quite slow growth of individual isolated strains in MSM media. Secondly, the selected strains were screened for BTEX degradation ability within 24 hours and two potent strains were selected. *Pseudomonas putida,* which is well-known for its BTEX degradation activity (Chicca et al., 2020a; H. J. Choi et al., 2013), was used as a reference strain to compare the degradation ability of isolated strains in all performed experiments. For these batch experiments, 100 mL serum bottles were used, with 20 mL MSM, 200 mg/L BTEX, and 2% inoculum at 15±1 °C, 28±1 °C, and 40±1 °C. The temperature range was selected based on the temperature conditions found with a working GHP (Park et al., 2015; Roohidehkordi & Krol, 2021a). The concentration of BTEX was in equal proportion for all four compounds and was present at less than their aqueous solubility limit at room temperature. The 200 mg/L BTEX concentration was selected to balance aqueous solubility, analytical detection limit, and microbial tolerance to enable clear evaluation of biodegradation dynamics under controlled laboratory conditions. Negative (without inoculum with and without BTEX) and positive (only inoculum without BTEX) control experiments were also used to assess background contamination and volatilization of BTEX. To record the growth rate, the samples were collected periodically every 6 hours using a micro-syringe, and cell count was obtained using a spectrophotometer (96-well plate reader, Gen5, Epoch (BioTek)) at 600 nm by observing optical density and the dry biomass was also analyzed by drying 1 mL of a culture sample at 60±1 °C, overnight in an oven (Precision, Thermo Scientific).

The specific growth rate and duplication time of bacteria were observed using equations 4.1 and 4.2 respectively.

$$\mu = \frac{dX}{X_o dT} \tag{4.1}$$

$$T_d = \frac{ln2}{\mu} \tag{4.2}$$

Where μ is the specific growth rate, dX is the mass of cells produced, X_o is the original cell mass, T is time in equation 4.1 and T_d is the duplication time of bacteria.

To obtain BTEX concentration, samples were collected from the serum bottles at 10 or 12-hour intervals and analyzed using a headspace GC-MS (Clarus 500 (Perkin Elmer)). For GC sample preparation, 100 μL sub-samples from the liquid phase of serum bottles were taken, using a gas-tight syringe, and added to 5 mL of ultrapure water in 20 mL GC-headspace vials. 30μL of fluorobenzene-D5 (4 mg/L diluted in methanol) was added as an internal standard and then sealed immediately with crimp caps. All experiments were done in triplicates to check the reproducibility.

4.6 Enzymatic assay

To study the enzymes involved in the degradation of BTEX, the activities of ToMO, C1,2D, and C2,3D were measured using colorimetric methods. Briefly, the conversion of toluene to p-cresol by ToMO was quantitatively determined using a UV-visible spectrophotometer (GENESYS 50, Thermo Scientific). The cellular lysate was prepared by washing it twice with PBS buffer and then sonicated at a 20 kHz wavelength for 10 minutes, with a 10-second on and off pulse cycle. For the reaction mixture, the cellular lysate was mixed with 35 μL of N, N-dimethylformamide containing 4% (vol/vol) toluene and incubated at 28 ± 1 °C. 1 mL sample was mixed with 100 μL of 1 M NH_4OH, 100 μL of 2% 4-amino antipyrine and 100 μL of 8% $K_3Fe(CN)_6$ after incubation. The reaction mixtures were briefly centrifuged at 14,000 × *g* and the absorbance was recorded immediately at 500nm (Miri et al., 2021). A reference curve was drawn by using 0–50 μg/mL of p-cresol as a product of the reaction.

Likewise, to assess the activity of C1,2D and C2,3D, the conversion rate of catechol as a substrate to muconic acid at 260 nm and 2-hydroxymuconic semialdehyde at 375 nm was measured, respectively. For the reaction mixture, 0.6 mL of catechol (10 mM) was added to 2.0 mL of phosphate buffer and 0.4 mL of cellular lysates (Y. Li et al., 2014).

4.7 Metabolites analysis

To analyze the product and intermediates formed during BTEX biodegradation *via* two potent selected strains: *Bacillus infantis* and *Microbacterium esteraromaticum,* 5 mL of media in 20

mL GC vials was inoculated with the seed inoculum and supplemented with 200 mg/L BTEX (see details in section 4.5). The vials were immediately closed with crimp caps to prevent any loss through volatilization and then incubated at 28±1 °C. Negative (without inoculum) and positive (without BTEX) controls were also included to analyze any interference of the matrix and potential losses. Samples (vials) were collected after 24 and 48 h and heated at 80±1 °C in a pre-heated water bath to kill the live bacteria and analyzed using GC-MS for the presence of the metabolites.

Objective 2: Analyze BTEX biodegradation under anoxic conditions using response surface methodology.

4.8 Microorganism, culture maintenance, and inoculum preparation

B. infantis (GenBank Accession Number: OQ582092) *and M. esteraromaticum* (GenBank Accession Number: OQ582078) were used for the BTEX degradation studies. The bacterial strains were isolated by enrichment from soil obtained from a geothermal borehole. Detailed information about the isolation process and characteristics is reported in section 4.3 and 4.4. The isolated bacterial strains were grown in 20 mL TSB media to their exponential phase and the culture was centrifuged at 1000 *x g* for 10 minutes. The supernatant was discarded, and the pellet was resuspended in 10 mL of a 40% (v/v) glycerol solution. The suspended bacterial culture was aliquoted to 1 mL volume in Eppendorf tubes and preserved as stock at -80 °C to maintain the bacterial activity for long-term storage. For conducting experiments, the culture from stored glycerol stock was first streaked on TSA plates and incubated at 28 °C in a static incubator (Thermo Scientific). After 36 hours, a single colony of *B. infantis* and *M. esteraromaticum* from the Petri plate was inoculated individually in 5 mL TSB media for primary inoculum. The cultures were incubated for 24 hours at 28 °C and 200 rpm in a shaking incubator (Infors Multitron Incubator Shaker, Switzerland). Secondary inoculum was prepared by using 2% of the primary inoculum and mixing it with 50 mL of fresh TSB media (For example, 1 mL of primary culture was added to 50 mL of TSB). After 24 hours of incubation under the same conditions, the bacteria from the secondary culture at their exponential phase around OD 1 were collected by centrifuging at 1000 *x g* for 10 minutes. The bacterial pellet was suspended in 10 mL autoclaved distilled water. The number of bacteria cells in suspension was

calculated via OD at 600 nm with a 96-well plate reader (BioTek Epoch Microplate Spectrophotometer, Agilent, Canada), where 1 OD refers to 1 x 10^8 bacterial cells. The bacterial suspension was used as inoculum for all the experiments with 2% of the experimental volume at OD 2. The volume of inoculum to be added was calculated by dilution formula (C1V1 = C2V2) and then added to the treatment sets in the following experiments.

4.9 Growth and biodegradation analysis with individual electron acceptors

The growth of *B. infantis* and *M. esteraromaticum* was observed in MSM media. Because of the volatile nature of BTEX, the experiments were performed in gas-tight 100 ml serum bottles with crimp caps with 0.5 mg/L dissolved oxygen. Each serum bottle contained 20 ml of MSM media with and without BTEX at a total concentration of 200 mg/L in equal proportion (50 mg/L) at a 1:1:1:1 ratio. 200 mg/L was chosen based on the tolerance of the selected microorganisms to BTEX and the solubility of BTEX in aqueous media at room temperature. Further, to analyze the effect of these ions on BTEX biodegradation, a range from 0 to 1000 mg/L has been chosen with four concentrations (0, 250, 500, and 1000 mg/L). In this set of experiments, bacterial growth and biodegradation were analyzed in three different anoxic environments, i.e., nitrate-only, sulfate-only, and ferric-only, as electron acceptors. The treatment and positive controls were inoculated with 2% bacteria (*B. infantis* and *M. esteraromaticum*) at OD 2 at 600 nm. The negative controls were only supplemented with ions and BTEX. The serum bottles were incubated at 28 °C and 200 rpm. The bacterial growth rate was analyzed by collecting the samples periodically for up to 48 hours using a gas tight syringe, and cell count was noticed by OD using a spectrophotometer at 600 nm. The samples for biodegradation analysis were also collected after 24 and 48 hours.

4.10 Growth and biodegradation analysis with different combinations of electron acceptors

In this set of experiments, BTEX biodegradation was explored under different anoxic conditions using different combinations of mixed nitrate/sulfate/ferric as electron acceptors in MSM media as well as soil matrix. The experiment was designed *via* the Box Behnken method with Response Surface Methodology in OriginLab2023b as shown in Table 4.1. Serum bottles were used for the treatment where each bottle had 20 mL of MSM, the specific amount of nitrate, sulfate, and ferric iron solution from a stock solution of 10g/L KNO_3, $MgSO_4$, and $FeCl_3$,

respectively, as per the design of the experiment, 200 mg/L of BTEX solution (from a stock of 20,000 mg/L), and 2% of bacteria inoculum at 2 OD Positive controls with 20 mL of MSM, the maximum amount of nitrate, sulfate, and ferric ions as per the design of the experiment, and with bacterial culture were used. Likewise, the negative controls without any bacterial inoculum were run in parallel to determine any BTEX losses through volatilization.

Table 4.1: Experimental design using the Box-Behnken* method.

Standard Order	*Point Type**	*Nitrate (mg/L)*	*Sulfate (mg/L)*	*Ferric (mg/L)*
1	2	10	10	105
2	2	500	10	105
3	2	10	500	105
4	2	500	500	105
5	2	10	255	10
6	2	500	255	10
7	2	10	255	200
8	2	500	255	200
9	2	255	10	10
10	2	255	500	10
11	2	255	10	200
12	2	255	500	200
13	0	255	255	105
14	0	255	255	105
15	0	255	255	105

*In the Box-Behnken design, three levels are considered for each input factor (low, center, and high). The point type describes the location of input factors in the design.

To analyze the effect of selected ions on *in-situ* biodegradation, the experiments were conducted in a soil slurry using the selected strains. The physicochemical soil properties confirmed that the soil was a silty loam with 25% sand, 52% silt, and 20% clay content (Figure C2). The soil samples had 76 mg/L nitrate, 184 mg/L sulfate, and 1.2% iron (w/w) (Table C1, *Appendix C*). To set up the experiments, 4 g of saturated soil was supplemented with the different

combinations of ions (as per Table 4.1) in 8 mL of media (containing the nutrients for bacterial growth) along with 200 mg/L of BTEX. Two control analyses were conducted: one that included only BTEX and soil without bacteria (for adsorption analysis) and one with only media with BTEX (for volatilization analysis). These controls were run parallelly. Samples were collected after 24- and 48- hours of incubation with a sterilized syringe and needle. For bacterial count, serial dilution and colony forming units' method was used as shown in Figure C1. For residual BTEX concentration quantification, headspace gas chromatography (HS-GC) samples were prepared as mentioned in section 4.20.

Objective 3: Perform a bench-scale GHP system in a bioreactor to study the effect of cyclic heat on BTEX biodegradation.

4.11 Soil characterization

Soil properties, which are important for microbial growth and biodegradation, were obtained before setting up the experiment. Briefly, the parameters such as soil texture by sieve and hydrometer test (ASTM D7928 and D6913), moisture content by gravimetric method (ASTM D2974 – 20), soil organic matter by dry combustion method (ASTM D2974 – 20), pH by electrochemical method (ASTM G51), cation exchange capacity (CEC) by ammonium acetate method (Chapman, 2016), and soil redox potential (Eh) (ASTM G200-20) were obtained according to standard ASTM protocols (details in *Appendix A*. Nitrate and sulfate content of the soil was measured with Ion chromatography (Dionex Integrion HPIC, Thermo Fisher Scientific), and iron was analyzed by Inductively coupled plasma-optical emission spectroscopy (Agilent 5110 ICP-OES Dual View*)*.

4.12 BTEX adsorption studies

Partitioning of BTEX compounds onto soil affects the bioavailability of soil for biodegradation. Hence, it is essential to quantify the soil adsorption capacity (the adsorbent) to understand how much BTEX will partition onto soil during bioremediation experiments. Sorption kinetics experiments were performed in 20 mL glass vials with air-tight septum crimp caps. Soil samples were air-dried and sieved through a 2 mm sieve. After analyzing the gravimetric moisture content, the samples were oven-dried at 105 °C. For each batch experiment, glass vials

contained 1 g of different soil samples (silty loam, fine sand, and coarse sand) separately and 18 mL of BTEX solution, minimizing the headspace to prevent volatilization. BTEX stocks were prepared at a concentration of 0, 100, 200, and 500 mg/L (1:1:1:1) and added to vials containing soil in a fume hood. Control samples for volatilization were prepared with only the BTEX solution in the vials, without any soil. Vials were sealed immediately and agitated on an orbital shaker at 150 rpm (Thermo Scientific, Canada). Samples were prepared in sacrificial sets and sampled at 0, 0.25, 0.5, 1, 2, 4, 8, 16, 24, 48, and 72 h. During sampling, the vials were centrifuged at 3000 rpm for 5 minutes, and the supernatant was used to prepare GC vials for quantifying the aqueous concentration by headspace GC-FID (details in section 4.20). Adsorption capacity of soil (qt) was calculated using equation 4.3:

$$q_t = \frac{(C_o - C_t).V}{m} \qquad (4.3)$$

Where q_t= amount adsorbed at time t (mg/g), C_o = initial concentration (mg/L), C_t= concentration at time t (mg/L), V = volume of solution (L), m = mass of adsorbent (g).

At equilibrium, C_t is replaced with C_e to get equilibrium sorption (q_e). The BTEX distribution coefficient (K_d), assuming linear and reversible sorption, was calculated by plotting q_e (mg/kg) vs C_e (mg/L).

$$K_d = \frac{q_e}{C_e} \qquad \ldots\ldots (4.4)$$

4.13 Small-scale cyclic temperature batch experiments

The batch biodegradation experiments were conducted in 20 mL vials with 4 g of soil and 8 mL of MSM media supplemented with 200 mg/L of BTEX (1:1:1:1) in equal proportions. The soil and media were autoclaved and inoculated with 2% bacterial culture at 2 OD. These experiments were conducted with monocultures of *B. infantis, M. esteraromaticum* and consortia. Consortia in this thesis refer to mixed consortia, which means mixed communities of bacteria from soil. After inoculation, vials were incubated at 15 °C for 24 hours and sampled for bacterial growth and residual BTEX concentration. After every 24 hours, the temperature was increased by 5 °C till 40 °C and then reversed back to 15 °C by a decrement of 5 °C. Transitions between adjacent setpoints occurred over approximately 30 – 45 min (average ramp

rate 0.133 °C/min). After each setpoint was reached, the temperature was allowed to stabilize, and samples were maintained for a total of 24 hours per step prior to the next temperature change. The 5 °C increase/decrease was chosen to reflect realistic temperature fluctuations anticipated within the thermal plume and adjacent gradient produced by shallow geothermal operations in the subsurface, while ensuring adequate resolution to assess temperature-dependent BTEX biodegradation without introducing noise from extremely small increments. Samples were collected at each specific temperature to determine the influence of temperature on bacterial growth and BTEX residual concentration. Control sets were used for adsorption and volatilization analysis. The control vials were prepared similarly. For adsorption controls, vials contain soil and BTEX in the same ratio as treatment vials, without the bacterial cells. In volatilization controls, 12 mL of MSM media with 200 mg/L of BTEX was used to maintain the same headspace when measuring BTEX loss. All the samples were prepared in duplicates and in sacrificial samples to avoid the loss through sampling by needle injection. The bacterial cell counts were performed by the serial dilution agar plating method to count for colony-forming units. The specific growth rate (μ) (equation 4.5) and doubling time (equation 4.6) were measured as per the equations below.

$$\mu = \frac{lnN_2 - lnN_1}{t_2 - t_1} \quad (4.5)$$

$$t_d = \frac{ln2}{\mu} \quad (4.6)$$

Where N_2 and N_1 are the number of bacterial cells at time t_2 and t_1, respectively.

The residual BTEX concentration was measured at each temperature with headspace GC-FID. The concentration of BTEX in soil samples was back-calculated by the following formula in equation 4.7.

$$C_{soil} = \frac{C_{GC} \cdot V_{water}}{m_{soil}} \quad (4.7)$$

Where C_{soil} is the BETX concentration in soil (mg/kg), C_{GC} is the BTEX concentration of diluted samples in GC vials (ug/L), V_{water} = extraction volume (5 mL) in GC vials, and m_{soil} is the amount of soil added in GC vials (g).

For BTEX biodegradation concentration analysis in soil, the mass balance of BTEX was performed by using equation 4.8.

$$C_d = C_r - C_a - C_v \qquad (4.8)$$

Where C_d is the biodegraded fraction of BTEX, C_r is the total removed concentration at time t (hours) ($C_r = C_o - C_t$) in treated samples, C_a is the fraction of absorbed BTEX in control samples with only BTEX, and C_v is the BTEX volatilized fraction in control samples with media containing BTEX (without soil and bacteria), C_o is the initial BTEX concentration at time 0 and C_t is BTEX concentration at time t. All concentrations were measured in mg/L.

4.14 Fed-batch soil column

A stainless steel column (15 cm x 3.5 cm) setup was fabricated for continuous study of cyclic temperature (5 °C to 40 °C) on bacterial growth and BTEX degradation to simulate geothermal heating cycles. Figure 4.1 shows the schematic diagram of the column setup. The soil columns were packed individually with coarse sand, fine sand, and silty loam soils (sieved through a 2 mm mesh). To isolate the effect of soil physicochemical properties (Table 5.4) on BTEX biodegradation and microbial growth among the different soils, all experimental and operational conditions were kept constant across the column experiments. Specifically, identical column dimensions, packing procedures, influent composition, flow rate, temperature regime, and incubation duration were used for all soils. The columns were packed using the same method and mass of soil to achieve comparable porosity and hydraulic conditions. The soil mass was chosen to target a porosity of <50% to maintain stable flow conditions and avoid pressure buildup, particularly in fine-grained soils. The soil was packed uniformly using lifts to target homogeneous porosity and to avoid preferential flow of water and contaminants through the column. Soil packing and saturation were performed according to (Martel & Gélinas, 1996). Briefly, soil columns consisted of a stainless-steel cylinder between two PTFE plates with a Teflon reservoir for the homogenous distribution of injected samples. To avoid water leakage and BTEX volatilization while experimenting, Vitton© O-rings were used with endplates to seal the cylinder completely. Soil packing was carried out by adding soil in layers of 1 cm and compacting 20 times with a plunger before adding the next layer. A stainless steel mesh was used at the bottom and top of the column to prevent the blockage of the inlet and outlet pipes

with soil. After packing, the columns were tested for any leaks by the air bubble method. Afterwards, CO_2 was circulated through the columns to remove trapped air from the void space at a pressure of 4 psi for 30 min. This helped with saturation, as CO_2 is a water-soluble gas and can dissolve in water.

Table 4.2: Details of column packing and the incubation method.

	Treatment	***Bacteria***	***Soil type***	***Temperature regime***
Column 1	Control	-	Coarse sand	Cyclic temperature
Column 2	Control	-	Coarse sand	Constant temperature
Column 3	Treatment	Consortia	Coarse sand	Cyclic temperature
Column 4	Treatment	Consortia	Coarse sand	Constant temperature
Column 5	Control	-	Fine sand	Cyclic temperature
Column 6	Control	-	Fine sand	Constant temperature
Column 7	Treatment	Consortia	Fine sand	Cyclic temperature
Column 8	Treatment	Consortia	Fine sand	Constant temperature
Column 9	Control	-	Silty loam	Cyclic temperature
Column 10	Control	-	Silty loam	Constant temperature
Column 11	Treatment	Consortia	Silty loam	Cyclic temperature
Column 12	Treatment	Consortia	Silty loam	Constant temperature
Column 13	Control	-	Coarse sand	Initial concentration (Day 0)
Column 14	Control	-	Fine sand	Initial concentration (Day 0)
Column 15	Control	-	Silty loam	Initial concentration (Day 0)

The columns were water-saturated by continuously flowing milliQ water (more than 5 PV) from the bottom using a peristaltic pump (MINIPULS 3, Gilson) at a rate of 1 mL/min. The columns' weight was measured at different time intervals until the weight of the columns stabilized, thus assuming that the soil column is fully saturated. After saturation, the porosity, pore volume

(PV), and bulk density of the column were calculated according to the following equations 4.9 – 4.11.

$$PV = \frac{m_{sat} - m_{dry}}{\rho_w} \quad (4.9)$$

$$n = \frac{PV}{V_{total}} \quad (4.10)$$

$$\rho_b = \rho_p(1 - n) \quad (4.11)$$

Where PV is pore volume (cm^3), m_{sat} is mass of packed column after saturation with water (g), m_{dry} is column mass before saturation (g), ρ_w is water density (1 g/cm^3), V_{total} is volume of column in cm^3, n is porosity (dimensionless), ρ_b is bulk density (g/cm^3), and ρ_p is particle density (2.65 g/cm^3). After complete saturation, PV is equal to the mass of water in g (water density 1 g/cm^3). The mass of water was converted into volume at ambient temperature to recalculate the porosity as shown in Table 4.3.

Table 4.3: Calculated parameters of packed columns.

Soil type	Column volume (cm^3)	Pore volume (cm^3)	Porosity (n)	Bulk density (g/cm^3)
Silty loam	144.244	68.4±1.02	0.474±0.01	1.395±0.21
Fine sand	144.244	65.5±1.71	0.454±0.00	1.447±0.19
Coarse sand	144.244	60.7±0.67	0.421±0.01	1.534±0.48

A total of 15 columns were prepared, including three that were opened on day 0 to know the initial BTEX concentration, and the rest continued according to their treatment details (Table 4.2). Two PV of BTEX solution at a concentration of 200 mg/L was injected into the columns to initialize contamination. The treatment columns were also injected with bacterial cells at 2% V/V along with nutrients. The columns were incubated at different temperatures in a cyclic form (from 5 °C to 40 °C and from 40 °C to 5 °C) to mimic the thermal plume effect on sorption and biodegradation with geothermal heating. This range reflects the thermal fluctuations typically found in a subsurface plume during active heating and recovery. Each temperature was maintained for 48 hours, enough time for 5 to 6 bacterial replication cycles based on typical

generation times of 7 – 8 hours, ensuring sufficient time to measure the impact of heat on microbial growth and BTEX degradation. Control columns at a constant temperature of 12 °C were used as a reference for the subsurface without geothermal heating. A steady 12 °C was selected based on the average annual temperature of the shallow subsurface (8 – 14 °C) to mirror the site's natural, undisturbed ground temperature (Z. Chen et al., 2004; Smith et al., 2023).

Once the experiments started, injections were done at a 1 mL/min flow rate. The lowest flow rate was selected that could be maintained by a peristaltic pump, and to approximate the slow groundwater velocities found in the subsurface systems. Two PV of BTEX solution at a concentration of 200 mg/L were injected into control columns, and 2 PV of BTEX solution (200 mg/L) with bacterial consortia (2 OD) were injected into the treatment columns. Following injection, columns were stored in chambers with regulated temperature. One set of columns was stored at changing temperature (5 – 40 °C and 40 – 5 °C), and one set was kept at a constant temperature (12 °C), as shown in Figure 4.1. After 48 hours, respective injections were made again, and outlet samples were collected for analysis. The outlet samples were analyzed for bacterial cell count using the colony-forming method, residual BTEX concentration using gas chromatography, and enzyme activity using spectrophotometry methods.

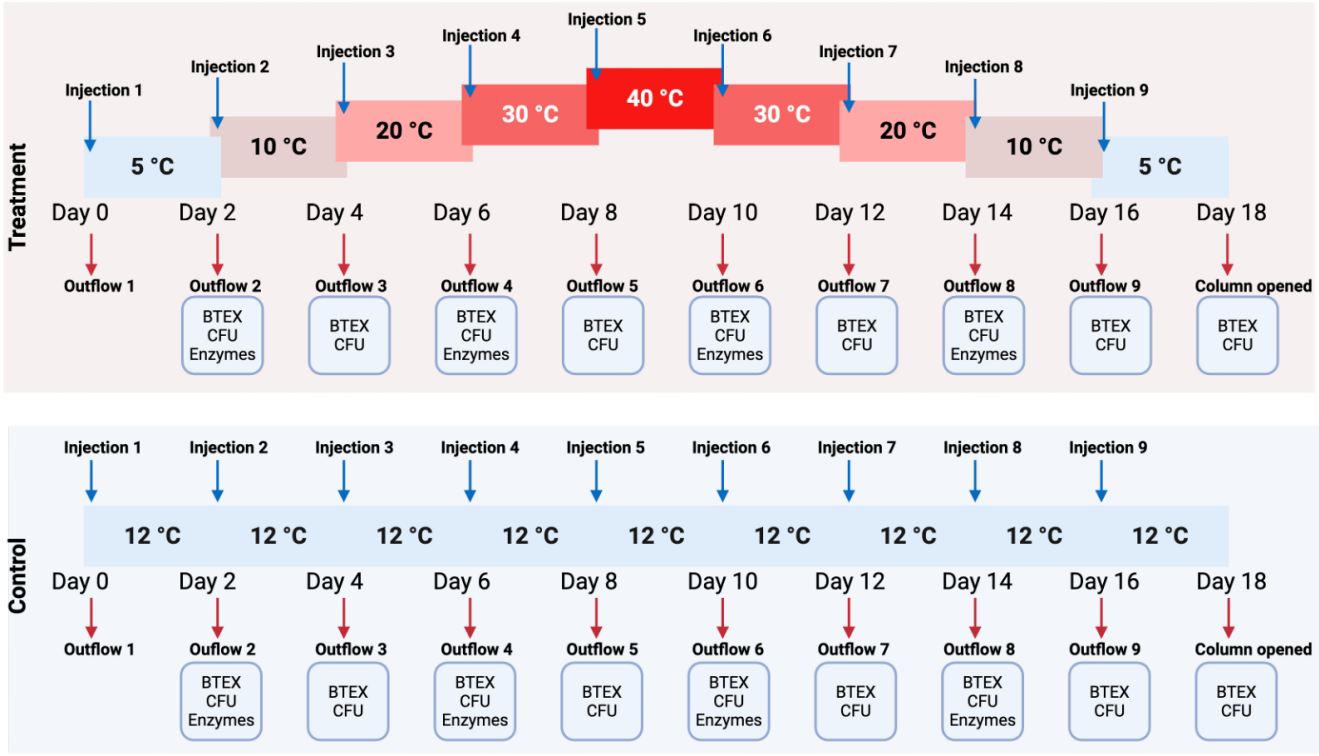

Figure 4.1: Schematic for the fed-batch soil column experiment with time of injection and sampling from outflow representing cyclic and constant temperature sets. The outlet samples were analyzed for BTEX concentration, Colony-forming units (CFU) for bacterial count and enzyme activity.

4.15 Enzymatic analysis

Biodegradation was mainly controlled by the microbial metabolism through intracellular and extracellular enzymes. Hence, to support the biodegradation in treated columns, enzyme activity was analyzed from the outlet samples of all control and treated samples at five time points corresponding to three temperatures, i.e., 5, 20, 40 °C, as shown in the Figure 4.1. Activity of major enzymes reported for BTEX degradation in literature, such as Catechol 1,2 dioxygenase (C1,2D), Catechol 2,3 dioxygenase (C2,3D), and Toluene monooxygenase (ToMO), was measured using the spectrophotometric method as per section 4.6. In short, the enzyme cocktail was prepared from bacterial cells of the outflow. The cells were sonicated at 20 kHz for 10 minutes with a 10-second on-and-off pulse cycle. The cellular lysate was used for the enzyme assay. For ToMO, the rate of change of toluene to p-cresol was quantified with a UV-visible spectrophotometer (GENESYS 50, Thermo Scientific). The reaction mixture was

prepared with 35 µL of N, N-dimethylformamide containing 4% (vol/vol) toluene, along with the cellular lysate, and incubated at 28 ± 1 °C. After incubation, a 1mL sample was mixed with 100 µL of 1 M NH_4OH, 2% 4-aminoantipyrine, and 8% $K_3Fe(CN)_6$, followed by centrifugation at 14,000 × g and direct absorbance measurement at 500 nm. A reference curve was created using concentrations of p-cresol ranging from 0 to 50 µg/mL as the reaction product. For C1,2D and C2,3D activity, the reaction was prepared by adding 0.6 mL catechol (10 mM), 2.0 mL phosphate buffer, and 0.4 mL cellular lysates. The conversion rate of catechol to muconic acid at 260 nm and 2-hydroxymuconic semialdehyde at 375 nm was measured (Y. Li et al., 2014).

Objective 4: Investigate geothermal heating impacts on soil microbiome communities along with the borehole depth by 16S rRNA sequencing.

4.16 Soil treatment with BTEX at different temperatures

Six soil samples were collected – three from each borehole. Two treatment sets were prepared: uncontaminated soil (without BTEX) and BTEX-treated soils at three different temperatures (15, 28, and 40 °C) as shown in Table 4.4. To represent the upper, mid, and lower parts of the 280 ft geothermal borehole profile, soil samples were taken from depths of 10, 120, and 240 ft in each borehole. Because subsurface environments frequently display vertical gradients in factors that strongly control biodegradation (such as organic carbon availability, oxygen/redox conditions, moisture content, nutrient availability, and sorption capacity), this stratified approach was chosen to assess how indigenous microbial communities and BTEX biodegradation potential vary with depth. Instead of using a continuous profile, the study sampled three representative depths, which allowed to capture depth-driven community alterations. For the treated samples, 1 g of each soil type was added to 20 mL vials, supplemented with 10 mL MSM media, and then spiked with 200 mg/L BTEX (1:1:1:1). After 200 mg/L BTEX supplementation, the GC vials were crimp-capped with Teflon septum caps to avoid the volatilization loss of BTEX. Control samples (uncontaminated soil) without BTEX were prepared in a similar manner. The soil samples were incubated for two months at the specified temperature and then used for downstream processing in metagenomics.

Table 4.4: Experimental treatment details for soil spiked with BTEX at different temperatures and depths.

Soil sample	Borehole	Depth (feet)	Soil type	BTEX (mg/L)	Temperature (°C)
SS1	BH1	10	Fine sand	-	15, 28, 40
SS2	BH1	120	Silty loam	-	15, 28, 40
SS3	BH1	240	Fine sand	-	15, 28, 40
SS4	BH2	10	Fine sand	-	15, 28, 40
SS5	BH2	120	Fine sand	-	15, 28, 40
SS6	BH2	240	Silty loam	-	15, 28, 40
SS7	BH1	10	Fine sand	200	15, 28, 40
SS8	BH1	120	Silty loam	200	15, 28, 40
SS9	BH1	240	Fine sand	200	15, 28, 40
SS10	BH2	10	Fine sand	200	15, 28, 40
SS11	BH2	120	Fine sand	200	15, 28, 40
SS12	BH2	240	Silty loam	200	15, 28, 40

** Each set incubated separately at 15, 28 and 40 °C

4.17 DNA extraction

For metagenomic analysis, genomic DNA (gDNA) was isolated from the BTEX-treated and uncontaminated soil samples using a DNA Isolation Kit according to the manufacturer's protocol (Quick-DNA Soil Microbe MicroPrep Kit from Zymo Research, New England). The purity and concentration of extracted DNA were analyzed by Nanodrop 2000 (Thermo Scientific, USA), and the extracted DNA was amplified for 16S rRNA using universal primers 27 F (5′-AGAGTTTGATCCTGGCTCAG-3′), 1492 R (5′-GGTTACCTTGTTACGACTT-3′) by Polymerase Chain Reaction (PCR).

4.18 Illumina 16S rRNA sequencing

Next-generation sequencing was performed to investigate the impact of BTEX and temperature on the taxonomic composition of the microbial community. To analyze the major communities

of bacteria present at different depths, the V4 region of the 16S rRNA gene was amplified using 515F- GTGYCAGCMGCCGCGGTAA and GGACTACNVGGGTWTCTAAT, then the amplified sequences were analyzed by the IlluminaMiSeqq platform (Metagenomics Facility at McMaster University, Canada). The process of demultiplexing was carried out for sequence runs using Illumina's Casava software. Then, the cutadapt tool was used to remove primers from the sequencing data. The filtered and trimmed forward and reverse paired-end reads at the opposing primers proceeded in DADA2. The chimeric sequences were removed, and the output sequences were clustered into operational taxonomic units (OTUs) at a 97% threshold using Abundant OTU+. The output sequences were identified taxonomically using the SILVA 132 database (version 4).

4.19 Data Compilation

The results were analyzed using the web-based software Microbiome Analyst to determine the taxonomic composition and diversity of the microbiome data, community abundance, OTU counts, and alpha and beta diversity analysis (Chong et al., 2020). Prior to the computation of microbial diversity, the data were filtered and normalized. Data filtering aims to remove low-quality or uninformative features to improve downstream statistical analysis. Low count features with a minimum count of 100 and low variance features with less than 10% cutoff, measured using *inter-quantile range (IQR)*, were removed. Likewise, normalization aims to address the variability in sampling depth and the sparsity of the data, enabling more biologically meaningful comparisons. The data was rarefied by the data scaling method, as rarefying is mainly used for 16S marker gene data to perform accurate statistical analysis.

Alpha diversity profiling was performed at the genus level using the Fisher index for diversity measure and the T-test/ANOVA for statistical analysis. The Bray-Curtis Index was used for beta diversity profiling, employing the PCoA (Principal Coordinates Analysis) ordination method and PERMANOVA (Permutational Multivariate ANOVA) statistical method. MaAsLin2 (Microbiome Multivariable Association with Linear Models) was used to determine the multivariable association between metadata, metagenomics features, covariates, and BTEX exposure. This model is a comprehensive R package that utilizes general linear models to fit microbial features.

Phylogenetic trees: For the evolutionary analysis of the microbiome, phylogenetic trees were made using MEGA 7 (Molecular Evolutionary Genetics Analysis Version 7). OTU sequence was saved as a Notepad file, and sequences were aligned using the Muscle tool (Multiple Sequence Comparison Log-Expectation) on MEGA 7 software. Phylogeny was constructed for each sample by the neighbour-joining algorithm with the Bootstrap method. Phylogeny revealed ancestral relationships by clustering the most closely related taxa into different clades, based on a similarity percentage of sequences with 1000 bootstraps.

Random Forest modelling: Random Forest is a supervised learning algorithm which combines the output of multiple decision trees to reach a single result. In this study, a random forest model was employed to investigate the correlation between physicochemical parameters and microbial diversity using an online GitHub tool.

4.20 Analytical methods

BTEX analysis: Headspace Gas chromatography (HS-GC) samples for residual BTEX quantification were prepared in 20 mL HS-GC vials. HS-GC vials were prepared by adding 5 mL of distilled water, followed by 100 µL of sample taken from each serum bottle with a gas-tight syringe. Lastly, 50 µL of D5 Fluorobenzene, used as an internal standard from a stock solution of 4 mg/L, was added to the vials. HS-GC vials were capped with air-tight metallic crimp caps and stored at 4 °C until analyzed.

For objective 1, the BTEX degradation rate was measured using a GC-MS (Clarus 500 (PerkinElmer) coupled with a headspace system (TurboMatrix 40 Trap (PerkinElmer)) at INRS, Quebec. The headspace system has a temperature of 90±1 °C and 120±1 °C for the needle and transfer line, respectively. The sample was heated and shaken for 10 minutes at 80±1 °C in an oven, then collected with a needle and transferred to the column. Analysis was performed using helium as the carrier gas at a flow rate of 2 mL/min, a 50:1 split ratio, and an inlet temperature of 180 °C. The oven was operated using a Chrom-624 (30 m x 0.25 mm x 1.4 µm) column at an initial temperature of 45 °C, held for 4 minutes, and then raised to 145 °C for 2 minutes at a rate of 17 °C/min. The BTEX was detected with an MS (Mass Spectrometry) detector using scan mode (40-150 m/z). A standard curve was prepared using standard concentrations and was used to calculate the concentration of compounds from their corresponding peak areas.

For objectives 2, 3, and 4, BTEX concentrations were analyzed using Headspace Gas Chromatography-Flame Ionization Detector (GC-FID) (Agilent Technologies, Canada) at York University. The autosampler (PAL-RSI) was equipped with an instrument for efficient and precise headspace gas-phase sampling. A method for BTEX quantification was developed on the OpenLab Chemstation software. Detailed information on instrument configuration and detection method used for BTEX analysis is provided in the *Appendix A*. Each time, standard samples were analyzed to prepare a standard curve with $R^2 > 0.95$ for each BTEX compound, allowing for the estimation of the unknown concentration of BTEX in samples.

Metal analysis: HMs and iron content in soil were analyzed by Inductively coupled plasma-optical emission spectroscopy (Agilent 5110 ICP-OES Dual View).

Ion analysis: Nitrate and sulfate content of the soil was measured with Ion chromatography (Dionex Integrion HPIC, Thermo Fisher Scientific).

Metabolite analysis: The metabolomics analysis for metabolites or intermediate compounds' identification was performed with Liquid chromatography with tandem mass spectrometry (LC-MS-MS) (ZenoToF™ 7600 from Sciex). The samples from treatments were centrifuged at 1000 x g for 10 minutes, and the supernatant was filtered through a 0.22 µm syringe filter. The filtrate was analyzed for metabolites using both positive and negative polarity ionization modes with a 1-hour gradient. The detected compounds were identified with the NIST (National Institute of Standards and Technology) Library.

4.21 Statistical analysis

The results of all experiments were recorded as the average of triplicates, with their standard deviations. The significance of the calculated parameters was confirmed by calculating the R^2 (R-squared or the coefficient of determination) value as follows in equation 4.12:

$$R^2 = 1 - \frac{S^2(residual)}{S^2(total)} \qquad (4.12)$$

Where S^2 is the sum of squares. Using the software Origin 2023b, ANOVA was employed to establish a 95% confidence interval for each parameter calculation to compare statistical data.

ANOVA was used to determine their statistical significance with a *p*-value of 0.05 as the level of significance.

In soil column experiments, all experiments were performed in duplicate with three technical replicates. The average of the replicates was calculated, along with the standard deviation. The significance of the data was analyzed using the p-test and t-test with ANOVA in Origin and Microsoft Excel.

CHAPTER 5: RESULTS AND DISCUSSION

Objective 1: Identify novel BTEX-degrading strains from subsurface soil: Isolation, Identification and Growth Evaluation

This objective focused on isolating and selecting soil bacteria from geothermal borehole soils capable of degrading BTEX compounds and performing at different temperatures. The results are published as a peer-reviewed article in "*Environmental Pollution*" with DOI: https://doi.org/10.1016/j.envpol.2023.122303

Background

Monoaromatic hydrocarbons such as BTEX are high-risk pollutants because of their mutagenic and carcinogenic nature. These pollutants are found with elevated levels in groundwater and soil in Canada at several contaminated sites. The intrinsic microbes present in the subsurface have the potential to degrade pollutants by their metabolic pathways and convert them to non-toxic products. However, the low subsurface temperature (5 – 10 °C) limits their growth and degradation ability. This study examined the feasibility of subsurface heat augmentation using geothermal heating for BTEX bioremediation. Novel potent BTEX-degrading bacterial strains were isolated from soil at 3.0, 42.6, and 73.2 m depths collected from a geothermal borehole during installation and screened using an enrichment technique. The selected strains were identified by Sanger sequencing and phylogenetic analysis, revealing that all strains except *Bacillus subtilis* are novel for BTEX degradation. The isolates, *Microbacterium esteraromaticum* and *Bacillus infantis,* showed the highest degradation with 67.98 and 65.2% for benzene, 72.8 and 71.02% for toluene, 77.52 and 76.44% for ethylbenzene, and 74.58 and 74.04% for xylenes, respectively. Further, temperature influence at 15±1 °C, 28±1 °C and 40±1 °C was observed, which showed increased growth by two-fold and on average 35 – 49% more biodegradation at higher temperatures. Results showed that temperature is a positive stimulant for bioremediation, hence geothermal heating could also be a stimulant for ISB.

Results and discussion

5.1 Microbial isolation and identification

The number of isolated aerobic BTEX-degrading strains in treated soils was 70-fold lower than in the untreated soils (*Appendix B,* Figure B2). Only the bacteria which can consume or degrade BTEX survived in the BTEX-treated soils after a month of incubation and while others diminished. Such bacteria could utilize hydrocarbons as their carbon and energy source for growth and then metabolize them into non-toxic products. The primary pathway of aerobic degradation that led to mineralization is bound to two enzymatic groups: dioxygenase and monooxygenase (H. A. Hassan & Aly, 2018; Siqueira et al., 2018).

For the identification of isolates, 16S rRNA was sequenced and aligned using Blastn. For each isolate, five strains with the highest similarities (Percent identity > 98% and Query cover > 97%

(Except for sample 7)) were selected and used for phylogenetic tree analysis using the neighbour-joining algorithm with 1000 bootstraps in MEGA 7.0 software (Figure 5.1). Based on the highest fit match, the isolates are identified as follows in Table 5.1. Five strains are identified as *Microbacterium paraoxydans* from different soil depths, and most strains are mostly novel and least studied concerning their BTEX degradation ability, except *Bacillus subtilis*. 16S rRNA was submitted to GenBank (NCBI- National Center for Biotechnology Information), and an accession number has been assigned to each isolate (Table 5.1).

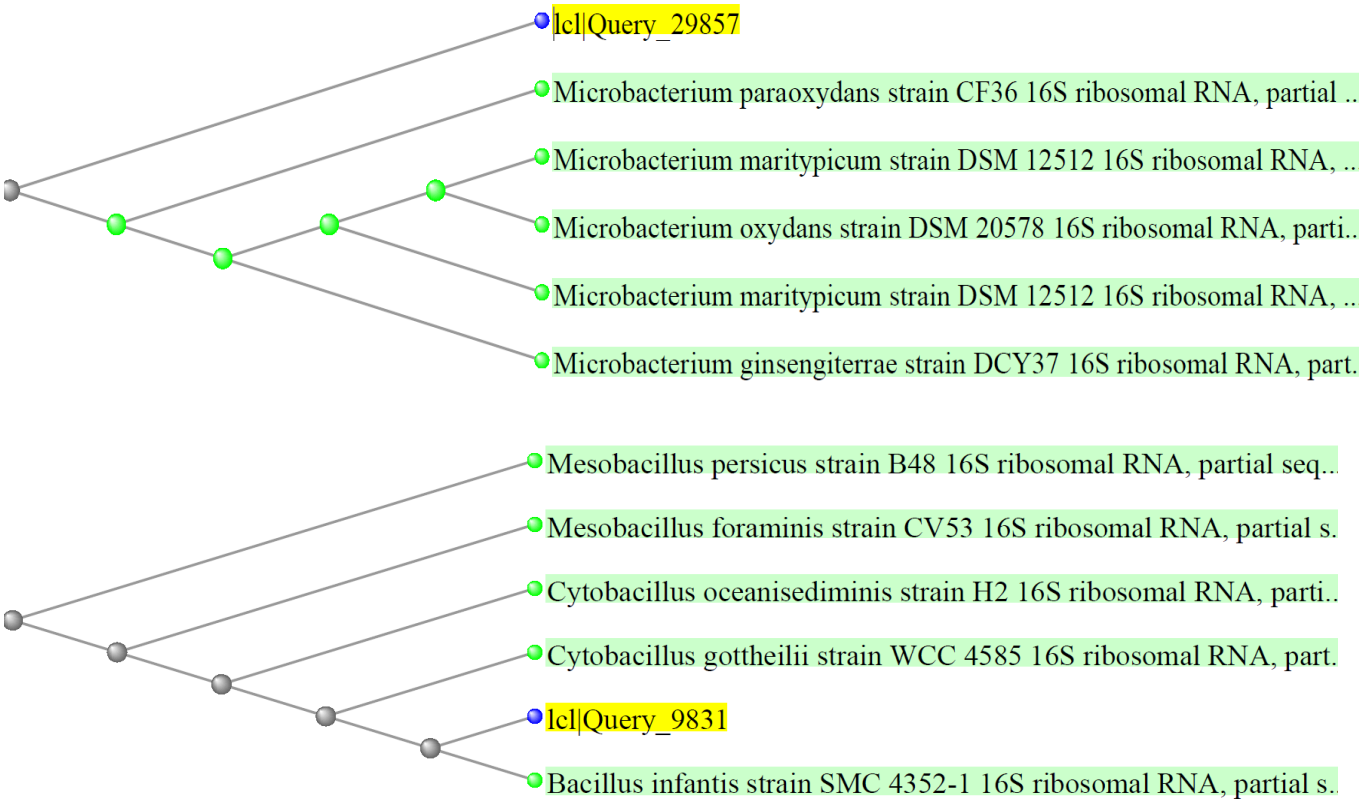

Figure 5.1: Phylogenetic tree of the identified sequence of *Microbacterium paraoxydans* and *Bacillus infantis* with 1000 bootstraps in MEGA 7.0 software (for other strains, it is provided as Figure B4 in *Appendix B*).

Table 5.1: Identification of soil-isolated strains using Blastn from NCBI.

Sample		Identity	Percent identity (%)	Query cover (%)	Accession Number by GenBank
Pseudomonas putida		*Pseudomonas putida*	99.42	97	OQ581996
Borehole 1 3.0 m	1	*Microbacterium paraoxydans*	99.42	97	OQ582075
	2	*Microbacterium paraoxydans*	98.48	97	OQ582076
42.6 m	3	*Bacillus subtilis*	98.19	97	OQ582077
	4	*Microbacterium esteraromaticum*	99.06	97	OQ582078
73.2 m	5	*Microbacterium paraoxydans*	98.27	98	OQ582079
	6	*Microbacterium lacusdiani*	98.71	97	OQ582080
Borehole 2 3.0 m	7	*Nocardia asteroides*	97.85	90	OQ582088
	8	*Peribacillus simplex*	98.98	97	OQ582089
42.6 m	9	*Microbacterium maritypicum*	98.59	97	OQ582090
	10	*Microbacterium paraoxydans*	98.58	96	OQ582091
73.2 m	11	*Bacillus infantis*	98.95	95	OQ582092
	12	*Exiguobacterium mexicanum*	99.11	97	OQ582093

5.2 Growth kinetics at different temperatures

The growth kinetics of the 12 isolated strains showed sigmoidal growth with similar cell counts within 48 hours at 28±1 °C. The results (Figure 5.2) clearly show the influence of temperature on growth. As a low temperature of 15±1 °C is a growth challenge for the bacteria, a decline in growth, especially in the lag phase, was observed. At 15±1 °C, the lag phase is comparatively long in comparison to the optimum temperature of 28±1 °C, but at 40±1 °C, the lag phase of fewer than 4 hours was observed. A small lag phase suggested the bacteria's acclimatization towards the initial BTEX concentration in the media. All the strains show good growth at 40±1

°C, but some of the strains including *Pseudomonas putida* and *Peribacillus simplex*, which show highest at 15±1 °C, didn't reach the maximum O.D. at 40±1 °C. On average, a 30% decline in growth has been observed for all other isolates at 15±1 °C. But from the comparison of all three temperatures, strains like *Microbacterium esteraromaticum, Peribacillus simplex,* and *Bacillus infantis* show good growth at all temperatures. Among the 12 strains, all four strains of *Microbacterium paraoxydans* showed significantly high growth at the highest temperature with a p-value of 0.001 at α=0.05, whereas in the case of *Bacillus subtilis, Exiguobacterium mexicanum, Peribacillus simplex* no significant difference of growth in different temperatures was observed. A 5±2% decrease has been seen for the treated samples in comparison to the control (without BTEX).

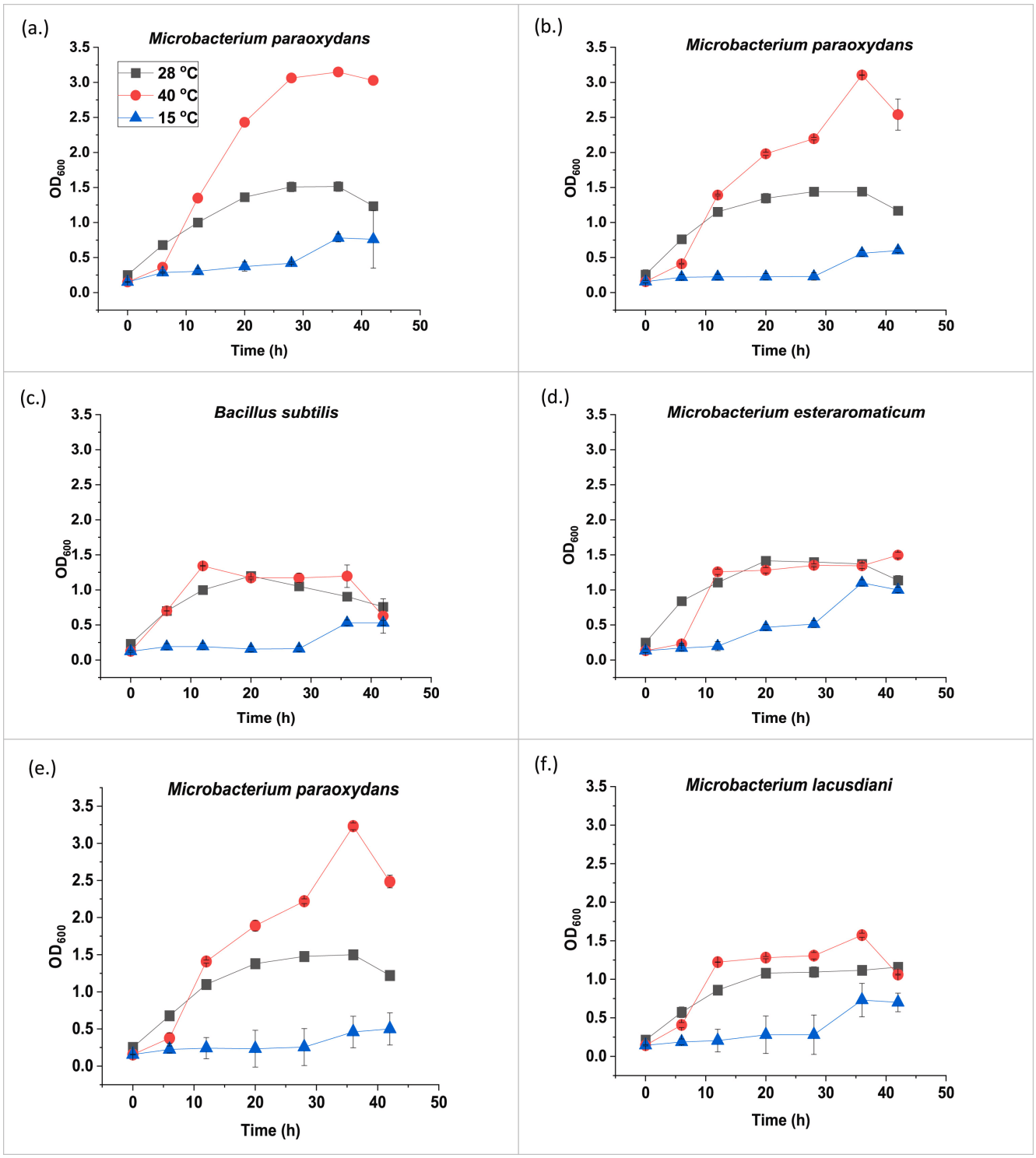
(a.)
Microbacterium paraoxydans
28 °C
40 °C
15 °C
OD600
Time (h)
(b.)
Microbacterium paraoxydans
OD600
Time (h)
(c.)
Bacillus subtilis
OD600
Time (h)
(d.)
Microbacterium esteraromaticum
OD600
Time (h)
(e.)
Microbacterium paraoxydans
OD600
Time (h)
(f.)
Microbacterium lacusdiani
OD600
Time (h)

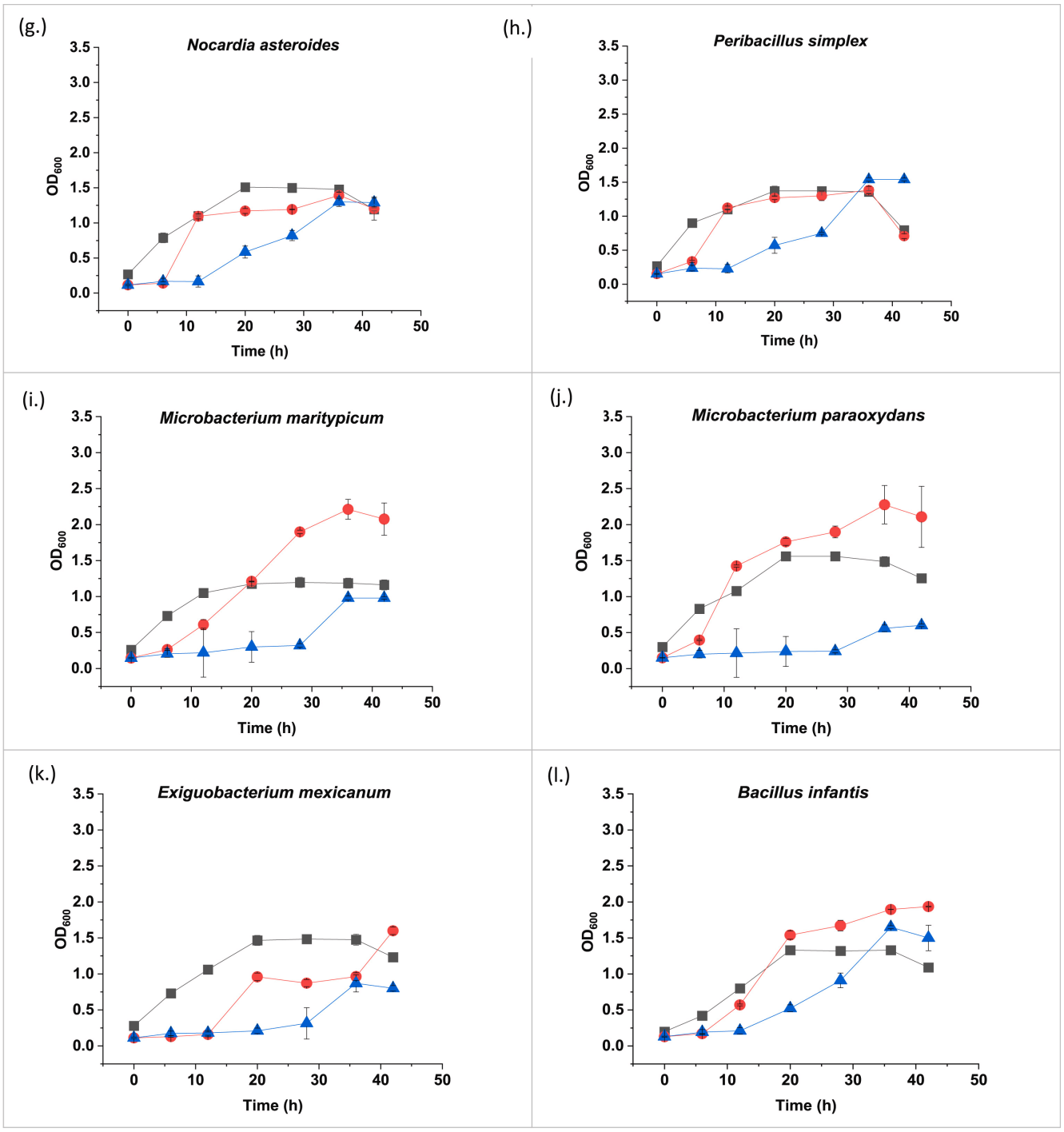
(g.)
Nocardia asteroides
(h.)
Peribacillus simplex
(i.)
Microbacterium maritypicum
(j.)
Microbacterium paraoxydans
(k.)
Exiguobacterium mexicanum
(l.)
Bacillus infantis
OD600
Time (h)

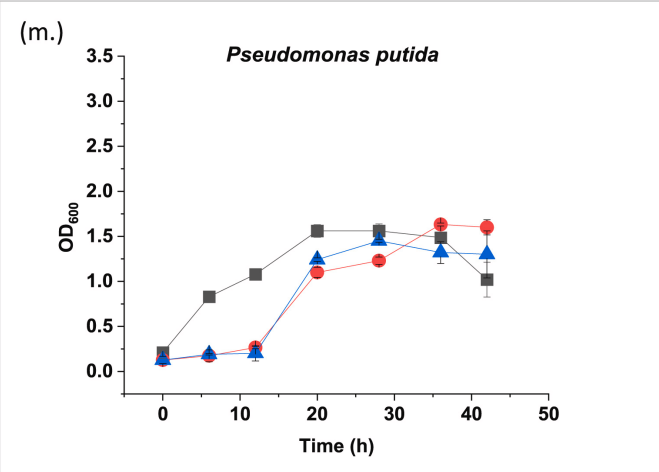

Figure 5.2: Isolate growth rate at temperatures found in the subsurface with a working Geothermal heat pump.

Table 5.2 also shows that the increasing temperature results in a higher specific growth rate and lower duplication time. This data demonstrates that when the temperature increases due to the injected heat from a GHP system, the bacterial community will proliferate at a faster rate within a small period. This in turn can lead to a decrease in substrate/pollutant molecules as they are metabolized into non-toxic compounds. The correlation study indicated that as the growth rate of microbes increased, the biodegradation rate also increased, showing a positive correlation (*Appendix B*, Figure B6).

Table 5.2: Growth parameters of selected strains at different temperatures

	Temperature (°C)	**μ (h^{-1})**	**T_d (h)**
Microbacterium esteraromaticum	15	0.063	11.00
	28	0.092	7.533
	40	0.099	7.00
Bacillus infantis	15	0.075	9.240
	28	0.095	7.295
	40	0.104	6.663
Pseudomonas putida	15	0.080	8.652
	28	0.083	8.329

40	0.091	7.615

At lower temperatures, the metabolic activity of microorganisms is generally slower, which can result in a slower growth rate. It is likely that cold temperatures may severely impact cellular function, which could be the cause of lower growth and biodegradation at 15±1 °C. This cellular function includes alteration in solute transport rates, enzyme kinetics, breakdown of macromolecules, solidification and stabilisation of membrane fluidity (M. Wang et al., 2017; Welander, 2005).

5.3 BTEX degradation ability of isolates

The biodegradation of all four BTEX compounds shows a sharp decline from the initial concentration of 50 mg/L of each four compounds, within 24 hours, with more than 65% degradation. The rate of biodegradation was the highest for ethylbenzene and decreased as follows: ethylbenzene > xylenes > toluene > benzene. Benzene seems to be recalcitrant as the residual benzene concentration was relatively higher as compared to the other three compounds in all treated cultures after 24 and 48 hours as shown in Figures 5.3 and 5.4. This could be due to the chemical stability of benzene, as it doesn't have any potential reactive substituent and has stabilized structure by the π-electron aromatic ring system (C. Vogt et al., 2011). The other possible reason could be competitive inhibition or substrate inhibition (El-Naas et al., 2014). The isolates *Microbacterium esteraromaticum* and *Bacillus infantis* showed the highest degradation potential with 67.98, 72.8, 77.52, 74.58 and 65.2, 71.02, 76.44, 74,04% for benzene, toluene, ethylbenzene, and xylenes respectively, as such these strains were selected for further analysis. The complete degradation pattern of these two strains and *Pseudomonas putida* is illustrated in Figure 5.4, where around overall 75-85% degradation was noticed after 48 hours for all four compounds. For individual compounds, Benzene showed the lowest degradation rate with approximately 75% within 48 hours, while for toluene, ethylbenzene and xylene, a 90% decline in concentration was observed (Figure 5.4). A 7% loss has been observed in controlled samples due to volatilization. To calculate the residual BTEX concentration in samples, calibration curves were prepared using a standard solution with known BTEX concentration (*Appendix B*, Figure B5).

Similar findings of intrinsic microbes' BTEX degradation ability has been previously reported by several articles (Benedek et al., 2021; Chicca et al., 2020b; Hocinat et al., 2020; Khodaei et al., 2017b; Wongbunmak et al., 2017a, 2020).

Based on the growth ability at all temperature ranges and high BTEX degradation rate, *Bacillus infantis* and *Microbacterium esteraromaticum* were selected for further analysis along with a consortium of all 12 isolates. *Bacillus infantis* is a rod-shaped, gram-positive, aerobic, catalase-positive, and endospore-forming bacteria. It is previously known to have a dye degradation ability (W.-Y. Chen et al., 2013). *Bacillus infantis* is a facultative aerobic bacterium meaning it can survive even if little oxygen is available in its surroundings. The sample for our experiment was taken from 70 meters below the ground, and there have been instances where species of *Bacillus* was taken even further down the surface level of Earth. For instance, Logan & Vos (2015), isolated *Bacillus infernus*, from Triassic shales at depths of around 2.7 km below the land surface. They also isolated *Bacillus subterraneus*, at depths of 2 km in the Great Artesian Basin of Australia (Logan & Vos, 2015) and live *Bacillus* has been extracted from the soil more than 1000 meters deep.

Microbacterium esteraromaticum is also a gram-positive, rod-shaped rhizosphere bacterium, previously reported for the ability to degrade organophosphorus, organosulfur, and aromatic compounds. Likewise, *Microbacterium esteraromaticum* was reported to found at ex-situ landfarming or *in-situ* hydrocarbons bioremediation sites in the central Patagonia, Argentina, and has the ability to proliferate in different temperature and salinity variations that takes place (Logeshwaran et al., 2020). A genomic study by Panneerselvan et al. showed that the presence of monoamine oxidase, gentisate 1,2-dioxygenase, shikimate 5-dehydrogenase, catechol 1,2-dioxygenase, salicylate hydroxylase, and phosphopyruvate hydratase (Panneerselvan et al., 2018). To the best of our knowledge, no study was conducted with *Bacillus infantis* for BTEX degradation analysis, however, there is only one report with *Microbacterium esteraromaticum*. The mentioned study isolated *M. esteraromaticum* SBS1-7 from estuarine sediment in Thailand. They reported the biodegradation of all BTEXs compounds, in both liquid medium and soil slurry systems with the help of monooxygenase and dioxygenase enzymes (Wongbunmak et al., 2017a).

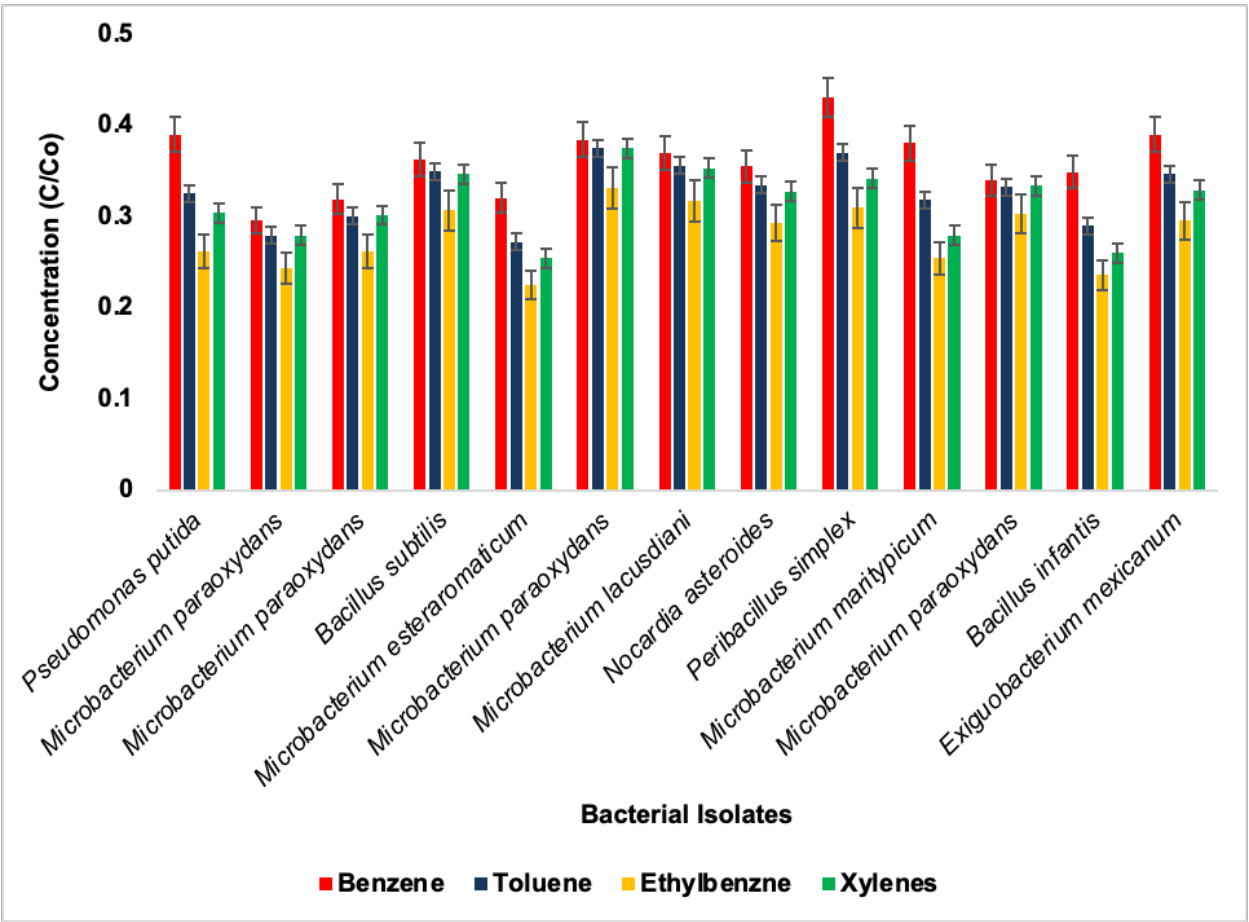

Figure 5.3: Biodegradation of BTEX by bacterial isolates after 24 hours of treatment; C and C_o represent actual concentration at different sampling times and the initial concentration (50 mg/L of each BTEX compound, respectively).

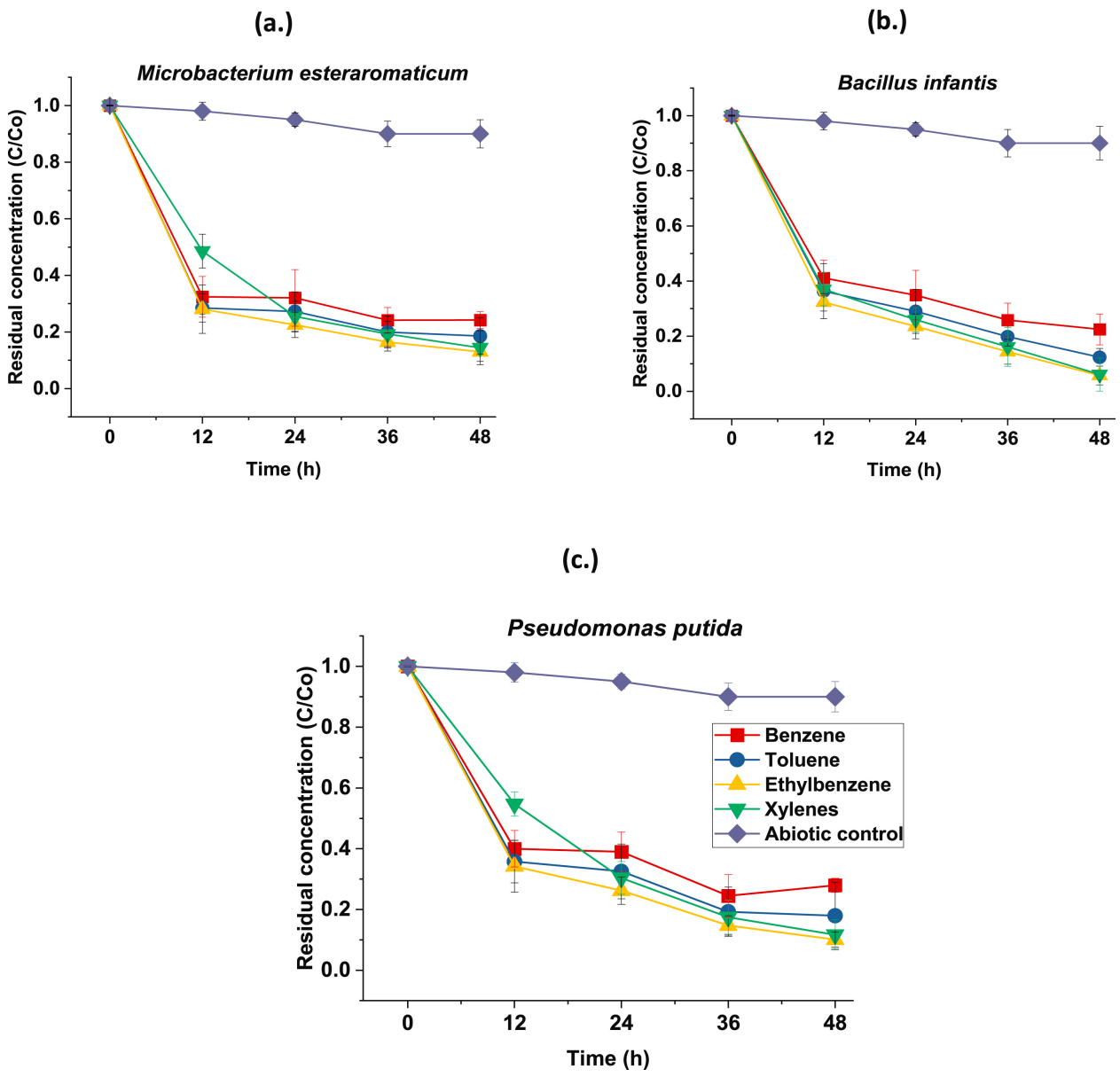

Figure 5.4: Complete BTEX-degradation pattern of: (a). *Microbacterium esteraromaticum*, *(b). Bacillus infantis* and *(c). Pseudomonas putida*. C and C_o represent the actual concentration at different sampling times and the initial concentration, respectively.

5.4 Effect of temperature on BTEX biodegradation

The growth of microbes depends on several factors including temperature, as each microorganism needs an optimum temperature for multiplication. Enhanced growth corresponds to higher degradation; therefore, temperature is a key factor in biodegradation. As

an illustration, increased temperature enhances the activity of mesophilic and thermophilic microorganisms, which can help to decontaminate brownfield sites as these microorganisms are in a proactive state. It is important to note that the optimal temperature for biodegradation may vary depending on the specific microorganisms that are present, and the type of compound being degraded (Benedek et al., 2021; Godin et al., 2020).

The results from the degradation pattern at three different temperatures showed that with an increase in temperature (15±1 °C to 28±1 °C), the biodegradation of all four BTEX compounds increased significantly ($p < 0.005$) for all bacteria except for *Microbacterium esteraromaticum*. However, when degradation was observed at 40±1 °C, a higher degradation with 35.87, 21.05, 34.72 and 41.24% for benzene; 42.03, 27.26, 38.83, and 47.24% for toluene; 47.89, 34.42, 43.96 and 51.51% for ethylbenzene; and 46.19, 30.66, 40.99 and 49.44% for xylenes was observed for *Pseudomonas putida*, *Microbacterium esteraromaticum*, *Bacillus infantis*, and consortia-treated cultures respectively (Figure 5.5).

The positive relationship between temperature and biodegradation rate is observed because most microorganisms that can degrade BTEX are mesophiles, which means they grow best at moderate temperatures between 20 – 40 °C. At temperatures outside of this range, the growth and metabolic activity of these microorganisms may be inhibited, resulting in a slower rate of biodegradation (as seen in the 15 °C experiments). A study by Deeb and Alvarez-Cohen showed also that the aerobic degradation of BTEX by *Rhodococcus rhodochrous* and toluene-enriched consortia has exhibited high degradation at 35 °C in comparison to 20 °C (Deeb & Alvarez-Cohen, 1999a). Likewise, a response surface methodology study by Khodaei et al. showed the optimized temperature of 28.9 °C for *Pseudomonas sp.* BTEX-30 (Khodaei et al., 2017b). Furthermore, an aerobic biodegradation study reported benzene and toluene degradation by an enrichment culture obtained from the salt flats showed higher degradation at 37 °C when analyzed at different temperatures ranging from 5 to 60 °C (Nicholson & Fathepure, 2005).

Results in Figure 5.5 showed that the increasing temperature had a positive correlation with the degradation of all four BTEX compounds. The biodegradation for all compounds and all the treated groups at 15±1 °C is significantly lower than at 40±1 °C, with a p-value of 0.00156.

Further, the correlation between the biodegradation percentage of BTEX and the growth of bacteria in optical density at 600 nm was observed in Origin graphs using linear fitting at all three different temperatures after 24 h of incubation. Fitting showed a linear correlation with an R-squared (coefficient of determination) value of 0.94 and Pearson's coefficient of 0.97, (*Appendix B*, Figure B6).

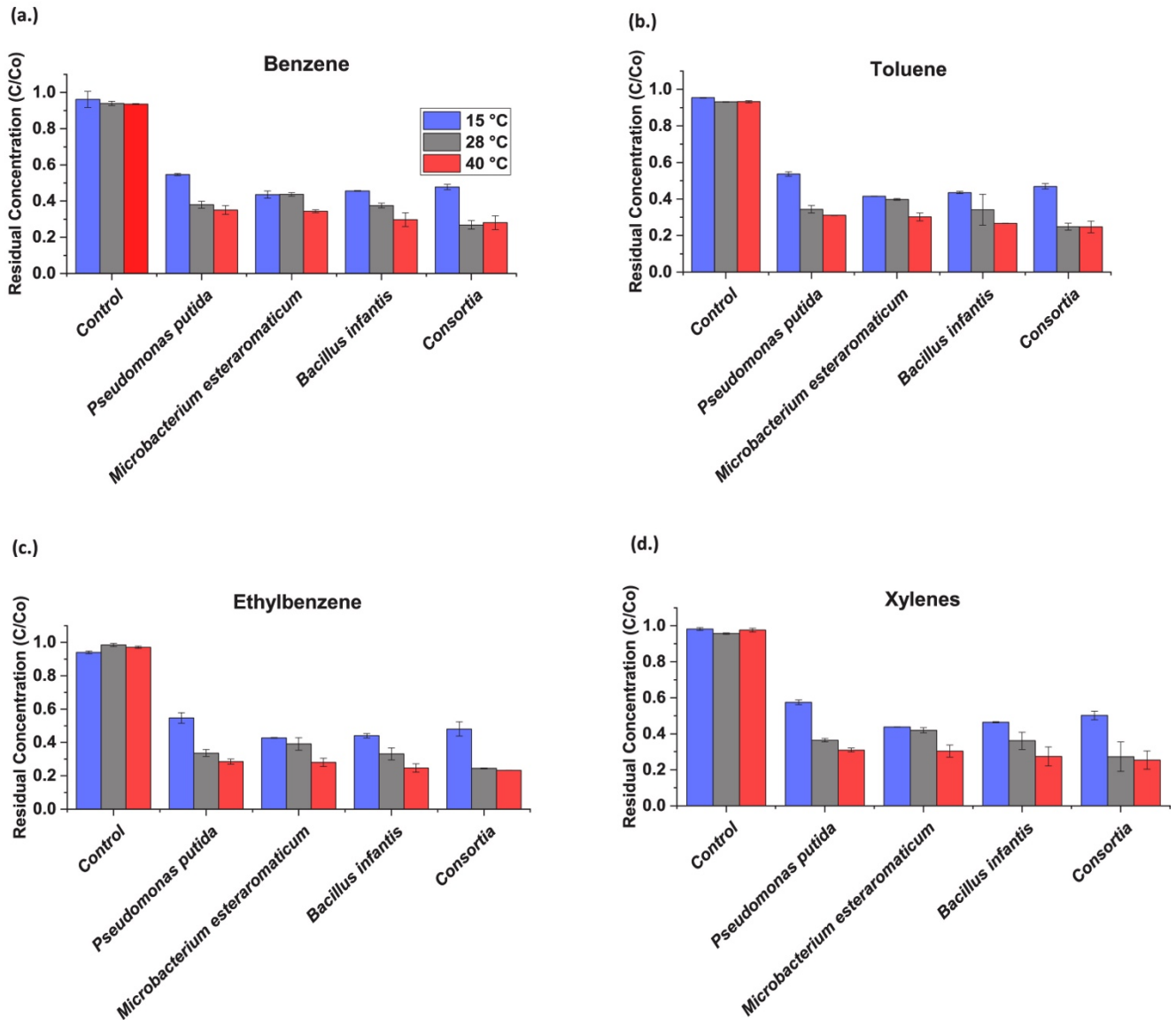

Figure 5.5: Effect of temperature on the degradation of: (a). Benzene, (b). Toluene, (c). Ethylbenzene, and (d). Xylenes by *Pseudomonas putida, Microbacterium esteraromaticum, Bacillus infantis* and Consortia. C and C_o represent the actual concentration after 24 hours of biodegradation and the initial concentration, respectively.

5.5 Enzymatic activity

In aerobic BTEX biodegradation processes, intermediate catecholic or non-catecholic compounds are formed by mono-oxidizing the alkyl side chains. The key stage in detoxification is the ortho, meta, or para cleavage of aromatic ring of the core intermediates by catechol dioxygenases. Most of the BTEX biodegradation pathways involve several monooxygenases and dioxygenases that attack the aromatic hydrocarbon ring (Leung et al., 2019; Miri et al., 2019). For example, it is reported that *Pseudomonas stutzeri* OX1 can oxidize the individual BTEX compounds by toluene o-xylene monooxygenase (ToMO) (Cafaro et al., 2004). Likewise, *Paraburkholderia aromaticivorans* BN5, a strain isolated from petroleum-contaminated soil showed the gene cluster encoding 29 monooxygenase including Toluene monooxygenase which tends to degrade BTEX and naphthalene (Y. Lee et al., 2019)

Toluene/*o*-Xylene Monooxygenase (ToMO) can metabolize a variety of aromatic compounds including BTEX. In two subsequent monooxygenation processes, ToMO is capable of hydroxylating more than one position of an aromatic ring. Catechol 1,2-dioxygenase (C1,2D) and Catechol 2,3-dioxygenase (C2,3D) are iron-containing enzymes able to cleave the ring of catechol (the converted product from ToMO) for complete detoxification of BTEX. Many studies have reported the role of C1,2D and C2,3D in the biodegradation of BTEX by meta-cleavage pathway (Chicca et al., 2020b; H. A. Hassan & Aly, 2018; Miri et al., 2021; Wongbunmak et al., 2020).

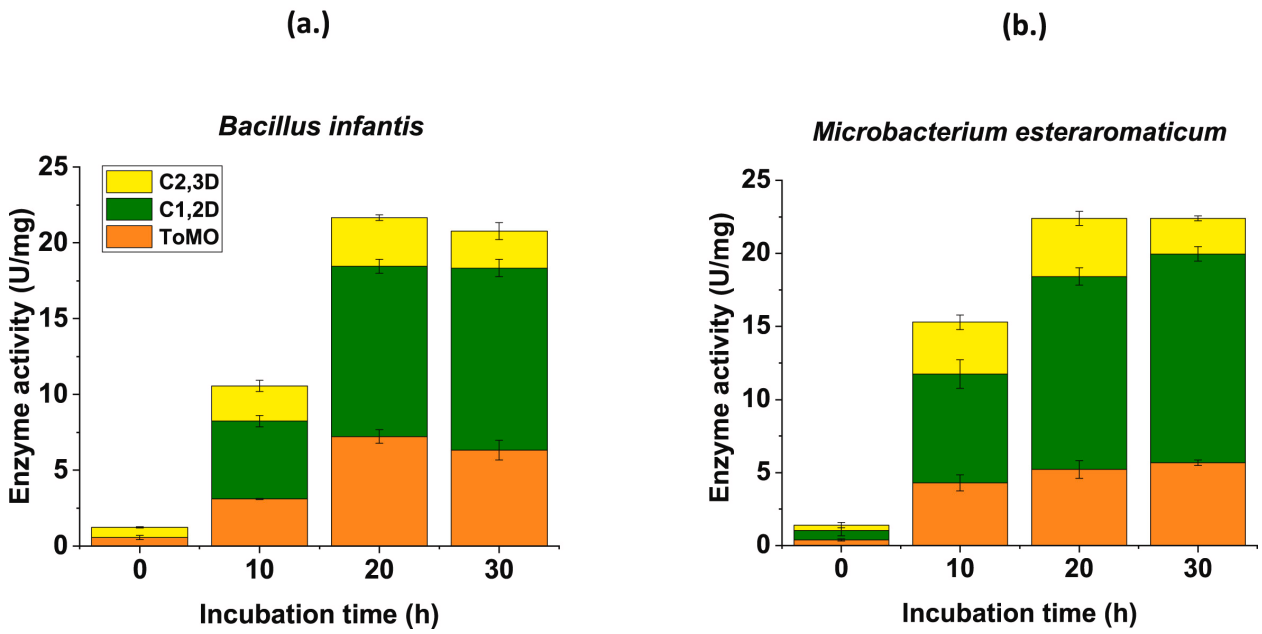

Figure 5.6: Enzymatic activity of Toluene/*o*-Xylene Monooxygenase (ToMO), Catechol 1,2-dioxygenase (C1,2D) and Catechol 2,3-dioxygenase (C2,3D) in (a) *Bacillus infantis* and (b) *Microbacterium esteraromaticum.*

Figure 5.6 shows that the activity of three tested enzymes ToMO, C1,2D, and C2,3D during BTEX degradation in bacteria-treated cultures. The enzymatic studies showed that these strains use *tod* and *tol* pathway for the BTEX metabolism, where ToMO start the cleavage of aromatic rings by hydroxylation and followed the by the cleavage of catecholic ring by C1,2D and C2,3D. The enzyme activity was higher at 20 hours of incubation after inoculation except for the abiotic control. Similar trend in BTEX decline was observed in degradation within 20 hours of incubation (Figure 5.4), which showed that these enzymes degraded the BTEX. Likewise, metabolites studies showed the intermediate compounds formed by these enzymes after metabolism. C1,2D (> 10 U and 12.5 U) give higher activity than ToMO (7 U and 5 U) and C2,3D (3.2 U and 4.1 U) after 20 hours in *Bacillus infantis* and *Microbacterium esteraromaticum*-treated cultures, respectively. This reveals that the activity of enzymes starts after the activation of metabolic pathways to consume or degrade a pollutant (A. Kumar et al., 2020). The decline in enzyme activities could also be because of the stationary phase around 30 hours of incubation for both bacteria as depicted in their growth kinetics (Figure 5.2), as bacteria

are more metabolically active in their exponential phase. Most BTEX removal occurred within the first 24–30 h (> 70%), so enzyme measurements were focused there.

Results are in agreement with the literature findings. Several reports have recognized the role of monooxygenase and dioxygenase in BTEX biodegradation. For instance, Khodaei et al. reported the co-metabolism of xylene-benzene mixture by catechol 2,3 dioxygenase with a relative activity of 9.43 IU/ mg through catechol oxidation (Khodaei et al., 2017). Likewise, 92-94% p-xylene biodegradation has been reported by an enzyme cocktail of xylene monooxygenase and catechol 2, 3 dioxygenases obtained from co-culture of two *Pseudomonas* strains in a soil column experiment (Miri et al., 2022).

5.6 Proposed degradation pathways

To the best of our knowledge, there is no report on the metabolic biodegradation pathway of BTEX by *Bacillus infantis*, however, there is one report, which demonstrates the potential of *Microbacterium esteraromaticum* and explained the possible degradation pathway for BTEX metabolism (Wongbunmak et al., 2017a). According to previously described pathways, benzene is either converted into phenol by toluene monooxygenase or to cis-dihydrobenzenediol by benzene 1,2-dioxygenase. Wongbunmak et al. (2017) reported that intermediates such as phenol, catechol, *cis*-*cis*-muconate, *cis*-2-hydroxypenta-2,4-dienoate, and 4-hydroxy-2-oxovalerate were observed when *M. esteraromaticum* was supplemented with benzene as the carbon source showing degradation by ToMO enzyme (Wongbunmak et al., 2017a). Therefore, the mechanism of BTEX degradation has been proposed based on the activity of enzymes during biodegradation and metabolites analysis as shown in Figure 5.7. In the GC-HS results for metabolites, the analysis did not show any new peak in the MS spectra, while a high-intensity peak of 44 amu at 1.2 retention time was observed in treated groups in comparison to abiotic control (Figure B7). This 44 amu peak might correspond to carbon dioxide or acetaldehyde, but further detailed genomic studies and metabolic tracking is required to confirm the same.

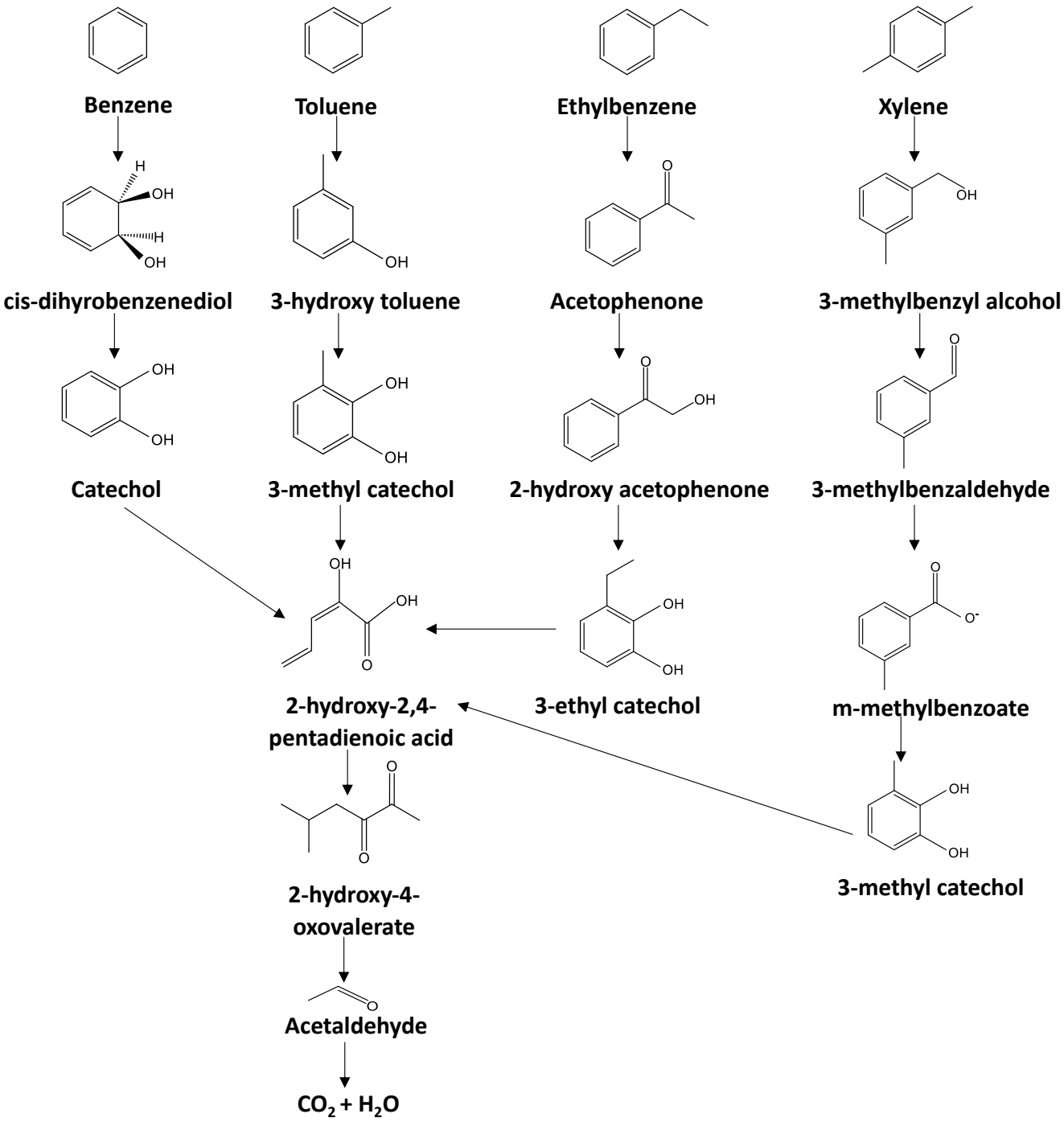

Figure 5.7: Proposed biodegradation pathway for BTEX.

5.7 Conclusions

The studies showed that the subsurface has numerous bacteria which can degrade pollutants during ISB. Among the 48 BTEX-tolerant isolated strains, *Bacillus infantis* and *Microbacterium esteraromaticum* degraded all four BTEX compounds within 48 hours. An in-vitro temperature-based study in synthetic media was performed to observe the effects of heat, to simulate the heat injected into the subsurface by geothermal heat pumps. Thus, geothermal heating could be a potential source for heat augmentation to the subsurface for enhancing the rate of natural ISB. Temperature increment from 15±1 °C to 40±1 °C, resulted in two-to-three-fold increase in bacterial growth and helped to achieve approximate double biodegradation rates for *Pseudomonas putida*, *Microbacterium esteraromaticum*, *Bacillus infantis*, and consortia cultures. These bacterial strains are new towards BTEX degradation, and their degradation mechanisms have not been studied. The enzymatic analysis revealed that both strains use ToMO, C1,2D, and C2,3D enzymes for degrading BTEX. Further studies will focus on analyzing the effect of temperature in soil and groundwater matrices, to mimic *in-situ* conditions using the potential isolated strains and consortium. Identifying bacteria and enzymes that can degrade BTEX compounds under moderately heated environments could result in new remediation methods for brownfield sites, where heat generated from geothermal applications can be used to enhance bioremediation.

Objective 2: Analyze BTEX biodegradation under anoxic conditions using response surface methodology

The two potent selected strains i.e. *B. infantis* and *M. esteraromaticum* from objective 1, were further analyzed for their potential for BTEX biodegradation under different anoxic conditions, to understand their bioremediation potential in subsurface. The results are published as a peer-reviewed article in "*International Biodeterioration & Biodegradation"* with DOI: https://doi.org/10.1016/j.ibiod.2024.105973

Background

The biodegradation potential and metabolism of bacteria depend on the terminal electron acceptors present at contaminated sites. Due to the quick consumption of oxygen, microorganisms tend to use substitute electron acceptors such as nitrate, sulfate, manganese, and iron for biodegradation. This objective aims to investigate the effect of electron acceptors (nitrate, sulfate, and ferric ions) on BTEX biodegradation using *Bacillus infantis (B. infantis)* and *Microbacterium esteraromaticum (M. esteraromaticum)*. The experiment was designed with response surface methodology using the Box-Behnken method. All four compounds of BTEX biodegraded with removal efficiencies ranging from 46% to 57% in *Bacillus*-treated samples, while 88-98% biodegradation occurred in *Microbacterium*-treated cultures. The optimal growth of *B. infantis* was observed at 250 mg/L of nitrate and iron, while no effect of sulfate was observed. For *M. esteraromaticum*, 250 mg/L of nitrate and sulfate showed the maximum growth of more than 1 optical density (OD); however, no change in growth was noticed with iron treatment. The investigation showed a maximum BTEX biodegradation of 57% by *B. infantis* under sulfate reduction and overall, 98% by *M. esteraromaticum* in combined nitrate and sulfate reduction. This provides new insights into soil microbial community responses to electron acceptors under anoxic conditions, signifying that intrinsic microorganisms could be successfully stimulated for ISB with electron acceptors as a supplement.

Results and discussion

5.8 Growth and biodegradation analysis with individual electron acceptors

5.8.1 Effect of nitrate-reducing conditions

Figures 5.8a and 5.8b show the growth pattern of *B. infantis* and *M. esteraromaticum* with different concentrations of nitrate (0, 250, 500, and 1000 mg/L) in the presence of BTEX (at 200 mg/L). The highest growth was observed with 250 mg/L of nitrate, with a significant difference (p-value < 0.05) in comparison to the control with 0 mg/L nitrate and the lowest growth with 1000 mg/L of nitrate amendment for both the bacteria. This showed that *B. infantis* and *M. esteraromaticum* have a threshold value for nitrate between 250 – 500 mg/L. The results for the control treatment of nitrate effect without BTEX have been provided in *Appendix C* as

Figure C3. However, without the presence of BTEX, a similar growth trend was observed in all nitrate treatment sets, which signifies that the selected bacteria utilize nitrate as a reducing agent while redox reactions oxidize BTEX for degradation.

Xu et al., 2014 also observed similar findings, where the percentage of unique genes had significantly increased ($p<0.05$) in the treatment samples after 24 h of nitrate amendment. The results showed that the genes involved in nitrogen, carbon and sulfur cycling processes were higher (22.5% to 37.1%) in nitrate treated PAHs contaminated sediments in comparison to control(7.9% to 16.7%) showing a positive metabolic change in microbes towards contaminants removal in sediments (Xu et al., 2014).

Previous studies from Tang et al. and Xu et al. also demonstrated that the structure of the microbial community changed significantly during the phases of sediment remediation by introducing electron acceptors or donors. Amendment of nitrate as electron acceptors into the contaminated subsurface enhanced ISB and completely degrade the organic contaminants (Tang et al., 2005; Xu et al., 2014).

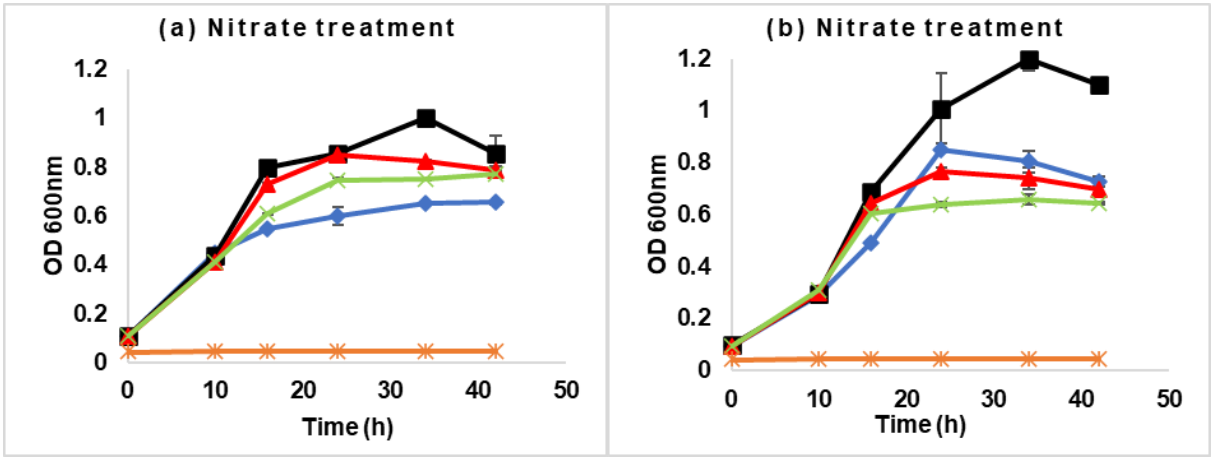

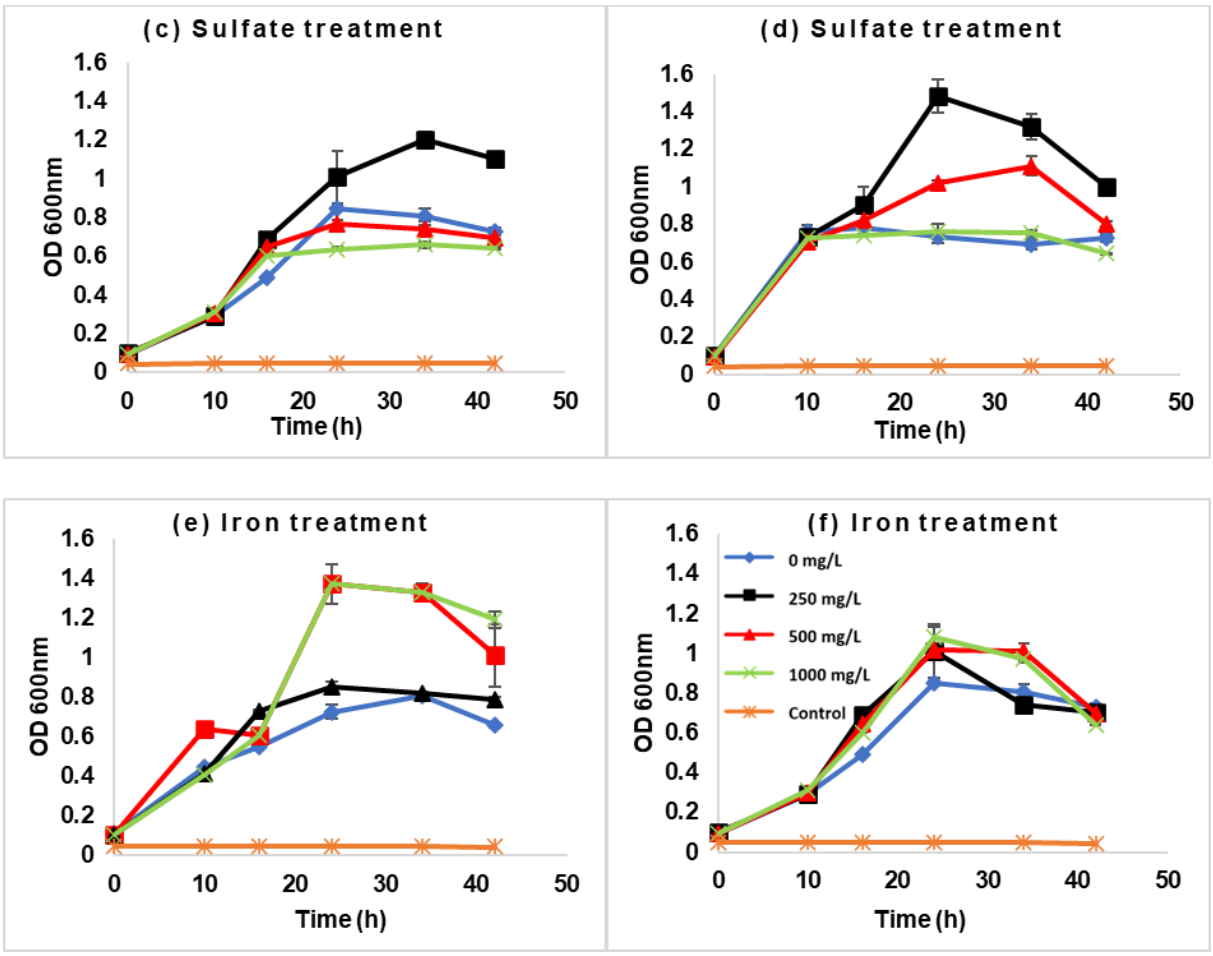

Figure 5.8: Growth of (a) *B. infantis* (b) *M. esteraromaticum* with nitrate treatment; (c) *B. infantis* (d) *M. esteraromaticum* with sulfate treatment; and (e) *B. infantis,* (f) *M. esteraromaticum* with iron treatment in the presence of BTEX (200 mg/L). The legend refers to the concentration of the treatment compound (nitrate in a, b; sulfate in c, d; and iron in e, f).

5.8.2 Effect of sulfate-reducing conditions

In Figures 5.8c and 5.8d, the extent of sulfate-reducing conditions under anoxic conditions for bacterial growth was measured up to an incubation period of 40 hours in artificial media. In *B. infantis*-treated cultures, a similar growth pattern and average maximum growth of 1.2 OD has been observed at all concentrations of sulfate ranging from 0 to 1000 mg/L with and without BTEX-supplemented treatments. This outcome shows that sulfate has the least effect on Bacillus growth (Figure 5.8c).

For *M. esteraromaticum*, no lag phase was observed, and bacteria grew at the same pace at all sulfate concentrations in treatments without BTEX. However, when *M. esteraromaticum* is supplemented with 200 mg/L BTEX along with different sulfate contents, the bacteria tend to behave differently. Collectively, a significant 40% higher growth has been observed at 250 mg/L of sulfate, followed by 500 mg/L sulfate. Cultures with 0 and 1000 mg/L of sulfate showed similar patterns with no significant difference (Figure 5.8d).

A similar trend was observed in a study by Chen and Taylor in 1997, where BTEX biodegradation was coupled with sulfate reduction in anaerobic conditions. Two anaerobic bacterial consortia (ALK-1 and LLNL-1) were observed to use BTEX as a sole carbon and energy source. The experiment was set up with 50-ml serum bottles, containing 30 mL mineral salts medium with 3.5 mg BTEX. The degradation of BTEX was coupled with sulfate reduction and H_2S generation. ALK-1 was observed to degrade 22% benzene, 38% toluene, 42% ethylbenzene, 40% m-xylene, and 38% o- and p-xylenes mixture, after 14 days of incubation. LLN-1 showed a lower degradation rate than ALK-1. In the experiment, no degradation was noticed when sulfate was removed from the serum bottles. The experimenter concluded that BTEX biodegradation is most probably due to sulfate-reducing bacteria (C.-I. Chen & Taylor, 1997a). Likewise, among the selected strains in the present study, growth results show that *M. esteraromaticum* could be a potential sulfate-reducing bacterium. The extent of sulfate ions on BTEX biodegradation by *M. esteraromaticum* has been further explained in section 5.10.

5.8.3 Effect of iron-reducing conditions

Like nitrate and sulfate, Figures 5.8e and 5.8f show the growth pattern of *B. infantis* and *M. esteraromaticum* with 0, 250, 500, and 1000 mg/L ferric ions treatment. With ferric ions, no significant effect was observed in BTEX-supplemented media in *M. esteraromaticum*-treated culture, while directly proportional growth was observed in control (without BTEX) cultures (Figure C3 in *Appendix C*). In the case of *B. infantis*, approximately two-fold more growth was observed in 250 and 1000 mg/L treated cultures (O.D- 1.37) after 24 hours of incubation in comparison to 500 mg/L treated culture (O.D- 0.85). It was evident in the literature that several iron-reducing bacteria (IRB) can cause BTEX degradation. For instance, benzene metabolization by the IRB, *Geobacter metallireducens* with phenol as an intermediate in the benzene biodegradation has been reported (Müller et al., 2017; Yoshikawa et al., 2017). The

presence of phenol was detected as a common intermediate under sulfate-reducing and denitrifying environments in early studies of benzene anaerobic biodegradation (Firmino et al., 2018; Siqueira et al., 2023; Weelink et al., 2010). However, various other studies have also suggested benzoate as a biodegradation intermediate along with phenol under all the types of electron acceptors mentioned above, which suggests that strains tend to maintain syntrophic relationships (Coates et al., 2002; Siqueira et al., 2023). It is important to note that iron is the most common metallic terminal electron acceptor involved in aromatic hydrocarbon degradation due to its abundance in the earth's crust. However, the growth results showed that iron only affected the *B. infantis'* growth showing its potential to use iron as a reducing agent for BTEX degradation.

5.9 Growth analysis with different combinations of electron acceptors

The growth of bacteria under different electron acceptors' presence shows that the presence of more than one type of electron acceptor has a direct influence on the growth pattern of microbes. Microbes prefer to consume selected ions during the growth and biodegradation process. Figures 5.9 and 5.10 show the growth patterns of *B. infantis* and *M. esteraromaticum* with nitrate, sulfate, and iron in two-way interaction plots.

The presence of sulfate has a positive effect (p-value 0.014) on *B. infantis* growth in the presence of nitrate and iron, while ferric ions show the opposite effect with nitrate for concentrations of nitrate being approximately less than 250 mg/L (p-value 0.154). However, when the concentration of nitrate was higher than ≈ 250 mg/L, Fe showed a positive effect on bacterial growth (p-value 0.019). While with constant iron and varying sulfate conditions, sulfate had the opposite effect where the growth of *B. infantis* was seen below the sulfate concentration of ≈ 350 mg/L and then a decline was observed as the concentration of sulfate increased after ≈ 350 mg/L.

Although *M. esteraromaticum* tends to show enhanced growth under sulfate-reducing conditions along with ferric and nitrate ions (p-value 0.001) while in nitrate-reducing conditions only ferric ions show a positive effect (p-value 0.036). No significant effect on growth was observed in constant nitrate and sulfate concentrations and varying iron content. In terms of

bacterial cells by OD_{600}, both the strains grow in an average of 0.264 to 0.528 x 10^8 and 0.264 to 0.80 x 10^8 cells.

These results show that both bacteria show more growth in both nitrate- and sulfate-reducing conditions, and not in iron conditions. Similar observations have been made previously by using consortia and other bacterial strains in the literature (da Silva & Corseuil, 2012; Müller et al., 2017; Xu et al., 2014). However, no report shows the physiological behavior of *B. infantis* and *M. esteraromaticum* under anoxic conditions and their potential for BTEX degradation. The results of the experiments showed that BTEX degraders i.e. *B. infantis* and *M. esteraromaticum* could potentially remediate a BTEX-contaminated site using nitrate and sulfate as terminal electron acceptors. That's why it is important to study the intrinsic strains for their degradation potential to design sustainable and fast ISB strategies.

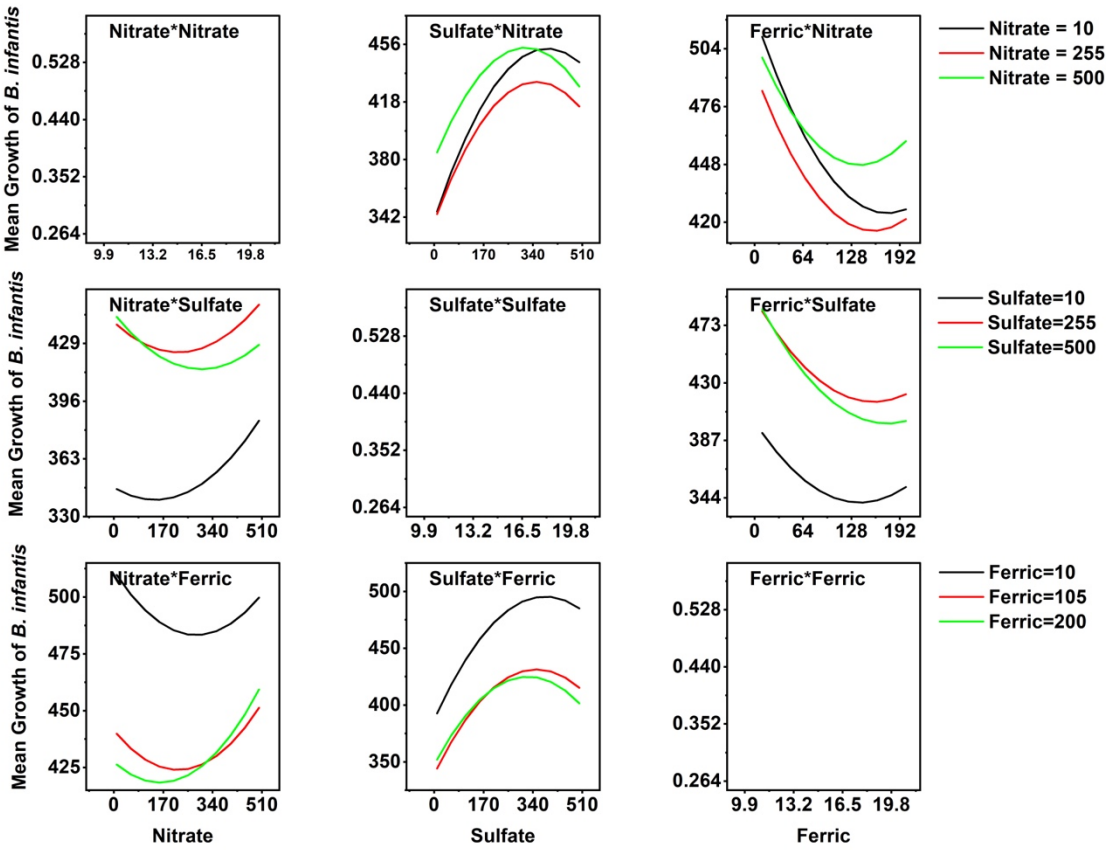

Figure 5.9: Two-way interaction between electron acceptors (Nitrate, sulfate and ferric ions) towards the growth of *B. infantis.*

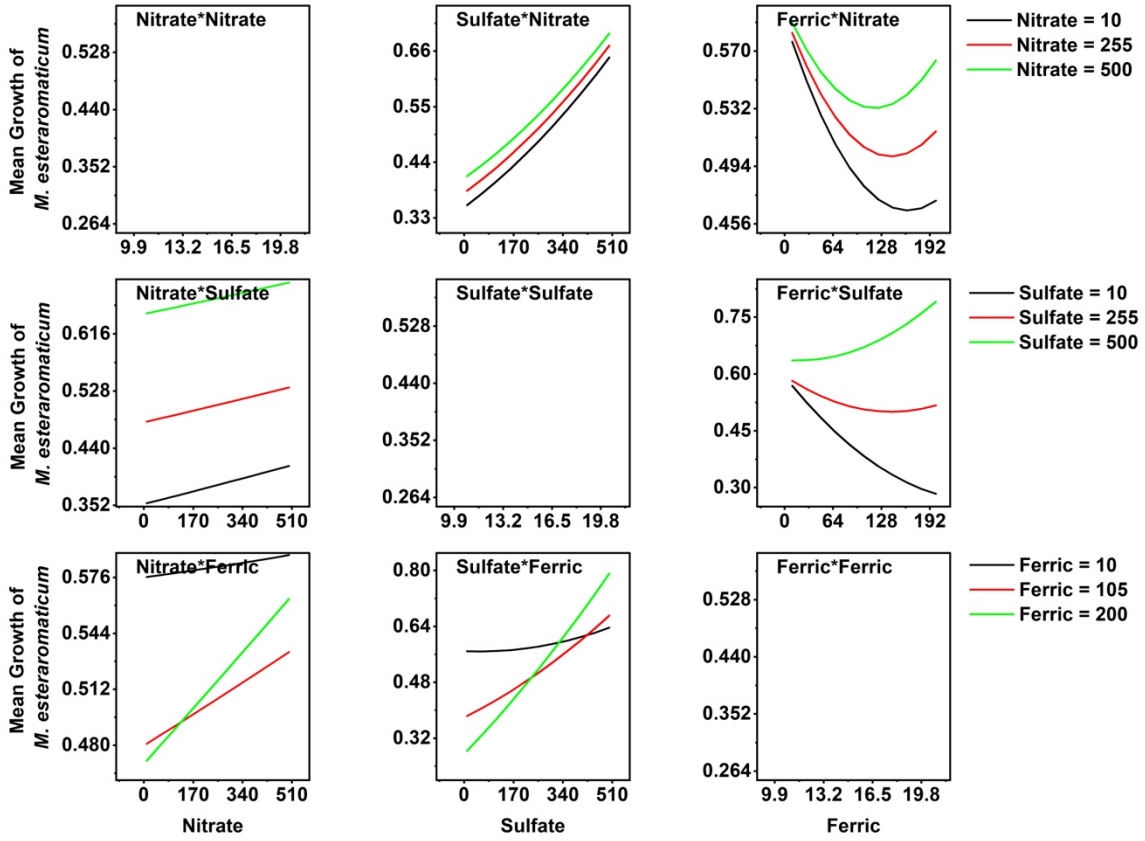

Figure 5.10: Two-way interaction between electron acceptors (Nitrate, sulfate and ferric ions) towards the growth of *M. esteraromaticum.*

5.10 BTEX biodegradation analysis with different combinations of electron acceptors

When different electron acceptors were amended to the artificial media, an overall significant change in biodegradability of *B. infantis* and *M. esteraromaticum* was observed as shown in Table 5.3 and Table C2.

Table 5.3: Overall BTEX biodegradation with different combinations of electron acceptors (* shows the significant difference between the biodegradation with a p-value of 0.05).

Degradation percentage (%)	***B. infantis***		***M. esteraromaticum***	
	MSM	Soil	MSM	Soil
Benzene	35-56*	73-80	63-88*	77-79
Toluene	36-57*	55-66	66-94*	56-58
Ethylbenzene	18-46*	7-40*	64-98*	46-51
Xylene (s)	27-52*	23-50*	72-98*	33-43
R^2 value				
Benzene	0.705	0.665	0.776	0.655
Toluene	0.695	0.657	0.919	0.686
Ethylbenzene	0.697	0.735	0.953	0.622
Xylene (s)	0.702	0.712	0.946	0.672

In the case of *B. infantis* treated cultures, higher degradation was observed in lower nitrate and higher sulfate conditions when ferric ions were held at 200 mg/L (Figure 5.11). Similar trend was observed for all four compounds of BTEX; however, more degradation was noticed for benzene (56%) and toluene (57%) in comparison to ethylbenzene and xylene (s) (46%) as shown in Figure C5. The results showed that *B. infantis* tends to undergo sulfate reduction for BTEX degradation rather than nitrate reduction.

However, in *M. esteraromaticum*-treated media, higher degradation was observed for all four compounds of BTEX as compared to *B. infantis* and electron acceptors (nitrate and sulfate) had a significant effect on BTEX degradation rate (Table 5.3). Like *B. infantis,* the same pattern was observed for all four compounds of BTEX; however, an overall increase from 66.60 to 92.50% degradation was noticed for BTEX. Higher degradation was observed in lower nitrate and lower sulfate conditions when ferric ions were held at 200 mg/L (Figure 5.11). The degradation pattern for all four BTEX compounds was similar (Figure C5). The possible reason for higher degradation could be the physiological nature of *M. esteraromaticum.* Being an anaerobic facultative microbe, it has more ability to use anaerobic electron acceptors at a wide range for hydrocarbon oxidation and degradation (Logeshwaran et al., 2020; Wongbunmak et al., 2017a).

Both the microbes *B. infantis* and *M. esteraromaticum* were also tested for their BTEX biodegradability in small-scale soil slurry samples. The soil samples were supplemented with the same concentrations of nitrate, sulfate, and ferric ions as MSM media (Chapter 4, Table 4.1). However, in soil, no significant influence of amended ions was observed for both bacteria except for ethylbenzene and xylene biodegradation by *B. infantis* (Figure C5). Similar findings have been reported by Wongbunmark et al., 2020, where *Bacillus amyloliquefaciens* was used to degrade BTEX in a soil slurry system and liquid medium system. The results showed that *Bacillus amyloliquefaciens* showed higher growth for the first three days and was able to degrade all 6 types of BTEX with the initial concentration of 60 mg/L. The degradation in liquid medium was higher than in soil and the reason for this was the complexity of soil matrix and absorption, which eventually led to a slower BTEX degradation rate (Wongbunmak et al., 2020).

In the case of *B. infantis,* the same degradation pattern was observed for TEX. For benzene, maximum biodegradation of 80% has been observed at higher concentrations of sulfate and medium range of nitrate. However, the opposite trend has been noted for other compounds. At lower concentrations of sulfate (10 mg/L) and higher levels of nitrate (500 mg/L); maximum 66% toluene, 40% ethylbenzene, and 50% xylene biodegradation were served as demonstrated in Figure 5.11 and A14.

Furthermore, in *M. esteraromaticum*-treated cultures, a similar degradation pattern has been observed for all four compounds (Figure C5). However, no significant change in biodegradation at the different supplements of nitrate and sulfate with a hold value of 200 mg/L of iron was noticed as shown in Table 5.3 and Figure 5.11. The R-squared values were also less than 0.7 for all BTEX compounds in soil treatment (Table 5.3) using linear regression analysis. The optimized conditions of electron acceptors for BTEX biodegradation (Figure C7) were validated by running an experiment at optimized values. The experimental results of total biodegradation have been reported in *Appendix C* as Table C3. The experimental values of BTEX degradation in MSM and soil by *B. infantis* and *M. esteraromaticum* matched the quadratic polynomial model and observed within 95% prediction interval and 95% confidence interval, indicating a good fit of the model.

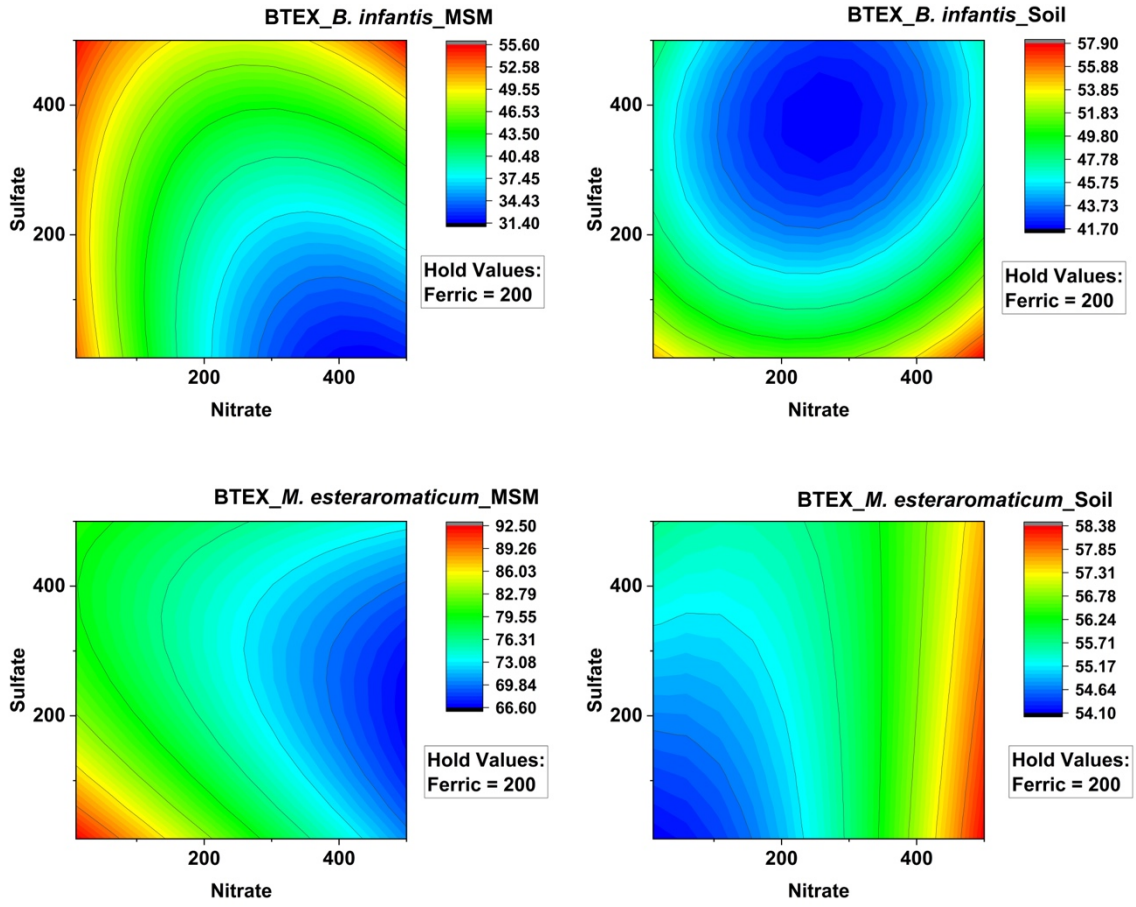

Figure 5.11: Contour plot of BTEX biodegradation by *B. infantis* in MSM (a) and soil (b) and *M. esteraromaticum* in MSM (c) and soil (d) at different concentrations of nitrate and sulfate at a hold value of 200 mg/L ferric ions.

In a study by Lu et al., 2012, anoxic conditions were studied for mixed PAHs biodegradation in soil. An overall 42% to 77% biodegradation was observed for two-, three-, and four-ring PAHs. In contrast, the degradation of five- and six-ring PAHs was minimal. Higher biodegradation rate of 4.01×10^{-2}–6.42×10^{-2} d^{-1} for two- to three-ring PAHs was reported with nitrate-reducing conditions in comparison to the sulphate-reducing conditions (X.-Y. Lu et al., 2012). However, these findings are contradictory with the biodegradation pattern of BTEX in *Bacillus*-treated samples, where sulfate-reducing conditions prevail and show high degradation.

Another study conducted by Chen et al, (2008) observed that ferric iron along with nitrate can promote BTEX degradation for all its six compounds. In the experiment, a Microcosm M5 was

used which was filled with 5 ml ferric iron stock solution and 100 ml MBH medium. This gave an initial electron acceptor pool which included 1.25 mM nitrate, 1.85 mM sulfate, and 3.58 mM ferric iron. Degradation of ethylbenzene and m/p-xylene continued to occur as the conditions switched from denitrifying to iron-reducing conditions. However, biodegradation of both, benzene and o-xylene significantly enhanced. It was observed that most of the benzene was degraded when the concentration of ethylbenzene decreased, and the environment was shifted to iron-reducing conditions. The study further explained that the presence of aromatic hydrocarbons such as ethylbenzene may have inhibited the degradation of benzene. This trend was observed in their experiment when one of the microcosms only had iron and sulfate, and the degradation of benzene was not seen. The study concludes that denitrifying microorganisms promotes the degradation of aromatic hydrocarbons, and from there onwards, iron-reducing conditions can significantly biodegrade all other compounds of BTEX (Y. D. Chen et al., 2008). These findings support the growth pattern of *M. esteraromaticum* but contradict the *B. infantis* growth for iron and nitrate combination.

A study done by Su et al, (2022) used Produced Water (PW) in the experiment to show the degradation of BTEX. PW is obtained from natural gas production and conventional oil, it consists of many organic and inorganic chemicals, heavy metals, polymers, etc. BTEX along with some other aromatic compounds is considered a major toxicant in PW. PW used for incubation in the experiment consisted of 14 µmol/L of benzene, 2.1 µmol/L of toluene, < 0.5 µmol/L of ethylbenzene, m-xylene, and p-xylene, and 4.5 µmol/L of o-xylene. Under anaerobic BTEX degradation, nitrate was seen to degrade BTEX at a four times higher rate than iron and sulfate-reducing conditions using bacterial enrichments obtained from gasoline-contaminated soils and sediments. This degradation rate was explained by the thermodynamics principles. Higher reaction energy was obtained when nitrate was used as an electron acceptor during denitrification, compared to iron and sulfate. For instance, standard free energy changes ($\Delta G^{\circ\prime}$) of benzene oxidation was −2990 kJ/mol with NO_3^-, while it was −2660 kJ/mol and −200 kJ/mol for Fe (III) and SO_4^{2-}, respectively (Su et al., 2022).

Furthermore, in a study, Winderl et al. concluded that the BTEX degradation in aquifers is mainly dependent on the reduction of sulfate. In addition, the concentration of electron acceptors may be a key factor for benzene biodegradation (Winderl et al., 2010). Likewise,

other previous studies have shown that there may be differences in biodegradation under different electron acceptors reduction conditions, and the biodegradation efficiency depends on the strength of interaction between pollutant degradation and electron acceptors' reduction combination (G. Martins et al., 2022; Mirsaeidi, 2023; Z. Wu et al., 2022).

Therefore, residual redox capacity has been calculated for supplemented ions towards BTEX degradation at their highest concentration as shown in Table C4. These calculations have shown that sulfate will be a potential electron acceptor for *B. infantis* for benzene degradation. For *M. esteraromaticum*, both nitrate and sulfate could be a reducing agent while BTEX degradation processes. The standard redox potential of nitrate is 0.420V, iron is 0.771V, and sulfate is 2.5V. Sulfate has the highest redox potential rather than nitrate and iron. Based on these values, sulfate will reduce at a faster rate than the other two ions under anoxic conditions (Laverman et al., 2012).

5.11 Metabolic pathway under anoxic conditions

Anaerobic biodegradation of BTEX resulted in high concentrations of uncleaved aromatics acids. These acids are potential intermediates during the degradation of alkylated phenols. Such aromatic acids are terephthalic acid, toluic acid, and 3, 4-dimethylbenzoic acid. Several pathways involve reactions of carboxylation, methylation, and hydroxylation. Such pathways could have been used to degrade BTEX, some examples of these pathways are benzoyl-CoA, hydroxy hydroquinone, resorcinol, phloroglucinol, etc. (Su et al., 2022). In the present study, the biodegradation pathway of BTEX by *B. infantis* and *M. esteraromaticum* was proposed based on the intermediates and metabolites products analyzed through LC-MS/MS. Similar intermediate compounds were identified for both the microbes under all the anoxic conditions of nitrate reduction, sulfate reduction and iron reduction. Hence, a common degradation pathway has been proposed as shown in Figure 5.12. The major identified intermediates identified are reported in the literature which further justify the proposed mechanism under anoxic conditions using these electron acceptors. Key metabolites of BTEX degradation, such as benzyl alcohol (Hernández-Ospina et al., 2024; Wu et al., 2022), benzaldehyde (Hernández-Ospina et al., 2024; Yuxuan et al., 2023), benzoic acid (Yuxuan et al., 2023; Fedorov et al., 2021), propionic acid (Hernández-Ospina et al., 2024), hydroxy acetophenone (Huang et al.,

2021; Kaur et al., 2023), dimethyl benzaldehyde (Godin et al., 2020; Kaur et al., 2023); were detected. The mass/charge spectra of the identified compounds have been provided in *Appendix C* as Figure C8. Pantothenic acid was also detected during the analysis, which is a precursor for synthesis of Coenzyme A (Leonardi and Jackowski., 2007). Various Coenzyme A has been reported previously as an important degradation enzyme while hydrocarbon biodegradation (Hernández-Ospina et al., 2024; Jiang et al., 2023; Wongbunmak et al., 2020). BTEX mainly mineralize through four different mechanisms of methylation, carboxylation, hydroxylation and fumarate addition under anoxic conditions (Hernández-Ospina et al., 2024).

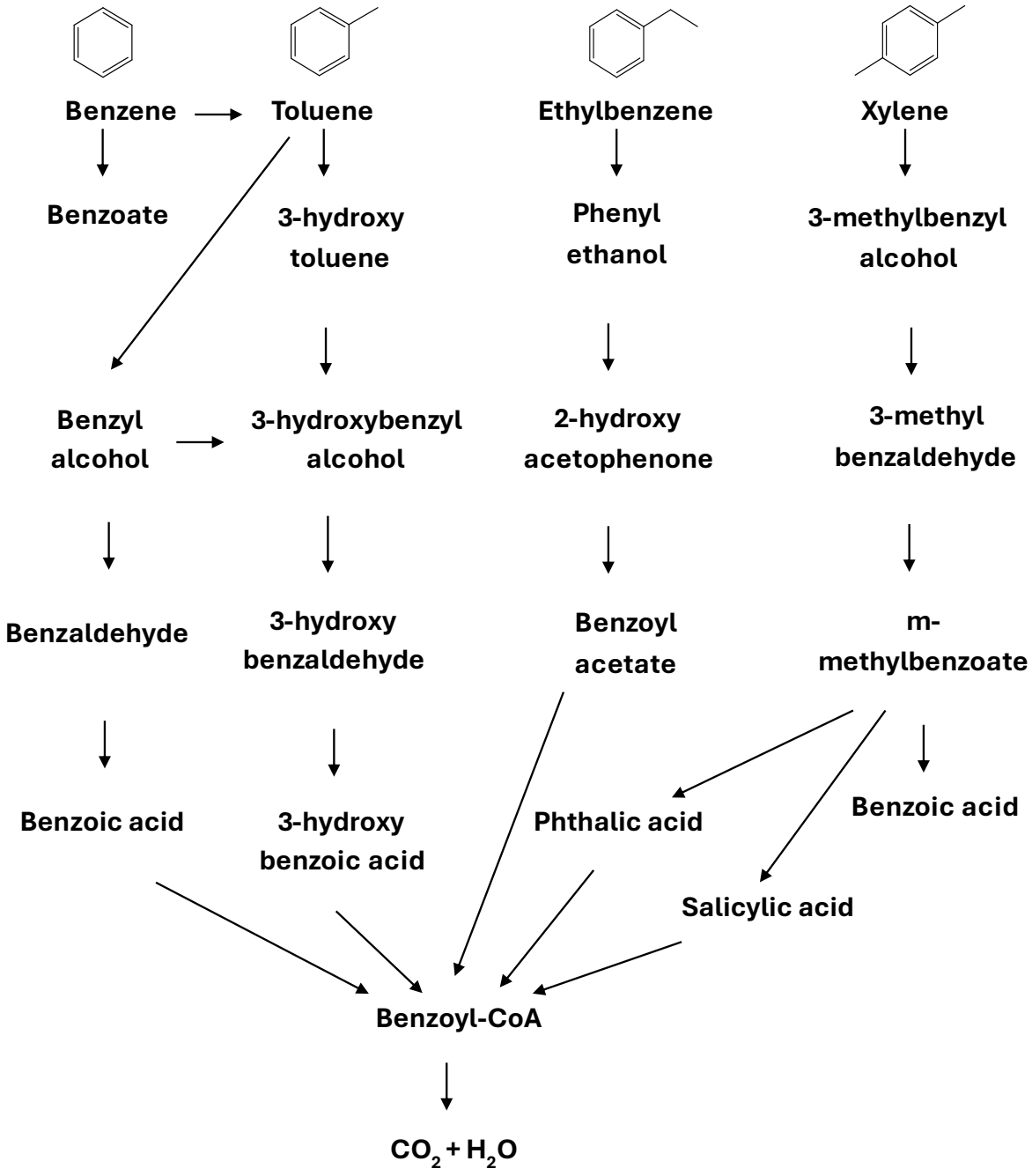

Figure 5.12: Proposed biodegradation pathway of BTEX by *B. infantis* and *M. esteraromaticum* under anoxic conditions using nitrate, sulfate and ferric ions as terminal electron acceptors.

Lastly, metabolic profiling provides insights into the intrinsic microorganisms' metabolism, elucidating the specific growth demands of various species at a given location and the interplay between distinct electron acceptors. This knowledge can be utilised to devise an effective remediation strategy and approximate the time required to remove contaminants from a contaminated site.

5.12 Conclusions

Two pure culture strains *B. infantis* and *M. esteraromaticum* were investigated for their role in different redox conditions under anoxic conditions. When supplemented individually, 250 mg/L nitrate showed maximum effect for both strains. While in sulfate-reducing conditions, a 40% higher growth was observed when augmented with 250 mg/L of sulfate, followed by 500 mg/L sulfate. With ferric iron, no significant effect was observed in BTEX-supplemented media, while direct proportional growth was observed in control (without BTEX) cultures. When ions (nitrate, sulfate, and iron) are supplemented in different combinations using the Box-Behnken method, higher degradation in denitrifying and sulfate-reducing conditions was observed in the presence of iron. However, no significant effect of iron-reducing conditions in the presence of other ions has been observed. This suggests that *B. infantis* tends to degrade more BTEX under sulfate-reducing than nitrate-reducing conditions. However, for *M. esteraromaticum*, the supplement of anaerobic electron acceptors enhanced the degradation at both denitrifying and sulfate-reducing conditions, because of the facultative anaerobic nature of microbes. These results show that a combination of electron acceptors could potentially affect the degradation pattern of hydrocarbons during bioremediation. For instance, the presence of sulfate helped to degrade BTEX with *B. infantis* and the combination of coupled nitrate and sulfate ions leads to higher degradation of benzene with *M. esteraromaticum*. Therefore, a proper supply of these ions, depending on pollutants, can remediate the site completely under anoxic conditions.

Objective 3: Perform a bench-scale GHP system in a bioreactor to study the effect of injected heat on BTEX degradation

After biodegradation studies at different temperatures and under anoxic conditions, the selected strains, i.e., *B. infantis, M. esteraromaticum,* and soil consortia, were used for geothermal cyclic-temperature studies in batch and fed-batch soil columns. This objective helped to understand the feasibility of geothermal-assisted bioremediation. The results are submitted as a peer-reviewed article in "*Energy and Environmental Science"*.

Background

The *in-situ* bioremediation in the subsurface can be slow due to the low subsurface temperatures (10 – 15 °C), which limit microbial degradation activity. Providing optimum growth temperatures through geothermal heat pumps may proliferate microbial growth and enhance bioremediation sustainably, using renewable energy sources. Hence, in this objective, the effect of cyclic temperature fluctuations (from 15 to 40 °C) on a small scale has been studied in BTEX-contaminated soil using *B. infantis, M. esteraromaticum* and consortium. To understand the real matrix influence, three different soil types were studied in continuous soil column experiments with cyclic temperature. The results revealed that cyclic temperature of 5±1 °C to 40±1 °C (shallow low enthalpy geothermal temperature range) enhanced the BTEX biodegradation by 2-fold in silty loam soil (> 80%) in comparison to constant aquifer temperature (12±1 °C). Higher K_{bio} for all four compounds was observed above 25±1 °C in cyclic treatment for the studied soil types compared to the isothermal 12±1 °C treatment. The study demonstrated that increased and cyclic temperatures facilitated enhanced microbial metabolism and simultaneous BTEX biodegradation, thereby promoting a cleaner approach to subsurface remediation.

Results and discussion

5.13 Soil characterization and column parameters

Using a combination of sieve and hydrometer analysis, the particle size distribution of the three soils was determined, and they were then categorized using the USDA textural classification system (Baillie, 2001). The USDA classification system was adopted because it is designed for soil science, environmental processes, and biological activity. Soil sample 1 had a silt loam texture with roughly 29% sand, 56% silt, and 13% clay. Soil sample 2 consisted of 91% sandy soil, with silt and clay accounting for 3% and 1%, respectively. The third soil sample was classified as coarse sand because it contained 98% sand, 1% silt, and 1% clay (Figure D1). The classification of the soil revealed significant textural differences between the soils, which could affect other soil properties, such as hydraulic conductivity, pore structure (porosity), and contaminant transport behaviour.

The detailed parameters for columns and soil properties are provided in Table 5.4. The three soils have a foc value of 0.021, 0.013, and 0.011 for silty loam, fine sand and coarse sand,

respectively, which is essential for adsorption and biodegradation in columns (obtained using dry combustion method). K_{oc} (organic carbon-water partition coefficient), K_d (soil adsorption coefficient) values were calculated accordingly and provided in Table 5.5.

Table 5.4: Soil and column parameters

Physiochemical property	**Silt loam**	**Fine sand**	**Coarse sand**
pH	7.6±0.30	7.1±0.25	7.5±0.21
Soil type	Silty loam	Fine sand	Coarse sand
Clay content	13%	1%	1%
Silt content	56%	3%	1%
Sand content	29%	91%	98%
Moisture content	13.80%	11.23%	13.12%
Plasticity index	10.1	8.01	11.47
Nitrate	76±3.04 mg/L	69±2.94 mg/L	73±4.22 mg/L
Sulfate	184±6.33 mg/L	101±4.85 mg/L	178±7.41 mg/L
Ferric	1.2%	0.9%	1.01%
foc	0.021	0.013	0.011
CEC	2.15±0.52 mg/kg	1.67±0.15 mg/kg	2.22±0.46 mg/kg
Heavy metals	ND	ND	ND
Column parameters			
Bulk density	1.395±0.21 g/cm^3	1.447±0.19 g/cm^3	1.534±0.48 g/cm^3
Porosity	0.474±0.01	0.454±0.00	0.421±0.01
Pore Volume	68.4±1.02 mL	65.5±1.71 mL	60.7±0.67 mL

ND = Not detected, foc = Fraction of organic carbon, CEC = Cation exchange capacity

Table 5.5: BTEX adsorption coefficients on three soils

Compound	K_{oc} (L/kg)	Silty loam K_d (L/kg)	Fine sand K_d (L/kg)	Coarse sand K_d (L/kg)
Benzene	62	1.302	0.806	0.682
Toluene	140	2.94	1.82	1.54
Ethylbenzene	204	4.284	2.652	2.244
Xylene	241	5.061	3.133	2.651

5.14 Batch scale experiment with cyclic temperature

5.14.1 Volatilization

The equilibrium volatilization of BTEX compounds was analyzed in 20 mL sealed vials containing 12 mL aqueous solution (200 mg/L in 1:1:1:1) with a 4 mL headspace. Figure 5.13(a) shows the volatilization fraction at different temperatures ranging from 15 °C to 40 °C. The increased temperature resulted in higher volatilization. For example, at 15 °C, 1.73 mg/L benzene, 1.41 mg/L toluene, 0.81 mg/L ethylbenzene, and 0.76 mg/L xylene(s) were lost in headspace. In comparison, at 40 °C, the loss was comparatively higher by more than two-fold, i.e. 6.88 mg/L benzene, 4.58 mg/L toluene, 3.7 mg/L ethylbenzene, and 2.25 mg/L xylene. These results revealed a clear temperature-dependent increase in volatilization for all compounds, consistent with their thermodynamic partitioning behaviour. At each temperature, benzene showed the highest fraction in the gas phase, followed by toluene, ethylbenzene, and xylene, reflecting their relative volatilities and vapour pressures. These findings also corroborate literature-reported Henry's constants confirming that benzene is the most volatile and environmentally mobile of the BTEX constituents (Schwardt et al., 2021).

The overall gas-phase partitioning remained below 10 % due to the limited headspace volume, indicating that equilibrium constraints strongly control volatilization under closed-system laboratory conditions. According to Henry's law, the partial pressure of a compound in the gas phase is directly proportional to its dissolved concentration in water, with the proportionality constant (Henry's constant) indicating the compound's tendency to escape from the liquid phase. Environmental factors such as temperature, pressure, and salinity significantly influence this process – an increase in temperature or ionic strength enhances volatilization by increasing

Henry's constant (Cagliari et al., 2009; Chao, 2009). In subsurface environments, however, reduced oxygen availability and limited gas exchange suppress volatilization, even for compounds with high volatility. Various parameters like soil physicochemical, soil packing, hydrodynamics, and gas-phase conditions influence the volatilization of these compounds

5.14.2 Adsorption

The BTEX adsorption equilibrium compounds were analyzed in 20 mL sealed vials containing 4 g of soil and 8 mL aqueous solution (200 mg/L in 1:1:1:1) with a 4 mL headspace. Figure 5.13(b) shows the adsorption of all four compounds at temperatures ranging from 15 °C to 40 °C for control sets in silty loam soil. During both the heating and cooling phases, a noticeable temperature-dependent trend was observed in the adsorption behaviour of BTEX compounds on silty loam soil. The BTEX adsorption was higher at low temperature and gradually dropped over the course of the heating cycle (15 °C – 40 °C), demonstrating that adsorption is an exothermic process controlled by physisorption mechanisms. The kinetic energy of BTEX molecules increases with temperature, weakening van der Waals forces and lowering the surface affinity between the adsorbates and organic matter in the soil (M. Wu et al., 2022, p. 20). The temperature-dependent decrease in adsorption is also consistent with Vant Hoff relation, suggesting lower partitioning coefficients at higher temperatures (Njobuenwu et al., 2005).

The compounds with the highest adsorption fraction (0.56 – 0.60 at 15 °C) are xylene and ethylbenzene. This is due to their larger molecular sizes and greater hydrophobicity, which enhance their partitioning into the organic phase of the soil. Benzene showed the lowest adsorption (0.21 – 0.23 at 15 °C), consistent with its higher aqueous solubility and smaller molecular radius, leading to greater mobility in subsurface environments.

Adsorption increased during the cooling phase (40 °C – 15 °C), but not to the initial values of the heating cycle. This suggests partial hysteresis in the sorption–desorption dynamics. Especially for the heavier aromatics (xylene and ethylbenzene), this hysteresis most likely results from irreversible sorption to organic binding sites or micropores. Slow equilibration kinetics, characterized by desorption during heating being faster than re-adsorption during cooling, are suggested by the slight asymmetry between the heating and cooling curves.

The partial hysteresis upon cooling and the observed temperature-driven decrease in BTEX adsorption align with results from the soil and adsorption literature. (M. Wu et al., 2022) demonstrated that benzene and toluene adsorb onto clay mineral surfaces via weak interactions that weaken with increasing temperature. In contrast, Sun et al. (2020) showed concentration-dependent hysteresis and particle-size effects in red soils, demonstrating that the desorption of benzene from soils proceeds more slowly than adsorption (Sun et al., 2020). The plausibility of hysteresis observations is supported by a more comprehensive review of BTEX behaviour in soils, which shows that desorption lags and adsorption decreases with increasing temperature, particularly for heavier aromatic compounds (Ren et al., 2009). The findings demonstrate that adsorption significantly slows down BTEX transport, especially in low-temperature subsurface settings. However, the decreased adsorption capacity caused by geothermal heating raises the subsurface temperature, which increases the bioavailability of BTEX compounds and promotes their volatilization and biodegradation in thermally active zones.

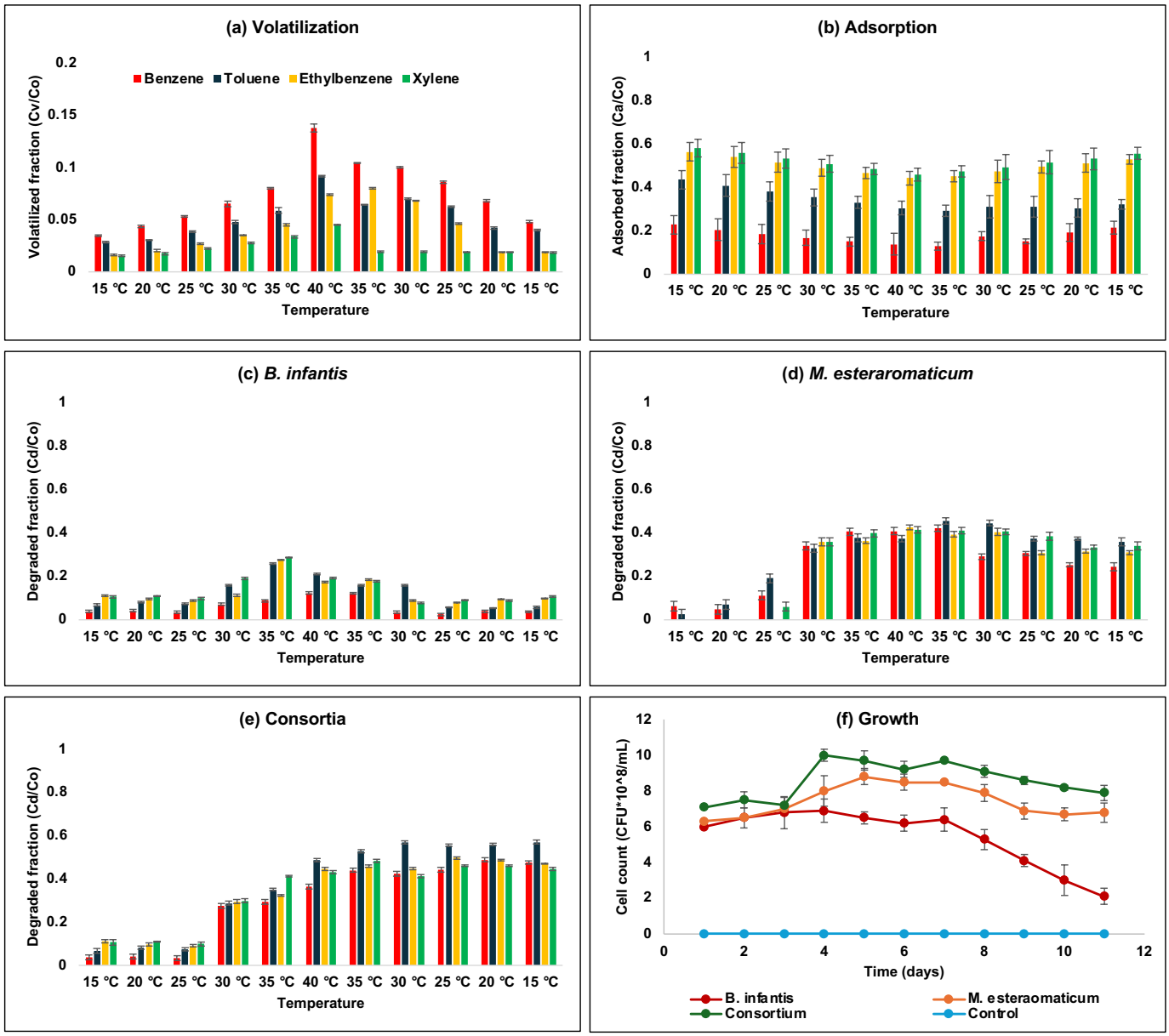

Figure 5.13: Temperature-dependent BTEX removal in silty loam soil (a) Volatilization fraction, (b) Adsorbed fraction, (c) Biodegradation with *B. infantis*, (d) Biodegradation with *M. esteraromaticum*, (e) Biodegradation with Consortium, (f) Growth of biotic treatments. C_o is the initial BTEX concentration, C_v is the volatilized BTEX, C_a is the adsorbed BTEX, and C_d is the degraded fraction of BTEX calculated from the equation 9.

5.14.4 Biodegradation

Figures 5.13(c), 5.13(d), and 5.13(e) show the biodegradation rate of BTEX at different temperatures in a cyclic form for *B. infantis, M. esteraromaticum,* and consortia-treated sets. During the simulated geothermal heating–cooling cycle (15 – 40 °C), the biodegradation profiles of BTEX showed clear temperature-dependent dynamics. A strong correlation between microbial activity and thermal conditions was shown, as all microbial systems increased their degradation efficiency with temperature up to 40 °C, followed by a slight decline during the cooling phase. Above 25 °C, all biological treatments achieved significantly higher removal fractions than the abiotic adsorption control, which was responsible for a maximum of 0.58 to 0.60 of total BTEX retention at 15 °C (*Appendix D*, Figure D2). This indicates that biodegradation became the dominant process beyond this threshold.

Biodegradation by monocultures: At lower temperatures (≤ 25 °C), *B. infantis* showed moderate activity, breaking down less than 0.1 of the total BTEX fraction. However, above 30 °C, biodegradation efficiency increased significantly by threefold with a p-value of 0.004, reaching peak fractions of 0.29 – 0.36 for benzene and up to 0.45 for xylene at 40 °C. The observed thermal activation is consistent with earlier research showing that *Bacillus* species have optimal BTEX degradation rates around 35 – 40 °C because of increased enzyme turnover and membrane fluidity (Daniel et al., 2008; Feller, 2010). The degradation of benzene and toluene by *M. esteraromaticum* was relatively higher in the 20 – 35 °C range (0.04 – 0.38 fraction). Still, it plateaued or slightly decreased after 40 °C, either because of temperature drop or enzyme denaturation at higher temperatures (Arcus et al., 2016; Daniel et al., 2008), however further metabolic studies are required for proper justification of the decline. Similarly, the mesophilic preference of *Microbacterium spp*. during the degradation of aromatic hydrocarbons has been reported by (Logeshwaran et al., 2022; Wongbunmak et al., 2017b).

Biodegradation by Consortium: Across all BTEX components and temperature ranges, the mixed consortium demonstrated superior degradation efficiency compared to monocultures, with a significant difference of $p < 0.05$. The biodegraded fractions rose sharply between 25 and 40 °C during the heating phase, reaching a maximum of 0.36 to 0.49 degrees at 40 °C. The microbial consortium exhibited a fast metabolic adaptation to thermal fluctuations by

maintaining more than 0.40 fractions for all compounds at 25 °C and 20 °C, demonstrating high degradation rates even during the cooling phase. The consortial strains usually exhibit metabolic complementarity and syntrophic cooperation, which accelerate the initial oxidation of monoaromatics by different species. Some species also promote the utilization of secondary metabolites and ring cleavage, likely leading to improved performance. Previous reports of BTEX degradation in mixed culture settings (Gupta et al., 2016; Jo et al., 2008) have demonstrated the ecological benefit of microbial consortia. A strong temperature dependence of BTEX biodegradation under simulated geothermal conditions was indicated by the apparent biodegradation rate constants (K_{bio}), which increased by about two-fold from 15 °C to 30 °C, corresponding to a Q_{10} of 1.9–2.2 (K_{bio} value at each temperature is given as Table D1 in *Appendix D*).

Temperature functioned as a dual regulator, increasing both substrate bioavailability and enzymatic activity, as indicated by a comparison of total removal trends throughout the heating cycle. Firstly, as the temperature rose, BTEX desorption from the soil improved mass transfer to the aqueous phase, which aided microbial uptake. This was demonstrated by decreasing adsorption fractions (Figure 5.13b). Secondly, the ideal temperature range for the oxygenase and dehydrogenase enzymes involved in BTEX catabolism is between 35 and 40 °C, where the maximum degradation rates were also observed (Daniel et al., 2008; Feller, 2010). On the other hand, the modest decline in biodegradation during the cooling phase points to a brief metabolic stress and a delayed recovery of enzyme kinetics after thermal downshift.

5.14.5 Growth

The three biotic treatments were analyzed for bacterial growth at 24-hour intervals at each temperature across heating and cooling cycles throughout the experiment, as shown in Figure 5.13(f). Growth was reported as CFU per mL for *B. infantis, M. esteraromaticum,* consortia-treated, and control samples. The *growth of B. infantis* remained saturated at approximately 6.5±0.3 × 10^8 cells/mL for 7 days until the temperature decreased to 35 °C, after which a sharp decline was observed. For *M. esteraromaticum* and consortia-treated samples, the cell count started at 6.3 × 10^8 cells/mL and 7.1 × 10^8 cells/mL at 15 °C. Bacterial growth increased significantly in the temperature range 30 °C (heating phase, day 4) to 30 °C (cooling phase, day

8). Afterwards, growth showed a modest decline, but the cell count remained above 6.8 × 10^8 cells/mL due to the mesophile ceiling. The consortium and *M. esteraromaticum* showed the highest growth around 30 °C with an optimum specific growth rate (μ) of 0.329 d^{-1} and 0.134 d^{-1}, while *B. infantis* grew at a rate of 0.015 d^{-1}. The data for μ and doubling time (t_d) are provided as Table D2 (*Appendix D*).

Experiments on temperature-dependent biodegradation showed that the isolates and the microbial consortium had different kinetic responses. Synergistic substrate utilization and metabolic cooperation were confirmed by the consortia's consistently higher degradation activity compared to monocultures. Enzymatic activity peaked between 30 and 35 °C, after which it began to decline, as per mesophilic behaviour. In comparison to *B. infantis*, which exhibited a limited response to temperature, *M. esteraromaticum* showed greater thermal tolerance and activity among monocultures.

Together, these results show that geothermal heating increases microbial activity, improving biodegradation kinetics, and decreases adsorption, thereby increasing bioavailability. The suitability of the microbial consortium for geothermal-assisted bioremediation of subsurface BTEX contamination was confirmed when it outperformed the monocultures, achieving higher and more stable degradation efficiencies under dynamic temperature regimes.

5.15 Fed-batch soil columns with cyclic temperature

5.15.1 Outlet BTEX concentration trend

The breakthrough curve of BTEX from the fed-batch soil columns indicated the trend of adsorption and biodegradation, as shown in Figure 5.14. The columns were injected with 9 injections of 50±3 mg/L of each compound, and the effluent concentration was compared in abiotic and biotic treatments to determine the biodegradation rate in consortia-treated columns. The abiotic adsorption treatment columns (T2 and T4) supported an exothermic sorption mechanism, as indicated by a definite inverse relationship between temperature and BTEX retention on silty loam soil. The soil showed a higher affinity for aromatic hydrocarbons at lower temperatures (10 – 15 °C); the adsorbed fractions for xylenes and ethylbenzene ranged from 0.52 to 0.60, while those for benzene ranged from 0.22 to 0.25. These values decreased to

0.13 – 0.45 as the temperature rose to 40 °C, indicating a decrease in sorptive forces and an increase in desorption into the aqueous phase. This change decreased possible substrate sequestration, which restricts microbial access, and increased the bioavailability of hydrocarbons (X. Chen et al., 2023; D. Zhang et al., 2023). The Vant Hoff relation is also consistent with the temperature-dependent decrease in adsorption, indicating lower partitioning coefficients at higher temperatures (Njobuenwu et al., 2005).

With compound-specific optima, temperature-wise degradation rates showed a strong positive temperature dependence for biodegradation (T1). Because of sorption dominance, slower enzymatic turnover, and microbial dormancy, biodegradation rates were either negligible or negative (apparent net accumulation) at lower temperatures (5 – 15 °C). Above 25 °C, rates increased dramatically, a sign of mesophilic hydrocarbon degraders' increased membrane permeability and enzyme activation (L. Meng et al., 2018; Sikkema et al., 1994). Lower or even negative apparent K_{bio} was consistently produced during the cooling phase (after 40 °C), indicating a brief lag or inhibition in the microbial metabolism's reactivation following thermal exposure.

Across the tested compounds, maximum rates followed the order: Toluene > Ethylbenzene > Xylene > Benzene**,** consistent with the relative ease of enzymatic activation of methylated aromatics. The findings are consistent with literature on aerobic BTEX degradation, where monoaromatic hydrocarbons with lower substitution (benzene) exhibit slower enzymatic oxidation rates (Jindrová et al., 2002; Kaur et al., 2023).

At 5 to 15 °C, the biodegradation rate (K_{bio}) values were almost zero or negative; at 30 to 40 °C, they ranged from 0.15 to 0.74 d^{-1}. Ethylbenzene and toluene showed the most noticeable enhancement, with sharp increases of 0.7 d^{-1} and 0.58 d^{-1}, respectively, near 30 °C. This illustrates the ideal catalytic range of the oxygenases and dehydrogenases that cleave aromatic rings (Dindar et al., 2015; Zazueta-Sandoval et al., 2003). A brief drop in apparent rates was brought on by cooling cycles; this was probably caused by desorption–resorption hysteresis or temporary metabolic dormancy rather than actual inhibition (W. Zhang et al., 2022).

Furthermore, when the biodegradation rates of all four compounds with cyclic treatment (T1) were compared to isothermal treatment (T3) in silty loam soil columns, rates were consistently

lower, as shown in Table 5.6. The geothermal system consistently yielded one to two orders of magnitude higher biodegradation constants than the constant 12 °C setup. Temperature cycling between 5 – 40 °C appeared to activate enzymatic mechanism, improve substrate desorption, and promote community adaptation through stress–response signalling.

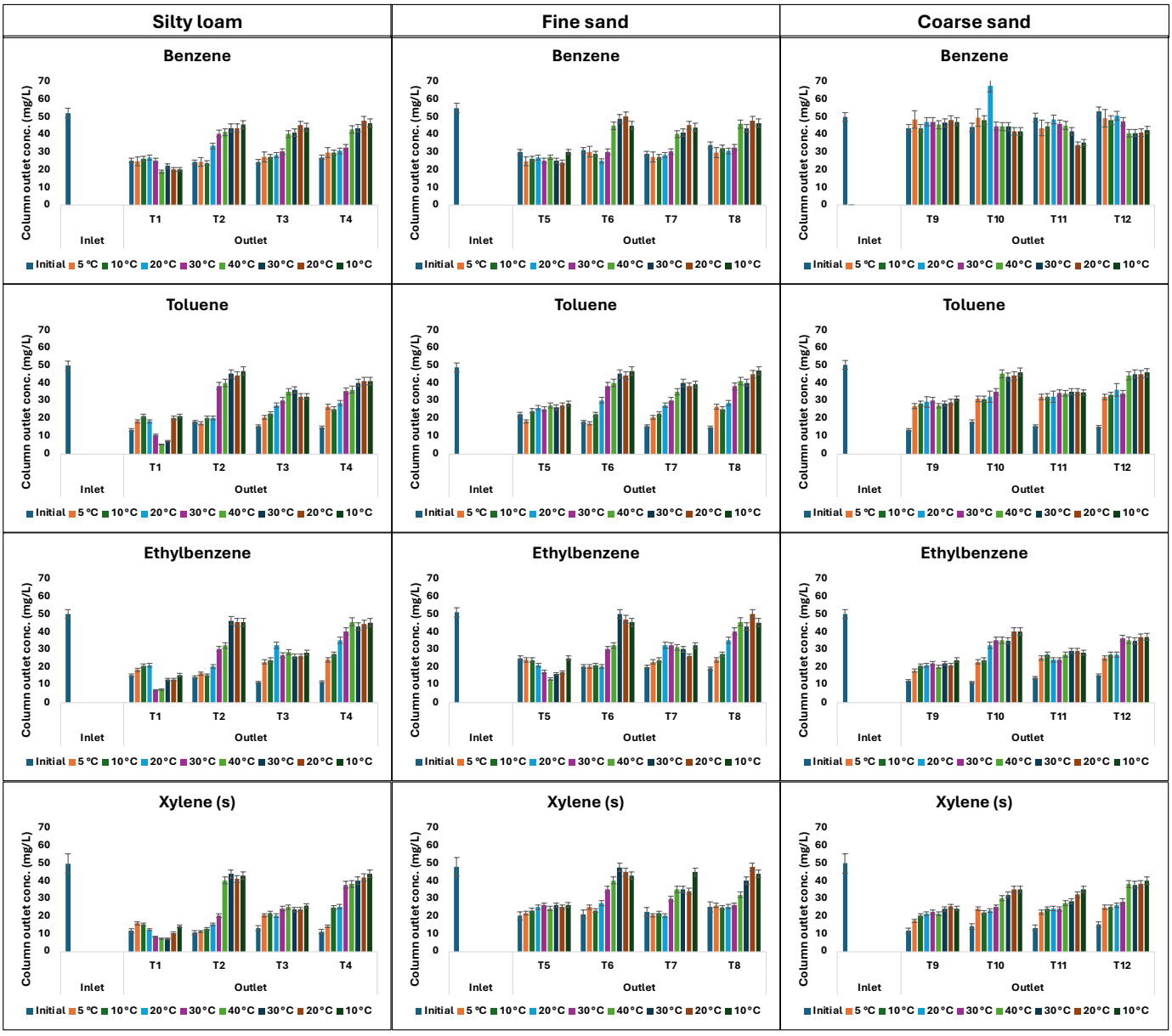

Figure 5.14: Outlet BTEX concentration after each temperature incubation. The total injected concentration was 450±6 mg/L of each compound (50 mg/L at each injection- total 9 injections). T1 is consortia-treated columns with cyclic temperature, T2 is control BTEX columns with cyclic temperature, T3 is consortia-treated columns at constant temperature (12 °C), and T4 is control BTEX columns at constant temperature with silty loam soil (in same pattern T5, T6, T7 and T8 with fine sand; T9, T10, T11, and T12 with coarse sand).

For fine sandy soil, the biotic outflow BTEX concentrations (T5) were consistently lower than those of the abiotic control (T6) under cyclic temperature conditions. Measurable biodegradation was observed near 20 – 40 °C, however, lower than in the silty loam columns. Compared to silty loam, fine sand soil exhibited significantly lower sorption (< 20 % across all BTEX). This resulted from its coarse texture, reduced clay minerals, and lower specific surface area. While this increases initial bioavailability, it also led to faster breakthrough in the effluent and reduced residence time for microbial degradation. Thus, the K_{bio} constants appear lower overall than in the silty loam geothermal system, even though bioactivity was evident.

Likewise, in coarse sand columns, the same temperature-dependent adsorption and biodegradation were observed (T9, T10, T11, and T12). Benzene has modest K_{bio} overall in coarse sand, suggesting faster breakthrough and lower residence time limit biotic removal, especially during cooling. Toluene and ethylbenzene show the strongest temperature response in coarse sand, with maximum K_{bio} value after 30 °C. Xylenes show consistently positive K_{bio} across the cycle, increasing toward the cooling phase, consistent with carryover of enzymatic activity and improved desorption. K_{bio} values under constant temperature were consistently lower (mostly 0.05 – 0.13 d^{-1}) than those observed under cyclic temperature conditions for fine sand and coarse sand (which reached up to 0.25 – 0.3 d^{-1}) (Table 5.6). The specific rate of degradation at each temperature in cyclic treatment is presented in Table D3 (*Appendix D*). The results indicate that reduced organic matter and surface area in sandy soil limit both adsorption and microbial colonization. Sandy soils facilitated rapid flow and lower residence times, which reduced overall biodegradation even when temperature cycling was favourable.

Overall, benzene being more polar and volatile, showed the lowest adsorption, thereby remaining more bioavailable at all temperature stages. Xylene and ethylbenzene exhibited the highest sorptive retention due to their larger molecular size and higher hydrophobicity (higher log K_{ow} and K_{oc}) (Sun et al., 2020; W. Zhang et al., 2022). This reduction in adsorption at higher temperatures implies that geothermal heating enhances substrate availability for microbial degradation**,** a critical link between abiotic and biotic processes in thermally perturbed soils.

During heating, increased diffusion and reduced viscosity improved contaminant–microbe contact, while cooling phases (10 – 5 °C) caused temporary decreases in degradation rates and

slight rebound of effluent concentrations. The maximum biological contribution to removal occurred at 30 – 35 °C, consistent with optimal mesophilic microbial metabolism.

Table 5.6: Biodegradation rate constant (K_{bio}) values in different columns.

Soil Type	Temperature Regime	Benzene (d^{-1})	Toluene (d^{-1})	Ethylbenzene (d^{-1})	Xylenes (d^{-1})
Silty loam	Cyclic (5–40 °C)	0.18	0.21	0.24	0.23
Silty loam	Constant (12 °C)	0.08	0.11	0.10	0.09
Fine sand	Cyclic (5–40 °C)	0.14	0.18	0.21	0.20
Fine sand	Constant (12 °C)	0.06	0.09	0.08	0.07
Coarse sand	Cyclic (5–40 °C)	0.12	0.16	0.19	0.18
Coarse sand	Constant (12 °C)	0.05	0.10	0.11	0.09

The remaining fraction of BTEX on the soil also supported the previous finding of cyclic temperature influence. Figure 5.15 illustrates the residual adsorbed concentration of each of the four compounds on soil at the end of the experiment from all column experiments. The finding suggested that silty loam soil, with cyclic heating and cooling phases, contains significantly lower concentration ($p = 0.003$) than the constant columns. Similarly, in fine sand and coarse sand columns, the fraction of BTEX in cyclic was lower than in constant isotherm treatment, but the magnitude of the difference was lower than in silty loam soil. The results confirm that temperature cycling stimulates microbial metabolism and enzyme activity**,** improving degradation kinetics, particularly for heavier BTEX components. Under isothermal conditions (12 °C)**,** biodegradation sustained but at a lower rate**,** consistent with the slower microbial kinetics reported for hydrocarbon degraders in cooler, constant environments.

In contrast to constant low-temperature (12 °C) operation, results clearly showed that thermal cycling (5 – 40 – 5 °C) significantly accelerated the biodegradation of BTEX compounds. K_{bio} under cyclic heating reached values 2 – 10 times higher than under isothermal 12 °C conditions across all soil types tested (silty loam, fine sand, and coarse sand). This improvement is in line with the known temperature dependence of microbial metabolism and hydrocarbon-degrading

enzymes (C.-I. Chen & Taylor, 1997b; Deeb & Alvarez-Cohen, 1999b). Furthermore, high temperatures increase the availability of substrate for microorganisms by reducing sorptive constraints and speeding up biochemical reaction steps (as the soil–aqueous partitioning weakens) (Sleep & McClure, 2001c)

For many BTEX-degrading consortia, the idea of a mesophilic optimum is supported by the fact that the highest K_{bio} values frequently occurred in the mid-high temperature window (30 – 40 °C) (Kaur et al., 2023). Even though K_{bio} decreased during cooling phases, positive values remained, suggesting that microorganisms can withstand heat stress and return to metabolic activity. Research on thermally exposed microbial communities supports this resilience, demonstrating changes in diversity but maintaining basal functioning under repeated heating (Ali et al., 2024).

The texture of the soil significantly influenced the observed rates of biodegradation. The observed differences in BTEX degradation and microbial growth kinetics across the three soil types can be directly linked to their contrasting physicochemical properties (Table 5.4). Despite stronger sorptive binding of BTEX (which slows immediate availability), silty loam generally showed the highest average K_{bio} across compounds during cyclic tests. Silty loam soil contained higher organic matter (foc = 0.021) and microporosity because of finer particles, supporting more surface area, better microbial colonization, nutrient retention and protection from washout. In addition, higher porosity (0.474) and higher adsorption improved the retention time of BTEX in the column and made them bioavailable in biologically active zones for enhanced degradation. In contrast, fine and coarse sand exhibited less sorption due to lower organic matter (foc = 0.013 and 0.011, respectively) and therefore faster breakthrough in the outlet. Lower organic carbon availability further resulted in less biomass retention and substrate contact time, resulting in somewhat lower but still noticeable rates under cyclic heating. The differences were more pronounced at a constant low temperature (12 °C): fine sand consistently displayed lower rates and more frequent negative (apparent) values, which are indicative of the dominance of abiotic processes or desorption lag, while soils with greater heterogeneity (loam) retained marginally positive biodegradation. Coarse sand, with the lowest porosity (0.421), highest bulk density (1.534 g/cm³), showed the weakest biodegradation performance, probably due to poor microbial colonization and faster breakthrough due to low adsorption coefficient. As a whole,

the findings indicate that soil properties such as soil texture, organic carbon, and porosity dictate how effectively bacteria can proliferate and degrade BTEX.

The activation energy (E_a) was calculated for all four compounds from Arrhenius slopes. E_a decreased with higher molecular weight; Benzene = 45 – 55 kJ/mol, toluene = 38 – 43 kJ/mol, ethylbenzene and xylene = 30 – 38 kJ/mol. Geothermal temperature cycling (5 – 40 °C) dramatically increased BTEX biodegradation rates by lowering sorption constraints and stimulating microbial metabolism. This suggests that geothermal heating could be a sustainable option for improved ISB.

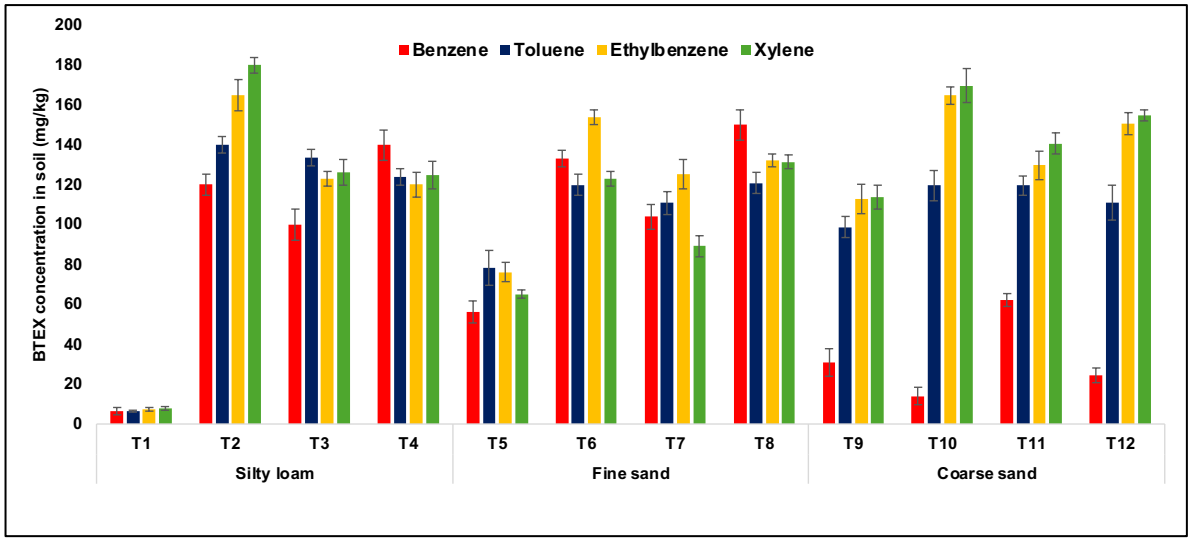

Figure 5.15: Remaining BTEX concentration in different soils after opening columns on completion of heating and cooling treatment. T1 is consortia-treated columns with cyclic temperature, T2 is control BTEX columns with cyclic temperature, T3 is consortia-treated columns at constant temperature (12 °C), and T4 is control BTEX columns at constant temperature with silty loam soil (in same pattern T5, T6, T7 and T8 with fine sand; T9, T10, T11, and T12 with coarse sand).

5.15.2 Mass balance

A complete mass balance was performed to quantify the fate of BTEX in the soil column systems under both cyclic and constant temperature regimes, as shown in Figure 5.16. Nine

injections of 50 mg/L of each compound were used to introduce the total mass, which was then divided into four main fractions: (i) effluent (outflow), (ii) adsorbed to soil, (iii) biodegraded (microbial transformation), and (iv) unaccounted (lost) fraction. The lost fraction was interpreted as either analytical uncertainty, irreversible sorption, possible adsorption to column cell walls or possible volatilization via microleaks.

Depending on the type of compound and soil, the biodegraded fraction accounted for 45–60% of the total BTEX introduced and was the dominant fraction under cyclic temperature conditions. The effluent outflow fraction stayed below 20% because of high microbial and sorptive retention, while adsorption made up 15–30%, mostly at lower temperatures. In most cases, the lost fraction was less than 10%, demonstrating strong system closure and analytical dependability. In contrast, under constant 12 °C incubation, adsorption (35–45%) and effluent outflow (25–35%) contributed proportionately more to the biodegradation, which was significantly lower (10–20%). These findings are consistent with earlier research showing that BTEX is more persistent in soil matrices in low-temperature systems due to slower desorption kinetics and decreased microbial metabolism (Sleep & McClure, 2001c; B. K. Yadav & Hassanizadeh, 2011).

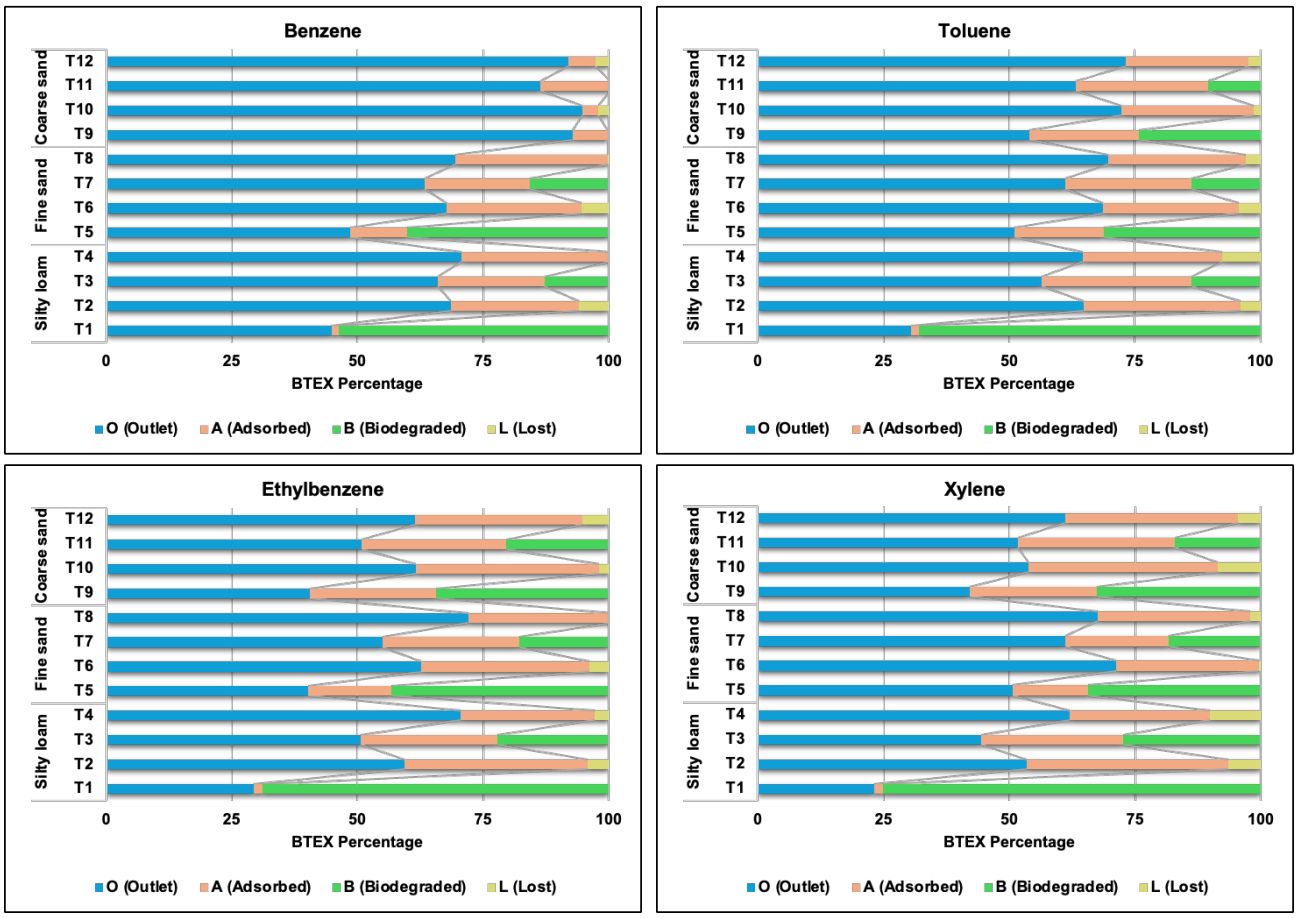

Figure 5.16: Overall mass balance of BTEX accounting for abiotic (outflow, adsorption, loss) and biotic loss (biodegradation) after completion. The total injected concentration was 450±6 mg/L of each compound (50 mg/L at each injection- total 9 injections). T1 is consortia-treated columns with cyclic temperature, T2 is control BTEX columns with cyclic temperature, T3 is consortia-treated columns at constant temperature (12 °C), and T4 is control BTEX columns at constant temperature with silty loam soil (in same pattern T5, T6, T7 and T8 with fine sand; T9, T10, T11, and T12 with coarse sand).

Benzene and toluene had higher effluent fractions and lower adsorption than ethylbenzene and xylenes. This is in line with their higher Henry's constants and lower hydrophobicity. On the other hand, xylenes had more adsorption and biodegradation during cyclic heating, which shows that they were more available to living things after thermal desorption. These patterns are similar to previous findings on how BTEX sorption and biodegradation work together in soils with varying amounts of organic carbon (Ran et al., 2003; Shi et al., 2020).

Headspace equilibrium experiment indicates that volatility losses under sealed column conditions were relatively minimal (< 10%). Consequently, temperature-modulated adsorption–desorption and microbial degradation constituted the primary mechanisms regulating BTEX attenuation. During the heating phase, the desorption of organics increased their concentration in water, which accelerated oxidation and microbial uptake. This dynamic coupling of biological and physical processes under geothermal cycles shows how controlled heating could be used to improve remediation.

The overall mass balance closure across all experiments surpassed 90%, confirming both analytical consistency and the dependability of the derived K_{bio} values. The remaining discrepancies (<10%) can be ascribed to unquantified intermediate metabolites, assimilation of BTEX-derived carbon in microbial biomass, or irreversible sorption to soil micropores or column walls. The convergence of adsorbed and biodegraded fractions under cyclic conditions illustrates that biological processes increasingly dictate the fate of BTEX, as thermal oscillations promote microbial activation and substrate release.

5.15.3 Enzyme activity

To further prove the biodegradation of BTEX in consortia-treated columns, the activity of enzymes was analyzed as shown in Figure 5.17. Activity of ToMO, C1,2D, and C2,3D was tested at different time intervals during heating and cooling phases. Most of the BTEX biodegradation pathways involve several monooxygenases and dioxygenases that attack the aromatic hydrocarbon ring (Leung et al., 2019; Miri et al., 2019). In two subsequent monooxygenation processes, ToMO is capable of hydroxylating more than one position of an aromatic ring. C1,2D and C2,3D are iron-containing enzymes able to cleave the ring of catechol (the converted product from ToMO) for complete detoxification of BTEX. Many studies have reported the role of C1,2D and C2,3D in the biodegradation of BTEX by the meta-cleavage pathway (Chicca et al., 2020b; H. A. Hassan & Aly, 2018; Miri et al., 2021; Wongbunmak et al., 2020).

The maximum change was reported and presented at incubation days 6 and 14 for cyclic and constant temperature columns (Chapter 4, Figure 4.1). The enzyme activity was higher at 20 °C during the heating and cooling phases, while the activity was comparatively slow in the effluent

collected from the isothermal columns. The biodegradation trend found in different soils in the previous section (silty loam, fine sand, coarse sand) was further supported by a similar enzyme activity trend in these soil columns; silty loam followed by fine sand and coarse sand.

On day 6, the activity of ToMO, C1,2D and C2,3D was 16, 12 and 23 U in silty loam soil, which was higher than 10, 7 and 10 U in fine sand, and 9, 10 and 15 U in coarse sand, respectively. These activities were further enhanced for all soil columns on day 16. Meanwhile, in constant temperature columns, the activity was consistently lower than the cyclic ones at days 6 and 14, with statistically significant differences of $p < 0.05$. This revealed that enzymes of metabolic pathways were more active at higher temperatures to consume or degrade a pollutant (A. Kumar et al., 2020). The enzymatic studies showed that the consortium used the *tod* and *tol* pathways for the BTEX metabolism, where ToMO started the cleavage of aromatic rings by hydroxylation and was followed by the cleavage of catecholic ring by C1,2D and C2,3D (Miri et al., 2022).

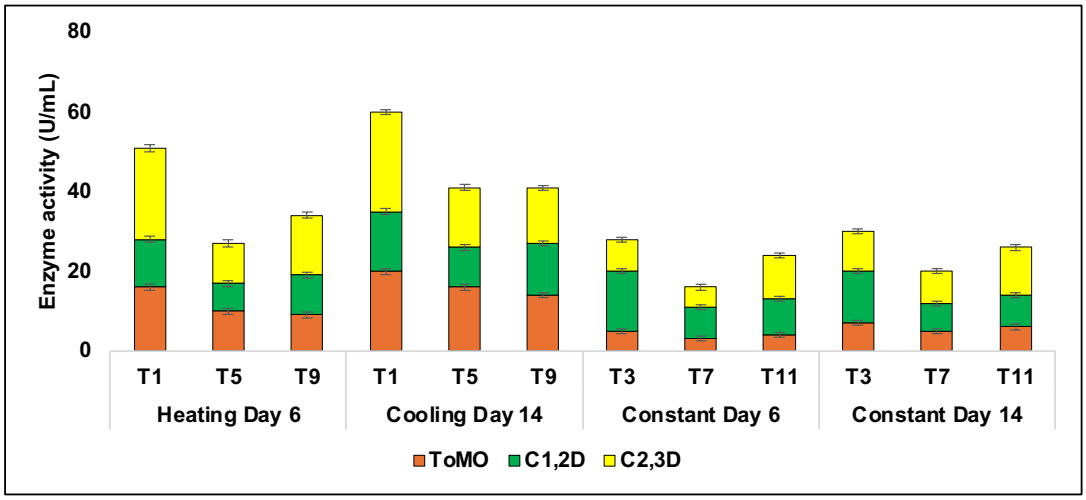

Figure 5.17: Enzymatic activity of Toluene monooxygenase (ToMO), Catechol 1,2-dioxygenase (C1,2D) and Catechol 2,3-dioxygenase (C2,3D) from cyclic and constant temperature columns at different incubation periods. T1 is consortia-treated columns with cyclic temperature, T3 is consortia-treated columns at constant temperature (12 °C) with silty loam soil (in the same pattern as T5 and T7 with fine sand; T9 and T11 with coarse sand).

5.16 Conclusions

The coupled processes of volatilization, adsorption, and biodegradation of BTEX compounds under thermal cycling (15 – 40 °C) were evaluated to understand the feasibility of geothermal Remediation. In batch experiments, volatilization increased predictably with temperature by 5 – 7 %, while adsorption onto silty loam soil showed a strong negative temperature relation (exothermic sorption); adsorption fractions declined systematically by 11 – 13% for all compounds from 15 °C to 40 °C. The reduced adsorption at elevated temperatures enhances the aqueous availability of BTEX compounds. The biodegradation became dominant above 25 – 30 °C. Monocultures achieved moderate removal with *<0.38 for B. infantis and ~ 0.40 for M. esteraromaticum*, but the consortium outperformed both, reaching biodegradation fractions approaching 0.36 – 0.48 for all BTEX compounds at 35 – 40 °C.

In fed-batch soil columns**,** cyclic heating and cooling enhanced BTEX biodegradation by more than two-fold in all three soil types, but overall significant removal was found in silty loam (53% benzene, 68% toluene, 68% ethylbenzene and 75% xylene) due to higher foc and enhanced microbial retention. Temperature remains the primary driver, with peak K_{bio} (0.335 – 0.739 d^{-1}) near 30 – 35 °C for all compounds. In contrast, constant low temperature systems (K_{bio} < 0.1 d^{-1} for all soils and BTEX biodegradation < 27%) are constrained by low metabolic rates, slow diffusion, and reversible sorption equilibrium that favours retention over degradation. This aligns with the broader body of BTEX biodegradation literature, which shows slow attenuation in cold groundwater unless stimulated. Soil types significantly govern the coupling efficiency between geothermal energy and microbial degradation with soil that had higher organic content (foc) resulted in higher degradation. Silty loam supported highest biodegradation, followed by sandy soils, due to higher organic matter, surface area, microporosity, adsorption, porosity, and nutrient retention. All these factors lead to better microbial colonization and increased BTEX bioavailability. It showed that Geothermal remediation systems must be tailored to local lithology by combining heating with nutrient addition or biofilm carriers in coarse sand soils to enhance performance. Overall, the results demonstrated that geothermal heating is a sustainable option to shift the balance from sorptive retardation toward biological removal.

Objective 4: Investigate geothermal heating impacts on soil microbiome communities along with the borehole depth by 16S rRNA sequencing

The experimental studies from previous objectives showed the potential of geothermal heating as a sustainable heat source for BTEX bioremediation. To better understand how this temperature range could affect the soil microcosm, advanced techniques such as sequencing were used to examine the effects of temperature and BTEX on the soil microcosm from a geothermal borehole. The results from this objective are submitted as a peer-reviewed article in "*Current Research in Biotechnology*".

Background

In-situ bioremediation of the subsurface can be enhanced with heat. A detailed understanding of subsurface microbial interactions, the effect of pollutants, and physicochemical parameters under heated conditions will help in the optimization and design of ISB of contaminated sites. Hence, in this objective, microbial communities were explored from different depths (10, 120, and 240 feet) in soil samples from a geothermal heat pump borehole. Soil samples were spiked with BTEX at different temperatures (15, 28, and 40 °C) to analyze the role of geothermal heating on the microbial community. The microbial profiling change was analyzed through 16S rRNA sequencing. The taxonomic results revealed that more than 0.75 relative abundance of bacteria belong to the phylum *Proteobacteria* in all the samples, followed by *Bacteroidota* and *Actinobacteriota*. Bacteria from these phyla have been previously reported for BTEX degradation and are mostly aerobic and facultatively anaerobic. The presence of BTEX significantly ($p < 0.05$) shifted microbiome diversity by >2-fold, especially *Proteobacteria* and *Bacteroidota, compared* with uncontaminated soil samples at all three temperatures. Specific species like *Methylotenera, Pseudomonas, Bacillus,* and *Arthrobacter* were identified as the major strains for BTEX tolerance. The knowledge derived from such studies and identified strains is pivotal for developing sustainable and efficient bioremediation strategies to address BTEX contamination in diverse environmental settings.

Results and Discussion

5.17 Soil characterization

Physicochemical factors such as temperature, pH, salinity, redox conditions, porosity, and the soil type all dictate the conditions in each habitat. Figure 5.18 shows the soil grain distribution performed with sieve analysis. As the depth increases from 10 to 240 ft, the soil becomes finer in both boreholes. Most of the soils were fine sand, while SS2 from 120 ft and SS6 from 240 ft were silty loam, as shown in Figure 5.18. Other soil parameters are defined in Table 5.7, for instance, CEC, moisture content, and plasticity. Liquid limit, plastic limit, and moisture content were similar for all soils, although the second borehole exhibited a slightly higher moisture content, differing by 10–15%. pH of all the soil samples was found to be around neutral or slightly alkaline, which is preferable for microbial growth and their proliferation.

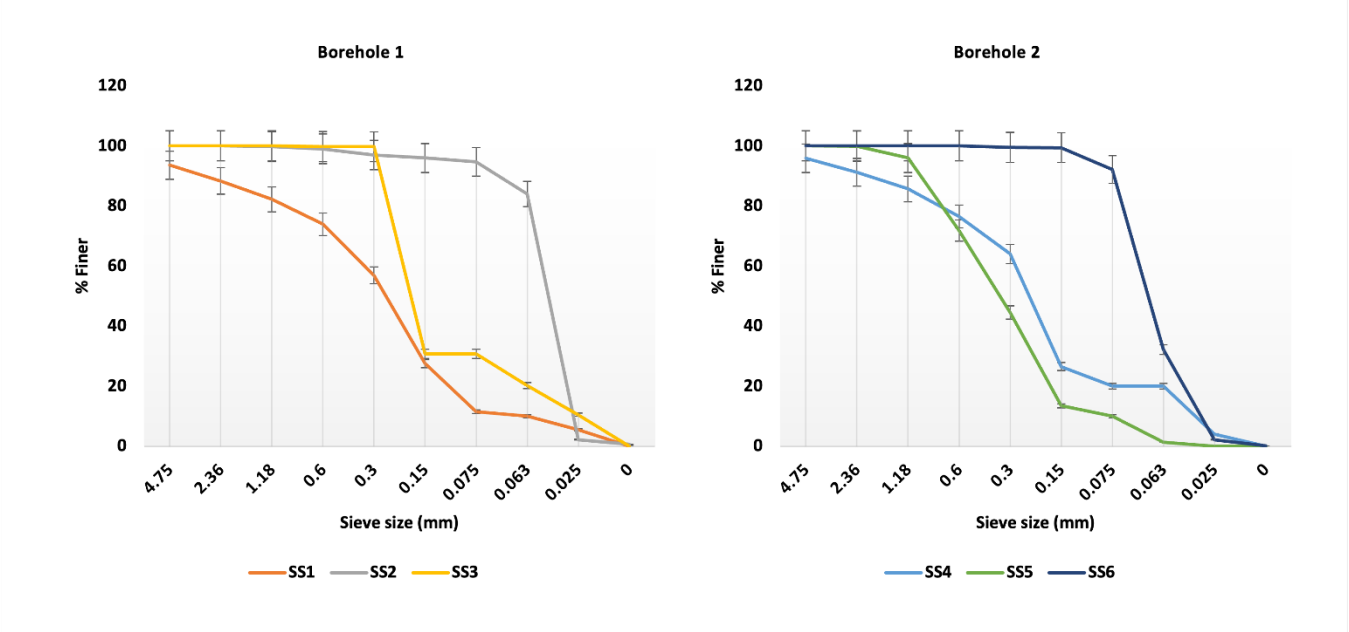

Figure 5.18: Grain size distribution curve of soil samples (SS) from different depths.

However, CEC was the only property among the analyzed factors that was higher in the topmost soil samples (from 10 ft) compared to the deeper soil samples for both boreholes. CEC measures the ability of soil to hold positively charged ions, and it is a crucial factor that allows us to understand soil structure stability, nutrient availability, and soil pH. Its value depends on clay mineral and organic matter content (Solly et al., 2020). The value of CEC showed lower cation and clay content in soils 2, 3 and 6 (SS2, SS3 and SS6). These soil samples also did not exhibit any plasticity properties, possibly due to low clay content; hence, the plastic limit could not be measured in SS2, SS3, and SS6.

Table 5.7: Physicochemical properties of soils.

Soil sample	pH	Moisture content (%)	Plastic limit (%)	Liquid limit (%)	CEC (ppb)
SS1	7.6±0.21	13.80±2.01	13.61±1.73	23.71±1.37	2152±32.35
SS2	8.6±0.35	11.23±1.22	-	26.73±1.72	477±7.99

SS3	8.8±0.46	13.12±1.99	-	25.82±1.64	402±9.12
SS4	7.1±0.23	14.52±2.01	14.42±1.96	22.43±1.24	2227±35.08
SS5	8.3±0.32	15.41±2.21	13.70±1.63	25.17±1.63	1677±27.06
SS6	8.6±0.35	15.32±2.32	-	25.61±1.48	1277±24.12

***CEC:** Cation exchange capacity

Likewise, HMs were also analyzed because they can affect microbial growth and hinder their metabolism when present in amounts higher than the regulatory concentration. Hence, it is essential to screen the soil samples for HMs because they may affect the rate of BTEX biodegradation (Fulke et al., 2024; Inobeme, 2021). Figure E1 (*Appendix E*) illustrates the analysis of HM by ICP, demonstrating that the soils had HM levels (<50 mg/kg) below the regulatory level, and therefore, it can be assumed that there was no HM contamination (L. Liu et al., 2018).

5.18 Metagenomic analysis

Metagenomic analyses were performed to estimate the overall diversity and similarity in microbial communities at depth. The V4 region of 16S rRNA was sequenced and analyzed by Microbiome Analyst software, as shown in Figure 5.19a. The results reveal that there is no monotonic trend in the microbial abundance as the depth increases. For instance, in borehole 1, the microbial richness is higher in SS2 at 140 ft, while in borehole 2, there is a continuous increase in the microbial community from 10 ft to 240 ft in SS4, SS5, and SS6.

Figure 5.19b demonstrates the dendrogram of the microbial community of all six soil samples. The clades are arranged according to how similar they are to each other; the greater the height difference, the more dissimilarity (Jarman, 2020). Figure 5.19b shows that there was high similarity in the topmost soil samples (SS1 and SS4 from 10 ft) with a remarkably similar number of reading counts, while other soil samples exhibit greater diversity. This could be because of the reason that surface microbial communities are influenced by relatively consistent and well-mixed environmental factors like temperature, moisture, oxygen availability, and

organic matter input from plant and atmospheric sources; they typically have more compositional similarity across boreholes. Additionally, microbial assemblages are homogenized by frequent nutrient exchange and physical mixing in these surface soils. Conversely, deeper subsurface environments exhibit greater physical and geochemical heterogeneity, with limited hydrological connectivity between boreholes and noticeable gradients in oxygen, redox potential, and nutrient availability. More community divergence occurs at depth as a result of these factors, which encourage the growth of highly specialized microbial populations tailored to localized energy sources and mineralogical conditions (Griebler & Lueders, 2009c; Hug, Baker, Anantharaman, Brown, Probst, Castelle, Butterfield, Hernsdorf, Amano, & Ise, 2016).

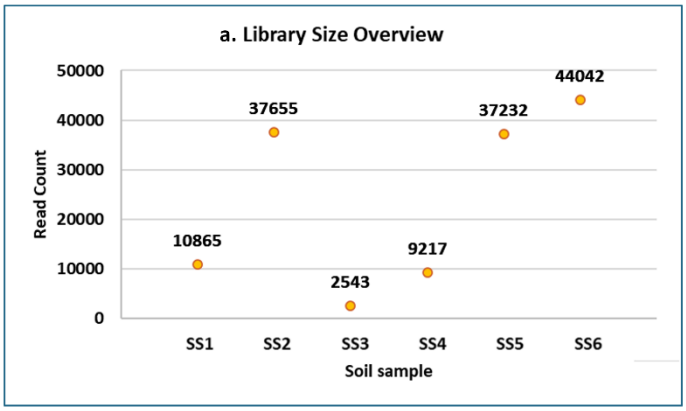

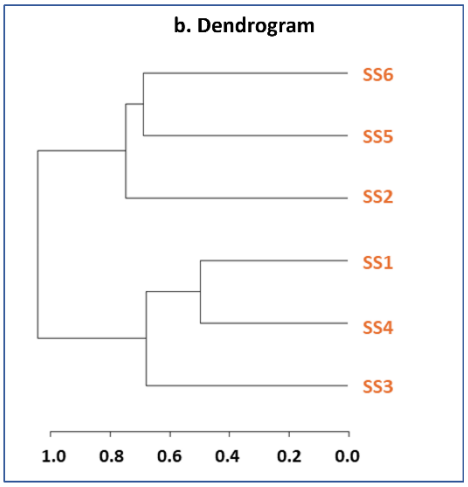

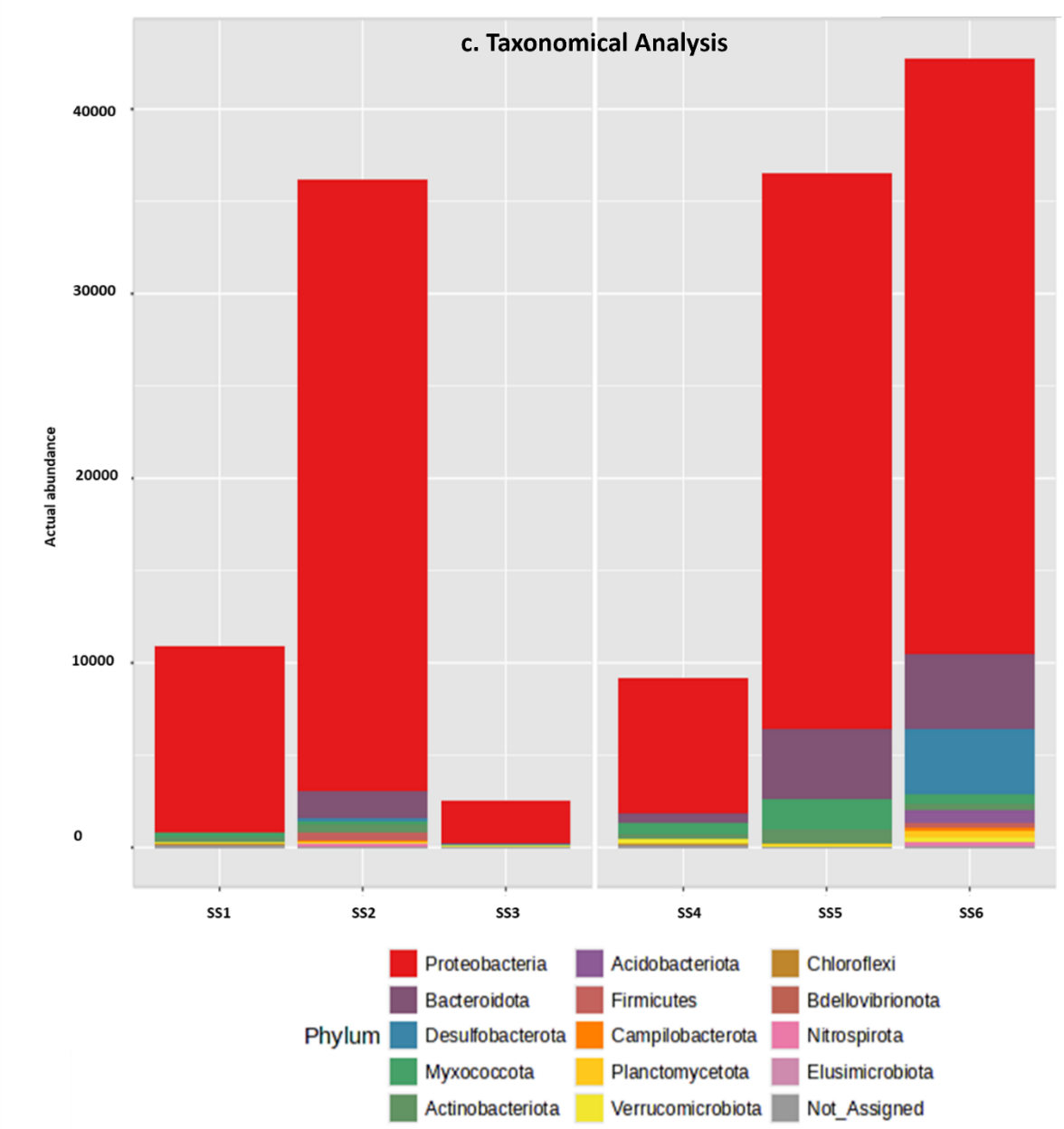

Figure 5.19: (a) Overall number of reads per soil sample, **(b)** Dendrogram of metagenomic analysis for microbial community similarity, **(c)** Taxonomy analysis of the microbial community in soil on a phylum basis.

The marker data profiling was performed on metagenomic data to determine the taxonomic composition, analyze the whole microbial community in the soil samples, and examine how the pattern of consortia changes with depth. This is shown in Figure 5.19c. The results revealed that more than 0.75 relative abundance of bacteria belong to the phylum *Proteobacteria* in all six

samples, followed by *Bacteroidota* and *Actinobacteriota*. Bacteria from these phyla are previously reported for BTEX degradation and are mostly aerobic and facultative anaerobic, for instance; *Pseudomonas putida and Pseudomonas fluorescens* (Chicca et al., 2020c; Feng et al., 2021; Miri et al., 2021), *Rhodococcus sp*. (Feng et al., 2021; You et al., 2018), and *Bacillus sp*. (Surendra et al., 2017; Wongbunmak et al., 2020).

Likewise, the microbes identified in the soil samples were further analyzed based on the genus to which they belong to (*Appendix E* Figure E2). The community and their abundance were drastically low in soil samples SS1 and SS4 from depth 10 ft and SS3 from depth 240 ft. The total count for OTUs was around 10,000, compared to the other three soil samples, which had higher counts (over 35,000 OTUs). More than 80 different bacterial genera were found in each sample; however, *Rhodoferax, Bacillus, Pseudomonas, and Microbacterium* genera were found in high abundance in each soil. These genera are recognized for their contributions to the decomposition of organic matter, the cycling of nutrients, the degradation of pollutants and metabolic versatility. Species of *Bacillus* and *Pseudomonas* are especially hardy; they are rhizobacteria that promote plant growth, generate antimicrobial compounds, and can withstand changes in their surroundings (Santoyo et al., 2012; A. N. Yadav et al., 2017). *Rhodoferax* thrives in redox-dynamic soils due to its facultative anaerobic metabolism, which allows it to reduce iron and oxidize carbon in low oxygen environments (Finneran, 2003). According to Sheng et al. (2009), *Microbacterium* species, which belong to the Actinobacteria family, break down complex organic polymers and endure in soils with low nutrient levels. When combined, these characteristics allow them to thrive in a variety of soil types and make significant contributions to soil biochemical processes (Sheng et al., 2009).

To study the hierarchical and evolutionary relationship among the identified microbes of each soil, phylogenetic trees were generated using the neighbour-joining algorithm with 1000 bootstraps in MEGA 7.0 software, as illustrated in Figure E5. Phylogenetic analysis showed the genetic diversity and similarity of microbes present in the soil. For instance, the Phylogenetic analysis showed that soil sample 3 has a microbiome with a diverse range of genetically linked microbes, with bacteria sharing between 8% and 99% of their genetic material. *Klebsiella* and *Serratia* have 98% similarity, while *Nitrospira* and *Corynebacterium* have only 8% similarity. As facultative anaerobic, Gram-negative bacteria with similar metabolic characteristics and

genomic makeup, Klebsiella and Serratia share a close phylogenetic relationship within the Enterobacteriaceae family, as evidenced by their high similarity (98%). They have similar ecological roles, including hydrocarbon degradation and heterotrophic growth in aerobic or low-oxygen environments, as well as conserved 16S rRNA gene sequences (Williams et al., 2022). On the other hand, the low similarity (8%) between Corynebacterium and Nitrospira can be explained by their divergent ecological roles, and they are members of completely different phyla, Actinobacteriota and Nitrospirota, respectively, with different metabolic strategies and evolutionary lineages. Corynebacteria are heterotrophic bacteria that are frequently found in soil or on hosts, while Nitrospira are chemolithoautotrophic nitrite oxidizers that are essential to nitrification (Bernard & Funke, 2015; Daims et al., 2015)(Daims et al., 2016; Bernard et al., 2010). The species or taxa identified as potential BTEX-tolerant bacteria belong to different clades, indicating that taxa from different phyla could possess hydrocarbon-degrading genes and the capacity to degrade BTEX. For instance, *Pseudomonas* and *Methylotenera* are from different clades, with an overall 58% similarity between them.

5.19 Temperature effect on the soil microbial community from different depths

Figure 5.19 shows the bacterial community and taxonomy in the collected soil before any treatment with temperature and BTEX. Untreated soil has a vast diversity of bacteria belonging to different phyla, such as *Proteobacteria*, *Bacteroidota*, *Desulfobacteriota*, *Myxococcota*, *Actinobacteriota*, and *Acidobacteriota*.

However, Figure 5.20 illustrates the effect of BTEX and temperature on the microbial community. When all six soil samples were spiked with BTEX at 15±1 °C, the abundance of bacteria decreased drastically. Only phyla like *Proteobacteria*, *Bacteroidota*, *Actinobacteriota*, and *Firmicutes* have been found. All the other bacteria belonging to different phyla have been diminished, showing their low tolerance to BTEX and cold shock (lower temperature) (Figure 5.20a). The dominance of these phyla at low temperatures indicates their metabolic versatility and psychrotolerant nature. Many of these groups' members have adaptive characteristics that allow them to survive and function in cold, nutrient-limited environments. Because of their adaptable metabolism and effective use of dissolved organic carbon, Proteobacteria and Bacteroidota are able to survive in low-temperature, low-energy environments. Firmicutes can

develop endospores or switch to anaerobic metabolism, which increases persistence under heat stress, while Actinobacteriota frequently produce cold-active extracellular enzymes that break down complex organic compounds. When the microbial growth and enzyme activity of less cold-tolerant taxa are inhibited, these adaptations work together to enable these phyla to predominate (Russell, 1998; Salwan & Sharma, 2020). However, at 28±1 °C, the abundance of some selective bacteria increased in all six soil samples when treated with BTEX. Especially, the *Proteobacteria* thrived more with BTEX, showing their ability to consume and grow in its presence. These results are comparable with the literature, as most studies reported that hydrocarbon-degrading bacteria belong to the *Proteobacteria* and *Actinobacteriota* phylum (Akmirza et al., 2017; Alfreider & Vogt, 2007; Techtmann & Hazen, 2016; Wani et al., 2022). In comparison to 15±1 °C, microbes belonging to two more phyla like *Acidobacteriota* and *Chloroflexi* were observed at 28±1 °C (Figure 5.20b). Alongside dominant Proteobacteria, Acidobacteriota and Chloroflexi have emerged, reflecting ecological and metabolic changes brought on by hydrocarbon enrichment and rising temperatures. Because of their quick growth rates and well-studied hydrocarbon-degrading enzymes, which allow for effective BTEX oxidation in both aerobic and microaerophilic environments, proteobacteria continue to be widely distributed (W. Lu et al., 2024; Spiers et al., 2000). In copiotrophic taxa, elevated temperature promotes metabolic activity by improving hydrocarbon solubility and enzyme kinetics. As hydrocarbon degradation acidifies the microenvironment, oligotrophic and acid-tolerant acidobacteriota are enriched, and Chloroflexi flourish under the resulting redox gradients and can take part in the anaerobic or cometabolic breakdown of aromatic intermediates (Ho et al., 2017; Hug, Baker, Anantharaman, Brown, Probst, Castelle, Butterfield, Hernsdorf, Amano, & Ise, 2016). These changes collectively show how temperature increases and BTEX exposure reorganize microbial communities toward taxa with complementary metabolic roles in hydrocarbon turnover. The findings of a study by Alfreider and Vogt, (2007) observed similar bacterial phyla at a BTEX-contaminated site. They performed metagenomics analysis on a BTEX-contaminated aquifer based on 16S rDNA. The classes of *Proteobacteria* and *Firmicutes* were found to be dominant in contaminated plumes (Alfreider & Vogt, 2007). Likewise, the dominance of *Proteobacteria* and *Actinobacteria* was reported in BTEX-contaminated soil samples and culture media. The possible reason for their ability to degrade and grow in the presence of aromatic and aliphatic hydrocarbons is the production of

hydrocarbon-hydrolyzing enzymes such as alkane monooxygenase, dioxygenase, and gluconolactonase (H. Wu et al., 2023).

At 40±1 °C, the same six taxonomical classes were found as those at 28±1 °C. However, at 40±1 °C, *Proteobacteria* proliferate more in the control group without BTEX (Figure 5.20c). Proteobacteria proliferate in untreated soils because they are copiotrophic mesophiles, which flourish on readily degradable native carbon sources in aerobic, nutrient-rich environments. As a result, although Proteobacteria thrive in warm, undisturbed soils, the combined effects of solvent toxicity, metabolic inhibition, and competition from thermotolerant degraders cause their relative abundance to decline in BTEX-treated systems (Khan et al., 2018; Morozkina et al., 2010). The abundance suggests that, at higher temperatures, only the classes or species of *Proteobacteria* that are tolerant to high temperatures have proliferated. At the same time, the degradation ability has been restricted due to the loss of enzymatic activities. It has been reported that most of the monooxygenase and dioxygenase enzymes, which are key players for BTEX degradation, show higher activity around 30 °C and activity decreases above 30 °C (W.-Y. Chen et al., 2013; Olukunle et al., 2015).

Furthermore, the microbial communities were compared at the genus level to gain a deeper understanding of the species that have the potential to degrade BTEX under different temperature conditions, as shown in Figure 5.21. When compared at 15±1 °C, both the uncontaminated and BTEX-spiked soil have the highest microbial community from the unidentified genera, followed by *Arthrobacter* and *Pseudomonas*. The *Janthinobacterium* genus was found in higher abundance in BTEX-treated soil in comparison to uncontaminated soil. In contrast, *Pedobacter* (second highest in uncontaminated soil) was drastically diminished from the BTEX-treated group (Figure 5.21a). At 28±1 °C, in uncontaminated soil, more than 50% of species belong to the genera *Brevundimonas* and *Bacillus,* followed by *Sediminibacterium.* In BTEX-spiked soil, the *Methylotenera* genus was found to be the most abundant, contributing 49%. Genera like *Arthrobacter, Pseudomonas* and unidentified genus were found in both the soil types with comparable counts (Figure 5.21b). Furthermore, when genera were compared at 40±1 °C, the *Brevundimonas* genus was found to be the dominant genus in uncontaminated soil with more than 60% abundance, but it was drastically reduced in BTEX-treated soil. A similar trend was found at 28±1 °C showing its intolerance to BTEX.

Meanwhile, the abundance of *Arthrobacter, Lysobacter, and Bacillus* increased in BTEX-treated soil samples compared to uncontaminated soil (Figure 5.21c). These results showed that the *Arthrobacter* genus is active at all three temperatures, particularly at 40±1 °C in the presence of BTEX. In contrast, *Janthinobacterium* and *Methylotenera* were the dominant species at 15±1 °C and 28±1 °C, respectively, for BTEX degradation. The predominance of Arthrobacter at all temperatures, particularly at 40±1 °C, suggests that it has a highly flexible metabolism and can withstand environmental stress. Because of their strong cell wall structure, resistance to solvents and desiccation, and wide range of enzymatic ability to break down aromatic hydrocarbons, *Arthrobacter* species are able to flourish in environments with high temperatures and hydrocarbon exposure (Cross et al., 2015; P. Roy & Kumar, 2020). On the other hand, psychrotolerant genus *Janthinobacterium* has effective low-temperature enzyme systems for the metabolism of aromatic and simple carbon compounds (Chernogor et al., 2022; Gillis & Logan, 2015), whereas *Methylotenera* focuses on methylotrophic pathways that function best in mesophilic, oxygenated environments, making it easier to use BTEX intermediates at 28±1 °C (Afshin et al., 2021; Kalyuzhnaya et al., 2006). Therefore, the observed succession of dominant BTEX-degrading genera across temperature regimes is determined by physiological resilience and temperature-driven enzyme activity profiles.

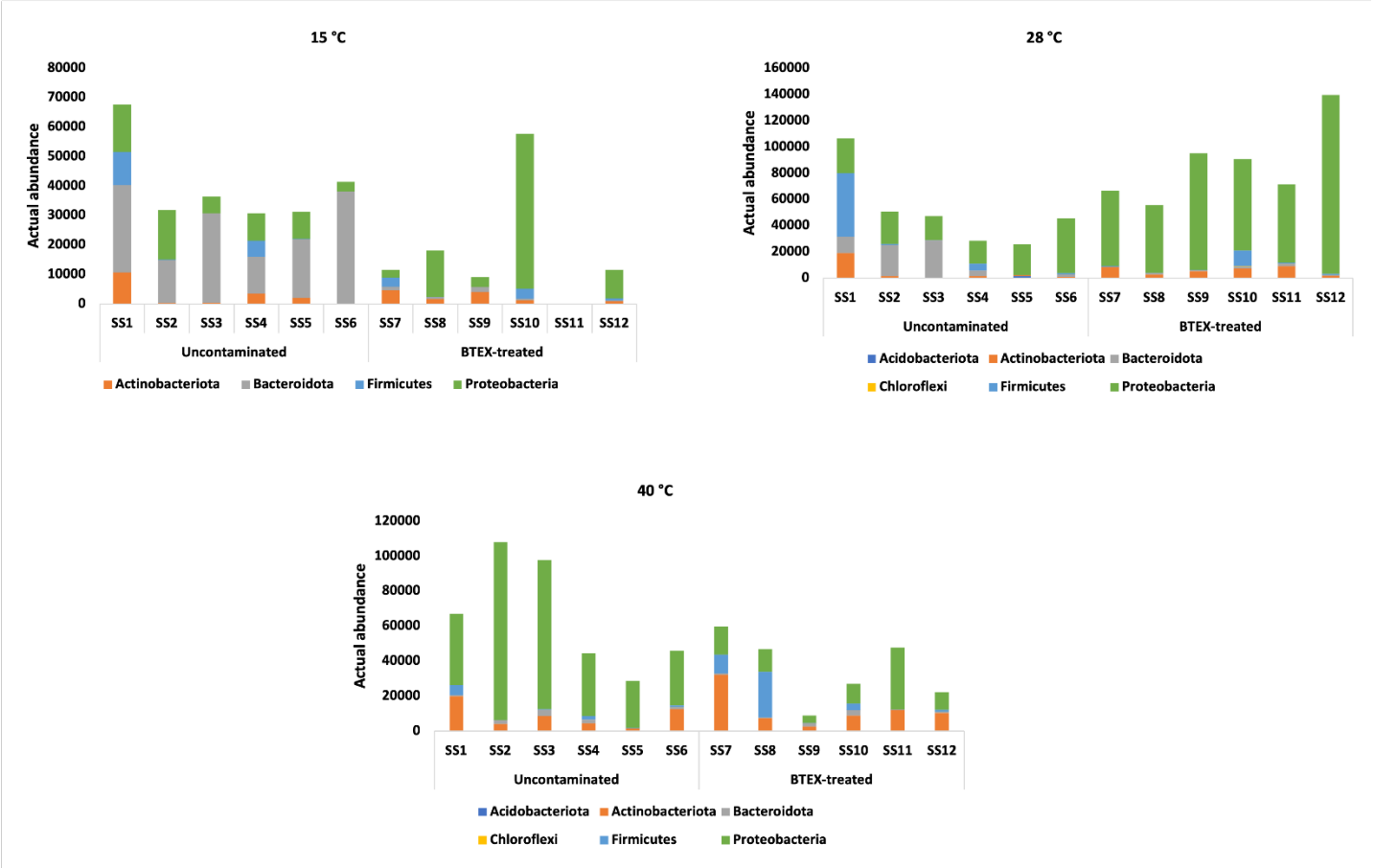

Figure 5.20: Microbial profiling of soil spiked with and without BTEX at different temperatures (a) 15 °C, (b) 28 °C, and (c) 40 °C compared at phylum level.

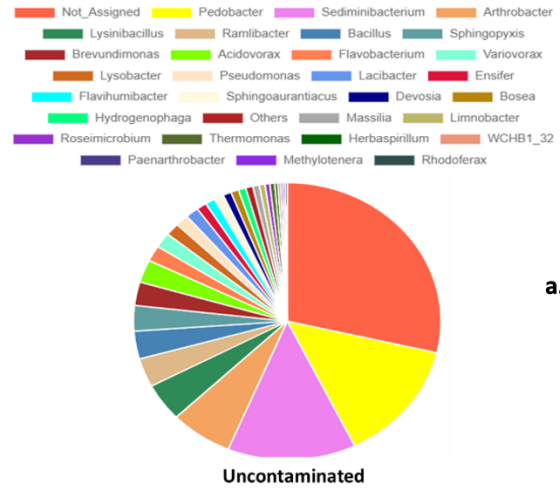

Uncontaminated

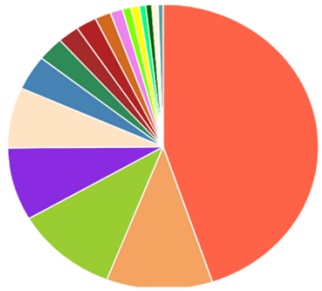

BTEX- treated

a. 15 °C

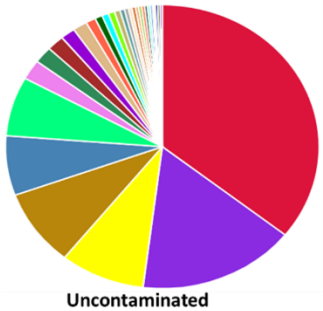

Uncontaminated

BTEX- treated

b. 28 °C

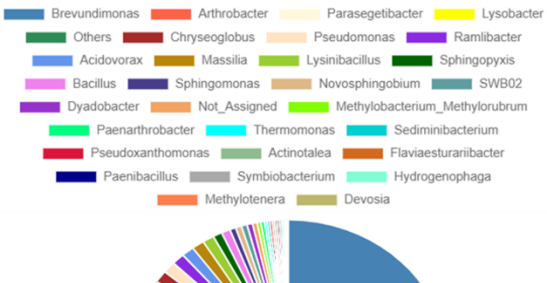

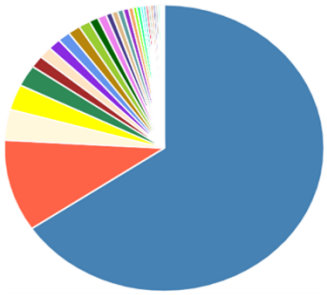

Uncontaminated

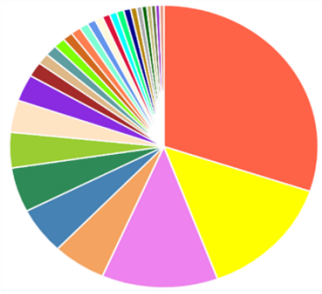

BTEX- treated

c. 40 °C

Figure 5.21: Comparison of microbial communities at genu level in treated and untreated soils and at different temperatures (a) 15 °C, (b) 28 °C, and (c) 40 °C.

5.20 Statistical analysis

To study the species' richness and diversity among the soil samples, alpha diversity and beta diversity analyses were performed as shown in Figure 5.22. For the observed OTUs, the Fisher index showed high species richness in all the soils except for the BTEX-treated soil at 15±1 °C. A significant difference was observed among the uncontaminated and BTEX-treated soil samples at 15±1 °C ($p = 0.000$), 28±1 °C ($p = 0.050$) and 40±1 °C ($p = 0.006$) (Figure 5.22a). To further analyze the differences between microbial communities, nonmetric multidimensional scaling analysis was performed using the Bray-Curtis index, as shown in Figure 5.22. The diversity among the phylotypes was significant when the uncontaminated and BTEX-treated soil samples were compared at all the temperatures: 15±1 °C (PERMANOVA $R = 0.266$, $p = 0.004$), 28±1 °C (PERMANOVA $R = 0.416$, $p = 0.003$), 40±1 °C (PERMANOVA $R = 0.514$, $p = 0.003$) (Figure 5.22b). Multiple linear regression performed with MaAsLin2 showed the significantly impacted bacterial genera with BTEX treatment in comparison to uncontaminated samples at all three temperatures (Figure E3). *Methylotenera* ($p = 0.000$) and *Pseudomonas* ($p = 0.002$) genera significantly increased in abundance at 15±1 °C with BTEX treatment (Log-transformed counts are given in *Appendix E* as Figure E4). At 28±1 °C, *Methylotenera* ($p = 0.001$) and at 40±1 °C, *Hydrogenophaga* ($p = 0.003$) and *Arthrobacter* ($p = 0.011$) proliferated more in BTEX treatment, showing their tolerance to BTEX and degradation capacity at these temperatures. *Pseudomonas* species are well known for their BTEX degradation capacity at lower temperatures since the 20th century. A study by Shim and Yang (1999) used *Pseudomonas putida* and *Pseudomonas fluorescens* as a coculture for BTEX degradation under hypoxic conditions with a 10 – 20 $mgL^{-1}h^{-1}$ degradation rate (Shim & Yang, 1999). Similarly, an enzymatic study using *Pseudomonas sp*. for BTEX degradation in groundwater and soil at 10 °C removed more than 80% of BTEX within 30 days (Miri et al., 2021). *Arthrobacter* is one of the most cited/reported species from the Actinobacteria phylum for aerobic BTEX biodegradation by several researchers (Hocinat et al., 2020; Y. Zhou et al., 2016). In contrast, *Methylotenera* is an obligately methylamine-utilizing bacterium, not reported directly for BTEX biodegradation. Some studies have reported its tendency to tolerate and utilize

hydrocarbons (Eze, 2021; A. Gomes et al., 2022). Hence, further metabolic studies are required to explore the ability of *Methylotenera* to degrade BTEX.

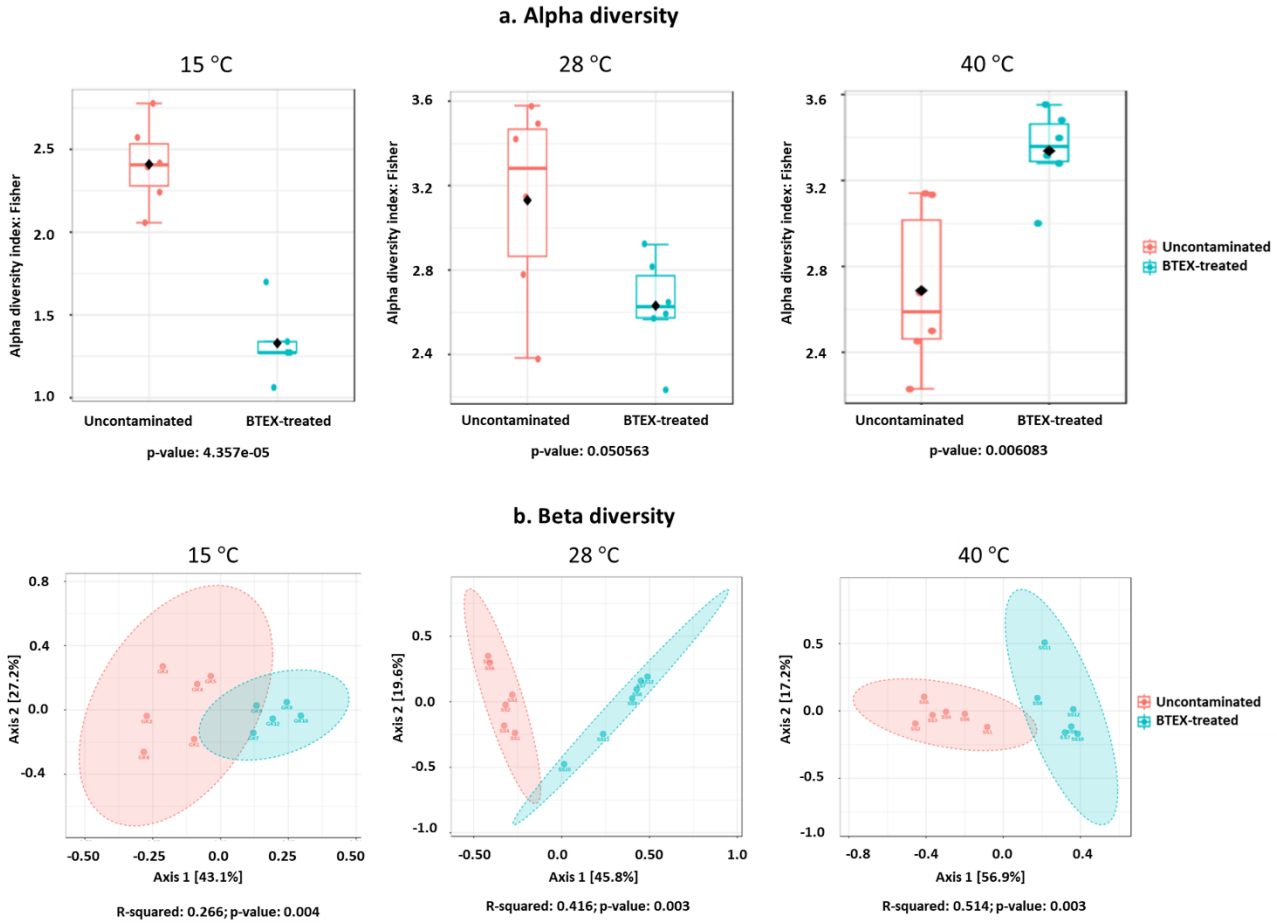

Figure 5.22: Alpha and beta diversity analysis of soil samples comparing uncontaminated and BTEX-spiked soil at different temperatures.

5.21 Correlation of physicochemical parameters and microbial profile

The microbes present in the subsurface are influenced by the surrounding environmental factors. Therefore, the soil parameters studied in this thesis (section 5.17) and temperature were further explored to correlate their effect on the microbial community of all six soil samples. Figure 5.23 shows the heat map of the top five microbial phylotypes, such as *Acidovorax, Arthrobacter, Bacillus, Methylotenera, and Pseudomonas*. Most of the parameters do not show any significant impact on microbial counts except for CEC and temperature. The figure shows the relative effect of these parameters on a scale of 0 to 1 concerning the main microbial genera.

Temperature was the most influential factor for microbes, followed by CEC. The effect of temperature is well explored in the literature, which indicates that there is a different preferred temperature range for different microbes depending on their phylotype and metabolic pathways (S. Li et al., 2024; C. Wang et al., 2021). A previous study by our group explored the effect of temperature on microbial growth and BTEX degradation. Results showed that microbes proliferate more and degrade more BTEX at 28±1 °C and 40±1 °C in comparison to 15±1 °C (Objective 1, section 5.5). Another study on the effect of temperature on microbes showed that the temperature sensitivity of microbes varies among different microbial taxa. Some microbes prefer low temperatures, while others prefer high temperatures (Wang et al., 2021). Likewise, CEC is an important parameter related to cations; a higher CEC will help retain a large quantity of nutrients by providing more exchange sites for ions. Soils with higher CEC have a high clay fraction, corresponding to more organic content, which affects microbial distribution in the soil. Therefore, CEC makes the soil fertile and a better place for microbial proliferation (Solly et al., 2020; Zheng et al., 2022). Other parameters like HMs did not show any effect as the measured levels of HMs in all six soils were below toxic levels.

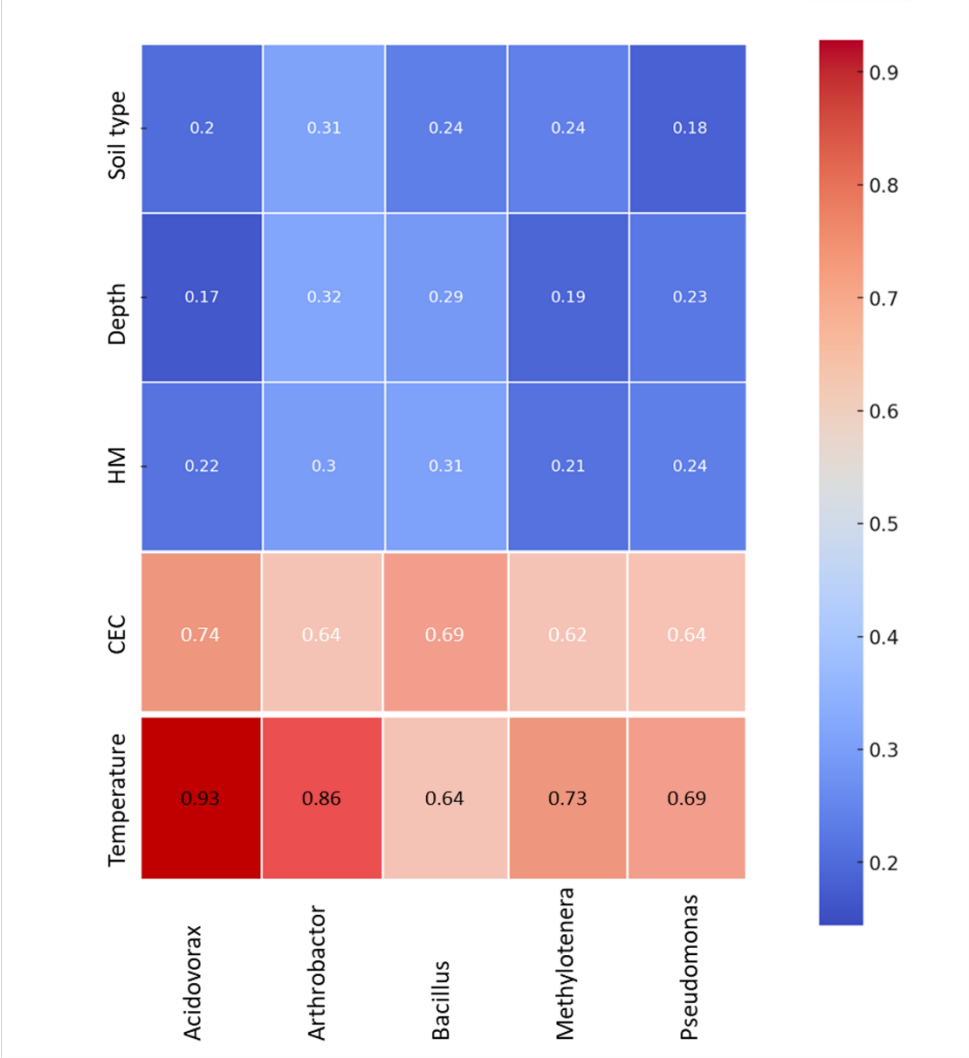

Figure 5.23: Heat map of five most dominant microbial genera showing impact of physiochemical parameters on their abundance.

Overall, this study helped to understand the diversity and change in the microbiome under different conditions. With an increase in temperature from 15 to 28 and 40 °C, the microbial community increased and became more diverse, with bacterial strains showing greater tolerance to BTEX. This suggests that geothermal heating is a potential source for enhanced bioremediation by augmenting heat into the subsurface sustainably, while also providing heating and cooling to buildings.

5.22 Conclusions

The study aimed to explore the microbiome present in six different soil samples from three different depths. It further investigated how this microbiome could change when subjected to BTEX contamination and three different temperatures (15±1, 28±1, and 40±1 °C) to understand the role of geothermal heating on microbial community and biodegradation. The findings showed that the untreated soil samples were rich in bacterial species belonging to more than 15 phyla. *Proteobacteria* dominated the other phyla by more than 50% of actual abundance. However, no correlation of microbial abundance was observed with increasing depth. Alpha and beta diversity analysis showed that the microbial communities were significantly ($p < 0.05$) different between uncontaminated and BTEX-treated soils. When treated with BTEX, the microbiome declined markedly at all three temperatures. Only four phyla at 15±1 °C and six phyla at 28±1 °C and 40±1 °C survived. The genus-based analysis revealed the major species that were active at each temperature. At 15±1 °C, *Methylotenera* and *Pseudomonas;* at 28±1 °C, *Methylotenera* and *Arthrobacter;* and at 40±1 °C, *Hydrogenophaga* and *Arthrobacter* proliferated more in BTEX-treated soil, demonstrating their temperature resilience and BTEX-degrading potential. Hence, these bacterial strains could be a potential tool for bioremediation purposes at various temperatures. Moreover, it showed that geothermal heating facilitated the proliferation of bacterial strains at elevated temperatures, suggesting it is a sustainable approach for supplementing heat for enhanced bioremediation of contaminated subsurface environments using natural microbes.

CHAPTER 6: CONCLUSIONS AND FUTURE RECOMMENDATIONS

6.1 Conclusions

This research focused on analyzing the impacts of geothermal heating on BTEX bioremediation, as defined by the experimental objectives. A central novelty of this thesis lies in evaluating cyclic low-enthalpy geothermal heating, representative of shallow geothermal operation, and its influence on BTEX biodegradation, microbial activity, and community structure. The findings provide both mechanistic and applied insight into the feasibility of coupling geothermal energy with bioremediation as a sustainable subsurface remediation strategy. Based on the defined objectives and the performed experimental work, the following conclusions can be made:

1. The soil microbiome comprises a diverse array of microorganisms beneath the surface, capable of consuming and degrading harmful pollutants such as BTEX. This research identified potent and novel bacterial isolates, namely *B. infantis* and *M. esteraromaticum*, which achieved more than 80% degradation of each BTEX compound (initial concentration of 50 mg/L) in enrichment media.
2. Batch experiments conducted at 15±1 °C**,** 28±1 °C**,** and 40±1 °C with isolates showed that raising the temperature increased both bacterial growth and BTEX biodegradation. When the temperature was increased from 15 °C to 28 °C and 40 °C, the bacterial growth increased by about two- to three-fold, and the BTEX biodegradation rate approximately doubled (25 – 50%) for *Pseudomonas putida, Microbacterium esteraromaticum, Bacillus infantis,* and consortia cultures at 28±1 °C and 40±1 °C. These bacterial strains are reported for the first time for BTEX degradation, and their degradation mechanisms have not been studied. The enzymatic analysis revealed that both strains use ToMO, C1,2D, and C2,3D enzymes for degrading BTEX. Identifying bacteria and enzymes that degrade BTEX compounds under moderately heated mesophilic conditions (20 – 40 °C) could lead to new remediation methods for brownfield sites, where heat generated by geothermal applications can enhance bioremediation.
3. The degradation pathway studies showed that *B. infantis* and *M. esteraromaticum* use tod and tol pathways for BTEX biodegradation using different enzymes like monooxygenases and dioxygenases. The metabolomics analysis revealed the intermediate compounds formed during the degradation like acetaldehyde, hydroxybenzyl alcohol, methyl propionic acid, acetophenone, among others which are non-toxic. This helped us understand that the bacteria

studied for biodegradation do not produce any harmful intermediates and are safe to use for future bioaugmentation studies.

4. Two pure culture strains *B. infantis* and *M. esteraromaticum* were investigated for their role in different redox conditions under anoxic conditions. When ions (nitrate, sulfate, and iron) were supplemented in different combinations using the Box-Behnken method, higher degradation in denitrifying and sulfate-reducing conditions was observed in the presence of iron. However, no significant effect of iron-reducing conditions in the presence of other ions has been observed. The investigation showed a maximum BTEX biodegradation of 57% by *B. infantis* under sulfate reduction and overall, 98% by *M. esteraromaticum* in combined nitrate and sulfate reduction. This suggests that *B. infantis* tends to degrade more BTEX under sulfate-reducing than nitrate-reducing conditions. However, for *M. esteraromaticum*, the supplement of anaerobic electron acceptors enhanced the degradation under both denitrifying and sulfate-reducing conditions, because of the facultative anaerobic nature of microbes. These results show that a combination of electron acceptors could potentially affect the degradation pattern of hydrocarbons during bioremediation.
5. The coupled processes of volatilization, adsorption, and biodegradation of BTEX compounds under thermal cycling (15 – 40 °C) were evaluated to understand the feasibility of Geothermal remediation. In batch experiments, volatilization increased predictably with temperature by 5 – 7%, while adsorption onto silty loam soil showed a strong negative temperature relation (exothermic sorption); adsorption fractions declined systematically by 11 – 13% for all compounds from 15±1 °C to 40±1 °C. The reduced adsorption at elevated temperatures enhances the aqueous availability of BTEX compounds. Biodegradation became dominant above 25–30 °C. Monocultures achieved moderate removal, with <0.38 for *B. infantis* and ~0.40 for *M. esteraromaticum*, but the consortium outperformed both, reaching biodegradation fractions of 0.36–0.48 for all BTEX compounds at 35 – 40 °C.
6. In fed-batch soil columns, cyclic heating and cooling enhanced BTEX biodegradation by more than two-fold in all three soil types, but overall significant removal was found in silty loam (53% benzene, 68% toluene, 68% ethylbenzene and 75% xylene) due to higher foc and enhanced microbial retention. Temperature remains the primary driver, with peak K_{bio} (0.335 – 0.739 d^{-1}) near 30 – 35 °C for all compounds. In contrast, constant low temperature systems ($K_{bio} < 0.1$ d^{-1} for all soils and BTEX biodegradation < 27%) were constrained by low metabolic

rates, slow diffusion, and reversible sorption equilibrium that favours retention over degradation. This degradation aligned with the broader body of BTEX biodegradation literature, which showed slow attenuation in cold groundwater unless stimulated. Overall, the results demonstrated that geothermal heating is a sustainable option to shift the balance from sorptive retardation toward biological removal.

7. The research further investigated how this soil microbiome could change when subjected to BTEX contamination and three different temperatures (15, 28 and 40 °C) to understand the role of geothermal heating on microbial community and biodegradation. Alpha and beta diversity analysis showed that the microbial communities were significantly ($p < 0.05$) different between uncontaminated and BTEX-treated soils. When treated with BTEX, the microbiome changed drastically at all three temperatures. Only four phyla at 15±1 °C and six phyla at 28±1 °C and 40±1 °C survived. The genus-based analysis revealed the major species that were active at each temperature. At 15±1 °C, *Methylotenera* and *Pseudomonas;* at 28±1 °C, *Methylotenera* and *Arthrobacter;* and at 40±1 °C, *Hydrogenophaga* and *Arthrobacter* proliferated more in BTEX treated soil showing their tolerance to BTEX and degradation capacity at these temperatures. Hence, these bacterial strains could be a potential tool for bioremediation purposes at various temperatures. Moreover, it showed that geothermal heating promoted the proliferation of bacterial strains at elevated temperatures, suggesting it is a sustainable approach for supplementing heat to enhance bioremediation of contaminated subsurface environments using natural microbes.

6.1.1: Fundamental and applied significance

This study highlights the complex, nonlinear relationship between temperature and BTEX breakdown. The depth-dependent microbial changes seen during BTEX exposure and heating offer new proof that subsurface microbial communities functionally adapt to changing thermal environments in response to the dual stress of contaminants and heat. This research demonstrates that geothermal heating can change the main BTEX attenuation process from sorptive retention to biological removal by enhancing bioavailability and microbial activity. The improvement of biodegradation through cyclic heating indicates that shallow geothermal systems could fulfill two roles: sustainable energy supply and contaminant removal, especially at polluted brownfield locations. Significantly, this method could eliminate the requirement for

chemical oxidants or harsh physical processes, promoting a more sustainable remediation framework.

6.1.2: Limitations of study

While the findings of this research are promising, multiple constraints need to be recognized. The experiments were conducted in a controlled lab environment, which might not entirely reflect the spatial variability, hydraulic intricacy, and prolonged dynamics of subsurface systems at a field scale. Measurements of enzymatic activity concentrated on the initial incubation phases and did not cover the entire length of all experiments. Moreover, microbial analyses focused on community structure rather than the direct measurement of functional genes related to BTEX degradation. Subsequent studies should emphasize validating at the field scale, conducting extended thermal cycling, and performing molecular analyses aimed at functional pathways to enhance the effectiveness of geothermal-assisted bioremediation.

6.2 Future Recommendations

The present research enhanced our understanding of the role of native microbes in BTEX bioremediation and how geothermal heat influences their activity and degradation capacity. The results showed a promising approach for coupling geothermal heating with BTEX bioremediation at the laboratory scale. However, based on the results of the objectives studied, further recommendations are proposed to explore in depth the feasibility of geothermal heating as a sustainable heat source for enhanced ISB. Specifically, the recommendations comprise:

1. **Microbial Isolation and Functional Enhancement**: The potent BTEX-degrading bacterial strains, i.e. *B. infantis* and *M. esteraromaticum*, showed promising degradation. Future work could focus on the development of formation of these bacterial strains for field-scale bioaugmentation to improve and accelerate the bioremediation of BTEX-contaminated sites. Advanced genomic and proteomic analyses should be used for real-time microbial gene expression profiling and metabolic pathways studies to ensure environmental safety while using them for bioaugmentation. Furthermore, these isolates could be used to design synthetic consortia optimized for environments with temperature fluctuations.
2. **Geothermal Microbiome Profiling**: 16S rRNA sequencing across borehole depths helped to elucidate temperature-dependent shifts in microbial community structure and identify keystone degraders**.** Future work should focus on implementing microbial consortia according to their thermal niches to improve modelling of long-term bioremediation performance under geothermal regimes.
3. **Optimization of Anoxic Biodegradation**: The electron acceptors play a vital role in the bioremediation process. Response Surface Methodology (RSM) and kinetic modelling should be expanded to predict the interactive effects of electron acceptors (nitrate, sulfate, iron, and manganese), temperature, and BTEX concentration. Understanding anoxic pathways under geothermal gradients will help to understand substrate availability and electron transfer rates, which will improve ISB under varying anoxic conditions
4. **Integrated Mass-Balance and Modelling Approach**: This study investigates the adsorption–volatilization–biodegradation partitioning in soil columns. In future studies, adsorption–volatilization–biodegradation partitioning can be further combined with reactive transport and energy balance modelling to predict contaminant attenuation under natural geothermal

gradients. This will allow us to design site-specific geothermal-assisted bioremediation guidelines**.**

5. **Field-Scale Geothermal-Assisted Bioremediation Studies**: The bench-scale geothermal heating simulation demonstrated that cyclic temperatures accelerate desorption and enhance microbial activity. However, at the field scale, various other parameters come into play, like soil grain shape, groundwater flow, porosity, and soil type, which could affect the efficiency of GHPs to enhance bioremediation. Hence, field-scale studies are proposed for further validation.

CHAPTER 7: BIBLIOGRAPHY

List of References

Adams, G. O., Fufeyin, P. T., Okoro, S. E., & Ehinomen, I. (2015). Bioremediation, biostimulation and bioaugmention: A review. *International Journal of Environmental Bioremediation & Biodegradation*, *3*(1), 28–39.

Afrooz, A. N., Pitol, A. K., Kitt, D., & Boehm, A. B. (2018). Role of microbial cell properties on bacterial pathogen and coliphage removal in biochar-modified stormwater biofilters. *Environmental Science: Water Research & Technology*, *4*(12), 2160–2169.

Afshin, Y., Delherbe, N., & Kalyuzhnaya, M. G. (2021). *Methylotenera*. In W. B. Whitman (Ed.), *Bergey's Manual of Systematics of Archaea and Bacteria* (1st ed., pp. 1–11). Wiley. https://doi.org/10.1002/9781118960608.gbm02021

Agrawal, K., Bhardwaj, N., Kumar, B., Chaturvedi, V., & Verma, P. (2019). Microbial fuel cell: A boon in bioremediation of wastes. In *Microbial wastewater treatment* (pp. 175–194). Elsevier.

Akmirza, I., Pascual, C., Carvajal, A., Pérez, R., Muñoz, R., & Lebrero, R. (2017). Anoxic biodegradation of BTEX in a biotrickling filter. *Science of the Total Environment*, *587*, 457–465.

Alberti, L., Angelotti, A., Antelmi, M., La Licata, I., & Legrenzi, C. (2012). Low temperature geothermal energy: Heat exchange simulation in aquifers through Modflow/MT3DMS codes. *AQUA Mundi*, 039–051.

Alfreider, A., & Vogt, C. (2007). Bacterial Diversity and Aerobic Biodegradation Potential in a BTEX-Contaminated Aquifer. *Water, Air, and Soil Pollution*, *183*(1–4), 415–426. https://doi.org/10.1007/s11270-007-9390-4

Ali, M., Song, X., Wang, Q., Zhang, Z., Zhang, M., Ma, M., Che, J., Li, R., Chen, X., Tang, Z., Tang, B., & Huang, X. (2024). Effects of short and long-term thermal exposure on microbial compositions in soils contaminated with mixed benzene and benzo[*a*]pyrene: A short communication. *Science of The Total Environment*, *912*, 168862. https://doi.org/10.1016/j.scitotenv.2023.168862

Alisawi, H. A. O. (2020). Performance of wastewater treatment during variable temperature. *Applied Water Science*, *10*(4), 89. https://doi.org/10.1007/s13201-020-1171-x

Al-Khoury, R., Bonnier, P. G., & Brinkgreve, R. B. J. (2005). Efficient finite element formulation for geothermal heating systems. Part I: Steady state. *International Journal for Numerical Methods in Engineering*, *63*(7), 988–1013.

Alster, C. J., von Fischer, J. C., Allison, S. D., & Treseder, K. K. (2020). Embracing a new paradigm for temperature sensitivity of soil microbes. *Global Change Biology*, *26*(6), 3221–3229.

Amend, J., & Teske, A. (2005). Expanding frontiers in deep subsurface microbiology. *Geobiology: Objectives, Concepts, Perspectives*, *219*, 131–155. https://doi.org/10.1016/B978-0-444-52019-7.50012-7

Anderson, R., Brazelton, W., & Baross, J. (2011). Is the Genetic Landscape of the Deep Subsurface Biosphere Affected by Viruses? *Frontiers in Microbiology*, *2*, 219. https://doi.org/10.3389/fmicb.2011.00219

Andrade, L. B. L., Melloni, R., Silva, F. S., Rozenskỳ, L., Lípa, J., & Melloni, E. G. P. (2025). *Thermally Enhanced Bioremediation of Soil Contaminated by Naphthalene: An Assessment Using Bioindicators*. https://www.preprints.org/frontend/manuscript/875d0f1a016f092ba9c999f3417513f0/download_pub

Ang, E. L., Zhao, H., & Obbard, J. P. (2005). Recent advances in the bioremediation of persistent organic pollutants via biomolecular engineering. *Enzyme and Microbial Technology*, *37*(5), 487–496.

Ape, F., Manini, E., Quero, G. M., Luna, G. M., Sarà, G., Vecchio, P., Brignoli, P., Ansferri, S., & Mirto, S. (2019). Biostimulation of in situ microbial degradation processes in organically-enriched sediments mitigates the impact of aquaculture. *Chemosphere*, *226*, 715–725.

Arcus, V. L., Prentice, E. J., Hobbs, J. K., Mulholland, A. J., Van Der Kamp, M. W., Pudney, C. R., Parker, E. J., & Schipper, L. A. (2016). On the Temperature Dependence of Enzyme-Catalyzed Rates. *Biochemistry*, *55*(12), 1681–1688. https://doi.org/10.1021/acs.biochem.5b01094

Arndt, N. (2011). Geothermal gradient. In M. Gargaud, R. Amils, J. C. Quintanilla, H. J. (Jim) Cleaves, W. M. Irvine, D. L. Pinti, & M. Viso (Eds.), *Encyclopedia of Astrobiology* (pp. 662–662). Springer. https://doi.org/10.1007/978-3-642-11274-4_643

ASTM, R. version. (2017). *ASTM STANDARDS*.

Aulenta, F., Tucci, M., Cruz Viggi, C., Dolfing, J., Head, I. M., & Rotaru, A.-E. (2021). An underappreciated DIET for anaerobic petroleum hydrocarbon-degrading microbial communities. *Microbial Biotechnology*, *14*(1), 2–7. https://doi.org/10.1111/1751-7915.13654

Azadpour-Keeley, A., Wood, L. A., Lee, T. R., & Mravik, S. C. (2004). Microbial responses to in situ chemical oxidation, six-phase heating, and steam injection remediation technologies in groundwater. *Remediation Journal: The Journal of Environmental Cleanup Costs, Technologies & Techniques*, *14*(4), 5–17.

Bai, G., Brusseau, M. L., & Miller, R. M. (1997). Biosurfactant-enhanced removal of residual hydrocarbon from soil. *Journal of Contaminant Hydrology*, *25*(1), 157–170. https://doi.org/10.1016/S0169-7722(96)00034-4

Baillie, I. C. (2001). Soil Survey Staff 1999, Soil Taxonomy: A basic system of soil classification for making and interpreting soil surveys, 2nd edition. Agricultural Handbook 436, Natural Resources Conservation Service, USDA, Washington DC, USA, pp. 869. *Soil Use and Management*, *17*(1), 57–60. https://doi.org/10.1111/j.1475-2743.2001.tb00008.x

Banks, D. (2012). *An introduction to thermogeology: Ground source heating and cooling*. John Wiley & Sons.

Barba, S., López-Vizcaíno, R., Saez, C., Villaseñor, J., Cañizares, P., Navarro, V., & Rodrigo, M. A. (2018). Electro-bioremediation at the prototype scale: What it should be learned for the scale-up. *Chemical Engineering Journal*, *334*, 2030–2038.

Barla, M., Donna, A. D., & Baralis, M. (2018). City-scale analysis of subsoil thermal conditions due to geothermal exploitation. *Environmental Geotechnics*, 1–11. https://doi.org/10.1680/jenge.17.00087

Benedek, T., Szentgyörgyi, F., Gergócs, V., Menashe, O., Gonzalez, P. A. F., Probst, A. J., Kriszt, B., & Táncsics, A. (2021). Potential of Variovorax paradoxus isolate BFB1_13 for bioremediation of BTEX contaminated sites. *AMB Express*, *11*(1), 1–17.

Bernard, K. A., & Funke, G. (2015). *Corynebacterium*. In W. B. Whitman (Ed.), *Bergey's Manual of Systematics of Archaea and Bacteria* (1st ed., pp. 1–70). Wiley. https://doi.org/10.1002/9781118960608.gbm00026

Beyer, C., Popp, S., & Bauer, S. (2016). Simulation of temperature effects on groundwater flow, contaminant dissolution, transport and biodegradation due to shallow geothermal use. *Environmental Earth Sciences*, *75*(18), 1–20.

Bezelgues, S., Martin, J., Schomburgk, S., & Monnot, P. (2010). *Geothermal potential of shallow aquifers: Decision-aid tool for heat-pump installation*.

Bin Hudari, M. S., Deb, S., Vogt, C., Filippini, M., & Nijenhuis, I. (2025). Temperature-associated effects on methanogenesis and microbial reductive dechlorination of trichloroethene in contaminated aquifer sediments. *Frontiers in Water*, *7*, 1566161.

Bolden, A. L., Kwiatkowski, C. F., & Colborn, T. (2015). New Look at BTEX: Are Ambient Levels a Problem? *Environmental Science & Technology*, *49*(9), 5261–5276. https://doi.org/10.1021/es505316f

Bonte, M., Stuyfzand, P. J., van den Berg, G. A., & Hijnen, W. A. M. (2011). Effects of aquifer thermal energy storage on groundwater quality and the consequences for drinking water production: A case study from the Netherlands. *Water Science and Technology*, *63*(9), 1922–1931. https://doi.org/10.2166/wst.2011.189

Bonte, M., van Breukelen, B. M., & Stuyfzand, P. J. (2013). Temperature-induced impacts on groundwater quality and arsenic mobility in anoxic aquifer sediments used for both drinking water and shallow geothermal energy production. *Water Research*, *47*(14), 5088–5100. https://doi.org/10.1016/j.watres.2013.05.049

Boopathy, R. (2000). Factors limiting bioremediation technologies. *Bioresource Technology*, *74*(1), 63–67. https://doi.org/10.1016/S0960-8524(99)00144-3

Bourne-Webb, P., Burlon, S., Javed, S., Kürten, S., & Loveridge, F. (2016). Analysis and design methods for energy geostructures. *Renewable and Sustainable Energy Reviews*, *65*, 402–419. https://doi.org/10.1016/j.rser.2016.06.046

Bouwer, H. (2002). Artificial recharge of groundwater: Hydrogeology and engineering. *Hydrogeology Journal*, *10*(1), 121–142. https://doi.org/10.1007/s10040-001-0182-4

Boyd, E., & Barkay, T. (2012). The mercury resistance operon: From an origin in a geothermal environment to an efficient detoxification machine. *Frontiers in Microbiology*, *3*, 349.

Boyle, G. (2004). *Renewable energy*.

Brandl, H. (2006). Energy foundations and other thermo-active ground structures. *Géotechnique*, *56*(2), 81–122. https://doi.org/10.1680/geot.2006.56.2.81

Bryś, K., Bryś, T., Sayegh, M. A., & Ojrzyńska, H. (2020). Characteristics of heat fluxes in subsurface shallow depth soil layer as a renewable thermal source for ground coupled heat pumps. *Renewable Energy*, *146*, 1846–1866. https://doi.org/10.1016/j.renene.2019.07.101

Buettner, H. M., & Daily, W. D. (1995). Cleaning contaminated soil using electrical heating and air stripping. *Journal of Environmental Engineering*, *121*(8), 580–589.

Cafaro, V., Izzo, V., Scognamiglio, R., Notomista, E., Capasso, P., Casbarra, A., Pucci, P., & Di Donato, A. (2004). Phenol hydroxylase and toluene/o-xylene monooxygenase from Pseudomonas stutzeri OX1: Interplay between two enzymes. *Applied and Environmental Microbiology*, *70*(4), 2211–2219.

Cagliari, J., Fedrizzi, F., Rodrigues Finotti, A., Echevenguá Teixeira, C., & Do Nascimento Filho, I. (2009). Volatilization of monoaromatic compounds (benzene, toluene, and xylenes; BTX) from gasoline: Effect of the ethanol. *Environmental Toxicology and Chemistry*, *29*(4), 808–812. https://doi.org/10.1002/etc.111

Caird, S., Roy, R., & Potter, S. (2012). Domestic heat pumps in the UK: User behaviour, satisfaction and performance. *Energy Efficiency*, *5*(3), 283–301. https://doi.org/10.1007/s12053-012-9146-x

Canadell, J. G., Monteiro, P. M., Costa, M. H., Cotrim da Cunha, L., Cox, P. M., Eliseev, A. V., Henson, S., Ishii, M., Jaccard, S., & Koven, C. (2021). Global carbon and other biogeochemical cycles and feedbacks. *Climate Change*.

Carberry, J. B., & Wik, J. (2001). Comparison of ex situ and in situ bioremediation of unsaturated soils contaminated by petroleum. *Journal of Environmental Science and Health, Part A*, *36*(8), 1491–1503.

Carini, P. (2019). A "Cultural" Renaissance: Genomics Breathes New Life into an Old Craft. *mSystems*, *4*(3), e00092-19. https://doi.org/10.1128/mSystems.00092-19

Carotenuto, A., Ciccolella, M., Massarotti, N., & Mauro, A. (2016). Models for thermo-fluid dynamic phenomena in low enthalpy geothermal energy systems: A review. *Renewable and Sustainable Energy Reviews*, *60*, 330–355. https://doi.org/10.1016/j.rser.2016.01.096

Casasso, A., & Sethi, R. (2015). Modelling thermal recycling occurring in groundwater heat pumps (GWHPs). *Renewable Energy*, *77*, 86–93. https://doi.org/10.1016/j.renene.2014.12.003

Casasso, A., & Sethi, R. (2019). Assessment and minimization of potential environmental impacts of ground source heat pump (GSHP) systems. *Water*, *11*(8), 1573.

Casasso, A., Tosco, T., Bianco, C., Bucci, A., & Sethi, R. (2020). How Can We Make Pump and Treat Systems More Energetically Sustainable? *Water*, *12*(1), 67. https://doi.org/10.3390/w12010067

Castro, C., Urbieta, M. S., Plaza Cazón, J., & Donati, E. R. (2019). Metal biorecovery and bioremediation: Whether or not thermophilic are better than mesophilic microorganisms. *Bioresource Technology*, *279*, 317–326. https://doi.org/10.1016/j.biortech.2019.02.028

Chao, H.-P. (2009). Volatilization characteristics of organic solutes in stirred solution. *Journal of Environmental Management*, *90*(11), 3422–3428.

Chapman, H. D. (2016). Cation-Exchange Capacity. In A. G. Norman (Ed.), *Agronomy Monographs* (pp. 891–901). American Society of Agronomy, Soil Science Society of America. https://doi.org/10.2134/agronmonogr9.2.c6

Chatterjee, S. K., Bhattacharjee, I., & Chandra, G. (2010). Biosorption of heavy metals from industrial waste water by Geobacillus thermodenitrificans. *Journal of Hazardous Materials*, *175*(1), 117–125. https://doi.org/10.1016/j.jhazmat.2009.09.136

Chen, C.-I., & Taylor, R. T. (1997a). Thermophilic biodegradation of BTEX by two consortia of anaerobic bacteria. *Applied Microbiology and Biotechnology*, *48*(1), 121–128. https://doi.org/10.1007/s002530051026

Chen, C.-I., & Taylor, R. T. (1997b). Thermophilic biodegradation of BTEX by two consortia of anaerobic bacteria. *Applied Microbiology and Biotechnology*, *48*(1), 121–128. https://doi.org/10.1007/s002530051026

Chen, W.-Y., Wu, J.-H., Lin, Y.-Y., Huang, H.-J., & Chang, J.-E. (2013). Bioremediation potential of soil contaminated with highly substituted polychlorinated dibenzo-p-dioxins and dibenzofurans: Microcosm study and microbial community analysis. *Journal of Hazardous Materials*, *261*, 351–361. https://doi.org/10.1016/j.jhazmat.2013.07.039

Chen, X., Zhou, X., Geng, P., Zeng, Y., Hu, F., Sun, P., Zhuang, G., & Ma, A. (2023). Advancing biodegradation of petroleum contaminants by indigenous microbial consortia through assembly strategy innovations. *Chemical Engineering Journal*, *475*, 146142.

Chen, Y. D., Barker, J. F., & Gui, L. (2008). A strategy for aromatic hydrocarbon bioremediation under anaerobic conditions and the impacts of ethanol: A microcosm study. *Journal of Contaminant Hydrology*, *96*(1–4), 17–31.

Chen, Z., Grasby, S. E., & Osadetz, K. G. (2004). Relation between climate variability and groundwater levels in the upper carbonate aquifer, southern Manitoba, Canada. *Journal of Hydrology*, *290*(1–2), 43–62.

Chernogor, L., Bakhvalova, K., Belikova, A., & Belikov, S. (2022). Isolation and properties of the bacterial strain Janthinobacterium sp. SLB01. *Microorganisms*, *10*(5), 1071.

Chicca, I., Becarelli, S., Dartiahl, C., La China, S., De Kievit, T., Petroni, G., Di Gregorio, S., & Levin, D. B. (2020a). Degradation of BTEX mixture by a new Pseudomonas putida strain: Role of the quorum sensing in the modulation of the upper BTEX oxidative pathway. *Environmental Science and Pollution Research*, *27*(29), 36203–36214. https://doi.org/10.1007/s11356-020-09650-y

Chicca, I., Becarelli, S., Dartiahl, C., La China, S., De Kievit, T., Petroni, G., Di Gregorio, S., & Levin, D. B. (2020b). Degradation of BTEX mixture by a new Pseudomonas putida strain: Role of the quorum sensing in the modulation of the upper BTEX oxidative pathway. *Environmental Science and Pollution Research*, *27*(29), 36203–36214.

Chicca, I., Becarelli, S., Dartiahl, C., La China, S., De Kievit, T., Petroni, G., Di Gregorio, S., & Levin, D. B. (2020c). Degradation of BTEX mixture by a new Pseudomonas putida strain: Role of the quorum sensing in the modulation of the upper BTEX oxidative pathway. *Environmental Science and Pollution Research*, *27*(29), 36203–36214.

Choi, H. J., Seo, J.-Y., Hwang, S. M., Lee, Y.-I., Jeong, Y. K., Moon, J.-Y., & Joo, W. H. (2013). Isolation and characterization of BTEX tolerant and degrading Pseudomonas putida BCNU 106. *Biotechnology and Bioprocess Engineering*, *18*(5), 1000–1007. https://doi.org/10.1007/s12257-012-0860-1

Choi, H., Kim, J., Shim, B. O., & Kim, D. (2020). Characterization of aquifer hydrochemistry from the operation of a shallow geothermal system. *Water*, *12*(5), Article 5. https://doi.org/10.3390/w12051377

Chong, J., Liu, P., Zhou, G., & Xia, J. (2020). Using MicrobiomeAnalyst for comprehensive statistical, functional, and meta-analysis of microbiome data. *Nature Protocols*, *15*(3), 799–821. https://doi.org/10.1038/s41596-019-0264-1

Cimmino, M., & Bernier, M. (2015). Experimental determination of the g-functions of a small-scale geothermal borehole. *Geothermics*, *56*, 60–71. https://doi.org/10.1016/j.geothermics.2015.03.006

Coates, J. D., Chakraborty, R., & McInerney, M. J. (2002). Anaerobic benzene biodegradation—A new era. *Research in Microbiology*, *153*(10), 621–628.

Cross, T., Schoff, C., Chudoff, D., Graves, Li., Broomell, H., Terry, K., Farina, J., Correa, A., Shade, D., & Dunbar, D. (2015). An optimized enrichment technique for the isolation of Arthrobacter bacteriophage species from soil sample isolates. *Journal of Visualized Experiments: JoVE*, *98*, 52781.

da Silva, M. L. B., & Corseuil, H. X. (2012). Groundwater microbial analysis to assess enhanced BTEX biodegradation by nitrate injection at a gasohol-contaminated site. *International Biodeterioration & Biodegradation*, *67*, 21–27.

Daemi, N., & Krol, M. M. (2019). Impact of building thermal load on the developed thermal plumes of a multi-borehole GSHP system in different canadian climates. *Renewable Energy*, *134*, 550–557. https://doi.org/10.1016/j.renene.2018.11.074

Daims, H., Lebedeva, E. V., Pjevac, P., Han, P., Herbold, C., Albertsen, M., Jehmlich, N., Palatinszky, M., Vierheilig, J., & Bulaev, A. (2015). Complete nitrification by Nitrospira bacteria. *Nature*, *528*(7583), 504–509.

Daniel, R. M., Danson, M. J., Eisenthal, R., Lee, C. K., & Peterson, M. E. (2008). The effect of temperature on enzyme activity: New insights and their implications. *Extremophiles*, *12*(1), 51–59. https://doi.org/10.1007/s00792-007-0089-7

Decesaro, A., Machado, T. S., Cappellaro, Â. C., Reinehr, C. O., Thomé, A., & Colla, L. M. (2017). Biosurfactants during in situ bioremediation: Factors that influence the production and challenges in evalution. *Environmental Science and Pollution Research*, *24*(26), 20831–20843.

Deeb, R. A., & Alvarez-Cohen, L. (1999a). Temperature effects and substrate interactions during the aerobic biotransformation of BTEX mixtures by toluene-enriched consortia and Rhodococcus rhodochrous. *Biotechnology and Bioengineering*, *62*(5), 526–536.

Deeb, R. A., & Alvarez-Cohen, L. (1999b). Temperature effects and substrate interactions during the aerobic biotransformation of BTEX mixtures by toluene-enriched consortia andRhodococcus rhodochrous. *Biotechnology and Bioengineering*, *62*(5), 526–536. https://doi.org/10.1002/(SICI)1097-0290(19990305)62:5%253C526::AID-BIT4%253E3.0.CO;2-8

Dehkordi, S. E., & Schincariol, R. A. (2014). Effect of thermal-hydrogeological and borehole heat exchanger properties on performance and impact of vertical closed-loop geothermal heat pump systems. *Hydrogeology Journal*, *22*(1), 189–203.

Dindar, E., Şağban, F. O. T., & Başkaya, H. S. (2015). Variations of soil enzyme activities in petroleum-hydrocarbon contaminated soil. *International Biodeterioration & Biodegradation*, *105*, 268–275.

Dohrmann, R. (2006). Problems in CEC determination of calcareous clayey sediments using the ammonium acetate method. *Journal of Plant Nutrition and Soil Science*, *169*(3), 330–334.

Dowty, B. J., Laseter, J. L., & Storer, J. (1976). The transplacental migration and accumulation in blood of volatile organic constituents. *Pediatric Research*, *10*(7), 696–701.

Duncan, J., Bokhary, A., Fatehi, P., Kong, F., Lin, H., & Liao, B. (2017). Thermophilic membrane bioreactors: A review. *Bioresource Technology*, *243*, 1180–1193. https://doi.org/10.1016/j.biortech.2017.07.059

Earth energy systems in Ontario | Ontario.ca. (2013). https://www.ontario.ca/page/earth-energy-systems-ontario

El-Naas, M. H., Acio, J. A., & El Telib, A. E. (2014). Aerobic biodegradation of BTEX: Progresses and prospects. *Journal of Environmental Chemical Engineering*, *2*(2), 1104–1122.

Environment and Climate Change, C. (2007, January 9). *Groundwater contamination* [Research]. https://www.canada.ca/en/environment-climate-change/services/water-overview/pollution-causes-effects/groundwater-contamination.html

Eze, M. O. (2021). *Metagenome Analysis of a Hydrocarbon-Degrading Bacterial Consortium Reveals the Specific Roles of BTEX Biodegraders. Genes 2021, 12, 98*. s Note: MDPI stays neu-tral with regard to jurisdictional clai-ms in ….

Falkowski, P. G., Fenchel, T., & Delong, E. F. (2008). The Microbial Engines That Drive Earth's Biogeochemical Cycles. *Science*. https://doi.org/10.1126/science.1153213

Fang, H. H. P., Liang, D. W., Zhang, T., & Liu, Y. (2006). Anaerobic treatment of phenol in wastewater under thermophilic condition. *Water Research*, *40*(3), 427–434. https://doi.org/10.1016/j.watres.2005.11.025

Farber, R., Rosenberg, A., Rozenfeld, S., Banet, G., & Cahan, R. (2019). Bioremediation of artificial diesel-contaminated soil using bacterial consortium immobilized to plasma-pretreated wood waste. *Microorganisms*, *7*(11), 497.

Feller, G. (2010). Protein stability and enzyme activity at extreme biological temperatures. *Journal of Physics: Condensed Matter*, *22*(32), 323101.

Feng, S., Gong, L., Zhang, Y., Tong, Y., Zhang, H., Zhu, D., Huang, X., & Yang, H. (2021). Bioaugmentation potential evaluation of a bacterial consortium composed of isolated Pseudomonas and Rhodococcus for degrading benzene, toluene and styrene in sludge and sewage. *Bioresource Technology*, *320*, 124329.

Fernández Escalante, E. (2015). Practical management to minimize the effects of clogging in managed aquifer recharge wells at two sites in the guadiana basin, Spain. *Journal of Hydrologic Engineering*, *20*(3), B5014002. https://doi.org/10.1061/(ASCE)HE.1943-5584.0001047

Finneran, K. T. (2003). Rhodoferax ferrireducens sp. Nov., a psychrotolerant, facultatively anaerobic bacterium that oxidizes acetate with the reduction of Fe(III). *INTERNATIONAL JOURNAL OF SYSTEMATIC AND EVOLUTIONARY MICROBIOLOGY*, *53*(3), 669–673. https://doi.org/10.1099/ijs.0.02298-0

Firmino, P. I. M., Farias, R. S., Barros, A. N., Landim, P. G. C., Holanda, G. B. M., Rodríguez, E., Lopes, A. C., & Dos Santos, A. B. (2018). Applicability of Microaerobic Technology to Enhance BTEX Removal from Contaminated Waters. *Applied Biochemistry and Biotechnology*, *184*(4), 1187–1199. https://doi.org/10.1007/s12010-017-2618-x

Flemming, H.-C., & Wingender, J. (2010). The biofilm matrix. *Nature Reviews Microbiology*, *8*(9), Article 9. https://doi.org/10.1038/nrmicro2415

Fleuchaus, P., Godschalk, B., Stober, I., & Blum, P. (2018). Worldwide application of aquifer thermal energy storage–A review. *Renewable and Sustainable Energy Reviews*, *94*, 861–876.

Freedman, Z., Zhu, C., & Barkay, T. (2012). Mercury resistance and mercuric reductase activities and expression among chemotrophic thermophilic Aquificae. *Appl. Environ. Microbiol.*, *78*(18), 6568–6575.

Fulke, A. B., Ratanpal, S., & Sonker, S. (2024). Understanding heavy metal toxicity: Implications on human health, marine ecosystems and bioremediation strategies. *Marine Pollution Bulletin*, *206*, 116707.

Garcia-Blanco, S., Venosa, A. D., Suidan, M. T., Lee, K., Cobanli, S., & Haines, J. R. (2007). Biostimulation for the treatment of an oil-contaminated coastal salt marsh. *Biodegradation*, *18*(1), 1–15. https://doi.org/10.1007/s10532-005-9029-3

García-Gil, A., Epting, J., Ayora, C., Garrido, E., Vázquez-Suñé, E., Huggenberger, P., & Gimenez, A. C. (2016). A reactive transport model for the quantification of risks induced by groundwater heat pump systems in urban aquifers. *Journal of Hydrology*, *542*, 719–730. https://doi.org/10.1016/j.jhydrol.2016.09.042

Garnier, F., Lesueur, H., Motelica-Heino, M., & Ignatiadis, I. (2011). *Aquifer Biothermoremediation using Heat Pumps: Sound theoretical basis and results on thermal, geochemical and biological impacts on aquifers*.

Garrido Schneider, E. A., García-Gil, A., Vázquez-Suñè, E., & Sánchez-Navarro, J. Á. (2016). Geochemical impacts of groundwater heat pump systems in an urban alluvial aquifer with evaporitic bedrock. *Science of The Total Environment*, *544*, 354–368. https://doi.org/10.1016/j.scitotenv.2015.11.096

Gidudu, B., & Chirwa, E. M. N. (2021). Production of a bacterial biosurfactant in an electrochemical environment as a prelude for in situ biosurfactant enhanced bio-electrokinetic remediation. *Process Safety and Environmental Protection*.

Gillis, M., & Logan, N. A. (2015). *Janthinobacterium*. In W. B. Whitman (Ed.), *Bergey's Manual of Systematics of Archaea and Bacteria* (1st ed., pp. 1–12). Wiley. https://doi.org/10.1002/9781118960608.gbm00964

Ginn, T. R., Wood, B. D., Nelson, K. E., Scheibe, T. D., Murphy, E. M., & Clement, T. P. (2002). Processes in microbial transport in the natural subsurface. *Advances in Water Resources*, *25*(8), 1017–1042. https://doi.org/10.1016/S0309-1708(02)00046-5

Giovanella, P., Vieira, G. A. L., Ramos Otero, I. V., Pais Pellizzer, E., de Jesus Fontes, B., & Sette, L. D. (2020). Metal and organic pollutants bioremediation by extremophile microorganisms. *Journal of Hazardous Materials*, *382*, 121024. https://doi.org/10.1016/j.jhazmat.2019.121024

Godin, S., Kubica, P., Ranchou-Peyruse, A., Le Hecho, I., Patriarche, D., Caumette, G., Szpunar, J., & Lobinski, R. (2020). An LC-MS/MS method for a comprehensive determination of metabolites of BTEX anaerobic degradation in bacterial cultures and groundwater. *Water*, *12*(7), 1869.

Gomes, A., Christensen, J. H., Gründger, F., Kjeldsen, K. U., Rysgaard, S., & Vergeynst, L. (2022). Biodegradation of water-accommodated aromatic oil compounds in Arctic seawater at 0° C. *Chemosphere*, *286*, 131751.

Gomes, H. I., Dias-Ferreira, C., & Ribeiro, A. B. (2013). Overview of in situ and ex situ remediation technologies for PCB-contaminated soils and sediments and obstacles for full-scale application. *Science of the Total Environment*, *445*, 237–260.

Gou, Y., Zhao, Q., Yang, S., Qiao, P., Cheng, Y., Song, Y., Sun, Z., Zhang, T., Wang, L., & Liu, Z. (2020). Enhanced degradation of polycyclic aromatic hydrocarbons in aged subsurface soil using integrated persulfate oxidation and anoxic biodegradation. *Chemical Engineering Journal*, *394*, 125040.

Griebler, C., Brielmann, H., Haberer, C. M., Kaschuba, S., Kellermann, C., Stumpp, C., Hegler, F., Kuntz, D., Walker-Hertkorn, S., & Lueders, T. (2016). Potential impacts of geothermal energy use and storage of heat on groundwater quality, biodiversity, and ecosystem processes. *Environmental Earth Sciences*, *75*(20), 1391. https://doi.org/10.1007/s12665-016-6207-z

Griebler, C., & Lueders, T. (2009a). Microbial biodiversity in groundwater ecosystems. *Freshwater Biology*, *54*(4), 649–677. https://doi.org/10.1111/j.1365-2427.2008.02013.x

Griebler, C., & Lueders, T. (2009b). Microbial biodiversity in groundwater ecosystems. *Freshwater Biology*, *54*(4), 649–677. https://doi.org/10.1111/j.1365-2427.2008.02013.x

Griebler, C., & Lueders, T. (2009c). Microbial biodiversity in groundwater ecosystems. *Freshwater Biology*, *54*(4), 649–677. https://doi.org/10.1111/j.1365-2427.2008.02013.x

Guevara-Luna, J., Alvarez-Fitz, P., Ríos-Leal, E., Acevedo-Quiroz, M., Encarnación-Guevara, S., Moreno-Godinez, M. E., Castellanos-Escamilla, M., Toribio-Jiménez, J., & Romero-Ramírez, Y. (2018). Biotransformation of benzo [a] pyrene by the thermophilic bacterium Bacillus licheniformis M2-7. *World Journal of Microbiology and Biotechnology*, *34*(7), 88.

Gultekin, A., Aydin, M., & Sisman, A. (2016). Thermal performance analysis of multiple borehole heat exchangers. *Energy Conversion and Management*, *122*, 544–551.

Gupta, G., Kumar, V., & Pal, A. K. (2016). Biodegradation of Polycyclic Aromatic Hydrocarbons by Microbial Consortium: A Distinctive Approach for Decontamination of Soil. *Soil and*

Sediment Contamination: An International Journal, *25*(6), 597–623. https://doi.org/10.1080/15320383.2016.1190311

Hallsworth, J. E. (2018). Stress-free microbes lack vitality. *Fungal Biology*, *122*(6), 379–385.

Hassan, H. A., & Aly, A. A. (2018). Isolation and characterization of three novel catechol 2, 3-dioxygenase from three novel haloalkaliphilic BTEX-degrading Pseudomonas strains. *International Journal of Biological Macromolecules*, *106*, 1107–1114.

Hassan, I. A., Mohamedelhassan, E. E., Yanful, E. K., & Yuan, Z.-C. (2019). Mitigation of soil contaminated with diesel fuel using bioelectrokinetics. *Journal of Environmental Science and Health, Part A*, *54*(5), 416–426.

Hassan, I., Mohamedelhassan, E., Yanful, E. K., & Yuan, Z.-C. (2016). A review article: Electrokinetic bioremediation current knowledge and new prospects. *Advances in Microbiology*, *6*(01), 57.

Hatzinger, P. B., Whittier, M. C., Arkins, M. D., Bryan, C. W., & Guarini, W. J. (2002). In-situ and ex-situ bioremediation options for treating perchlorate in groundwater. *Remediation Journal*, *12*(2), 69–86.

Hazen, T. C. (2018). Bioremediation. In *The Microbiology of the Terrestrial Deep Subsurface* (pp. 247–266). CRC Press.

Health Canada. (2025, 01). *Guidelines for Canadian Drinking Water Quality—Summary Tables* [Guidance]. https://www.canada.ca/en/health-canada/services/environmental-workplace-health/reports-publications/water-quality/guidelines-canadian-drinking-water-quality-summary-table.html

Hendry, M. J., Mendoza, C. A., Kirkland, R. A., & Lawrence, J. R. (1999). Quantification of transient CO2 production in a sandy unsaturated zone. *Water Resources Research*, *35*(7), 2189–2198. https://doi.org/10.1029/1999WR900060

Hepbasli, A., & Akdemir, O. (2004). Energy and exergy analysis of a ground source (geothermal) heat pump system. *Energy Conversion and Management*, *45*(5), 737–753. https://doi.org/10.1016/S0196-8904(03)00185-7

Herbert, A., Arthur, S., & Chillingworth, G. (2013). Thermal modelling of large scale exploitation of ground source energy in urban aquifers as a resource management tool. *Applied Energy*, *109*, 94–103. https://doi.org/10.1016/j.apenergy.2013.03.005

Hernández-Ospina, D. A., Osorio-González, C. S., Miri, S., & Kaur Brar, S. (2024). New perspectives on the anaerobic degradation of BTEX: Mechanisms, pathways, and intermediates. *Chemosphere*, *361*, 142490. https://doi.org/10.1016/j.chemosphere.2024.142490

Heron, G., Parker, K., Galligan, J., & Holmes, T. C. (2009). Thermal treatment of eight CVOC source zones to near nondetect concentrations. *Groundwater Monitoring & Remediation*, *29*(3), 56–65. https://doi.org/10.1111/j.1745-6592.2009.01247.x

Ho, A., Di Lonardo, D. P., & Bodelier, P. L. (2017). Revisiting life strategy concepts in environmental microbial ecology. *FEMS Microbiology Ecology*, *93*(3), fix006.

Hocinat, A., Boudemagh, A., Ali-Khodja, H., & Medjemadj, M. (2020). Aerobic degradation of BTEX compounds by Streptomyces species isolated from activated sludge and agricultural soils. *Archives of Microbiology*, *202*(9), 2481–2492.

Hoekstra, N., Pellegrini, M., Bloemendal, M., Spaak, G., Gallego, A. A., Comins, J. R., Grotenhuis, T., Picone, S., Murrell, A. J., & Steeman, H. J. (2020). Increasing market opportunities for renewable energy technologies with innovations in aquifer thermal energy storage. *Science of the Total Environment*, *709*, 136142.

Hollander, A. K. (2018). Environmental impacts of genetically engineered microbial and viral biocontrol agents. In *Biotechnology for biological control of pests and vectors* (pp. 251–266). CRC Press.

Hong, S., Jung, Y., Han, S., Kim, J., Kim, J., & Kwon, S. (2019). Determining design parameters and an optimal design method for coaxial geothermal heat exchangers using verification experiments and GLHEPro numerical analysis. *Journal of the Korean Society of Hazard Mitigation*, *19*(2), 265–275.

Huang, J. (2021). Analytical model for volatile organic compound transport in the coupled vadose zone–groundwater system. *Journal of Hydrologic Engineering*, *26*(1), 04020058.

Huang, K., Chen, C., Shen, Q., Rosen, B. P., & Zhao, F.-J. (2015). Genetically engineering Bacillus subtilis with a heat-resistant arsenite methyltransferase for bioremediation of arsenic-contaminated organic waste. *Appl. Environ. Microbiol.*, *81*(19), 6718–6724.

Hubert, C., Loy, A., Nickel, M., Arnosti, C., Baranyi, C., Brüchert, V., Ferdelman, T., Finster, K., Christensen, F. M., & de Rezende, J. R. (2009). A constant flux of diverse thermophilic bacteria into the cold Arctic seabed. *Science*, *325*(5947), 1541–1544.

Hug, L. A., Baker, B. J., Anantharaman, K., Brown, C. T., Probst, A. J., Castelle, C. J., Butterfield, C. N., Hernsdorf, A. W., Amano, Y., & Ise, K. (2016). A new view of the tree of life. *Nature Microbiology*, *1*(5), 1–6.

Hug, L. A., Baker, B. J., Anantharaman, K., Brown, C. T., Probst, A. J., Castelle, C. J., Butterfield, C. N., Hernsdorf, A. W., Amano, Y., Ise, K., Suzuki, Y., Dudek, N., Relman, D. A., Finstad, K. M., Amundson, R., Thomas, B. C., & Banfield, J. F. (2016). A new view of the tree of life. *Nature Microbiology*, *1*(5), Article 5. https://doi.org/10.1038/nmicrobiol.2016.48

Huon, G., Simpson, T., Holzer, F., Maini, G., Will, F., Kopinke, F.-D., & Roland, U. (2012). In situ radio-frequency heating for soil remediation at a former service station: Case study and general aspects. *Chemical Engineering & Technology*, *35*(8), 1534–1544. https://doi.org/10.1002/ceat.201200027

Inobeme, A. (2021). Effect of Heavy Metals on Activities of Soil Microorganism. In C. O. Adetunji, D. G. Panpatte, & Y. K. Jhala (Eds.), *Microbial Rejuvenation of Polluted Environment* (Vol. 27, pp. 115–142). Springer Singapore. https://doi.org/10.1007/978-981-15-7459-7_6

Iqbal, J. (2003). *Effect of temperature on efficiency of in situ bioremediation technology: A laboratory microcosm and field study*.

Iqbal, J., Metosh-Dickey, C., & Portier, R. J. (2007). Temperature effects on bioremediation of PAHs and PCP contaminated south Louisiana soils: A laboratory mesocosm study. *Journal of Soils and Sediments*, *7*(3), 153–158. https://doi.org/10.1065/jss2007.01.204

Jarman, A. M. (2020). Hierarchical cluster analysis: Comparison of single linkage, complete linkage, average linkage and centroid linkage method. *Georgia Southern University*.

Jesußek, A., Grandel, S., & Dahmke, A. (2013). Impacts of subsurface heat storage on aquifer hydrogeochemistry. *Environmental Earth Sciences*, *69*(6), 1999–2012. https://doi.org/10.1007/s12665-012-2037-9

Jindrová, E., Chocová, M., Demnerová, K., & Brenner, V. (2002). Bacterial aerobic degradation of benzene, toluene, ethylbenzene and xylene. *Folia Microbiologica*, *47*(2), 83–93. https://doi.org/10.1007/BF02817664

Jo, M.-S., Rene, E. R., Kim, S.-H., & Park, H.-S. (2008). Removal of BTEX compounds by industrial sludge microbes in batch systems: Statistical analysis of main and interaction

effects. *World Journal of Microbiology and Biotechnology*, *24*(1), 73–78. https://doi.org/10.1007/s11274-007-9441-4

Johnston, A. S., & Sibly, R. M. (2018). The influence of soil communities on the temperature sensitivity of soil respiration. *Nature Ecology & Evolution*, *2*(10), 1597–1602.

Kadnikov, V. V., Mardanov, A. V., Beletsky, A. V., Karnachuk, O. V., & Ravin, N. V. (2020). Microbial Life in the Deep Subsurface Aquifer Illuminated by Metagenomics. *Frontiers in Microbiology*, *11*, 2146. https://doi.org/10.3389/fmicb.2020.572252

Kalyuzhnaya, M. G., Bowerman, S., Lara, J. C., Lidstrom, M. E., & Chistoserdova, L. (2006). Methylotenera mobilis gen. Nov., sp. Nov., an obligately methylamine-utilizing bacterium within the family Methylophilaceae. *International Journal of Systematic and Evolutionary Microbiology*, *56*(12), 2819–2823. https://doi.org/10.1099/ijs.0.64191-0

Kaur, G., Lecka, J., Krol, M., & Brar, S. K. (2023). Novel BTEX-degrading strains from subsurface soil: Isolation, identification and growth evaluation. *Environmental Pollution*, *335*, 122303.

Kensa, V. M. (2011). Bioremediation-an overview. *I Control Pollution*, *27*(2), 161–168.

Khan, M. A. I., Biswas, B., Smith, E., Mahmud, S. A., Hasan, N. A., Khan, M. A. W., Naidu, R., & Megharaj, M. (2018). Microbial diversity changes with rhizosphere and hydrocarbons in contrasting soils. *Ecotoxicology and Environmental Safety*, *156*, 434–442.

Khodaei, K., Nassery, H. R., Asadi, M. M., Mohammadzadeh, H., & Mahmoodlu, M. G. (2017a). BTEX biodegradation in contaminated groundwater using a novel strain (Pseudomonas sp. BTEX-30). *International Biodeterioration & Biodegradation*, *116*, 234–242.

Khodaei, K., Nassery, H. R., Asadi, M. M., Mohammadzadeh, H., & Mahmoodlu, M. G. (2017b). BTEX biodegradation in contaminated groundwater using a novel strain (Pseudomonas sp. BTEX-30). *International Biodeterioration & Biodegradation*, *116*, 234–242.

Kingston, J. L. T., Johnson, P. C., Kueper, B. H., & Mumford, K. G. (2014). In situ thermal treatment of chlorinated solvent source zones. In B. H. Kueper, H. F. Stroo, C. M. Vogel, & C. H. Ward (Eds.), *Chlorinated Solvent Source Zone Remediation* (pp. 509–557). Springer. https://doi.org/10.1007/978-1-4614-6922-3_14

Kosegi, J. M., Minsker, B. S., & Dougherty, D. E. (2000). Feasibility study of thermal in situ bioremediation. *Journal of Environmental Engineering*, *126*(7), 601–610. https://doi.org/10.1061/(ASCE)0733-9372(2000)126:7(601)

Koshlaf, E., & Ball, A. S. (2017). Soil bioremediation approaches for petroleum hydrocarbon polluted environments. *AIMS Microbiology*, *3*(1), 25.

Koul, B., & Taak, P. (2018). Ex situ soil remediation strategies. In *Biotechnological Strategies for Effective Remediation of Polluted Soils* (pp. 39–57). Springer.

Krol, M. M., Johnson, R. L., & Sleep, B. E. (2014). An analysis of a mixed convection associated with thermal heating in contaminated porous media. *Science of the Total Environment*, *499*, 7–17.

Krol, M. M., Mumford, K. G., Johnson, R. L., & Sleep, B. E. (2011). Modeling discrete gas bubble formation and mobilization during subsurface heating of contaminated zones. *Advances in Water Resources*, *34*(4), 537–549.

Krol, M. M., Sleep, B. E., & Johnson, R. L. (2011). Impact of low-temperature electrical resistance heating on subsurface flow and transport. *Water Resources Research*, *47*(5).

Kumar, A., Gudiukaite, R., Gricajeva, A., Sadauskas, M., Malunavicius, V., Kamyab, H., Sharma, S., Sharma, T., & Pant, D. (2020). Microbial lipolytic enzymes–promising energy-efficient biocatalysts in bioremediation. *Energy*, *192*, 116674.

Kumar Gupta, P. (2020). Fate, transport, and bioremediation of biodiesel and blended biodiesel in subsurface environment: A review. *Journal of Environmental Engineering*, *146*(1), 03119001.

Kumar, S., Dagar, V. K., Khasa, Y. P., & Kuhad, R. C. (2013). Genetically modified microorganisms (GMOs) for bioremediation. In *Biotechnology for environmental management and resource recovery* (pp. 191–218). Springer.

Kumar, S., Stecher, G., Li, M., Knyaz, C., & Tamura, K. (2018). MEGA X: Molecular evolutionary genetics analysis across computing platforms. *Molecular Biology and Evolution*, *35*(6), 1547.

Kuppusamy, S., Palanisami, T., Megharaj, M., Venkateswarlu, K., & Naidu, R. (2016). Ex-situ remediation technologies for environmental pollutants: A critical perspective. *Reviews of Environmental Contamination and Toxicology Volume 236*, 117–192.

Laloui, L., & Loria, A. F. R. (2019). *Analysis and design of energy geostructures: Theoretical essentials and practical application*. Academic Press.

Laverman, A. M., Pallud, C., Abell, J., & Van Cappellen, P. (2012). Comparative survey of potential nitrate and sulfate reduction rates in aquatic sediments. *Geochimica et Cosmochimica Acta*, *77*, 474–488.

\Lawniczak, \Lukasz, Woźniak-Karczewska, M., Loibner, A. P., Heipieper, H. J., & Chrzanowski, \Lukasz. (2020). Microbial degradation of hydrocarbons—basic principles for bioremediation: A review. *Molecules*, *25*(4), 856.

Lazzari, S., Priarone, A., & Zanchini, E. (2010). Long-term performance of BHE (borehole heat exchanger) fields with negligible groundwater movement. *Energy*, *35*(12), 4966–4974.

Lee, K. S. (2010). A Review on Concepts, Applications, and Models of Aquifer Thermal Energy Storage Systems. *Energies*, *3*(6), 1320–1334. https://doi.org/10.3390/en3061320

Lee, Y., Lee, Y., & Jeon, C. O. (2019). Biodegradation of naphthalene, BTEX, and aliphatic hydrocarbons by Paraburkholderia aromaticivorans BN5 isolated from petroleum-contaminated soil. *Scientific Reports*, *9*(1), 860.

Leung, K. T., Jiang, Z.-H., Almzene, N., Nandakumar, K., Sreekumari, K., & Trevors, J. T. (2019). Biodegradation and bioremediation of organic pollutants in soil. *Modern Soil Microbiology*, 381–402.

Li, K., Bian, H., Liu, C., Zhang, D., & Yang, Y. (2015). Comparison of geothermal with solar and wind power generation systems. *Renewable and Sustainable Energy Reviews*, *42*, 1464–1474.

Li, S., Delgado-Baquerizo, M., Ding, J., Hu, H., Huang, W., Sun, Y., Ni, H., Kuang, Y., Yuan, M. M., Zhou, J., Zhang, J., & Liang, Y. (2024). Intrinsic microbial temperature sensitivity and soil organic carbon decomposition in response to climate change. *Global Change Biology*, *30*(6), e17395. https://doi.org/10.1111/gcb.17395

Lin, Y.-T., Jia, Z., Wang, D., & Chiu, C.-Y. (2017). Effects of temperature on the composition and diversity of bacterial communities in bamboo soils at different elevations. *Biogeosciences*, *14*(21), 4879–4889. https://doi.org/10.5194/bg-14-4879-2017

Liu, H., Cheng, Y., Du, B., Tong, C., Liang, S., Han, S., Zheng, S., & Lin, Y. (2015). Overexpression of a novel thermostable and chloride-tolerant laccase from Thermus thermophilus SG0. 5JP17-16 in Pichia pastoris and its application in synthetic dye decolorization. *PLoS One*, *10*(3).

Liu, L., Li, W., Song, W., & Guo, M. (2018). Remediation techniques for heavy metal-contaminated soils: Principles and applicability. *Science of the Total Environment*, *633*, 206–219.

Liu, W., Luo, Y., Teng, Y., Li, Z., & Ma, L. Q. (2010). Bioremediation of oily sludge-contaminated soil by stimulating indigenous microbes. *Environmental Geochemistry and Health*, *32*(1), 23–29. https://doi.org/10.1007/s10653-009-9262-5

Liu, X., Jiang, X., Liu, J., Li, J., & Li, W. (2017). The effect of the injection salinity and clay composition on aquifer permeability. *Applied Thermal Engineering*, *118*, 551–560. https://doi.org/10.1016/j.applthermaleng.2017.02.098

Liu, Y., He, N., Wen, X., Xu, L., Sun, X., Yu, G., Liáng, L., & Schipper, L. (2018). The optimum temperature of soil microbial respiration: Patterns and controls. *Soil Biology and Biochemistry*, *121*, 35–42. https://doi.org/10.1016/j.soilbio.2018.02.019

Logan, N. A., & Vos, P. D. (2015). Bacillus. *Bergey's Manual of Systematics of Archaea and Bacteria*, 1–163.

Logeshwaran, P., Krishnan, K., Naidu, R., & Megharaj, M. (2020). Purification and characterization of a novel fenamiphos hydrolysing enzyme from Microbacterium esteraromaticum MM1. *Chemosphere*, *252*, 126549.

Logeshwaran, P., Subashchandrabose, S. R., Krishnan, K., Sivaram, A. K., Annamalai, P., Naidu, R., & Megharaj, M. (2022). Polycyclic aromatic hydrocarbons biodegradation by fenamiphos degrading Microbacterium esteraromaticum MM1. *Environmental Technology & Innovation*, *27*, 102465.

Long, P. E., Williams, K. H., Hubbard, S. S., & Banfield, J. F. (2016). Microbial metagenomics reveals climate-relevant subsurface biogeochemical processes. *Trends in Microbiology*, *24*(8), 600–610.

Lu, W., Zheng, Y., Wang, Y., Song, J., Weng, Y., Ma, W., Arslan, M., El-Din, M. G., Wang, D., & Wang, Q. (2024). Survival strategies and assembly mechanisms of microbial communities in petroleum-contaminated soils. *Environmental Research*, *262*, 119857.

Lu, X.-Y., Li, B., Zhang, T., & Fang, H. H. (2012). Enhanced anoxic bioremediation of PAHs-contaminated sediment. *Bioresource Technology*, *104*, 51–58.

Luo, Y., Guo, H., Meggers, F., & Zhang, L. (2019). Deep coaxial borehole heat exchanger: Analytical modeling and thermal analysis. *Energy*, *185*, 1298–1313.

Major, D. W., McMaster, M. L., Cox, E. E., Edwards, E. A., Dworatzek, S. M., Hendrickson, E. R., Starr, M. G., Payne, J. A., & Buonamici, L. W. (2002). Field demonstration of successful bioaugmentation to achieve dechlorination of tetrachloroethene to ethene. *Environmental Science & Technology*, *36*(23), 5106–5116. https://doi.org/10.1021/es0255711

Majorowicz, J., Grasby, S. E., & Skinner, W. R. (2009). Estimation of shallow geothermal energy resource in Canada: Heat gain and heat sink. *Natural Resources Research*, *18*(2), 95–108.

Martel, R., & Gélinas, P. J. (1996). Residual Diesel Measurement in Sand Columns After Surfactant/Alcohol Washing. *Groundwater*, *34*(1), 162–167. https://doi.org/10.1111/j.1745-6584.1996.tb01876.x

Martins, G., Campos, S., Ferreira, A., Castro, R., Duarte, M. S., & Cavaleiro, A. J. (2022). A mathematical model for bioremediation of hydrocarbon-contaminated soils. *Applied Sciences*, *12*(21), 11069.

Martins, V. G., Kalil, S. J., & Costa, J. A. V. (2009). In situ bioremediation using biosurfactant produced by solid state fermentation. *World Journal of Microbiology and Biotechnology*, *25*(5), 843–851.

Matsushita, M., Ishikawa, S., Magara, K., Sato, Y., & Kimura, H. (2020). The potential for CH4 production by syntrophic microbial communities in diverse deep aquifers associated with an accretionary prism and its overlying sedimentary layers. *Microbes and Environments*, *35*(1), ME19103.

Meckenstock, R. U., Elsner, M., Griebler, C., Lueders, T., Stumpp, C., Aamand, J., Agathos, S. N., Albrechtsen, H.-J., Bastiaens, L., & Bjerg, P. L. (2015). Biodegradation: Updating the concepts of control for microbial cleanup in contaminated aquifers. *Environmental Science & Technology*, *49*(12), 7073–7081.

Meng, L., Li, W., Bao, M., & Sun, P. (2018). Promoting the treatment of crude oil alkane pollution through the study of enzyme activity. *International Journal of Biological Macromolecules*, *119*, 708–716.

Meng, Y., & Li, P. (2025). Effects of environmental factors on groundwater BTEX pollution: A quantitative analysis. *Journal of Environmental Chemical Engineering*, 119915.

Meyer, J., Zakhary, S., Larocque, M., & Lazar, C. S. (2022). From Surface to Subsurface: Diversity, Composition, and Abundance of Sessile and Endolithic Bacterial, Archaeal, and

Eukaryotic Communities in Sand, Clay and Rock Substrates in the Laurentians (Quebec, Canada). *Microorganisms*, *10*(1), Article 1. https://doi.org/10.3390/microorganisms10010129

Miri, S., Naghdi, M., Rouissi, T., Kaur Brar, S., & Martel, R. (2019). Recent biotechnological advances in petroleum hydrocarbons degradation under cold climate conditions: A review. *Critical Reviews in Environmental Science and Technology*, *49*(7), 553–586. https://doi.org/10.1080/10643389.2018.1552070

Miri, S., Perez, J. A. E., Brar, S. K., Rouissi, T., & Martel, R. (2021). Sustainable production and co-immobilization of cold-active enzymes from Pseudomonas sp. For BTEX biodegradation. *Environmental Pollution*, *285*, 117678.

Mirsaeidi, A. (2023). The effects of nitrogen and phosphorus nutrients on the bioremediation of oil-contaminated waters by Gracilariopsis persica in the coastal areas of Bandar Abbas. *Marine Pollution Bulletin*, *188*, 114660.

Mishra, S., Huang, Y., Li, J., Wu, X., Zhou, Z., Lei, Q., Bhatt, P., & Chen, S. (2022). Biofilm-mediated bioremediation is a powerful tool for the removal of environmental pollutants. *Chemosphere*, *294*, 133609. https://doi.org/10.1016/j.chemosphere.2022.133609

Molnar, I. L., Pensini, E., Asad, M. A., Mitchell, C. A., Nitsche, L. C., Pyrak-Nolte, L. J., Miño, G. L., & Krol, M. M. (2019). Colloid transport in porous media: A review of classical mechanisms and emerging topics. *Transport in Porous Media*, *130*(1), 129–156.

Molnár, K., Lukács, R., Dunkl, I., Schmitt, A. K., Kiss, B., Seghedi, I., Szepesi, J., & Harangi, S. (2019). Episodes of dormancy and eruption of the Late Pleistocene Ciomadul volcanic complex (Eastern Carpathians, Romania) constrained by zircon geochronology. *Journal of Volcanology and Geothermal Research*, *373*, 133–147. https://doi.org/10.1016/j.jvolgeores.2019.01.025

Moradi, A., M Smits, K., & O Sharp, J. (2018). Coupled thermally-enhanced bioremediation and renewable energy storage system: Conceptual framework and modeling investigation. *Water*, *10*(10), 1288.

Morozkina, E. V., Slutskaya, E. S., Fedorova, T. V., Tugay, T. I., Golubeva, L. I., & Koroleva, O. V. (2010). Extremophilic microorganisms: Biochemical adaptation and biotechnological application (review). *Applied Biochemistry and Microbiology*, *46*(1), 1–14. https://doi.org/10.1134/S0003683810010011

Müller, J. B., Ramos, D. T., Larose, C., Fernandes, M., Lazzarin, H. S., Vogel, T. M., & Corseuil, H. X. (2017). Combined iron and sulfate reduction biostimulation as a novel approach to enhance BTEX and PAH source-zone biodegradation in biodiesel blend-contaminated groundwater. *Journal of Hazardous Materials*, *326*, 229–236.

Mustafa, G., Kookana, R. S., & Singh, B. (2006). Desorption of cadmium from goethite: Effects of pH, temperature and aging. *Chemosphere*, *64*(5), 856–865. https://doi.org/10.1016/j.chemosphere.2005.10.041

Naeimi, M., Shavandi, M., & Alaie, E. (2021). Determining the impact of biofilm in the bioaugmentation process of benzene-contaminated resources. *Journal of Environmental Chemical Engineering*, *9*(1), 104976.

Naicker, S. S., & Rees, S. (2010). Monitoring of a large scale ground source heat pump system. *1st IESD PhD Conference, De Montfort University, Leicester, UK*.

National Research Council. (1993). *In situ bioremediation: When does it work?* National Academies Press.

Nejat, P., Jomehzadeh, F., Taheri, M. M., Gohari, M., & Abd. Majid, M. Z. (2015). A global review of energy consumption, CO2 emissions and policy in the residential sector (with an overview of the top ten CO2 emitting countries). *Renewable and Sustainable Energy Reviews*, *43*, 843–862. https://doi.org/10.1016/j.rser.2014.11.066

Ni, Z., van Gaans, P., Rijnaarts, H., & Grotenhuis, T. (2018). Combination of aquifer thermal energy storage and enhanced bioremediation: Biological and chemical clogging. *Science of The Total Environment*, *613–614*, 707–713. https://doi.org/10.1016/j.scitotenv.2017.09.087

Ni, Z., van Gaans, P., Smit, M., Rijnaarts, H., & Grotenhuis, T. (2015). Biodegradation of cis-1, 2-dichloroethene in simulated underground thermal energy storage systems. *Environmental Science & Technology*, *49*(22), 13519–13527.

Ni, Z., van Gaans, P., Smit, M., Rijnaarts, H., & Grotenhuis, T. (2016). Combination of aquifer thermal energy storage and enhanced bioremediation: Resilience of reductive dechlorination to redox changes. *Applied Microbiology and Biotechnology*, *100*(8), 3767–3780.

Ni, Z., Wang, Y., Wang, Y., Chen, S., Xie, M., Grotenhuis, T. J., & Qiu, R.-L. (2020). Comparative life cycle assessment of aquifer thermal energy storage integrated with in-situ

bioremediation of chlorinated volatile organic compounds. *Environmental Science & Technology*.

Nicholson, C. A., & Fathepure, B. Z. (2005). Aerobic biodegradation of benzene and toluene under hypersaline conditions at the Great Salt Plains, Oklahoma. *FEMS Microbiology Letters*, *245*(2), 257–262.

Njobuenwu, D. O., Amadi, S. A., & Ukpaka, P. C. (2005). Dissolution Rate of BTEX Contaminants in Water. *The Canadian Journal of Chemical Engineering*, *83*(6), 985–989. https://doi.org/10.1002/cjce.5450830608

Olukunle, O. F., Babajide, O., & Boboye, B. (2015). Effects of temperature and pH on the activities of catechol 2, 3-dioxygenase obtained from crude oil contaminated soil in Ilaje, Ondo State, Nigeria. *The Open Microbiology Journal*, *9*, 84.

Oudega, T. J., Lindner, G., Derx, J., Farnleitner, A. H., Sommer, R., Blaschke, A. P., & Stevenson, M. E. (2021). Upscaling Transport of Bacillus subtilis Endospores and Coliphage phiX174 in Heterogeneous Porous Media from the Column to the Field Scale. *Environmental Science & Technology*, *55*(16), 11060–11069.

Panneerselvan, L., Krishnan, K., Subashchandrabose, S. R., Naidu, R., & Megharaj, M. (2018). Draft Genome sequence of Microbacterium esteraromaticum MM1, a bacterium that hydrolyzes the organophosphorus pesticide fenamiphos, isolated from Golf Course soil. *Microbiology Resource Announcements*, *7*(4), e00862-18.

Park, Y., Kim, N., & Lee, J.-Y. (2015). Geochemical properties of groundwater affected by open loop geothermal heat pump systems in Korea. *Geosciences Journal*, *19*(3), 515–526. https://doi.org/10.1007/s12303-014-0059-x

Pavelic, P., Dillon, P., Barry, K., Armstrong, D., Hodson, A., Callaghan, J., Gerges, N., Land, C., & Associates, L. (2008). *Lessons drawn from attempts to unclog an ASR well in an unconsolidated sand aquifer*.

Pellegrini, M., Bloemendal, M., Hoekstra, N., Spaak, G., Gallego, A. A., Comins, J. R., Grotenhuis, T., Picone, S., Murrell, A. J., & Steeman, H. J. (2019). Low carbon heating and cooling by combining various technologies with Aquifer Thermal Energy Storage. *Science of the Total Environment*, *665*, 1–10.

Perfumo, A., Banat, I. M., Marchant, R., & Vezzulli, L. (2007). Thermally enhanced approaches for bioremediation of hydrocarbon-contaminated soils. *Chemosphere*, *66*(1), 179–184. https://doi.org/10.1016/j.chemosphere.2006.05.006

Pieper, D. H., & Reineke, W. (2000). Engineering bacteria for bioremediation. *Current Opinion in Biotechnology*, *11*(3), 262–270.

Pietikäinen, J., Pettersson, M., & Bååth, E. (2005). Comparison of temperature effects on soil respiration and bacterial and fungal growth rates. *FEMS Microbiology Ecology*, *52*(1), 49–58. https://doi.org/10.1016/j.femsec.2004.10.002

Piga, B., Casasso, A., Pace, F., Godio, A., & Sethi, R. (2017). Thermal impact assessment of groundwater heat pumps (GWHPs): Rigorous vs. simplified models. *Energies*, *10*(9), 1385.

Pikaar, I., Koelmans, A. A., & van Noort, P. C. M. (2006). Sorption of organic compounds to activated carbons. Evaluation of isotherm models. *Chemosphere*, *65*(11), 2343–2351. https://doi.org/10.1016/j.chemosphere.2006.05.005

Plangklang, P., & Reungsang, A. (2011). Bioaugmentation of carbofuran residues in soil by Burkholderia cepacia PCL3: A small-scale field study. *International Biodeterioration & Biodegradation*, *65*(6), 902–905.

Pophillat, W., Attard, G., Bayer, P., Hecht-Méndez, J., & Blum, P. (2020). Analytical solutions for predicting thermal plumes of groundwater heat pump systems. *Renewable Energy*, *147*, 2696–2707. https://doi.org/10.1016/j.renene.2018.07.148

Prakash, A. A., Prabhu, N. S., Rajasekar, A., Parthipan, P., AlSalhi, M. S., Devanesan, S., & Govarthanan, M. (2020). Bio-electrokinetic remediation of crude oil contaminated soil enhanced by bacterial biosurfactant. *Journal of Hazardous Materials*, 124061.

Pujades, E., Jurado, A., Scheiber, L., Teixidó, M., Criollo Manjarrez, R. A., Vázquez-Suñé, E., & Vilarrasa, V. (2023). Potential of low-enthalpy geothermal energy to degrade organic contaminants of emerging concern in urban groundwater. *Scientific Reports*, *13*(1), 2642.

Qiao, W., Puentes Jácome, L. A., Tang, X., Lomheim, L., Yang, M. I., Gaspard, S., Avanzi, I. R., Wu, J., Ye, S., & Edwards, E. A. (2019). Microbial communities associated with sustained anaerobic reductive dechlorination of α-, β-, γ-, and δ-hexachlorocyclohexane isomers to monochlorobenzene and benzene. *Environmental Science & Technology*, *54*(1), 255–265.

Quintella, C. M., Mata, A. M., & Lima, L. C. (2019). Overview of bioremediation with technology assessment and emphasis on fungal bioremediation of oil contaminated soils. *Journal of Environmental Management*, *241*, 156–166.

Rafferty, K. D. (2004). Water chemistry issues in geothermal heat pump systems. *Ashrae Transactions*, *110*, 550.

Ran, Y., Xiao, B., Fu, J., & Sheng, G. (2003). Sorption and desorption hysteresis of organic contaminants by kerogen in a sandy aquifer material. *Chemosphere*, *50*(10), 1365–1376.

Raymond, J., & Therrien, R. (2014). Optimizing the design of a geothermal district heating and cooling system located at a flooded mine in Canada. *Hydrogeology Journal*, *22*(1), 217–231.

Rees, S. J., & He, M. (2013). A three-dimensional numerical model of borehole heat exchanger heat transfer and fluid flow. *Geothermics*, *46*, 1–13. https://doi.org/10.1016/j.geothermics.2012.10.004

Ren, W., Zhou, Q., & Wang, M. (2009). Environmental behavior of BTEX in soil: A review. *Chin. J. Ecol*, *28*, 1647–1654.

Roohidehkordi, I., & Krol, M. M. (2021a). Applicability of ground source heat pumps as a bioremediation-enhancing technology for monoaromatic hydrocarbon contaminants. *Science of The Total Environment*, *778*, 146235. https://doi.org/10.1016/j.scitotenv.2021.146235

Roohidehkordi, I., & Krol, M. M. (2021b). Applicability of ground source heat pumps as a bioremediation-enhancing technology for monoaromatic hydrocarbon contaminants. *Science of The Total Environment*, *778*, 146235.

Rossman, A. J., Hayden, N. J., & Rizzo, D. M. (2006). Low-temperature soil heating using renewable energy. *Journal of Environmental Engineering*, *132*(5), 537–544. https://doi.org/10.1061/(ASCE)0733-9372(2006)132:5(537)

Roy, A., Dutta, A., Pal, S., Gupta, A., Sarkar, J., Chatterjee, A., Saha, A., Sarkar, P., Sar, P., & Kazy, S. K. (2018). Biostimulation and bioaugmentation of native microbial community accelerated bioremediation of oil refinery sludge. *Bioresource Technology*, *253*, 22–32.

Roy, P., & Kumar, A. (2020). Arthrobacter. In *Beneficial microbes in agro-ecology* (pp. 3–11). Elsevier. https://www.sciencedirect.com/science/article/pii/B9780128234143000010

Russell, N. J. (1998). Molecular adaptations in psychrophilic bacteria: Potential for biotechnological applications. In G. Antranikian (Ed.), *Biotechnology of Extremophiles* (Vol. 61, pp. 1–21). Springer Berlin Heidelberg. https://doi.org/10.1007/BFb0102287

Sagia, Z., Stegou, A., & Rakopoulos, C. (2012). Borehole resistance and heat conduction around vertical ground heat exchangers. *The Open Chemical Engineering Journal*, *6*(1).

Salwan, R., & Sharma, V. (2020). Physiology of extremophiles. In *Physiological and biotechnological aspects of extremophiles* (pp. 13–22). Elsevier. https://www.sciencedirect.com/science/article/pii/B9780128183229000022

Sanscartier, D., Laing, T., Reimer, K., & Zeeb, B. (2009). Bioremediation of weathered petroleum hydrocarbon soil contamination in the Canadian High Arctic: Laboratory and field studies. *Chemosphere*, *77*(8), 1121–1126. https://doi.org/10.1016/j.chemosphere.2009.09.006

Sanscartier, D., Reimer, K., Zeeb, B., & Koch, I. (2011). The effect of temperature and aeration rate on bioremediation of diesel-contaminated soil in solid-phase bench-scale bioreactors. *Soil and Sediment Contamination*, *20*(4), 353–369.

Sanscartier, D., Zeeb, B., Koch, I., & Reimer, K. (2009). Bioremediation of diesel-contaminated soil by heated and humidified biopile system in cold climates. *Cold Regions Science and Technology*, *55*(1), 167–173. https://doi.org/10.1016/j.coldregions.2008.07.004

Santoyo, G., Orozco-Mosqueda, Ma. D. C., & Govindappa, M. (2012). Mechanisms of biocontrol and plant growth-promoting activity in soil bacterial species of *Bacillus* and *Pseudomonas*: A review. *Biocontrol Science and Technology*, *22*(8), 855–872. https://doi.org/10.1080/09583157.2012.694413

Sarkar, P., Roy, A., Pal, S., Mohapatra, B., Kazy, S. K., Maiti, M. K., & Sar, P. (2017). Enrichment and characterization of hydrocarbon-degrading bacteria from petroleum refinery waste as potent bioaugmentation agent for in situ bioremediation. *Bioresource Technology*, *242*, 15–27.

Sawle, L., & Ghosh, K. (2011). How do thermophilic proteins and proteomes withstand high temperature? *Biophysical Journal*, *101*(1), 217–227.

Sayler, G. S., & Ripp, S. (2000). Field applications of genetically engineered microorganisms for bioremediation processes. *Current Opinion in Biotechnology*, *11*(3), 286–289.

Schwardt, A., Dahmke, A., & Köber, R. (2021). Henry's law constants of volatile organic compounds between 0 and 95 C–Data compilation and complementation in context of urban temperature increases of the subsurface. *Chemosphere*, *272*, 129858.

Seagren, E. A., & Becker, J. G. (2002). Review of Natural Attenuation of BTEX and MTBE in Groundwater. *Practice Periodical of Hazardous, Toxic, and Radioactive Waste Management*, *6*(3), 156–172. https://doi.org/10.1061/(ASCE)1090-025X(2002)6:3(156)

Sheng, X. F., He, L. Y., Zhou, L., & Shen, Y. Y. (2009). Characterization of *Microbacterium* sp. F10a and its role in polycyclic aromatic hydrocarbon removal in low-temperature soil. *Canadian Journal of Microbiology*, *55*(5), 529–535. https://doi.org/10.1139/W09-005

Shi, B., Ngueleu, S. K., Rezanezhad, F., Slowinski, S., Pronk, G. J., Smeaton, C. M., Stevenson, K., Al-Raoush, R. I., & Van Cappellen, P. (2020). Sorption and desorption of the model aromatic hydrocarbons naphthalene and benzene: Effects of temperature and soil composition. *Frontiers in Environmental Chemistry*, *1*, 581103.

Shim, H., & Yang, S.-T. (1999). Biodegradation of benzene, toluene, ethylbenzene, and o-xylene by a coculture of Pseudomonas putida and Pseudomonas fluorescens immobilized in a fibrous-bed bioreactor. *Journal of Biotechnology*, *67*(2–3), 99–112.

Sikkema, J., de Bont, J. A., & Poolman, B. (1994). Interactions of cyclic hydrocarbons with biological membranes. *Journal of Biological Chemistry*, *269*(11), 8022–8028.

Singh, J. S., Abhilash, P. C., Singh, H. B., Singh, R. P., & Singh, D. P. (2011). Genetically engineered bacteria: An emerging tool for environmental remediation and future research perspectives. *Gene*, *480*(1), 1–9. https://doi.org/10.1016/j.gene.2011.03.001

Singh, S., Kang, S. H., Mulchandani, A., & Chen, W. (2008). Bioremediation: Environmental clean-up through pathway engineering. *Current Opinion in Biotechnology*, *19*(5), 437–444.

Siqueira, J. P. S., Firmino, P. I. M., & dos Santos, A. B. (2023). Anaerobic and microaerobic biodegradation of benzene: Effect of important intermediates. *Journal of Water Process Engineering*, *54*, 103953.

Siqueira, J. P. S., Pereira, A. M., Dutra, A. M. M., Firmino, P. I. M., & Dos Santos, A. B. (2018). Process bioengineering applied to BTEX degradation in microaerobic treatment systems. *Journal of Environmental Management*, *223*, 426–432.

Si-Zhong, Y., Hui-Jun, J., Zhi, W., Rui-Xia, H. E., Yan-Jun, J. I., Xiu-Mei, L. I., & Shao-Peng, Y. U. (2009). Bioremediation of oil spills in cold environments: A review. *Pedosphere*, *19*(3), 371–381.

Sleep, B. E., & McClure, P. D. (2001a). Removal of volatile and semivolatile organic contamination from soil by air and steam flushing. *Journal of Contaminant Hydrology*, *50*(1–2), 21–40.

Sleep, B. E., & McClure, P. D. (2001b). The effect of temperature on adsorption of organic compounds to soils. *Canadian Geotechnical Journal*, *38*(1), 46–52.

Sleep, B. E., & McClure, P. D. (2001c). The effect of temperature on adsorption of organic compounds to soils. *Canadian Geotechnical Journal*, *38*(1), 46–52. https://doi.org/10.1139/t00-067

Smith, K. A., O'Sullivan, A. M., Kennedy, G., Benz, S. A., Somers, L. D., & Kurylyk, B. L. (2023). Shallow groundwater temperature patterns revealed through a regional monitoring well network. *Hydrological Processes*, *37*(9), e14975. https://doi.org/10.1002/hyp.14975

Solly, E. F., Weber, V., Zimmermann, S., Walthert, L., Hagedorn, F., & Schmidt, M. W. (2020). A critical evaluation of the relationship between the effective cation exchange capacity and soil organic carbon content in Swiss forest soils. *Frontiers in Forests and Global Change*, *3*, 98.

Sommer, W. T. (2015). *Modelling and monitoring of Aquifer Thermal Energy Storage: Impacts of soil heterogeneity, thermal interference and bioremediation* [PhD Thesis]. Wageningen University.

Sommer, W. T., Doornenbal, P. J., Drijver, B. C., van Gaans, P. F. M., Leusbrock, I., Grotenhuis, J. T. C., & Rijnaarts, H. H. M. (2014). Thermal performance and heat transport in aquifer thermal energy storage. *Hydrogeology Journal*, *22*(1), 263–279. https://doi.org/10.1007/s10040-013-1066-0

Sommer, W. T., Drijver, B., Verburg, R., Slenders, H., de Vries, E., Dinkla, I., Leusbrock, I., & Grotenhuis, J. T. C. (2013). *Combining shallow geothermal energy and groundwater remediation*. 9.

Song, H.-G., Wang, X., & Bartha, R. (1990). Bioremediation potential of terrestrial fuel spills. *Applied and Environmental Microbiology*, *56*(3), 652–656.

Song, W., Liu, X., Zheng, T., & Yang, J. (2020). A review of recharge and clogging in sandstone aquifer. *Geothermics*, *87*, 101857. https://doi.org/10.1016/j.geothermics.2020.101857

Spiers, A. J., Buckling, A., & Rainey, P. B. (2000). The causes of Pseudomonas diversity. *Microbiology*, *146*(10), 2345–2350. https://doi.org/10.1099/00221287-146-10-2345

Staiti, M., & Angelotti, A. (2015). Design of borehole heat exchangers for ground source heat pumps: A comparison between two methods. *Energy Procedia*, *78*, 1147–1152.

Steiger, D. W., & Kees, E. J. (1981). *Geothermal heating system and method of installing the same*.

Su, Q., Albani, G., Sundberg, J., Andersen, H. R., Nielsen, T. G., Thamdrup, B., & Jensen, M. M. (2022). Microbial bioremediation of produced water under different redox conditions in marine sediments. *Water Research*, *218*, 118428.

Sun, J., Lin, G., Henghua, Z., Tang, X., & Zhang, L. (2020). Study on adsorption-desorption of benzene in soil. *IOP Conference Series: Earth and Environmental Science*, *546*(4), 042041. https://iopscience.iop.org/article/10.1088/1755-1315/546/4/042041/meta

Surendra, S. V., Mahalingam, B. L., & Velan, M. (2017). Degradation of monoaromatics by Bacillus pumilus MVSV3. *Brazilian Archives of Biology and Technology*, *60*.

Szulc, A., Ambrożewicz, D., Sydow, M., Ławniczak, Ł., Piotrowska-Cyplik, A., Marecik, R., & Chrzanowski, Ł. (2014). The influence of bioaugmentation and biosurfactant addition on bioremediation efficiency of diesel-oil contaminated soil: Feasibility during field studies. *Journal of Environmental Management*, *132*, 121–128. https://doi.org/10.1016/j.jenvman.2013.11.006

Tang, Y. J., Carpenter, S., Deming, J., & Krieger-Brockett, B. (2005). Controlled release of nitrate and sulfate to enhance anaerobic bioremediation of phenanthrene in marine sediments. *Environmental Science & Technology*, *39*(9), 3368–3373.

Techtmann, S. M., & Hazen, T. C. (2016). Metagenomic applications in environmental monitoring and bioremediation. *Journal of Industrial Microbiology and Biotechnology*, *43*(10), 1345–1354.

Thompson, I. P., Van Der Gast, C. J., Ciric, L., & Singer, A. C. (2005). Bioaugmentation for bioremediation: The challenge of strain selection. *Environmental Microbiology*, *7*(7), 909–915.

Tran, P. Q., & Anantharaman, K. (2021). Biogeochemistry Goes Viral: Towards a Multifaceted Approach To Study Viruses and Biogeochemical Cycling. *Msystems*, *6*(5), e01138-21.

Truex, M. J., Gillie, J. M., Powers, J. G., & Lynch, K. P. (2009). Assessment of in situ thermal treatment for chlorinated organic source zones. *Remediation Journal*, *19*(2), 7–17. https://doi.org/10.1002/rem.20198

Tsutsumi, H., Hirota, Y., & Hirashima, A. (2000). Bioremediation on the shore after an oil spill from the Nakhodka in the Sea of Japan. II. Toxicity of a bioremediation agent with microbiological cultures in aquatic organisms. *Marine Pollution Bulletin*, *40*(4), 315–319.

Tyagi, M., da Fonseca, M. M. R., & de Carvalho, C. C. (2011). Bioaugmentation and biostimulation strategies to improve the effectiveness of bioremediation processes. *Biodegradation*, *22*(2), 231–241.

Van Stempvoort, D., & Biggar, K. (2008). Potential for bioremediation of petroleum hydrocarbons in groundwater under cold climate conditions: A review. *Cold Regions Science and Technology*, *53*(1), 16–41.

Varjani, S., & Upasani, V. N. (2019). Influence of abiotic factors, natural attenuation, bioaugmentation and nutrient supplementation on bioremediation of petroleum crude contaminated agricultural soil. *Journal of Environmental Management*, *245*, 358–366.

Vogt, C., Kleinsteuber, S., & Richnow, H.-H. (2011). Anaerobic benzene degradation by bacteria. *Microbial Biotechnology*, *4*(6), 710–724.

Vogt, T., Schneider, P., Hahn-Woernle, L., & Cirpka, O. A. (2010). Estimation of seepage rates in a losing stream by means of fiber-optic high-resolution vertical temperature profiling. *Journal of Hydrology*, *380*(1), 154–164. https://doi.org/10.1016/j.jhydrol.2009.10.033

Wadgaonkar, S. L., Ferraro, A., Nancharaiah, Y. V., Dhillon, K. S., Fabbricino, M., Esposito, G., & Lens, P. N. (2019). In situ and ex situ bioremediation of seleniferous soils from northwestern India. *Journal of Soils and Sediments*, *19*(2), 762–773.

Walworth, J., Braddock, J., & Woolard, C. (2001). Nutrient and temperature interactions in bioremediation of cryic soils. *Cold Regions Science and Technology*, *32*(2), 85–91. https://doi.org/10.1016/S0165-232X(00)00020-3

Wang, C., Morrissey, E. M., Mau, R. L., Hayer, M., Piñeiro, J., Mack, M. C., Marks, J. C., Bell, S. L., Miller, S. N., & Schwartz, E. (2021). The temperature sensitivity of soil: Microbial biodiversity, growth, and carbon mineralization. *The ISME Journal*, *15*(9), 2738–2747.

Wang, G., Xiao, Y., Zuo, J., Wang, Y., Man, J., Tang, W., Chen, Q., Ma, S., & Yao, Y. (2020). Physically simulating the effect of lateral vapor source-building separation on soil vapor intrusion: Influences of surface pavements and soil heterogeneity. *Journal of Contaminant Hydrology*, *235*, 103712.

Wang, M., Zhang, D. Q., Dong, J. W., & Tan, S. K. (2017). Constructed wetlands for wastewater treatment in cold climate—A review. *Journal of Environmental Sciences*, *57*, 293–311.

Wani, A. K., Akhtar, N., Naqash, N., Chopra, C., Singh, R., Kumar, V., Kumar, S., Mulla, S. I., & Américo-Pinheiro, J. H. P. (2022). Bioprospecting culturable and unculturable microbial consortia through metagenomics for bioremediation. *Cleaner Chemical Engineering*, *2*, 100017.

Weelink, S. A. B., Van Eekert, M. H. A., & Stams, A. J. M. (2010). Degradation of BTEX by anaerobic bacteria: Physiology and application. *Reviews in Environmental Science and Bio/Technology*, *9*(4), 359–385. https://doi.org/10.1007/s11157-010-9219-2

Welander, U. (2005). Microbial degradation of organic pollutants in soil in a cold climate. *Soil and Sediment Contamination: An International Journal*, *14*(3), 281–291.

Westlake, D. W. S., Jobson, A., Phillippe, R., & Cook, F. D. (2011). Biodegradability and crude oil composition. *Canadian Journal of Microbiology*. https://doi.org/10.1139/m74-141

Whang, L.-M., Liu, P.-W. G., Ma, C.-C., & Cheng, S.-S. (2008). Application of biosurfactants, rhamnolipid, and surfactin, for enhanced biodegradation of diesel-contaminated water and soil. *Journal of Hazardous Materials*, *151*(1), 155–163. https://doi.org/10.1016/j.jhazmat.2007.05.063

Williams, D. J., Grimont, P. A., Cazares, A., Grimont, F., Ageron, E., Pettigrew, K. A., Cazares, D., Njamkepo, E., Weill, F.-X., & Heinz, E. (2022). The genus Serratia revisited by genomics. *Nature Communications*, *13*(1), 5195.

Winderl, C., Penning, H., Netzer, F. von, Meckenstock, R. U., & Lueders, T. (2010). DNA-SIP identifies sulfate-reducing Clostridia as important toluene degraders in tar-oil-contaminated aquifer sediment. *The ISME Journal*, *4*(10), 1314–1325.

Witthayaphirom, C., Chiemchaisri, C., Chiemchaisri, W., Ogata, Y., Ebie, Y., & Ishigaki, T. (2020). Organic micro-pollutant removals from landfill leachate in horizontal subsurface flow constructed wetland operated in the tropical climate. *Journal of Water Process Engineering*, *38*, 101581.

Wolf, H. B. (1982). *Geothermal heating and cooling system*.

Wongbunmak, A., Khiawjan, S., Suphantharika, M., & Pongtharangkul, T. (2017a). BTEX-and naphthalene-degrading bacterium Microbacterium esteraromaticum strain SBS1-7 isolated from estuarine sediment. *Journal of Hazardous Materials*, *339*, 82–90.

Wongbunmak, A., Khiawjan, S., Suphantharika, M., & Pongtharangkul, T. (2017b). BTEX-and naphthalene-degrading bacterium Microbacterium esteraromaticum strain SBS1-7 isolated from estuarine sediment. *Journal of Hazardous Materials*, *339*, 82–90.

Wongbunmak, A., Khiawjan, S., Suphantharika, M., & Pongtharangkul, T. (2020). BTEX biodegradation by Bacillus amyloliquefaciens subsp. Plantarum W1 and its proposed BTEX biodegradation pathways. *Scientific Reports*, *10*(1), 1–13.

Wu, H., Du, X., Wu, W., Zheng, J., Song, J., & Xie, J. (2023). Metagenomic analysis reveals specific BTEX degrading microorganisms of a bacterial consortium. *AMB Express*, *13*(1), 48. https://doi.org/10.1186/s13568-023-01541-y

Wu, M., Zhao, Z., Cai, G., Wang, C., Cheng, G., & Wang, X. (2022). Adsorption behaviour and mechanism of benzene, toluene and m-xylene (BTX) solution onto kaolinite: Experimental and molecular dynamics simulation studies. *Separation and Purification Technology*, *291*, 120940.

Wu, Z., Liu, G., Ji, Y., Li, P., Yu, X., Qiao, W., Wang, B., Shi, K., Liu, W., & Liang, B. (2022). Electron acceptors determine the BTEX degradation capacity of anaerobic microbiota via regulating the microbial community. *Environmental Research*, *215*, 114420.

Xu, M., Zhang, Q., Xia, C., Zhong, Y., Sun, G., Guo, J., Yuan, T., Zhou, J., & He, Z. (2014). Elevated nitrate enriches microbial functional genes for potential bioremediation of complexly contaminated sediments. *The ISME Journal*, *8*(9), 1932–1944.

Yabusaki, S. B., Fang, Y., Long, P. E., Resch, C. T., Peacock, A. D., Komlos, J., Jaffe, P. R., Morrison, S. J., Dayvault, R. D., White, D. C., & Anderson, R. T. (2007). Uranium removal from groundwater via in situ biostimulation: Field-scale modeling of transport and biological processes. *Journal of Contaminant Hydrology*, *93*(1), 216–235. https://doi.org/10.1016/j.jconhyd.2007.02.005

Yadav, A. N., Verma, P., Singh, B., Chauhan, V. S., Suman, A., & Saxena, A. K. (2017). Plant growth promoting bacteria: Biodiversity and multifunctional attributes for sustainable agriculture. *Adv Biotechnol Microbiol*, *5*(5), 1–16.

Yadav, B. K., & Gupta, P. K. (2022). Thermally enhanced bioremediation of NAPL polluted soil-water resources. *Pollutants*, *2*(1), 32–41.

Yadav, B. K., & Hassanizadeh, S. M. (2011). An Overview of Biodegradation of LNAPLs in Coastal (Semi)-arid Environment. *Water, Air, & Soil Pollution*, *220*(1–4), 225–239. https://doi.org/10.1007/s11270-011-0749-1

Yarwood, R. R., Rockhold, M. L., Niemet, M. R., Selker, J. S., & Bottomley, P. J. (2006). Impact of microbial growth on water flow and solute transport in unsaturated porous media. *Water Resources Research*, *42*(10). https://doi.org/10.1029/2005WR004550

Ye, S., Zeng, G., Wu, H., Zhang, C., Liang, J., Dai, J., Liu, Z., Xiong, W., Wan, J., Xu, P., & Cheng, M. (2017). Co-occurrence and interactions of pollutants, and their impacts on soil remediation—A review. *Critical Reviews in Environmental Science and Technology*, *47*(16), 1528–1553. https://doi.org/10.1080/10643389.2017.1386951

Yong, R. N. (2000). *Geoenvironmental engineering: Contaminated soils, pollutant fate, and mitigation*. CRC Press.

Yoshikawa, M., Zhang, M., & Toyota, K. (2017). Biodegradation of volatile organic compounds and their effects on biodegradability under co-existing conditions. *Microbes and Environments*, *32*(3), 188–200.

You, J., Du, M., Chen, H., Zhang, X., Zhang, S., Chen, J., Cheng, Z., Chen, D., & Ye, J. (2018). BTEX degradation by a newly isolated bacterium: Performance, kinetics, and mechanism. *International Biodeterioration & Biodegradation*, *129*, 202–208.

Yu, X., Hurley, M. T., Li, T., Lei, G., Pedarla, A., & Puppala, A. J. (2020). Experimental feasibility study of a new attached hydronic loop design for geothermal heating of bridge decks. *Applied Thermal Engineering*, *164*, 114507. https://doi.org/10.1016/j.applthermaleng.2019.114507

Yuniati, M. D. (2018). Bioremediation of petroleum-contaminated soil: A Review. *IOP Conference Series: Earth and Environmental Science*, *118*(1), 012063.

Zazueta-Sandoval, R., Novoa, V. Z., Jiménez, H. S., & Ortiz, R. C. (2003). A Different Method of Measuring and Detecting Monoand Dioxygenase Activities: Key Enzymes in Hydrocarbon Biodegradation. *Applied Biochemistry and Biotechnology*, *108*(1–3), 725–736. https://doi.org/10.1385/ABAB:108:1-3:725

Zhang, D., Hu, Q., Wang, B., Wang, J., Li, C., You, P., Zhou, R., Zeng, W., Liu, X., & Li, Q. (2023). Effects of single and combined contamination of total petroleum hydrocarbons and heavy metals on soil microecosystems: Insights into bacterial diversity, assembly, and ecological function. *Chemosphere*, *345*, 140288.

Zhang, T. C., Surampalli, R. Y., Tyagi, R. D., & Benerji, S. K. (2017). Biological Treatment of Hazardous Waste. In *Current developments in biotechnology and bioengineering* (pp. 311–340). Elsevier.

Zhang, W., Li, G., Yin, H., Zhao, K., Zhao, H., & An, T. (2022). Adsorption and desorption mechanism of aromatic VOCs onto porous carbon adsorbents for emission control and resource recovery: Recent progress and challenges. *Environmental Science: Nano*, *9*(1), 81–104.

Zheng, X., Xu, W., Dong, J., Yang, T., Shangguan, Z., Qu, J., Li, X., & Tan, X. (2022). The effects of biochar and its applications in the microbial remediation of contaminated soil: A review. *Journal of Hazardous Materials*, *438*, 129557.

Zhou, Y., Huang, H., & Shen, D. (2016). Multi-substrate biodegradation interaction of 1, 4-dioxane and BTEX mixtures by Acinetobacter baumannii DD1. *Biodegradation*, *27*(1), 37–46. https://doi.org/10.1007/s10532-015-9753-2

Zhou, Z., Tran, P. Q., Breister, A. M., Liu, Y., Kieft, K., Cowley, E. S., Karaoz, U., & Anantharaman, K. (2022). METABOLIC: High-throughput profiling of microbial genomes for functional traits, metabolism, biogeochemistry, and community-scale functional networks. *Microbiome*, *10*(1), 1–22.

Zuurbier, K. G., Hartog, N., Valstar, J., Post, V. E., & van Breukelen, B. M. (2013). The impact of low-temperature seasonal aquifer thermal energy storage (SATES) systems on chlorinated solvent contaminated groundwater: Modeling of spreading and degradation. *Journal of Contaminant Hydrology*, *147*, 1–13.

APPENDECIES

Appendix A (Methodology)

1. Moisture content:

The water content (w) is the ratio of the weight of water to the weight of the solids in each mass of soil. This ratio is usually expressed as a percentage as denoted in equation A1. When voids are filled with air, water content is equal to zero (dry soil).

$$w\ (\%) = (M_W / M_S) * 100 \qquad (A1)$$

Where M_W (W_3 - W_2) is the mass of water and M_S (W_3 – W_1).is the mass of dry soil. The moisture content is measured by the "Oven dry method" as described by the following steps (ASTM, 2017):

i. A clean and dry container was weighed (W_1).
ii. The same container with a specimen of the soil sample was measured (W_2).
iii. The sample was dried in the hot air oven, at 110 ± 5 °C temperature and allowed for complete drying.
iv. The final constant weight of the container with the dried soil sample was measured (W_3).
v. The moisture content (w) was measured according to equation 1.

2. Grain size distribution:

To classify the soil samples into sand, silt, loam, and clay; the size of the grain and their proportion were measured by sieve analysis. To obtain the grain size distribution, 100 g of dry soil sample was passed through 10 sieves with different opening diameters (Table A1). The amount of soil attained on each sieve was then measured and used to obtain grain distribution graphs (ASTM, 2017).

Table A1: Summary of sieve size and diameter

Sieve number	Opening diameter (mm)
4	4.75
10	2

20	0.85
40	0.425
60	0.25
100	0.15
140	0.105
200	0.075
300	0.063
500	0.025

3. Hydrometer test:

For clay content analysis, hydrometer test was performed. 50 g of soil was sieved through 2 mm sieve, then mixed with 125 mL of dispersant (sodium hexametaphosphate) for 24 hours and mixed in a mixer. The mixture was transferred to hydrometer cylinder and volume was made to 1000 mL and mixed well. Immediately after mixing, the hydrometer was added to cylinder and depth of hydrometer and temperature was recorded. Likewise, reading was taken up to 24 hours to measure the settlement of fine particles.

4. Plastic limit:

The consistency and moisture content of soil defines its engineering properties of soil. The liquid limit, plastic limit and shrinkage limit of soils, were determined by Atterberg limits methods outlined in ASTM D4318 (ASTM, 2017).

The plastic limit (PL or W_{PL}), also known as the lower plastic limit, is the water content at which a soil changes from a plastic state to a semisolid state. The plastic limit test is performed by repeated rolling of an ellipsoidal-sized soil mass by hand on a non-porous surface. Casagrande defined the plastic limit as the water content at which a thread of soil just crumbles when it is carefully rolled out to a diameter of 3 mm (1/8") (Figure A1). If the thread crumbles at a diameter smaller than 3 mm, the soil is too wet. If the thread crumbles at a diameter greater than 3 mm, the soil is drier than the plastic limit. The sample can then be remolded, and the test

repeated. Once the appropriate size rolls are made, their moisture content is assessed using oven drying.

Figure A1: 3 mm rolled thread to measure plastic limit.

5. Liquid limit:

The liquid limit (LL or W_{LL}), also known as the higher plastic limit, is the water content at which a soil changes from a liquid state to a plastic state. The liquid limit test was performed by the fall cone apparatus (Figure A2). Soil was prepared by sieving through the 40 sieve (0.425 mm) and mixed with water to make a uniform paste-like dough and filled in a sample cup (no air bubbles and smooth surface). The cone of the apparatus was adjusted using a rack adjustor knob so that it touches the surface of the soil. The penetrometer head was set, and the pointer was adjusted to zero. The cone was released, and the penetration was recorded (it should be around 20 mm). The water content at 20 mm penetration was recorded as the LL (ASTM, 2017).

6. Plasticity Index:

Plasticity index (PI or I_P) is an important value when classifying soil types and is calculated as the PL subtracted from the LL.

$$PI = LL - PL \qquad (A2)$$

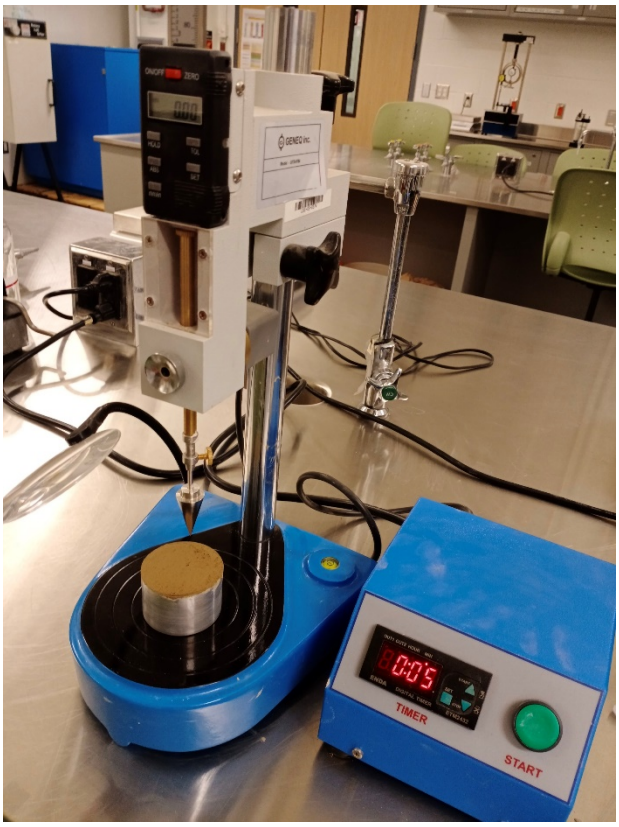

Figure A2: Fall cone apparatus for liquid limit.

7. Cation exchange capacity (CEC):

CEC is the ability of soil to hold positively charged ions and this can impact the soil structure stability, nutrient availability, and soil pH. Its value depends on clay mineral and organic matter content (Dohrmann, 2006). The CEC was measured by the Ammonium acetate method by the following procedure:

i. 25 mL of 1 M NH_4Oac was added to 5 g of soil in an Erlenmeyer flask and shaken thoroughly and kept overnight (16 – 24 hours) at room temperature.
ii. The solution was filtered through filter paper placed in a Buchner funnel.
iii. The soil was washed four times with 5 mL of the NH_4Oac, allowing each addition to filter through but not allowing the soil to crack or dry.
iv. Afterward, the soil was washed with eight separate additions of 95% ethanol to remove the excess saturating solution.

v. The adsorbed NH_4 was extracted by leaching the soil with eight separate 5 mL additions of 1 M KCl in a clean flask and diluted to additional KCl to 50 mL volume.

vi. The concentration of NH_4-N in the KCl extract was determined by colorimetry.

Calculations:

$$\text{CEC (Cmol/kg)} = (NH_4\text{-N in extract} - NH_4\text{-N in blank}) / 18 \quad \text{(A3)}$$

8. Gas chromatography method

Headspace GC-MS parameters:

The BTEX degradation rate was measured with a GC-MS (Clarus 500 (Perkin Elmer) coupled with a headspace system (Turbo matrix 40 Trap (Perkin Elmer). The headspace system has a temperature of 90 °C and 120 °C for the needle and transfer line, respectively. The sample was heated and shaken for 10 min at 80 °C in an oven and collected with a needle and transferred to the column. Analysis was performed using helium as carrier gas at a flow rate of 2 mL/min, 50:1 split ratio and 180 °C inlet temperature. The oven was operated using Chrom-624 (30 m x 0.25 mm x 1.4 µm) column at an initial temperature of 45 °C, hold for 4 minutes and raised to 145 °C for 2 minutes at a rate of 17 °C/min. BTEX concentration was detected with an MS detector using scan mode (40-150 m/z).

Headspace GC-FID parameters:

The BTEX degradation rate was measured with a GC-FID (Agilent Technologies, Canada) coupled with a headspace system (PAL-RSI) at York University. The headspace system was equipped with the SPME 1 tool. The sample was heated and extracted for 24 min at 80 °C, with an agitation of 1,000 rpm. The injections were made in splitless mode at an injection temperature of 290 °C. The oven was operated with a CP-Sil 5 GC column (30 m, 0.25 mm, 1.00 µm) and preheated to 30 °C. The oven was programmed for 30 °C for 4 minutes, and then increased to 100 °C at a rate of 4 °C/min with 0 minutes hold. Analysis was performed using helium as carrier gas at a flow rate of 3 mL/min. Air, hydrogen and nitrogen were used at a flow rate of 400 mL/min, 40 mL/min and 25 mL/min, respectively. BTEX concentration was detected with an FID detector, and data were analyzed with Chemstation software.

Appendix B

(Objective 1: Identify novel BTEX-degrading strains from subsurface soil: Isolation, Identification and Growth Evaluation**)**

Isolation process

The isolation of BTEX-degrading strains has been performed in enrichment media containing BTEX as a sole carbon source. 0.5 g of soil in 20 mL of media treated with 100 ppm BTEX for a week and sub-cultured in fresh media having 200 ppm BTEX. Similarly, three sub-cultures were done with increasing concentration of BTEX up to 200 ppm. After 28 days, 100 µL of the sample has been spread on TSA plates and the number of colonies was calculated in comparison to the control (Figure B1).

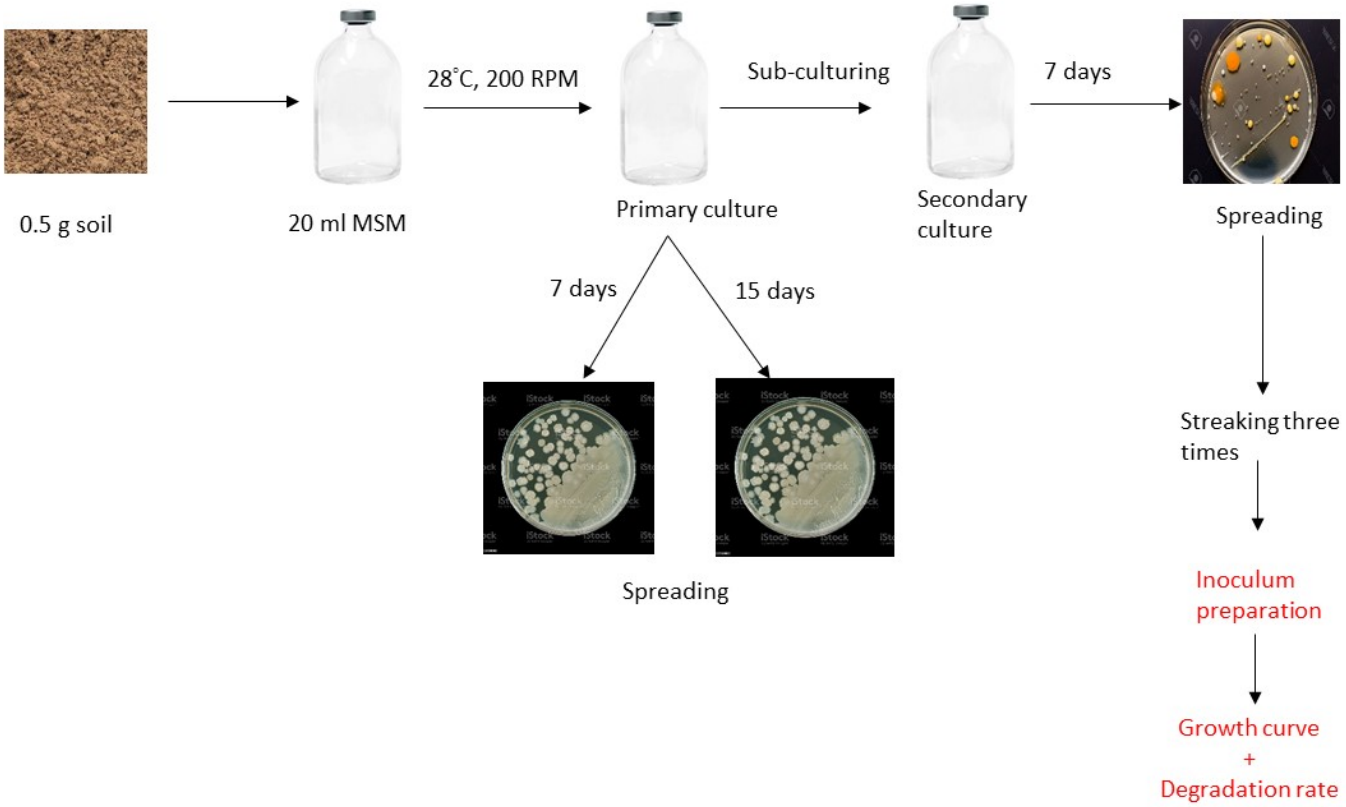

Figure B1: Schematic representation of the isolation experiment

The number of colonies in treated soils was 70-fold lower than the untreated soils (Figure B2). Only the bacteria which can consume or degrade BTEX survive in the BTEX-treated media for a month and others diminish. Such bacteria could utilize hydrocarbons as their carbon and energy source for growth and then degrade them into carbon dioxide and water. Such tolerant microorganisms (e.g., fungi, yeast, and bacteria) release various catalytic enzymes to carry out the breakdown of these hydrocarbon structures into simpler compounds. The primary pathway of aerobic degradation that led to mineralization is bound to two enzymatic groups: dioxygenase and monooxygenase (H. A. Hassan & Aly, 2018; Siqueira et al., 2018).

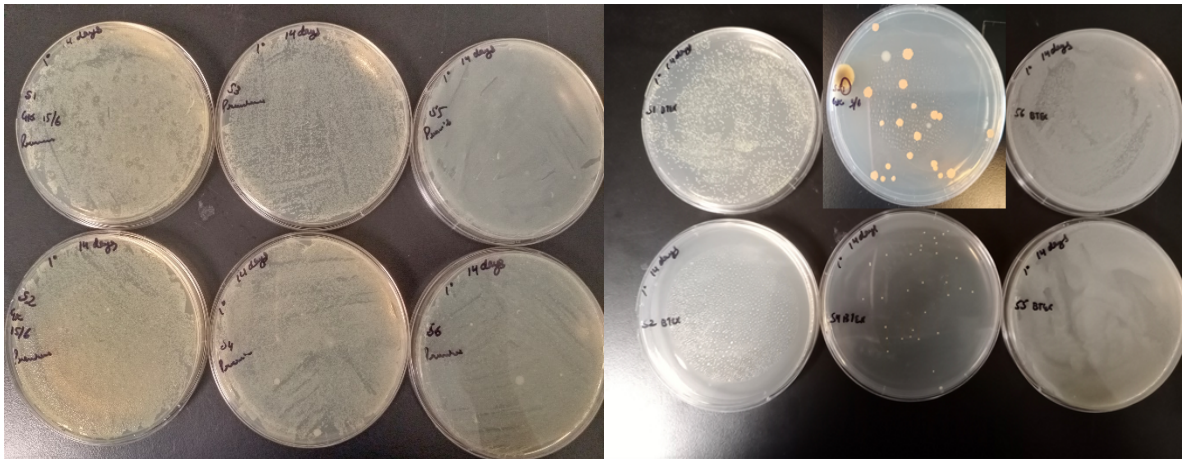

a. **b.**

Figure B2: Spreading of bacterial cells (a.) without BTEX and (b.) with BTEX

From the isolated tolerant bacteria, total of 12 isolates (two from each soil sample) with distinct morphology were selected and streaked twice on fresh agar plates to collect pure colonies (Figure B3). The single pure colony was then inoculated in TSB media for 24 hours and used for the preparation of glycerol stock of isolates for long-term storage and future experiments.

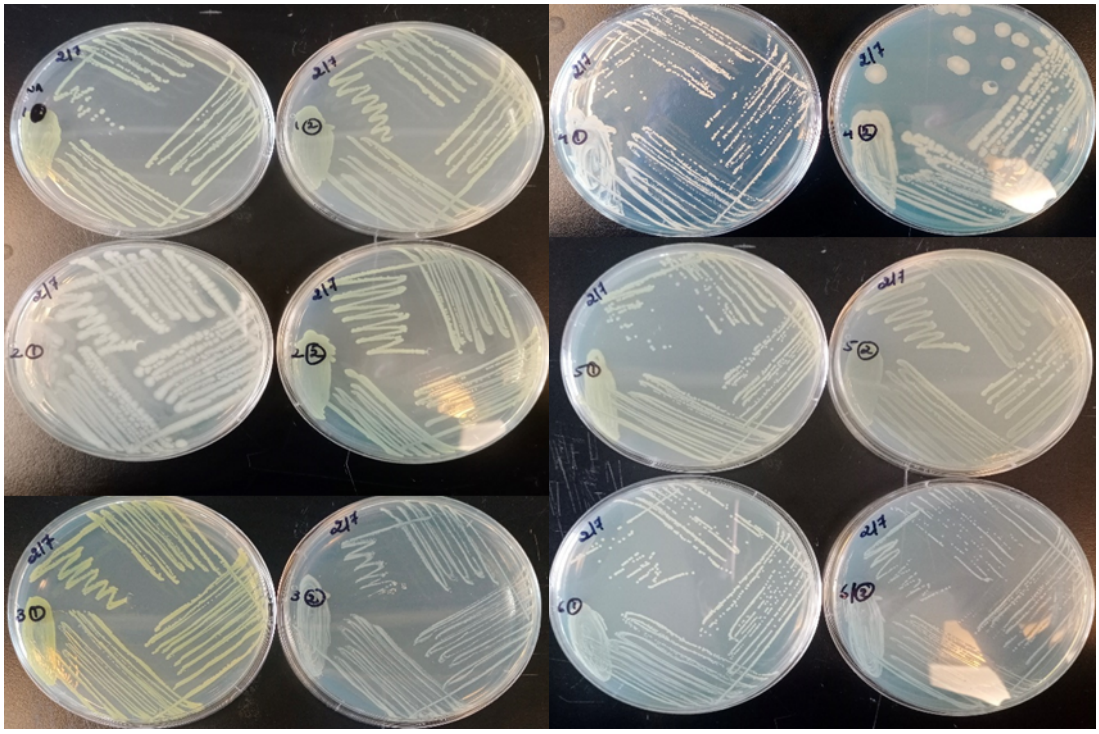

Figure B3: Quadrant streaking of 12 selected isolates

Identification of isolates

To identify the isolated strains, genomic DNA has been isolated using a DNA extraction kit (Miniprep kit from Zymo Research, New England) from an overnight grown culture of all isolates with O.D. of 2 x 10^8 cells/mL. The purity and concentration of extracted DNA were analyzed by Nanodrop (Table B1). Then the extracted DNA was amplified and sequenced for 16S rRNA using universal primers 27F (5′-AGAGTTTGATCCTGGCTCAG-3′), 1492R (5′-GGTTACCTTGTTACGACTT-3′).

Table B1: Analysis of DNA purity

Bacterial Isolate	ABS 260/280	Concentration (ng/ul)
Pseudomonas sp.	1.8	245
1	1.66	9.7
2	1.58	24.2
3	1.68	58
4	1.7	24.2
5	1.75	27.9
6	1.81	9.0
7	0.93	29.1
8	1.71	13
9	1.82	14.5
10	1.43	105.9
11	1.83	59.0
12	1.85	111.5

The resultant 16S rRNA sequence of each isolate was aligned with the five highest similar (>97%) 16S rRNA from the bacterial database using Blastn from NCBI to identify the strains. The five highest similar bacteria were selected and used for evolutionary and similarity analysis with the query strain by phylogenetic trees using MEGA 7 software (S. Kumar et al., 2018). The isolates were identified as the bacteria which showed the highest sequence alignment, for instance, isolate 1 has the highest similarity with *Microbacterium paraoxydans* with a 99.42% match, hence identified as *Microbacterium paraoxydans* (Figure B4).

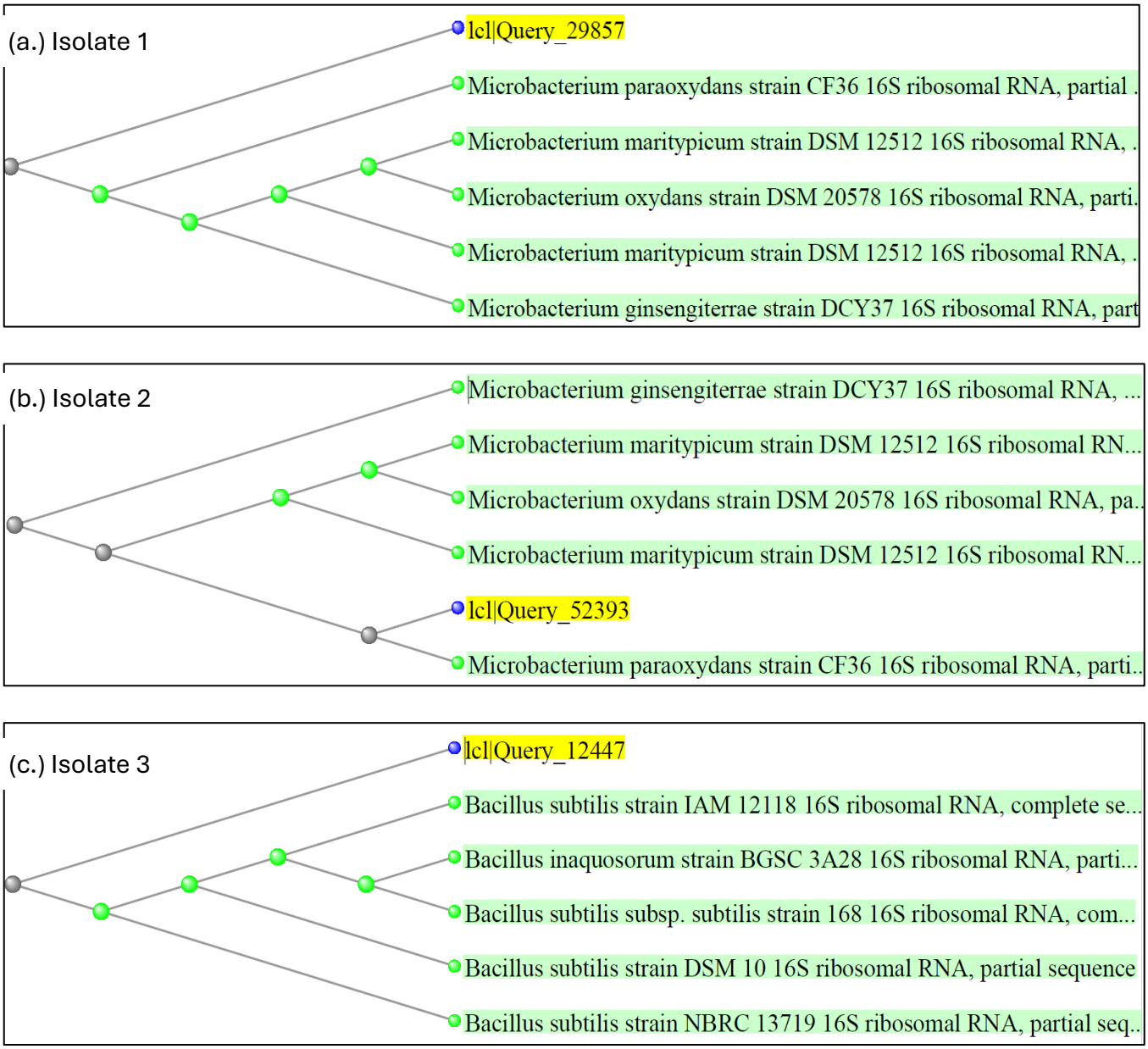

(d.) Isolate 4

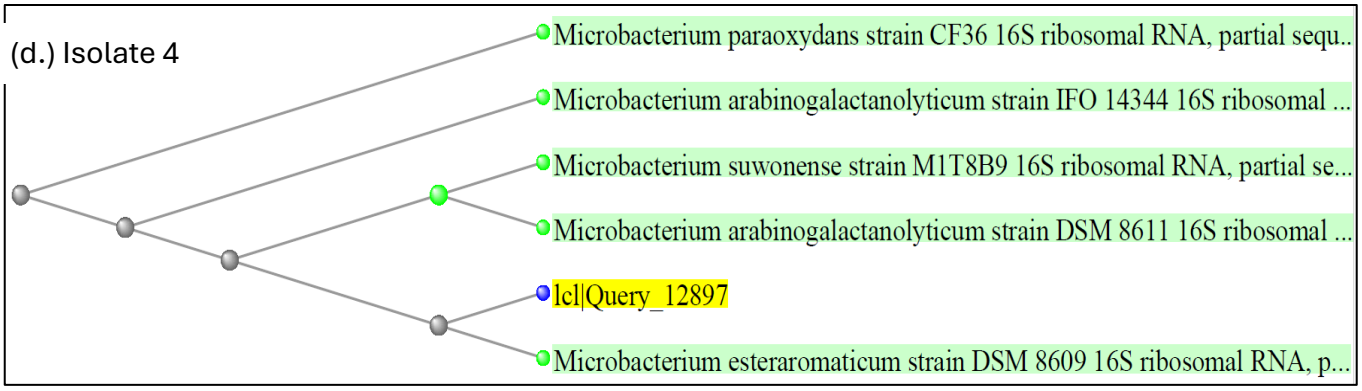

(e.) Isolate 5

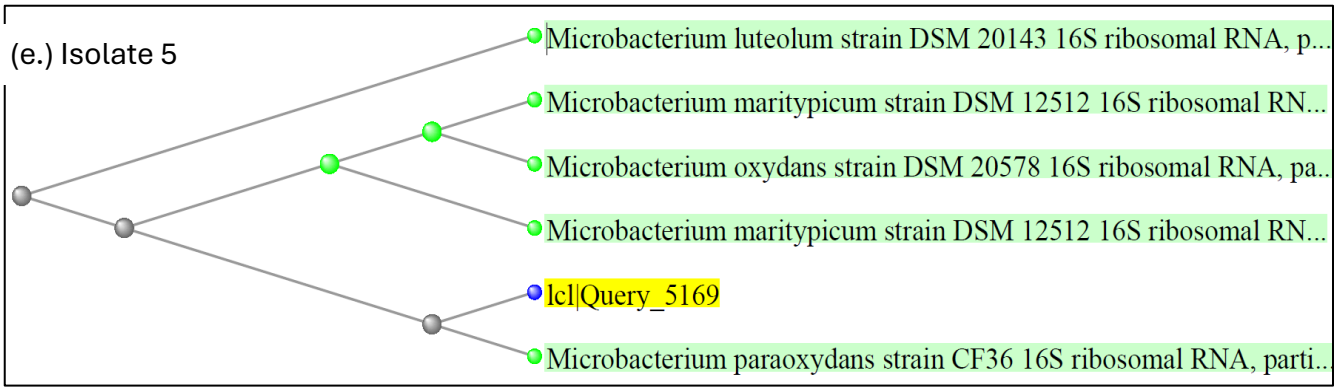

(f.) Isolate 6

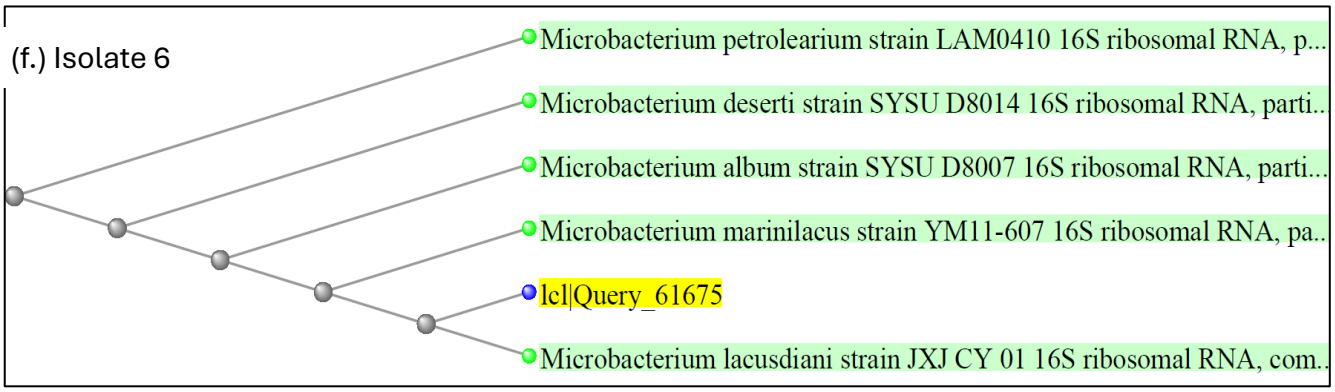

(g.) Isolate 7

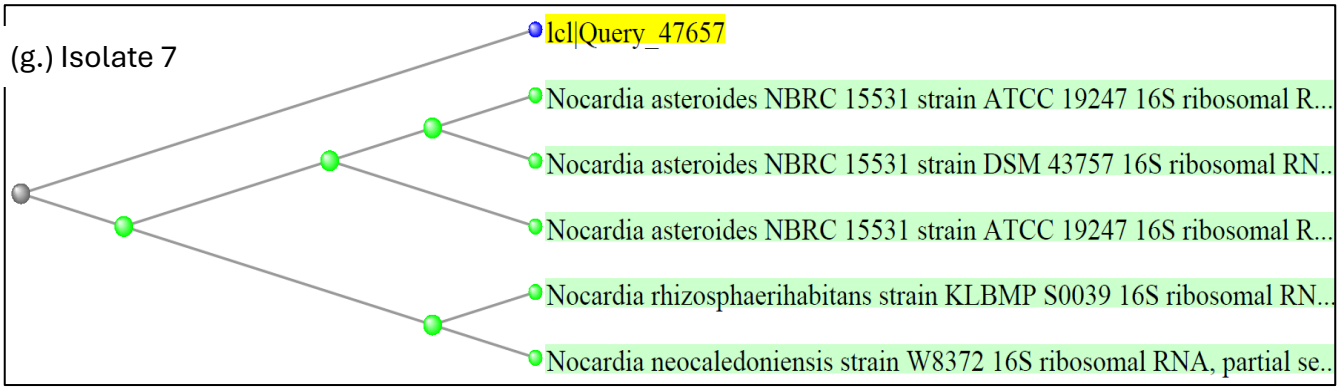

(h.) Isolate 8

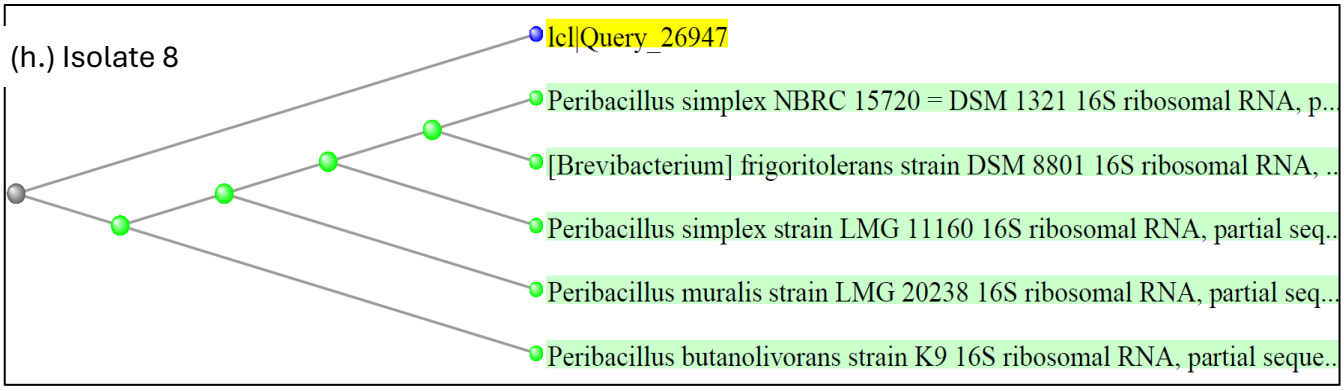

(i.) Isolate 9

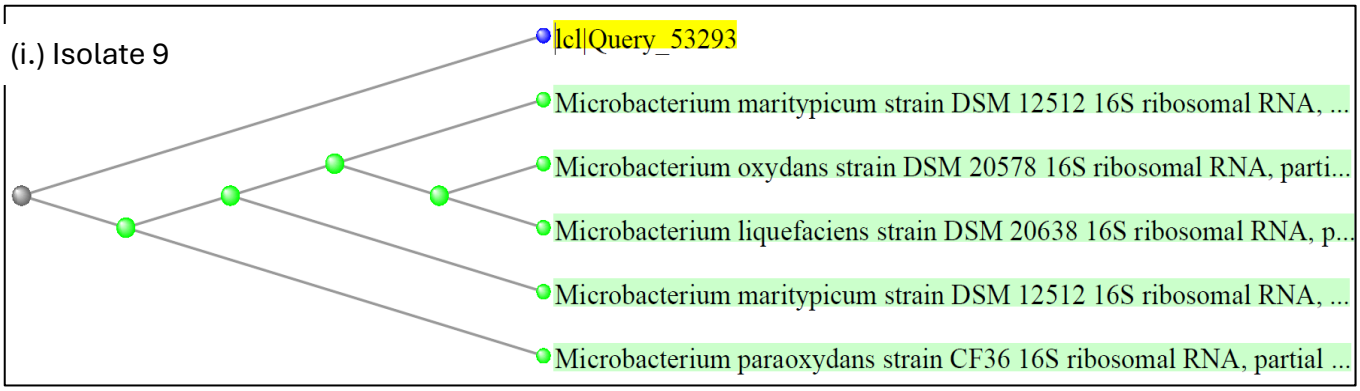

(j.) Isolate 10

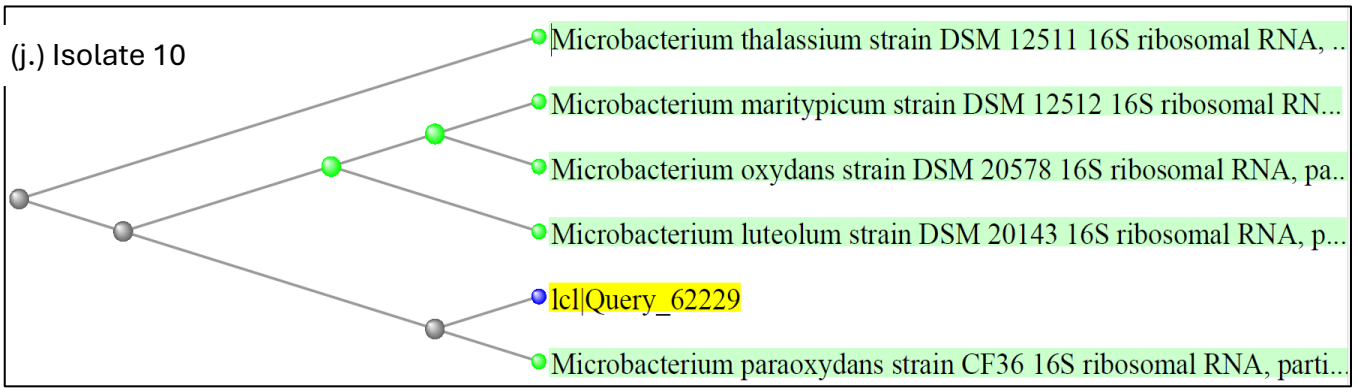

(f.) Isolate 11

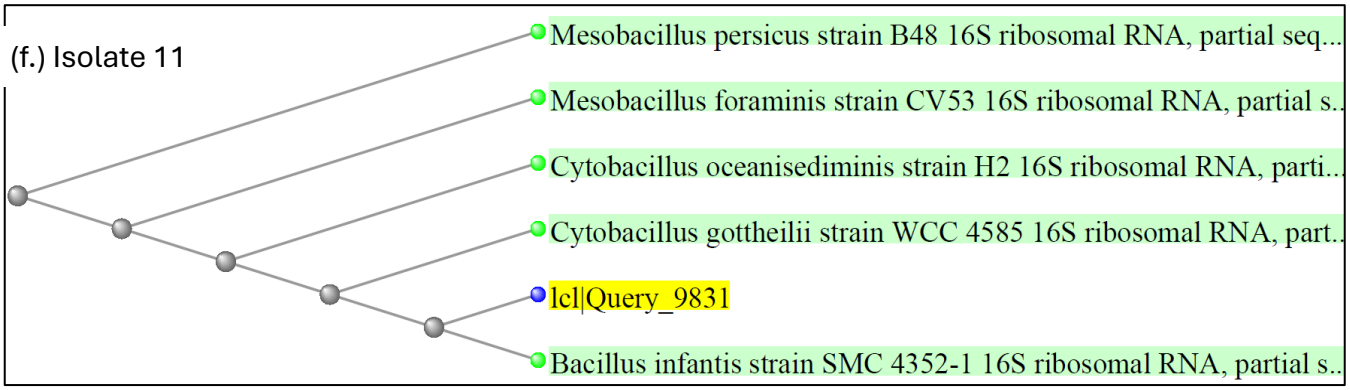

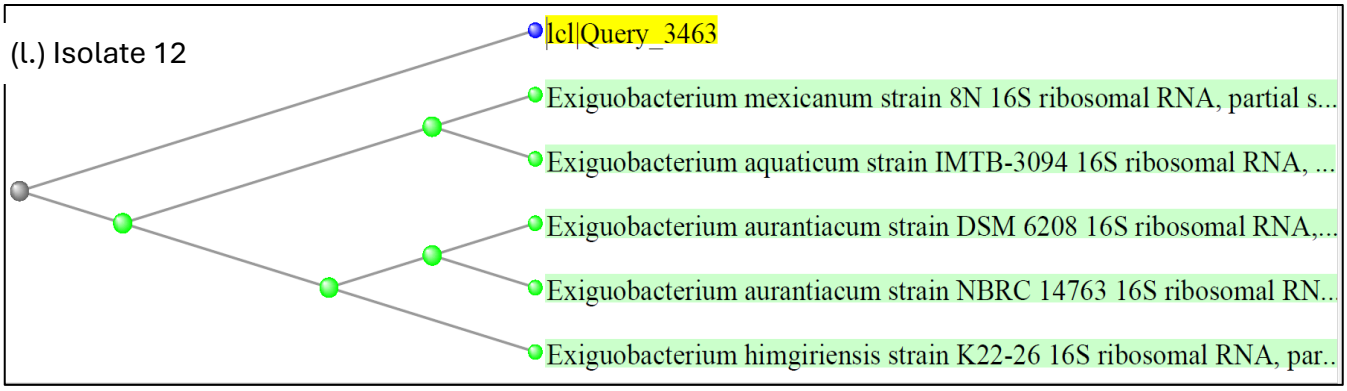

Figure B4: Phylogenetic trees of identified sequence

Analysis of isolates' degradation ability

GC samples were collected at 10-hour intervals to analyze the degradation pattern with headspace GC-MS (Clarus 500 (Perkin Elmer)). To calculate the residual BTEX concentration in samples, calibration curves were prepared using a standards solution with known BTEX concentration (Figure B5).

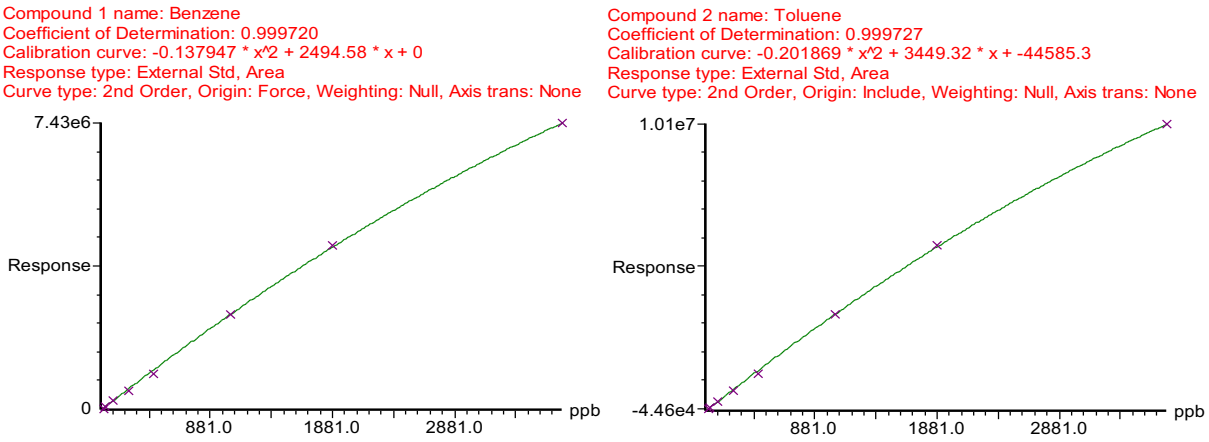

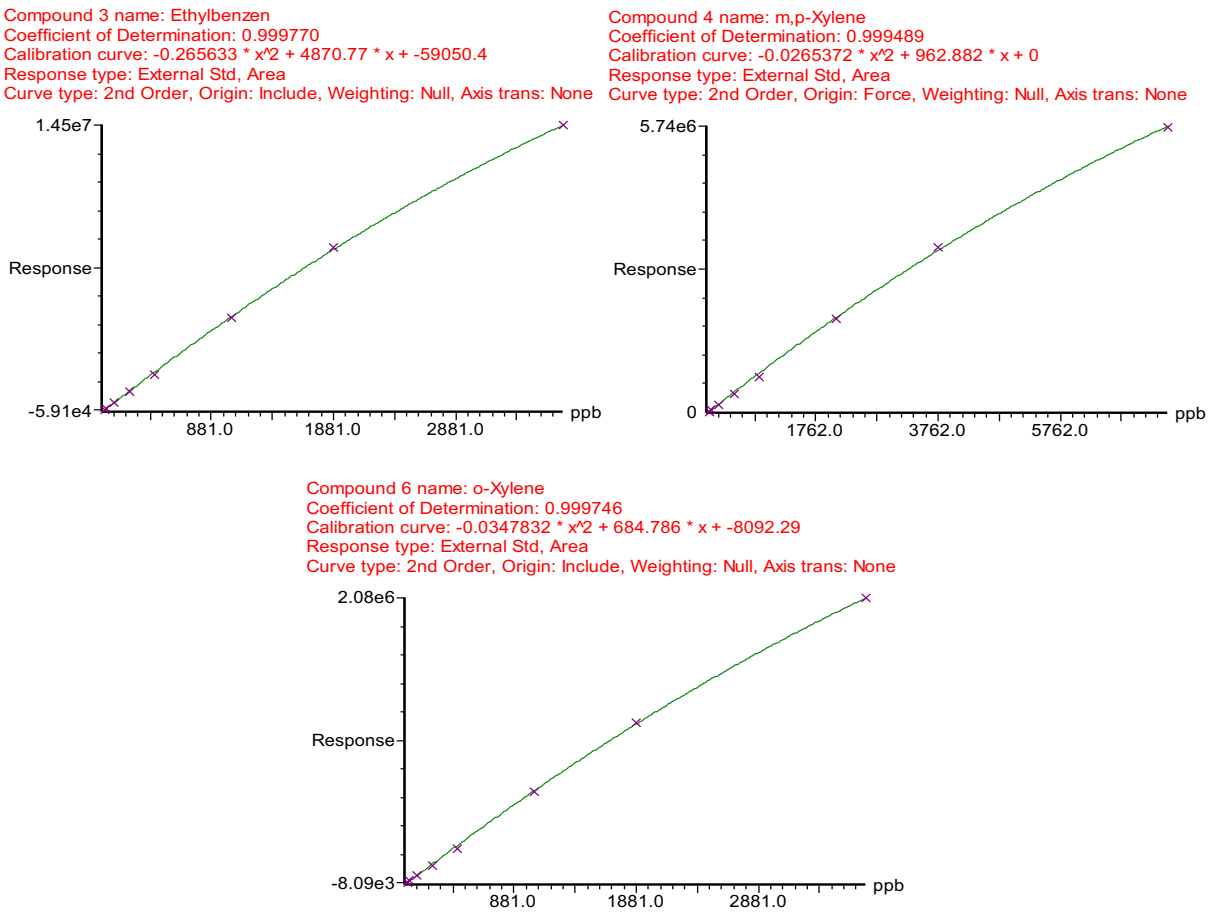

Figure B5: Calibration curves for Benzene, Toluene, Ethylbenzene and Xylenes

Further, the correlation between the biodegradation percentage of BTEX and the growth of bacteria in optical density at 600 nm was observed in Origin graphs using linear fitting at all three different temperatures after 24 h of incubation. Fitting showed a linear correlation with R-squared (Cofficient of determination) value of 0.83 and Pearson's coefficient of 0.91, Figure B6.

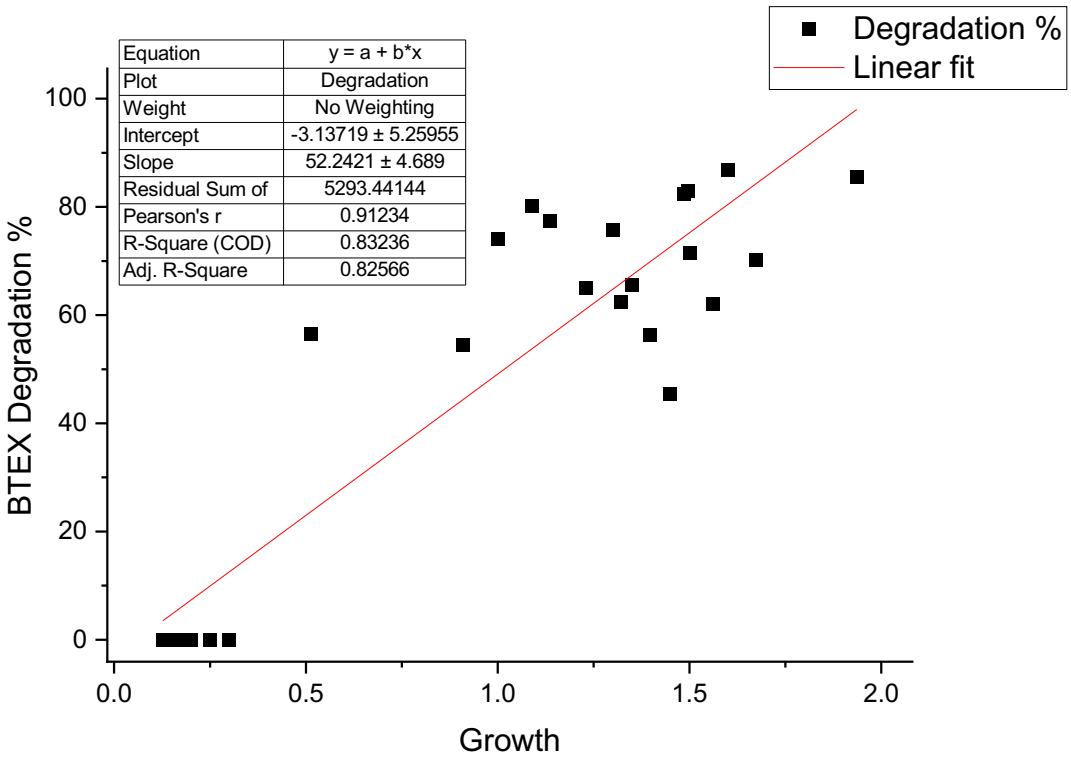
Degradation %
Linear fit
Equation y = a + b*x
Plot Degradation
Weight No Weighting
Intercept -3.13719 ± 5.25955
Slope 52.2421 ± 4.689
Residual Sum of 5293.44144
Pearson's r 0.91234
R-Square (COD) 0.83236
Adj. R-Square 0.82566
BTEX Degradation %
Growth
0
20
40
60
80
100
0.0
0.5
1.0
1.5
2.0

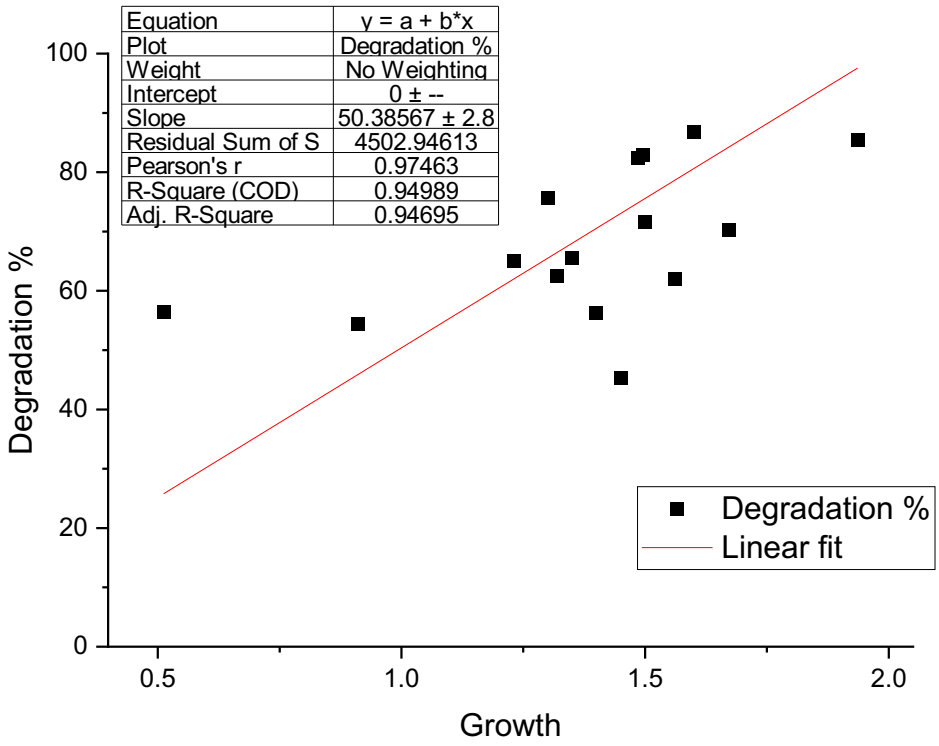

Figure B6: Linear fitting between the BTEX degradation percentage and bacteria growth in optical density at 600 nm at all three different temperatures after 24 h of incubation.

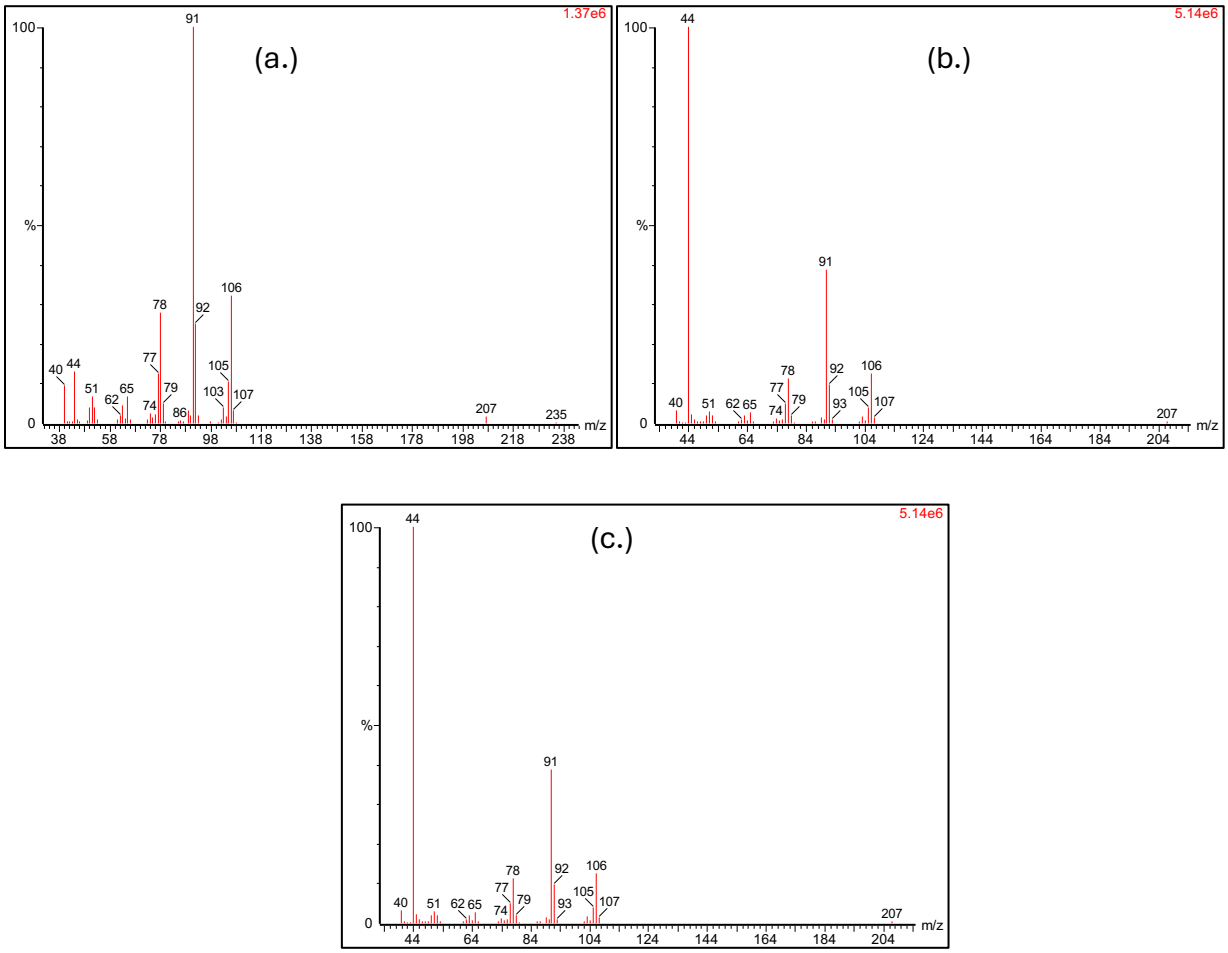

Figure B7: Mass spectra of: (a) abiotic control, (b) *Bacillus infantis* treated culture and, (c) *Microbacterium esteraromaticum* treated culture after 24 hours of incubation.

Appendix C

(Objective 2: Analyze BTEX biodegradation under anoxic conditions using response surface methodology**)**

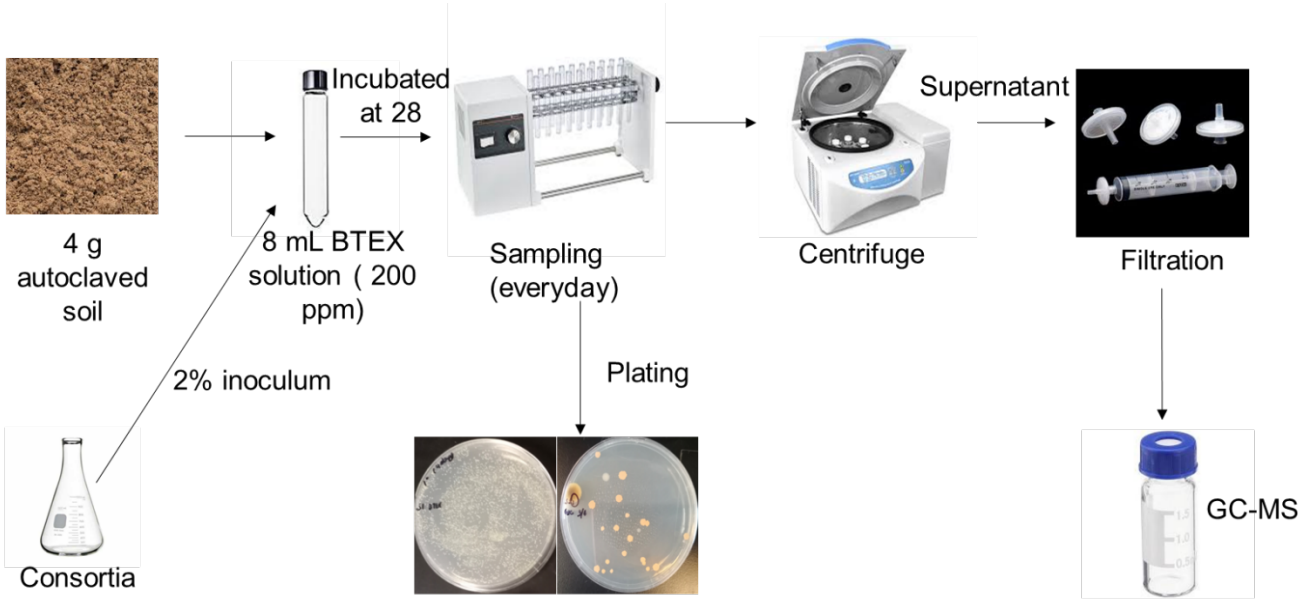

Figure C1: Methodology schematic for soil experiment.

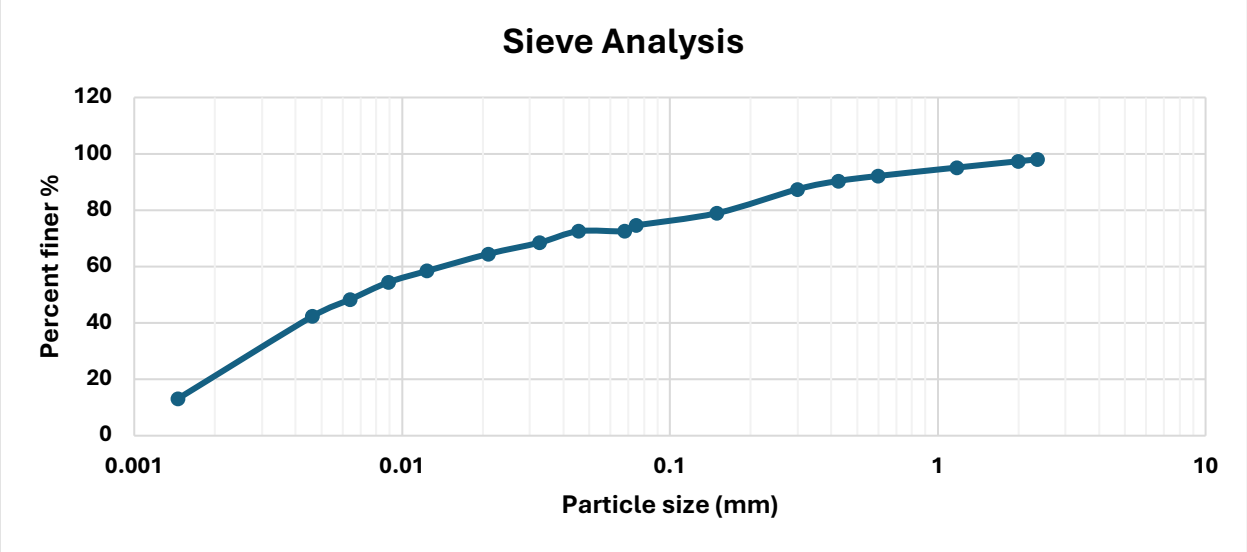

Figure C2: Soil particle size distribution curve by sieve and hydrometer analysis.

Table C1: Physicochemical properties of soil used for NSF experiment.

Physiochemical property	Amount
pH	6.8
Soil type	Silty loam
Clay content	20%
Silt content	52%
Sand content	25%
Nitrate	76 mg/L
Sulfate	184 mg/L
Ferric	1.2%

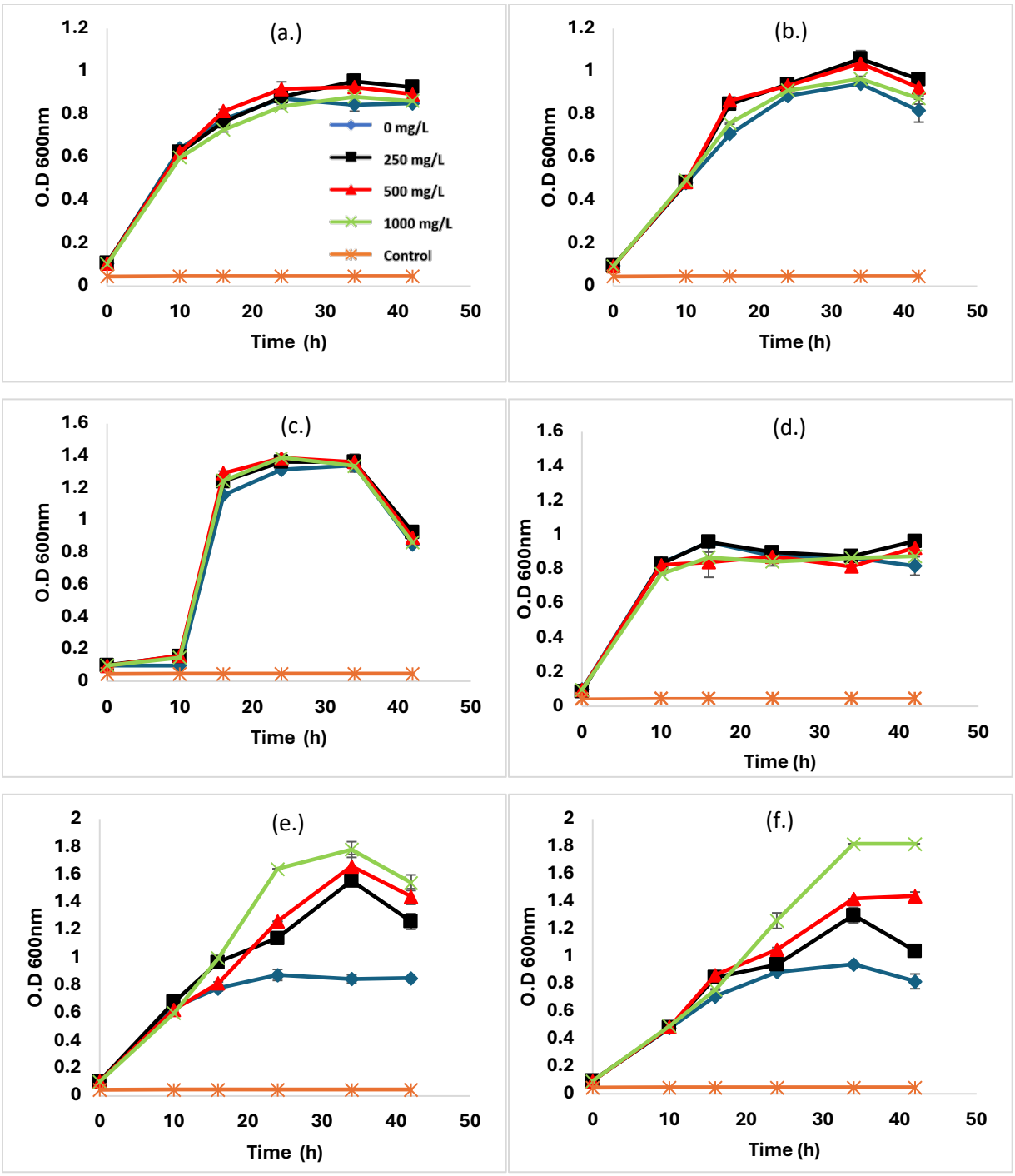

Figure C3: Growth of (a) *B. infantis* (b) *M. esteraromaticum* with nitrate treatment; (c) *B. infantis* (d) *M. esteraromaticum* with sulfate treatment; and (e) *B. infantis*, (f) *M. esteraromaticum* with iron treatment without BTEX.

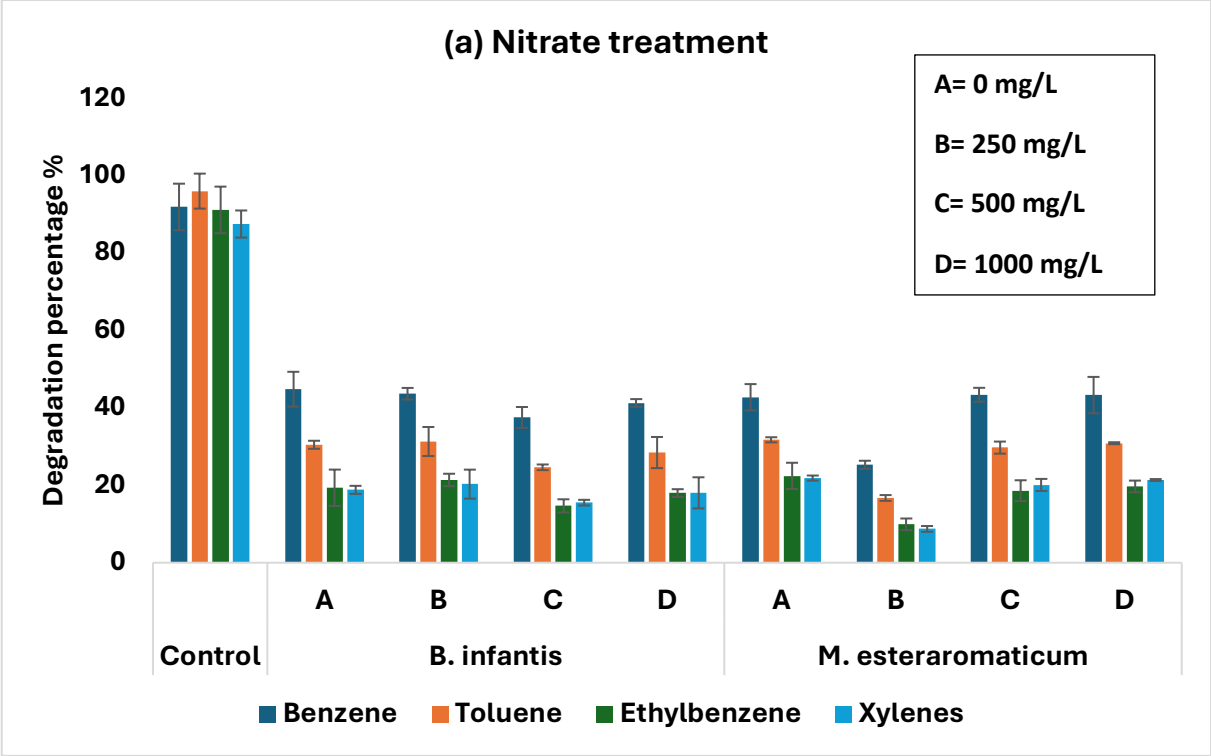
(a) Nitrate treatment
A= 0 mg/L
B= 250 mg/L
C= 500 mg/L
D= 1000 mg/L
Degradation percentage %
120
100
80
60
40
20
0
A
B
C
D
A
B
C
D
Control
B. infantis
M. esteraromaticum
Benzene
Toluene
Ethylbenzene
Xylenes

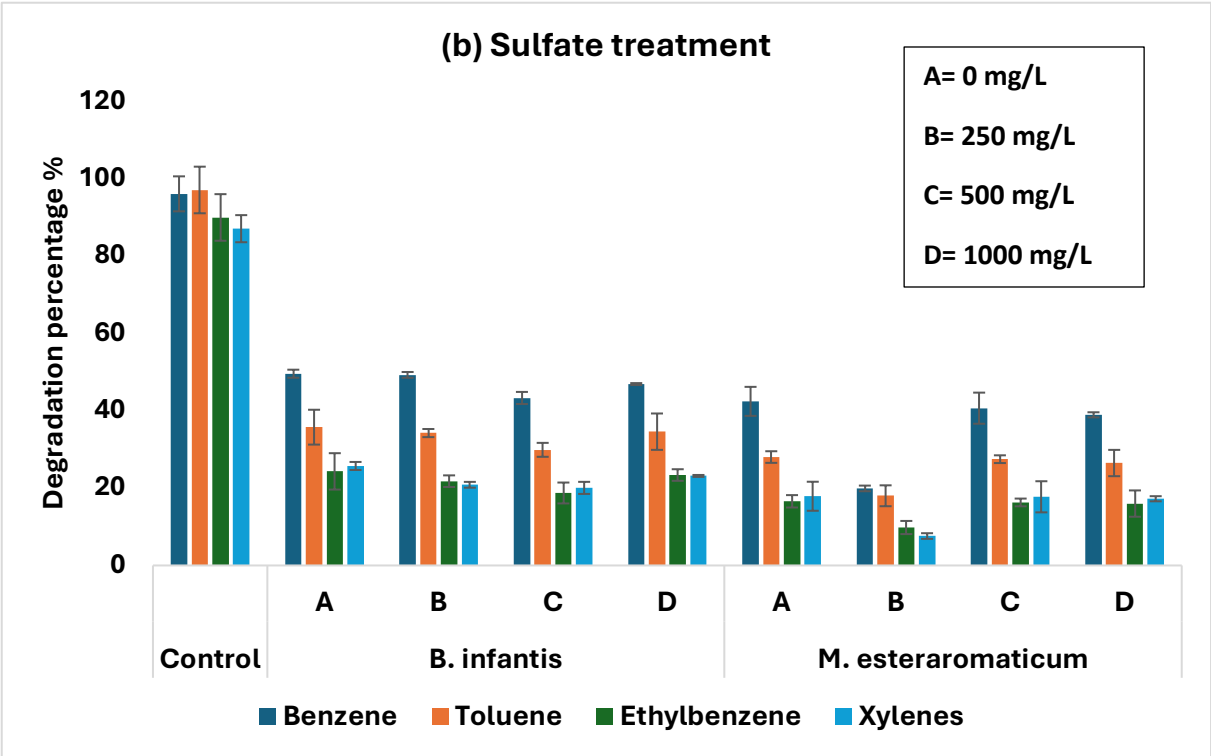
(b) Sulfate treatment
A= 0 mg/L
B= 250 mg/L
C= 500 mg/L
D= 1000 mg/L
Degradation percentage %
120
100
80
60
40
20
0
A
B
C
D
A
B
C
D
Control
B. infantis
M. esteraromaticum
Benzene
Toluene
Ethylbenzene
Xylenes

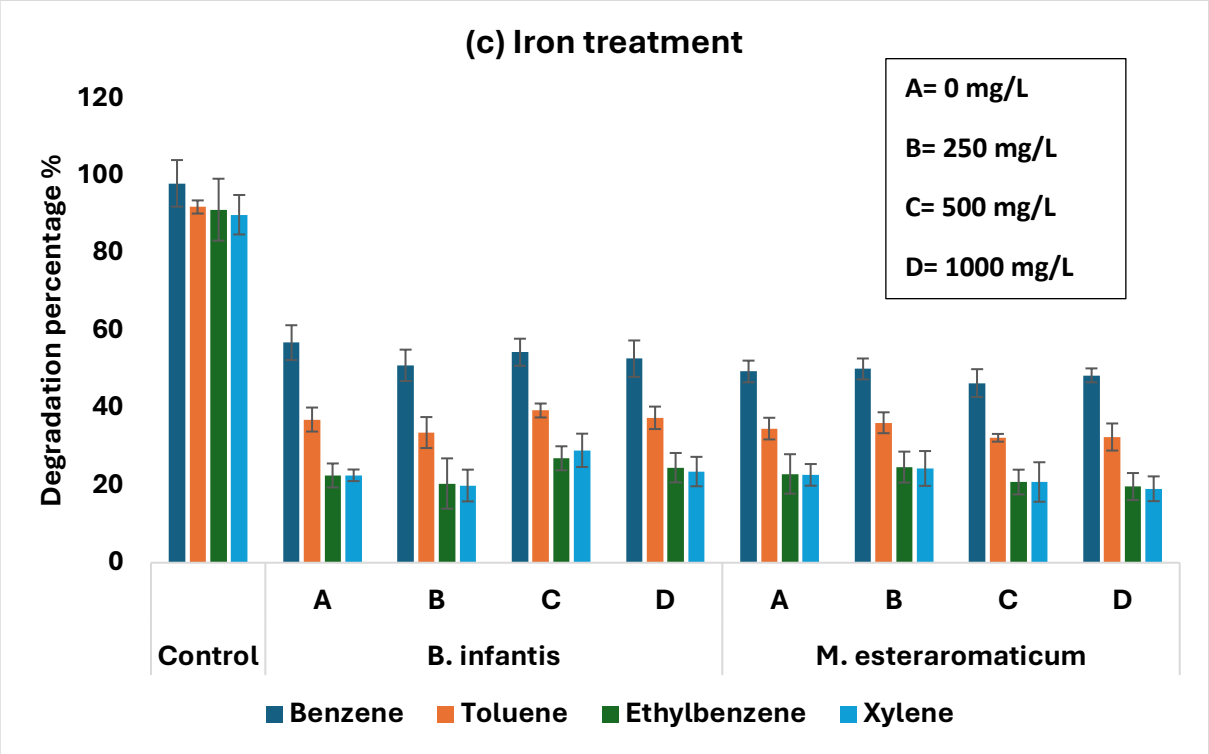

Figure C4: Degradation of BTEX compounds with individual ion treatment after 24 hours (a) Nitrate treatment, (b) Sulfate treatment and (c) Iron treatment

	B. infantis (MSM)	*B. infantis* (Soil)	*M. esteraromaticum* (MSM)	*M. esteraromaticum* (Soil)
Benzene	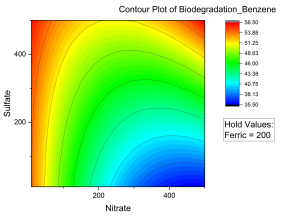	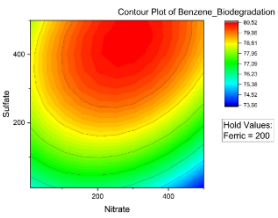	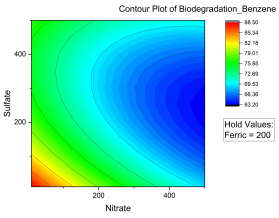	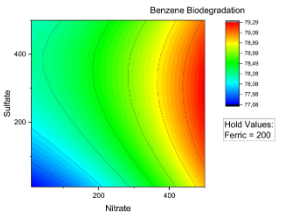
Toluene	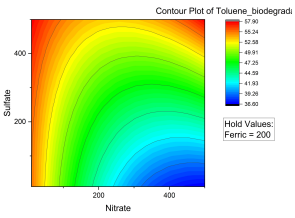	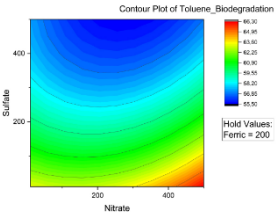	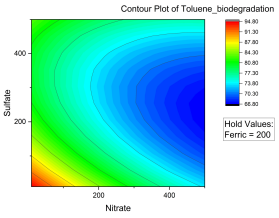	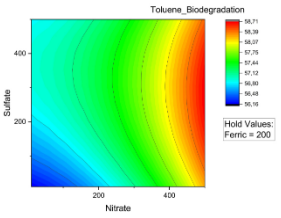
Ethylbenzene	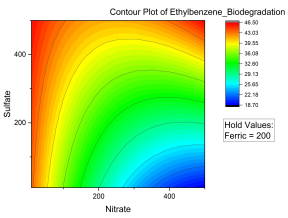	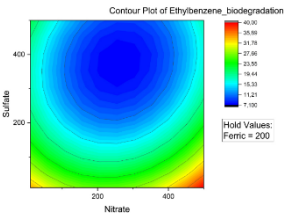	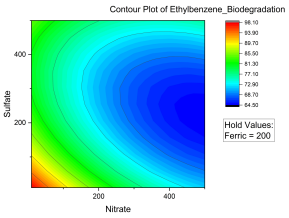	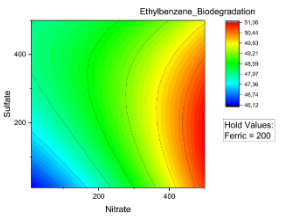
Xylene (s)	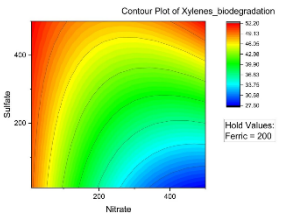	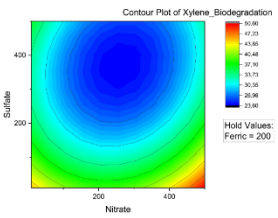	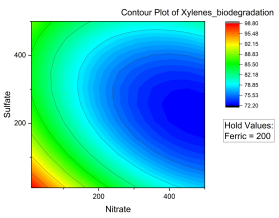	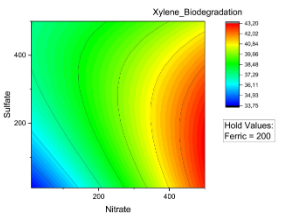

Figure C5: Contour plot of BTEX biodegradation by *B. infantis* and *M. esteraromaticum* with combinations of electron acceptors at a hold value of 200 mg/L ferric ions in artificial media and soil.

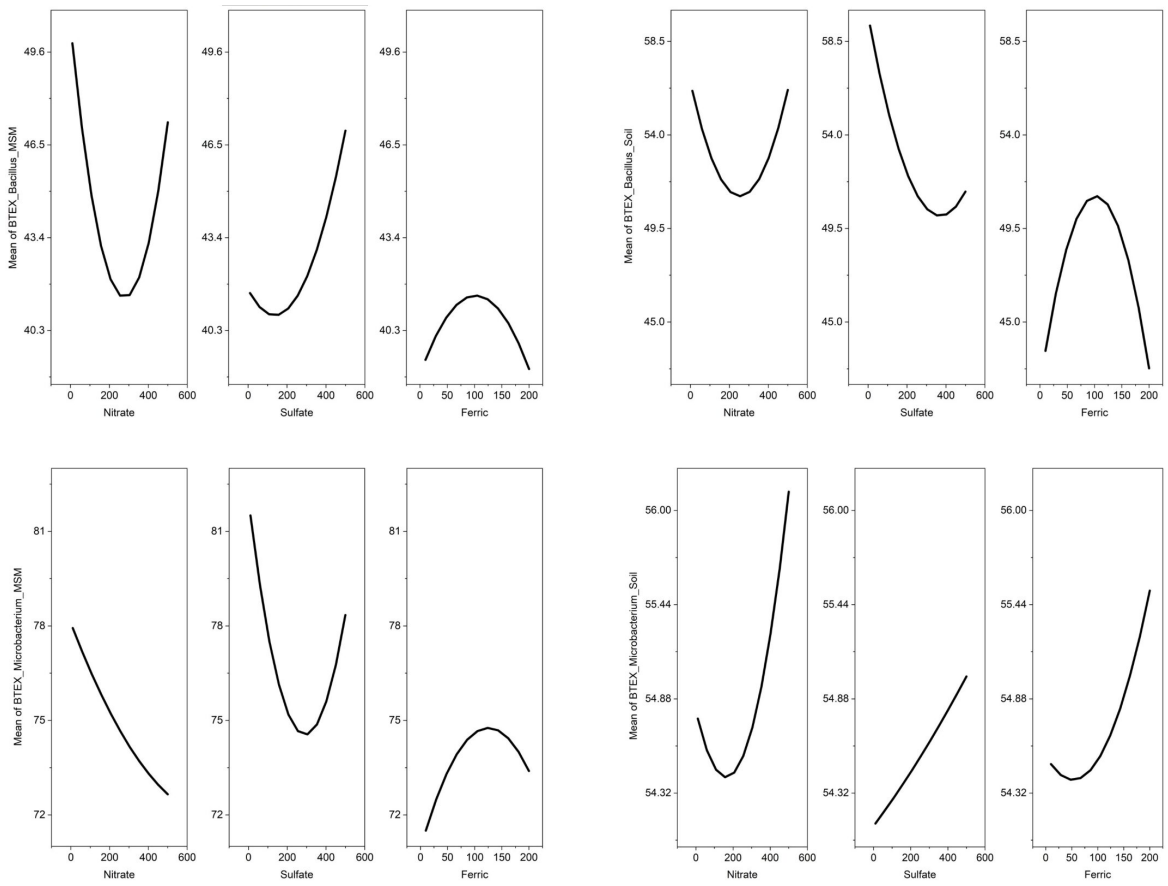

Figure C6: Effect of different ions on BTEX biodegradation through main plots.

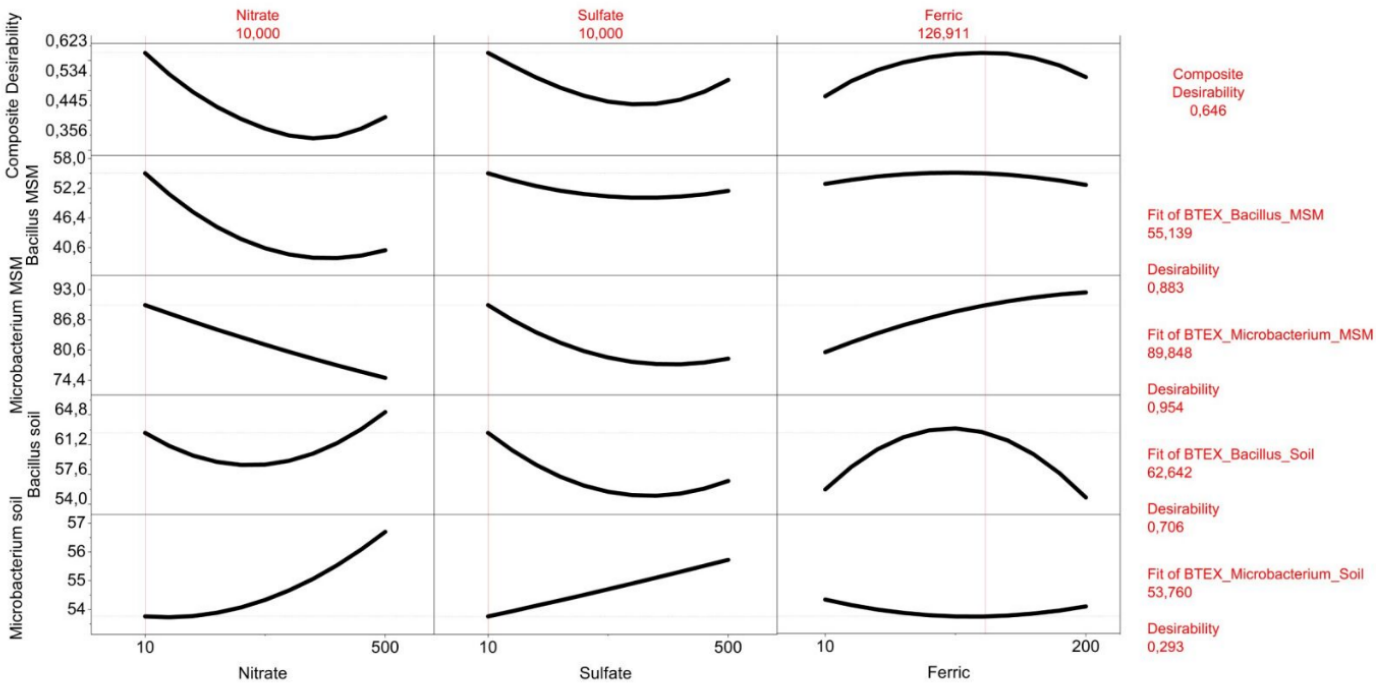

Figure C7: Optimization of BTEX biodegradation by *B. infantis* and *M. esteraromaticum* in MSM and soil.

Table C2: Statistical analysis of BTEX biodegradation by linear regression with ANOVA

	B. infantis		*M. esteraromaticum*	
	MSM	Soil	MSM	Soil
R^2 value				
B	0.705	0.665	0.776	0.655
T	0.695	0.657	0.919	0.686
E	0.697	0.735	0.953	0.622
X	0.702	0.712	0.946	0.672
Prob>F				
B	0.0047	0.5368	0.0239	5.03866E-34
T	0.0083	0.1851	0.0207	5.81405E-35
E	0.0034	0.0075	0.0249	2.55353E-34

X	0.0046	0.0231	0.0301	1.38929E-33

Table C3: Response optimization analysis

Response (BTEX Degradation %)	Fit	SE of Fit	95%LCL	95%UCL	95%LPL	95%UPL	Biodegradation at optimized values
*B. infantis*_MSM	55.138	6.106	39.442	70.835	31.347	78.930	52.750
*M. esteraromaticum*_MSM	89.848	3.737	80.239	99.456	75.283	104.412	94.521
*B. infantis*_Soil	62.642	5.748	47.864	77.419	40.243	85.040	59.636
*M. esteraromaticum*_Soil	53.760	1.242	50.565	56.955	48.917	58.603	55.345

LCL= Lower Confidence Interval

UCL= Upper Confidence Interval

LPL= Lower Perdicted Interval

UPL= Upper Perdicted Interval

Table C4: Residual redox capacity measurement for *B. infantis* and *M. esteraromaticum* from soil slurry experiment at highest electron acceptors' concentration.

B. infantis											
Benzene			Toluene			Ethylbenzene			Xylene		
Nitrate	Sulfate	Iron	Nitrate	Sulfate	Iron	Nitrate	Sulfate	Iron	Nitrate	Sulfate	Iron
0.601	0.434	1.100	0.447	0.781	2.054	0.739	1.432	4.068	0.598	1.123	3.330
0.429	0.429	1.077	0.803	0.803	1.968	1.547	1.547	3.950	1.250	1.250	3.212
0.434	0.426	1.112	0.797	0.788	2.067	1.579	1.558	4.165	1.298	1.268	3.472
0.431	0.423	1.057	0.787	0.804	2.010	1.580	1.626	4.065	1.284	1.340	3.350
M. esteraromaticum											
Benzene			Toluene			Ethylbenzene			Xylene		
Nitrate	Sulfate	Iron	Nitrate	Sulfate	Iron	Nitrate	Sulfate	Iron	Nitrate	Sulfate	Iron
0.438	0.424	1.087	0.866	0.844	2.151	1.035	1.004	2.595	1.231	1.182	3.132
0.418	0.418	1.028	0.837	0.837	2.049	1.009	1.009	2.425	1.193	1.193	2.813

0.435	0.441	1.077	0.863	0.869	2.140	1.045	1.050	2.566	1.260	1.264	3.044
0.411	0.438	1.097	0.819	0.868	2.170	0.970	1.056	2.641	1.125	1.274	3.185

1. **Amino Benzoic acid:**

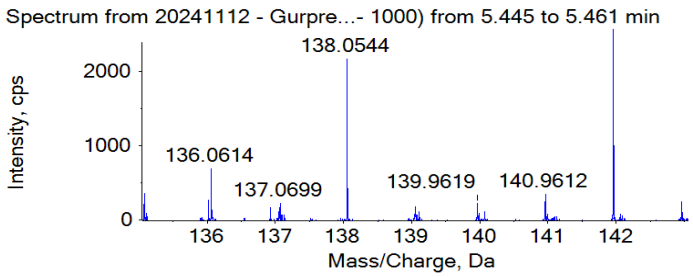

2. **Methylbenzoic acid:**

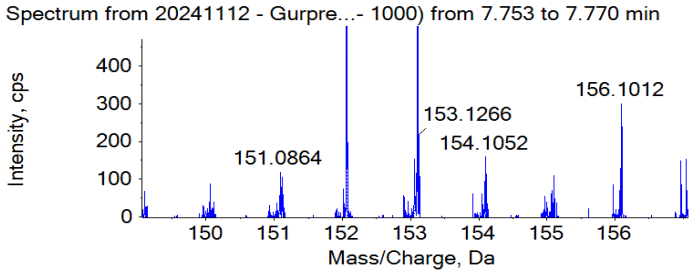

3. **2-hydroxybenzyl alcohol:**

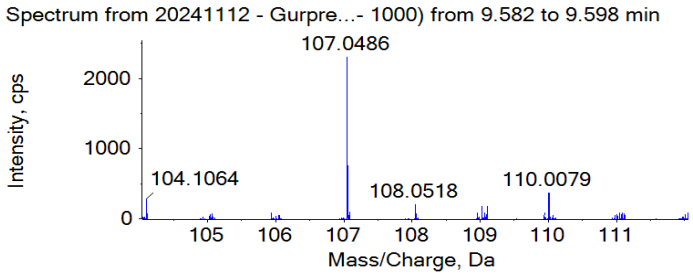

4. **3,4-Dimethylbenzaldehyde:**

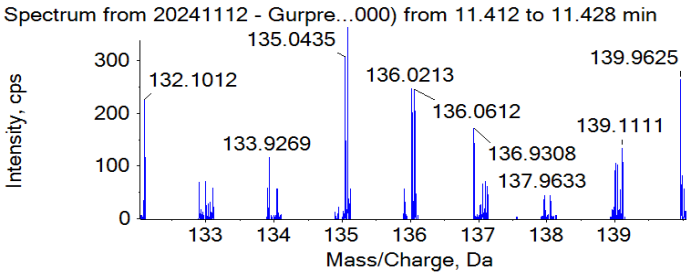

5. 2-methyl propionic acid:

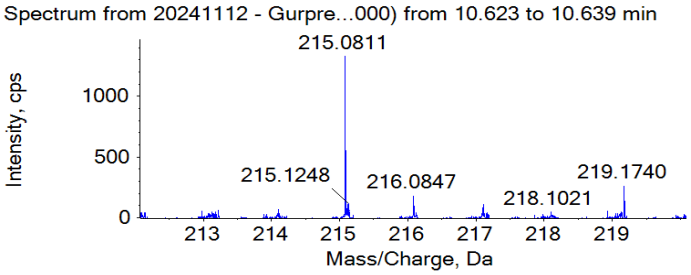

6. 2, 4-Dihydroxyacetophenone:

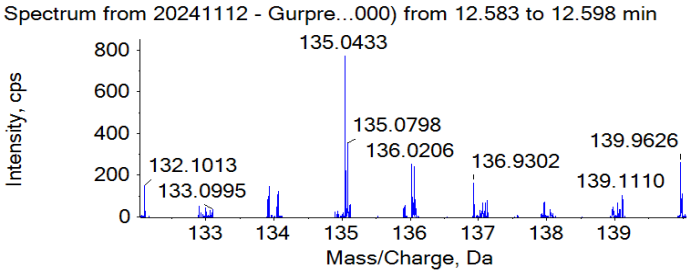

7. Pantothenic acid:

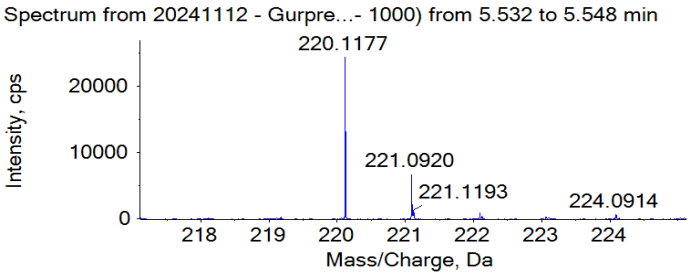

Figure C8: The MS spectra of the major identified compounds with their library and theoretical Hits confirmed with NIST Library.

The residual concentration of electron acceptors in different combination has been analyzed with Ion chromatography after 24 hours of treatment. Both the bacteria utilized the nitrate, sulfate and ferric ions at same rate. In combination ions, such as NS (Nitrate + Sulfate), nitrate was utilized first, likewise in NF (Nitrate + Ferric) and SF (Sulfate + Ferric), Nitrate and ferric ions were used in priority respectively. In NSF (Nitrate + Sulfate + Ferric) combination treatment, the utilize rate was as nitrate > ferric > sulfate ions as shown in Figure C9. Similar utilization rate has been reported by Pi et al., 2023 and Hernández-Ospina et al., 2023, based on their thermodynamics and redox potential.

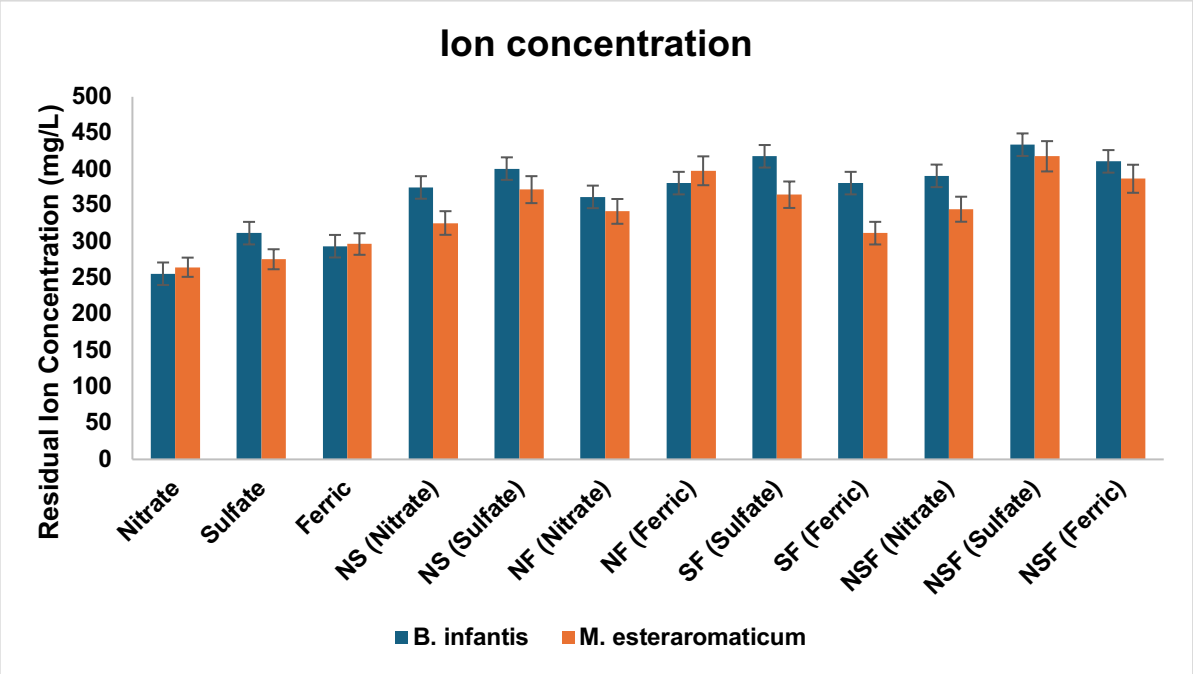

Figure C9: Residual concentration of electron acceptors after 24 h analyzed with Ion chromatography

Appendix D

(Objective 3: Perform a bench-scale GHP system in a bioreactor to study the effect of cyclic heat on BTEX biodegradation.**)**

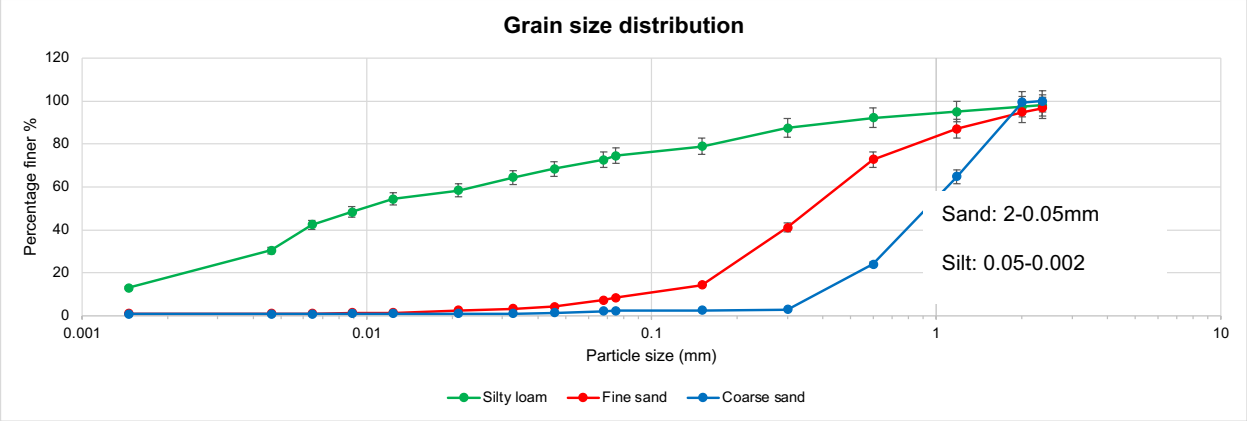

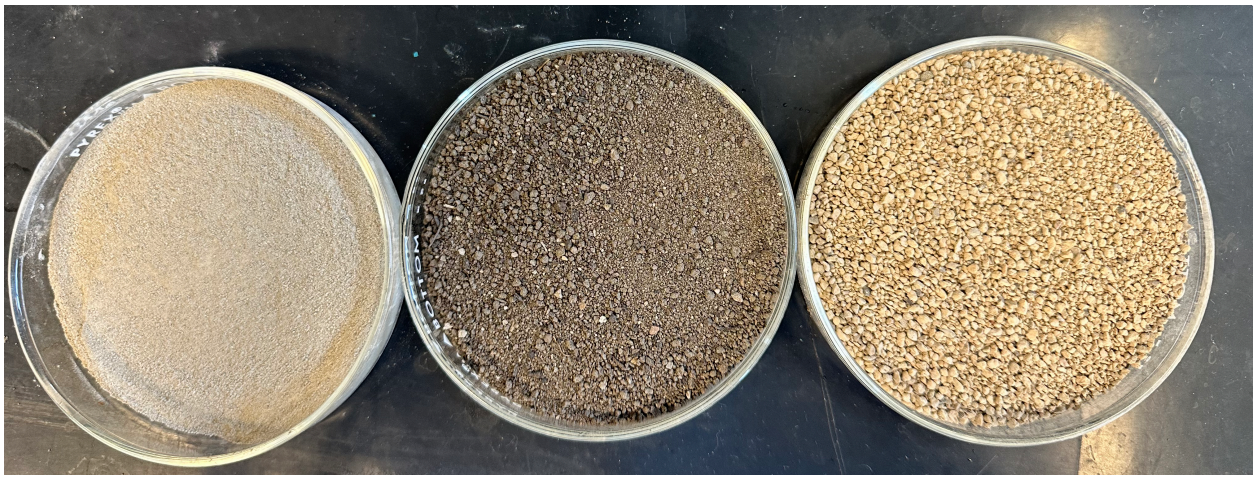

Figure D1: Particle size distribution and USDA textural classification of the three soils used in the column experiments.

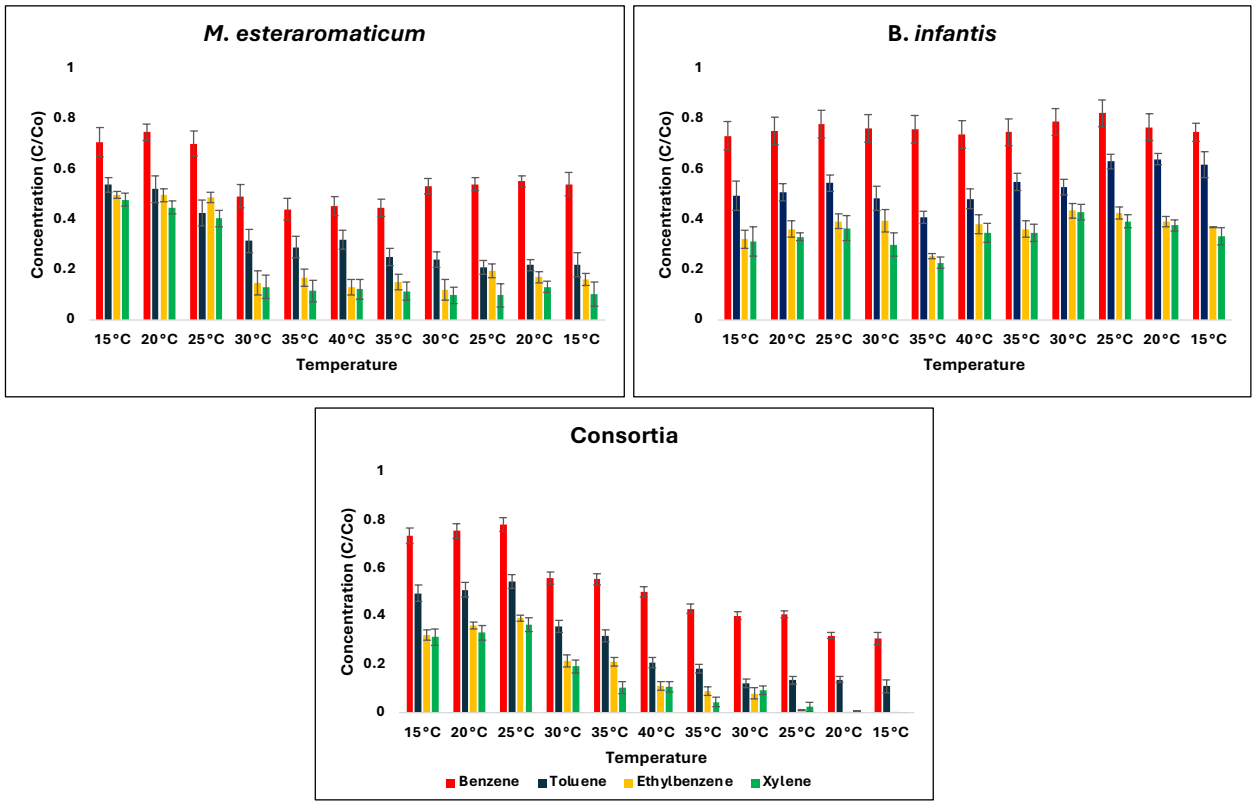

Figure D2: Residual BTEX concentration data from batch-scale experiments.

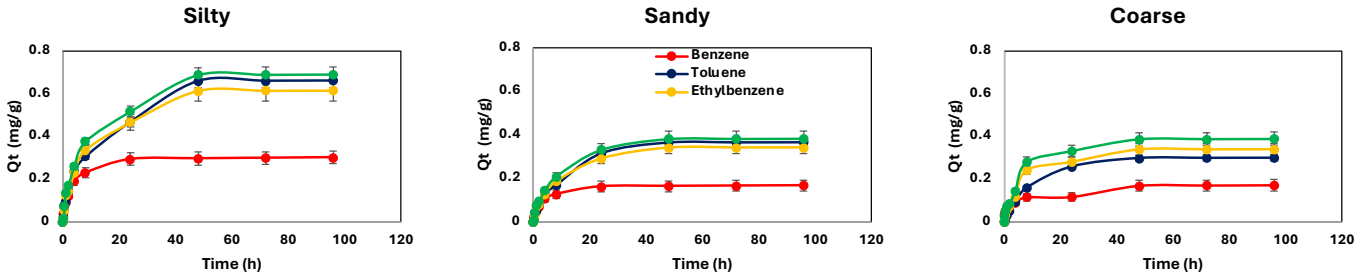

Figure D3: Adsorption rate of BTEX on Silty, Sandy and coarse soil at batch scale.

Table D1: Biodegradation rate constant (K_{bio}) values at different temperatures from batch experiments with silty loam soil.

	Consortia			
Temp (°C)	**Benzene (d^{-1})**	**Toluene (d^{-1})**	**Ethylbenzene (d^{-1})**	**Xylenes (d^{-1})**
10	0.028	0.063	0.042	0.035
15	0.04	0.09	0.06	0.05
20	0.056	0.127	0.085	0.071
25	0.08	0.18	0.12	0.1
30	0.113	0.254	0.169	0.141
35	0.16	0.36	0.24	0.2
40	0.226	0.509	0.339	0.282
	M. esteraromaticum			
Temp (°C)	**Benzene (d^{-1})**	**Toluene (d^{-1})**	**Ethylbenzene (d^{-1})**	**Xylenes (d^{-1})**
10	0.014	0.035	0.025	0.021
15	0.02	0.05	0.035	0.03
20	0.028	0.071	0.049	0.042
25	0.04	0.1	0.07	0.06
30	0.057	0.141	0.099	0.085
35	0.08	0.2	0.14	0.12
40	0.113	0.283	0.198	0.17

Table D2: Growth rate (μ) and doubling time of bacteria from batch experiments with silty loam soil.

	B. infantis		***M. esteraromaticum***		**Consortia**	
Temp (°C)	**μ (d^{-1})**	**t_d (d)**	**μ (d^{-1})**	**t_d (d)**	**μ (d^{-1})**	**t_d (d)**
15 → 20	0.08	8.7	0.031	22.1	0.055	12.7
20 → 25	0.045	15.4	0.074	9.4	–0.041	—
25 → 30	0.015	47.5	0.134	5.2	0.329	2.1
30 → 35	–0.059	—	0.095	7.3	–0.031	—
35 → 40	–0.047	—	–0.035	—	–0.052	—

Table D3: Biodegradation rate constant (K_{bio}) values at different temperatures from cyclic treatment of soil columns with silty loam, fine sand and coarse sand treated with Consortia.

	Cyclic_Silty loam			
Temp (°C)	**Benzene (d^{-1})**	**Toluene (d^{-1})**	**Ethylbenzene (d^{-1})**	**Xylenes (d^{-1})**
5	0.0178	−0.179	−0.018	−0.052
10	−0.0439	0.006	−0.090	0.087
20	0.1574	0.08	0.126	0.197
30	0.1299	0.575	0.739	0.335
40	0.15	0.196	0.024	0.339
30	−0.0467	−0.110	−0.144	0.031
20	0.0427	−0.517	−0.014	−0.227
10	0.0238	0.003	−0.092	−0.135
	Cyclic_Fine sand			
Temp (°C)	**Benzene (d^{-1})**	**Toluene (d^{-1})**	**Ethylbenzene (d^{-1})**	**Xylenes (d^{-1})**
5	0.015	−0.104	−0.105	0.022
10	0.101	−0.031	−0.087	0.074
20	0.054	−0.043	−0.064	−0.002
30	−0.038	0.074	−0.021	0.04
40	0.092	0.207	0.278	0.147
30	0.252	0.192	0.444	0.252
20	0.332	0.272	0.563	0.299
10	0.364	0.242	0.504	0.29
	Cyclic_Coarse sand			
Temp (°C)	**Benzene (d^{-1})**	**Toluene (d^{-1})**	**Ethylbenzene (d^{-1})**	**Xylenes (d^{-1})**
5	0.007	0.144	−0.037	0.093
10	0.009	0.071	0.123	0.167

20	0.049	0.044	0.075	0.039
30	0.179	0.046	0.21	0.041
40	−0.027	0.076	0.229	0.06
30	−0.012	0.254	0.278	0.171
20	−0.024	0.217	0.228	0.142
10	−0.073	0.206	0.322	0.16

Table D4: Activation energy for BTEX degradation on three soils calculated from the Arrhenius equation.

Soil	**Thermal regime**	**Benzene** (kJ/mol)	**Toluene** (kJ/mol)	**Ethylbenzene** (kJ/mol)	**Xylenes** (kJ/mol)	**Quality Fit**
Silty loam	Cyclic	43–48	35–45	30–40	30–40	$R^2 \approx 0.7–0.8$
Fine sand	Cyclic	35–42	32–42	34–42	36–44	R^2 0.5–0.8
Coarse sand	Cyclic	25–35	30–45	35–50	32–46	$R^2 \approx 0.4–0.8$
Silty loam	Constant	-	-	-	-	Arrhenius not estimable from a single temperature

In coarse sand, benzene exhibited the lowest apparent Ea (≈25–35 kJ/mol), while toluene, ethylbenzene, and xylenes showed higher Ea values (≈30–50 kJ/mol). This reversed trend compared to silty and sandy soils suggests that in coarse sand, benzene biodegradation is strongly limited by rapid advective transport and low contact time, resulting in weak temperature sensitivity. In contrast, heavier BTEX compounds are retained slightly longer, enabling greater temperature-dependent microbial activity and thus higher Ea.

Appendix E

(Objective 4: Investigate geothermal heating impacts on soil microbiome communities along with the borehole depth by 16S rRNA sequencing**)**

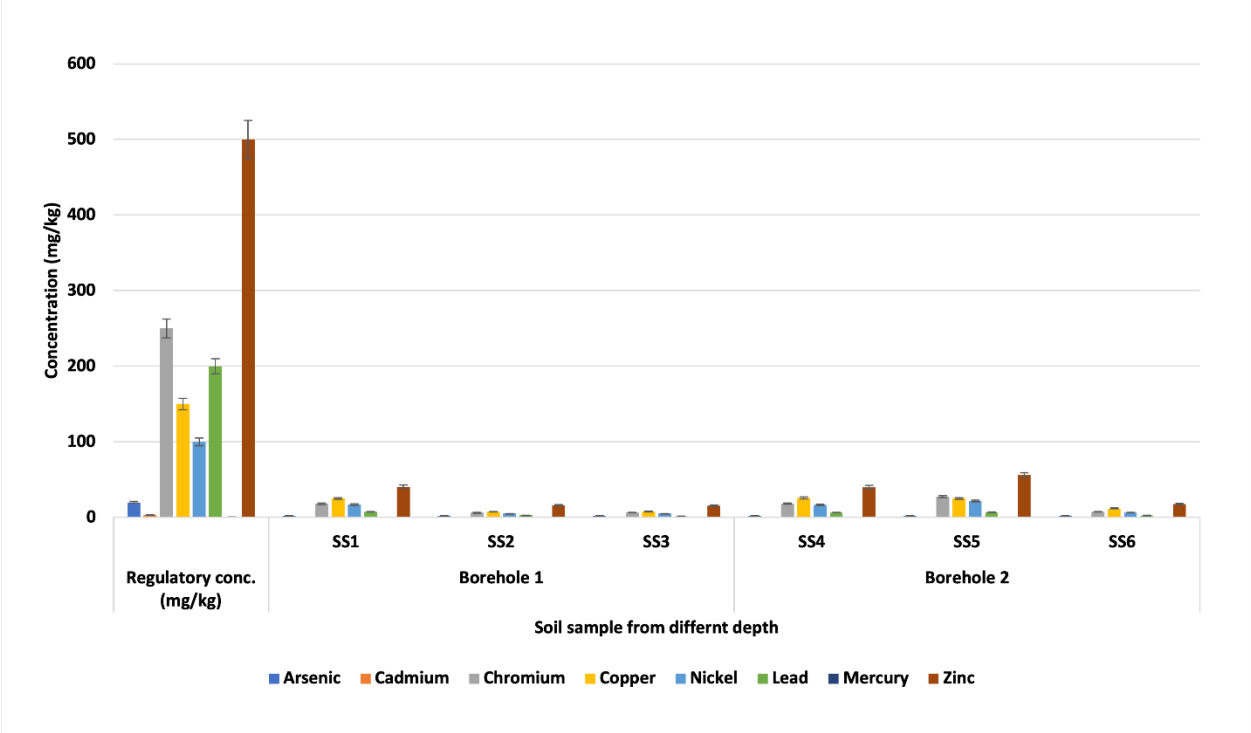

Figure E1: HM concentration in the soil samples of different depths along with regulatory concentration of HMs from Canadian soil regulatory policies (He, 2015).

Taxonomical analysis

The microbes identified in soil samples were further analyzed based on the genus to which they belong (Figure E2). Although the community and their amount vary a lot based on the genus in each sample, however, *Rhodoferax, Bacillus, Pseudomonas, Microbacterium* are found in high amounts in each soil.

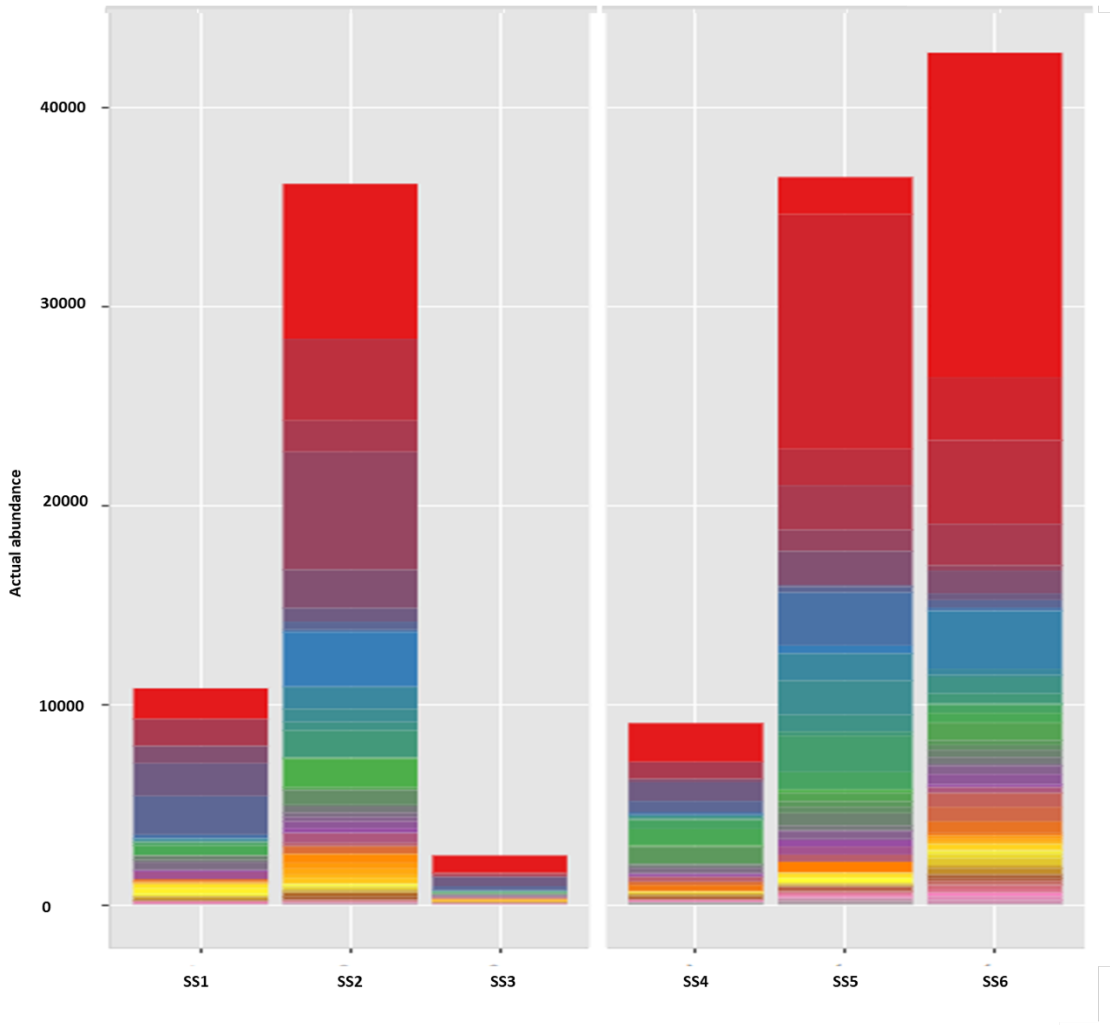

Genus

- Not_Assigned
- Rhodoferax
- Thiobacillus
- Cavicella
- Nevskia
- Hydrogenophaga
- Klebsiella
- Pseudomonas
- Ramlibacter
- Limnobacter
- Methylibium
- Pedobacter
- Curvibacter
- Methylotenera
- Phenylobacterium
- Flavihumibacter
- Haliangium
- C1_B045
- Bradyrhizobium
- Reyranella
- Acinetobacter
- Methyloversatilis
- Aquabacterium
- Serratia
- Sediminibacterium
- Devosia
- Chryseoglobus
- Legionella
- Sulfuricella
- Polaromonas
- Fluviicola
- OLB12
- Immundisolibacter
- Geothrix
- Janthinobacterium
- Sandaracinus
- Allorhizobium_Neorhizobium_Pararhizobium_Rhizobium
- GKS98_freshwater_group
- Erysipelothrix
- Pseudorhodobacter
- Acidovorax
- Algoriphagus
- Sulfuritalea
- Caenimonas
- Nocardioides
- Novosphingobium
- Shewanella
- Planctopirus
- Qipengyuania
- Simplicispira
- Noviherbaspirillum
- Sphingorhabdus
- Nitrospira
- Sulfuricurvum
- Arthrobacter
- Jahnella
- Mesorhizobium
- Bacteriovorax
- Lacunisphaera
- Geobacter
- Rhodococcus
- Gaiella
- Bryobacter
- Lacibacter
- Croceicoccus
- Sulfurospirillum
- Runella
- Afipia
- Bosea
- WCHB1_32
- Sphingopyxis
- ADurb_Bin063_1
- Pseudohongiella
- Pirellula
- Parasegetibacter
- Mycobacterium
- Brevundimonas
- Methylocella
- anthobacter
- Chryseolinea
- Staphylococcus
- Lysobacter
- Pseudarcobacter
- Peredibacter
- Massilia
- Thermomonas
- Desulfosporosinus
- Pseudoxanthobacter

Figure E2: Genus based classification of identified microbes from soil samples.

Multiple linear regression analysis

Multiple linear regression performed with MaAsLin2 showed the significantly impacted bacterial genera with BTEX treatment in comparison to uncontaminated samples at all three temperatures (Figure E3).

Significantly different bacterial genera using Multiple linear regression at 15 °C: MaAsLin2

Name	Log2FC	St.Error	P-value	FDR
Devosia	-2.61	0.586	0.00158	0.0132
Hydrogenophaga	-2.58	0.573	0.0015	0.0132
Methylotenera	4.99	1.0	7.7E-4	0.0132
Pseudomonas	4.22	0.99	0.00212	0.0133
Lacibacter	-6.69	1.68	0.00314	0.0157
Pedobacter	-3.16	0.893	0.00636	0.0265
Herbaspirillum	-2.99	0.938	0.011	0.0365
Mesorhizobium	-2.56	0.812	0.0117	0.0365
Thermomonas	-3.91	1.29	0.014	0.0389
Ensifer	-3.54	1.35	0.0275	0.053

Significantly different bacterial genera using Multiple linear regression at 28 °C: MaAsLin2

Name	Log2FC	St.Error	P-value	FDR
Brevundimonas	-7.67	1.11	4.13E-5	0.00116
Phyllobacterium	-4.15	0.636	6.64E-5	0.00116
Methylotenera	6.0	1.43	0.00181	0.0212
Methyloversatilis	5.72	1.77	0.00889	0.0778
Sphingopyxis	-4.34	1.6	0.0216	0.152
Allorhizobium_Neorhizobium_Pai	3.84	1.67	0.0446	0.175
Rhodobacter	-3.17	1.35	0.0414	0.175
Sphingoaurantiacus	-4.74	2.07	0.045	0.175
Thermomonas	-3.79	1.54	0.0333	0.175
Intrasporangium	3.51	1.66	0.0607	0.198

Significantly different bacterial genera using Multiple linear regression at 40 °C: MaAsLin2

Name	Log2FC	St.Error	P-value	FDR
Brevundimonas	-3.79	0.536	3.42E-5	0.00109
Not_Assigned	2.86	0.674	0.00169	0.027
Hydrogenophaga	2.32	0.621	0.00388	0.0414
Arthrobacter	1.96	0.631	0.011	0.0703
Methyloversatilis	4.89	1.55	0.0102	0.0703
Ancylobacter	3.34	1.13	0.0143	0.0732
Methylotenera	3.27	1.13	0.016	0.0732
Brevibacillus	2.01	0.82	0.034	0.136
Janthinobacterium	2.21	0.976	0.047	0.167
Pseudomonas	2.24	1.04	0.0565	0.181

Figure E3: Multiple linear regression performed with MaAsLin2.

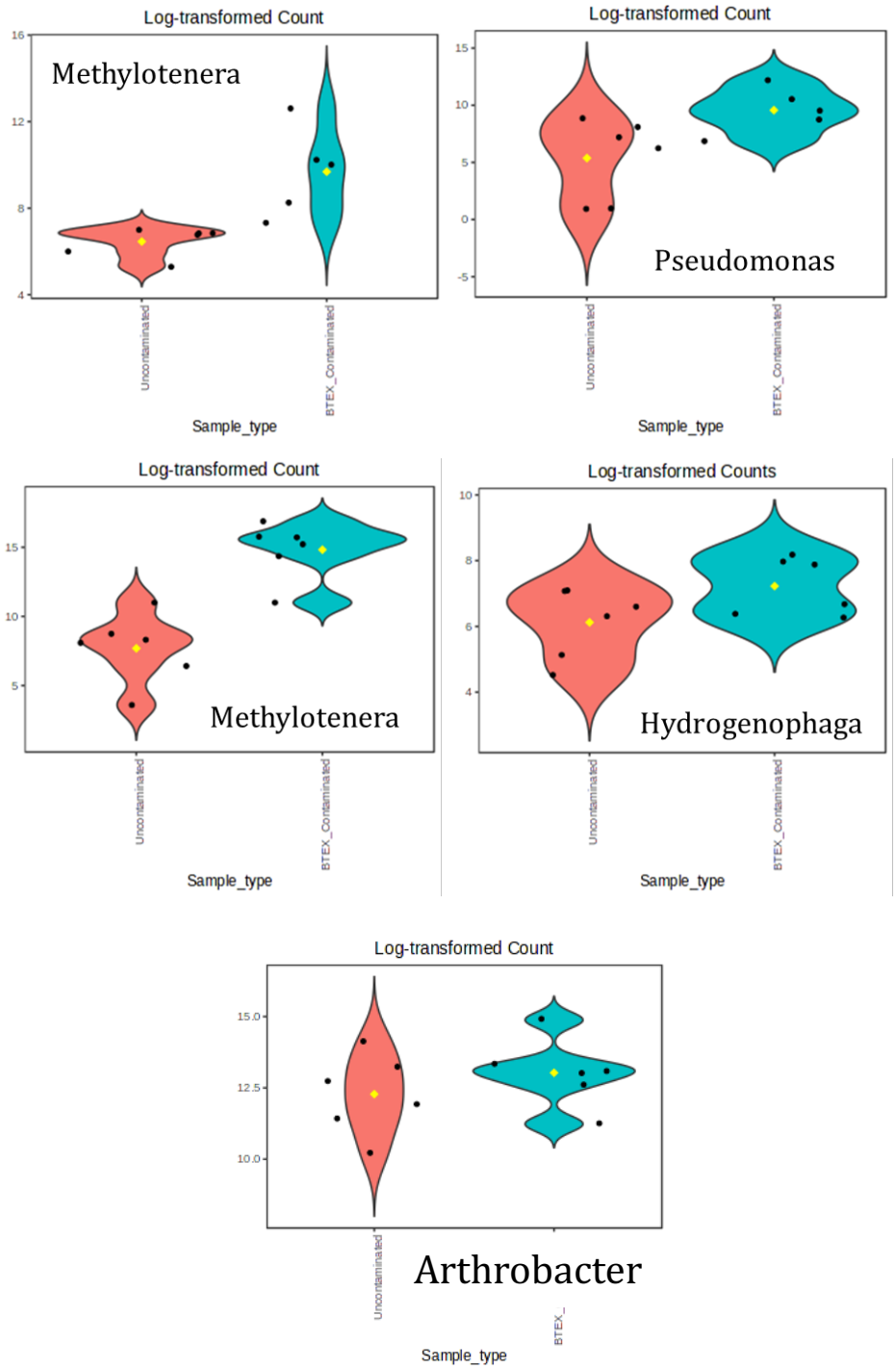

Figure E4: Log-transformed counts of significantly different bacterial genera by Multiple linear regression.

Phylogenetic analysis

To study the hierarchical and evolutionary relationship among the identified microbes of each soil, phylogenetic trees are generated using the neighbour-joining algorithm with 1000 bootstraps in MEGA 7.0 software, as illustrated in Figure E5.

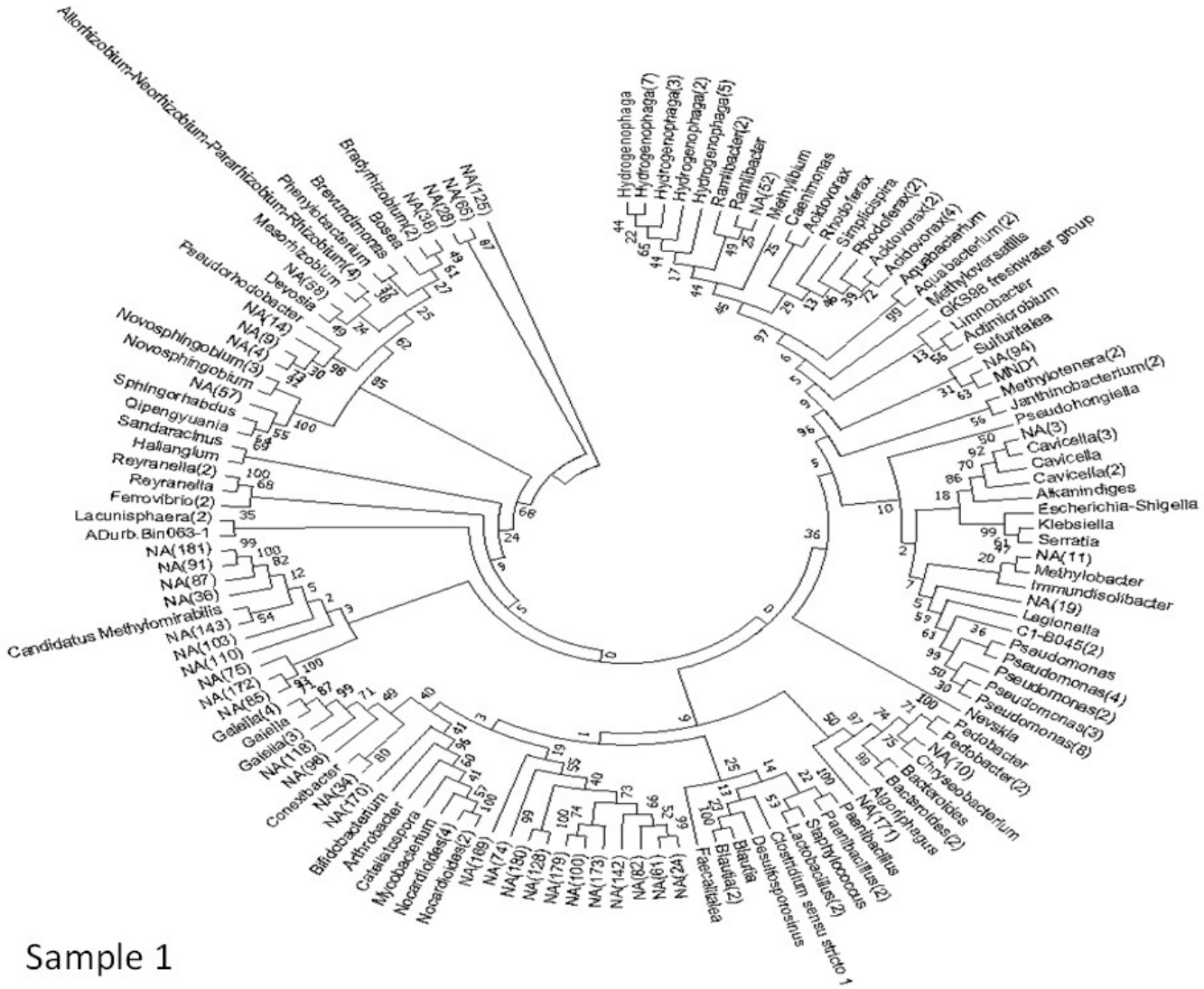

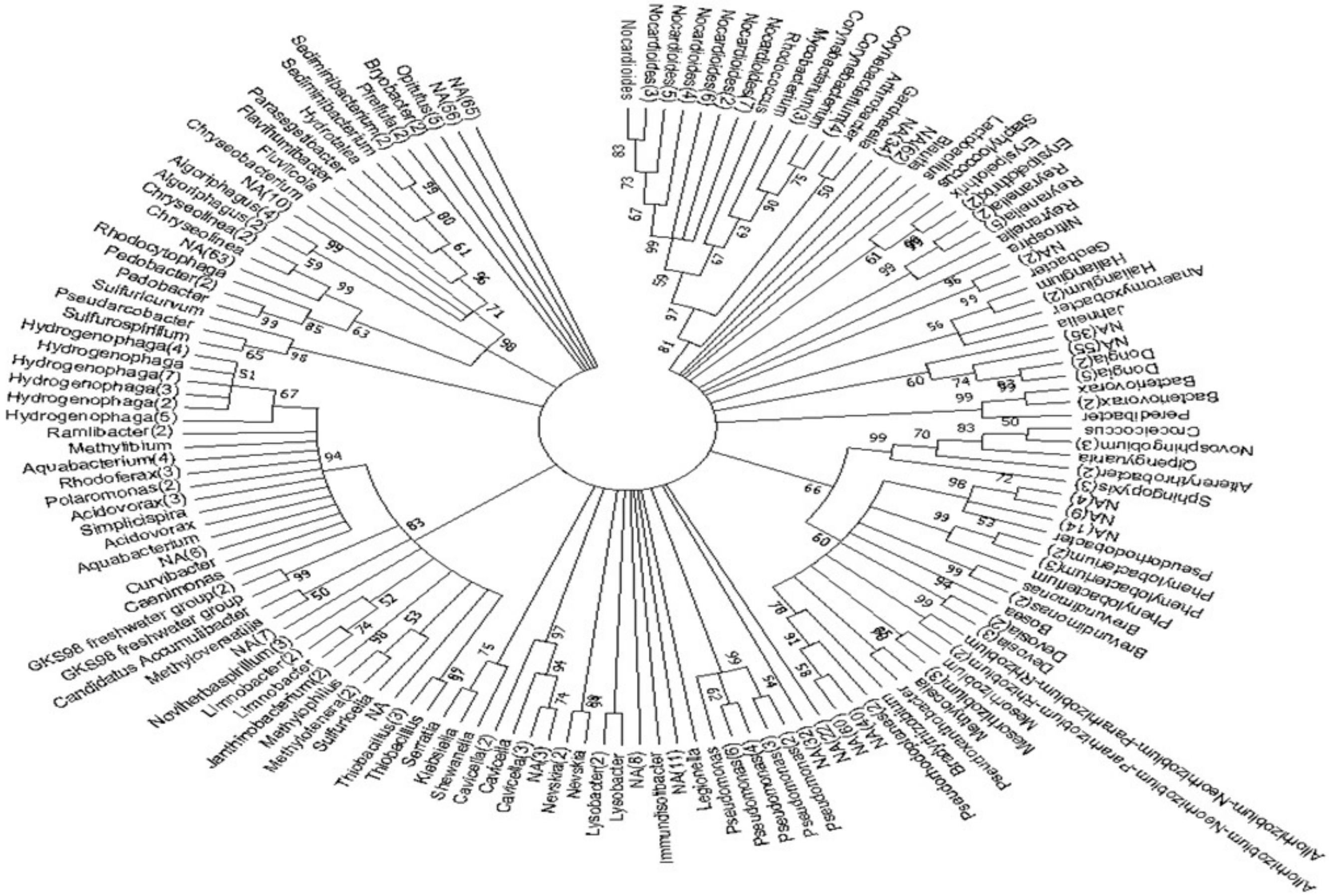
Nocardioides
Nocardioides(3)
Rhodococcus
Corynebacterium(4)
Gardnerella
Arthrobacter
Staphylococcus
Lactobacillus
Erysipelothrix
Reyranella
Nitrospira
Geobacter
Haliangium
Anaeromyxobacter
Jahnella
NA(35)
NA(55)
Dongia(2)
Dongia(5)
Bacteriovorax
Bacteriovorax(2)
Peredibacter
Crocelococcus
Novosphingobium(3)
Qipengyuania
Altererythrobacter(2)
Sphingopyxis(3)
Pseudorhodobacter
Pseudolabrys
Phenylobacterium(3)
Phenylobacterium
Brevundimonas(2)
Brevundimonas
Bosea
Devosia(3)
Devosia
Allorhizobium-Neorhizobium-Pararhizobium-Rhizobium
Mesorhizobium
Methylocella
Bradyrhizobium
Pseudoxanthobacter
Pseudorhodoplanes
Pseudomonas
Pseudomonas(4)
Legionella
NA(11)
Immundisolibacter
NA(8)
Lysobacter
Lysobacter(2)
Nevskia
Nevskia(2)
NA(3)
Cavicella(3)
Cavicella
Cavicella(2)
Shewanella
Klebsiella
Serratia
Thiobacillus
Thiobacillus(3)
NA
Sulfuricella
Methylotenera(2)
Methylophilus
Methylobacterium(2)
Janthinobacterium(2)
Limnobacter
Limnobacter(2)
Noviherbaspirillum(3)
NA(7)
Methyloversatilis
Candidatus Accumulibacter
GKS98 freshwater group
GKS98 freshwater group(2)
Caenimonas
Curvibacter
NA(6)
Aquabacterium
Acidovorax
Simplicispira
Acidovorax(3)
Polaromonas(2)
Rhodoferax(3)
Aquabacterium(4)
Methylibium
Ramlibacter(2)
Hydrogenophaga(5)
Hydrogenophaga(2)
Hydrogenophaga(3)
Hydrogenophaga(7)
Hydrogenophaga
Hydrogenophaga(4)
Sulfurospirillum
Pseudarcobacter
Sulfuricurvum
Pedobacter
Pedobacter(2)
NA(63)
Rhodocytophaga
Chryseolinea
Chryseolinea(2)
Algoriphagus(2)
Algoriphagus(4)
NA(10)
Chryseobacterium
Fluviicola
Flavihumibacter
Parasegetibacter
Hydrotalea
Sediminibacterium
Sediminibacterium(2)
Prellulla
Bryobacter(2)
Opitutus(2)
NA(5)
NA(56)
NA(65)

Sample 2

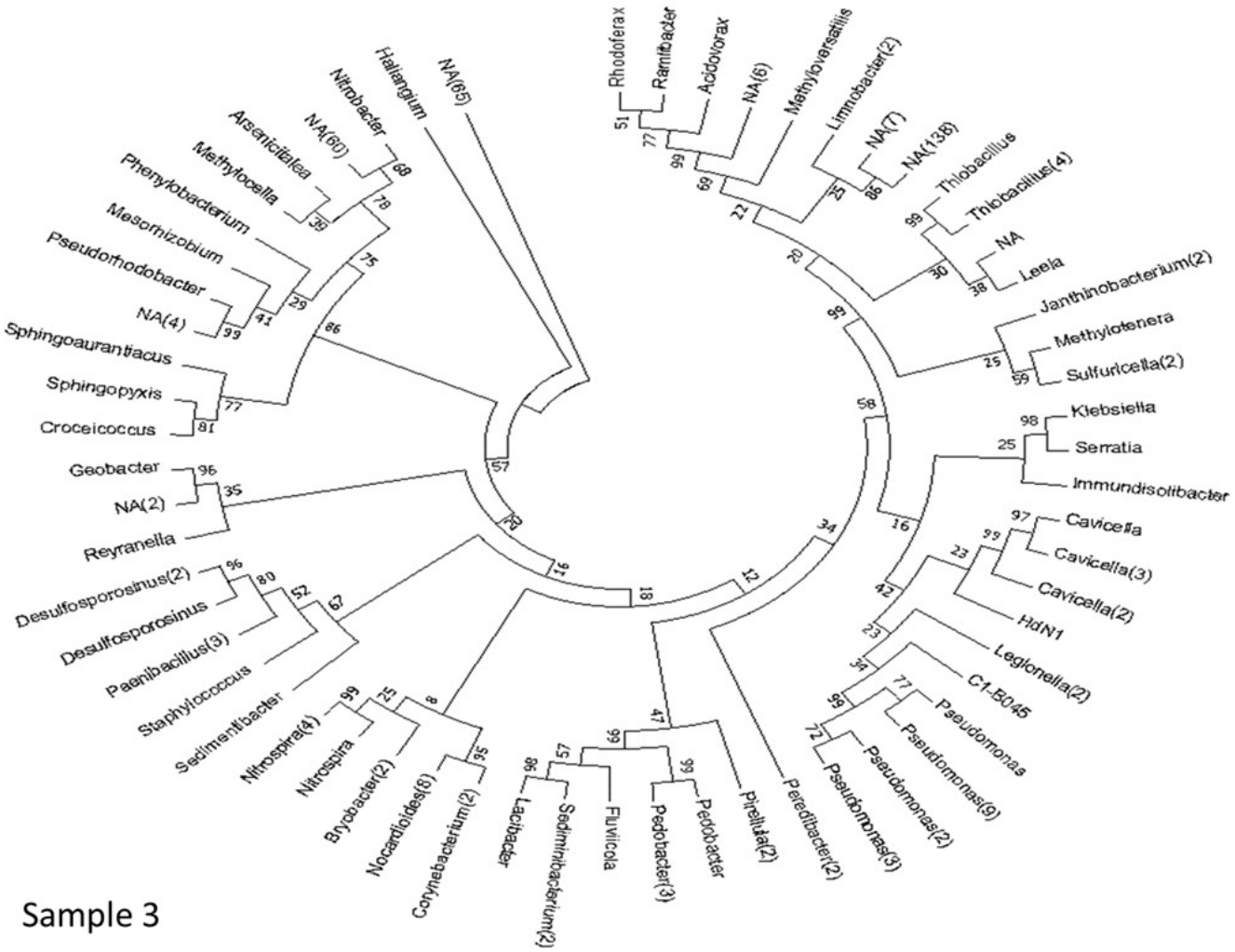
Rhodoferax
Ramlibacter
Acidovorax
NA(6)
Methyloversatilis
Limnobacter(2)
NA(7)
NA(138)
Thiobacillus
Thiobacillus(4)
NA
Leela
Janthinobacterium(2)
Methylotenera
Sulfuricella(2)
Klebsiella
Serratia
Immundisolibacter
Cavicella
Cavicella(3)
Cavicella(2)
HdN1
Legionella(2)
C1-B045
Pseudomonas
Pseudomonas(9)
Pseudomonas(2)
Pseudomonas(3)
Pirellula(2)
Pelodictyobacter(2)
Pedobacter
Pedobacter(3)
Fluviicola
Sediminibacterium(2)
Lacibacter
Corynebacterium(2)
Nocardioides(6)
Bryobacter(2)
Nitrospira
Nitrospira(4)
Sediminibacter
Staphylococcus
Paenibacillus(3)
Desulfosporosinus
Desulfosporosinus(2)
Reyranella
NA(2)
Geobacter
Croceicoccus
Sphingopyxis
Sphingoaurantiacus
NA(4)
Pseudorhodobacter
Mesorhizobium
Phenylobacterium
Methylocella
Arenicellales
NA(60)
Nitrobacter
Haliangium
NA(65)

Sample 3

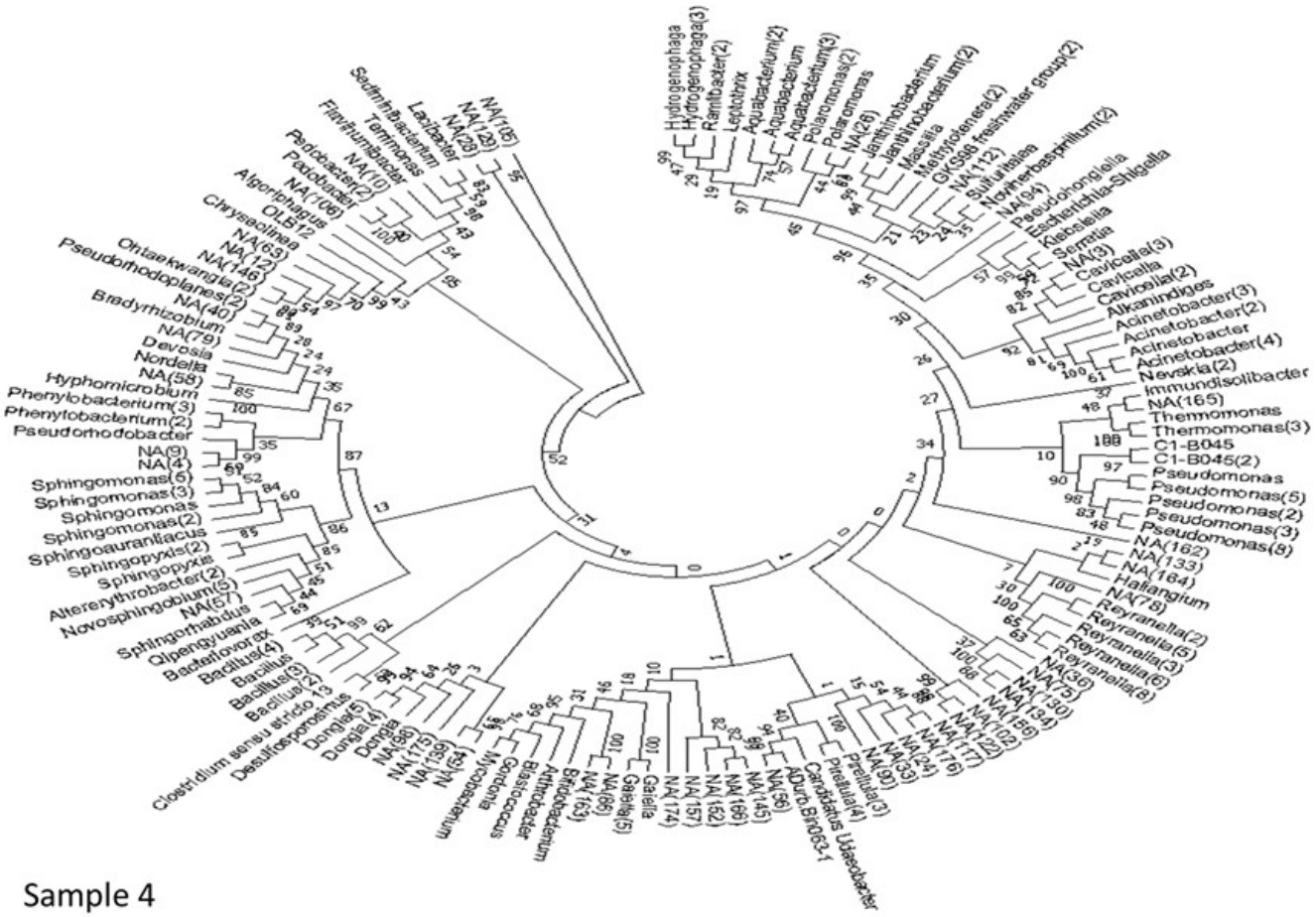
Hydrogenophaga
Hydrogenophaga(3)
Ramlibacter(2)
Leptothrix
Aquabacterium(2)
Aquabacterium
Aquitalea
Aquitalea(2)
Polaromonas(3)
Polaromonas(2)
NA(26)
Janthinobacterium
Janthinobacterium(2)
Massilia
Methylpilum
Methylpilum(2)
GKS98 freshwater group(2)
NA(112)
Sulfuritalea
Sulfuritalea(2)
Noviherbaspirillum(2)
NA(94)
Pseudohongiella
Escherichia-Shigella
Klebsiella
Serratia
NA(3)
Cavicella(3)
Cavicella
Caviciella(2)
Alkanindiges
Alkanindiges(3)
Acinetobacter(2)
Acinetobacter
Acinetobacter(4)
Acinetobacter
Acinetobacter(2)
Newskia(2)
Immundisolibacter
NA(165)
Thermomonas
Thermomonas(3)
C1-B045
C1-B045(2)
Pseudomonas
Pseudomonas(5)
Pseudomonas(2)
Pseudomonas(3)
Pseudomonas(8)
NA(162)
NA(133)
NA(164)
Haliangium
NA(75)
Reyranella(2)
Reyranella(5)
Reyranella(3)
Reyranella(6)
Reyranella(8)
NA(36)
NA(130)
NA(134)
NA(102)
NA(156)
NA(122)
NA(117)
NA(176)
NA(24)
NA(139)
NA(90)
Pirellula(3)
Pirellula(4)
Candidatus Udaeobacter
ADurb.Bin063-1
NA(36)
NA(145)
NA(166)
NA(162)
NA(157)
NA(174)
Gaiella(5)
Gaiella
NA(86)
NA(163)
Arthrobacterium
Blastococcus
Gordonia
Mycobacterium
NA(54)
NA(139)
NA(175)
NA(388)
Dongia
Dongia(4)
Dongia(5)
Desulfosporosinus
Clostridium sensu stricto 13
Bacillus(2)
Bacillus(3)
Bacillus
Bacillus(4)
Bacteriovorax
Olpenguyuania
Sphingorhabdus
NA(57)
Novosphingobium(5)
Altererythrobacter(2)
Sphingopyxis
Sphingopyxis(2)
Sphingoaurantiacus
Sphingomonas(2)
Sphingomonas
Sphingomonas(3)
Sphingomonas(5)
NA(4)
NA(9)
Pseudorhodobacter
Phenylobacterium(2)
Phenylobacterium(3)
Hyphomicrobium
NA(58)
Nordella
Devosia
NA(79)
Bradyrhizobium
NA(40)
Pseudorhodoplanes(2)
Chitinaekwangsia(2)
NA(12)
NA(146)
NA(63)
Chrysaclinea
OLB12
Alpiniphaga
NA(106)
Paludibacter
Paludibacter(2)
NA(10)
Flavihumibacter
Terrimonas
Sediminibacterium
Lacibacter
NA(29)
NA(125)

Sample 4

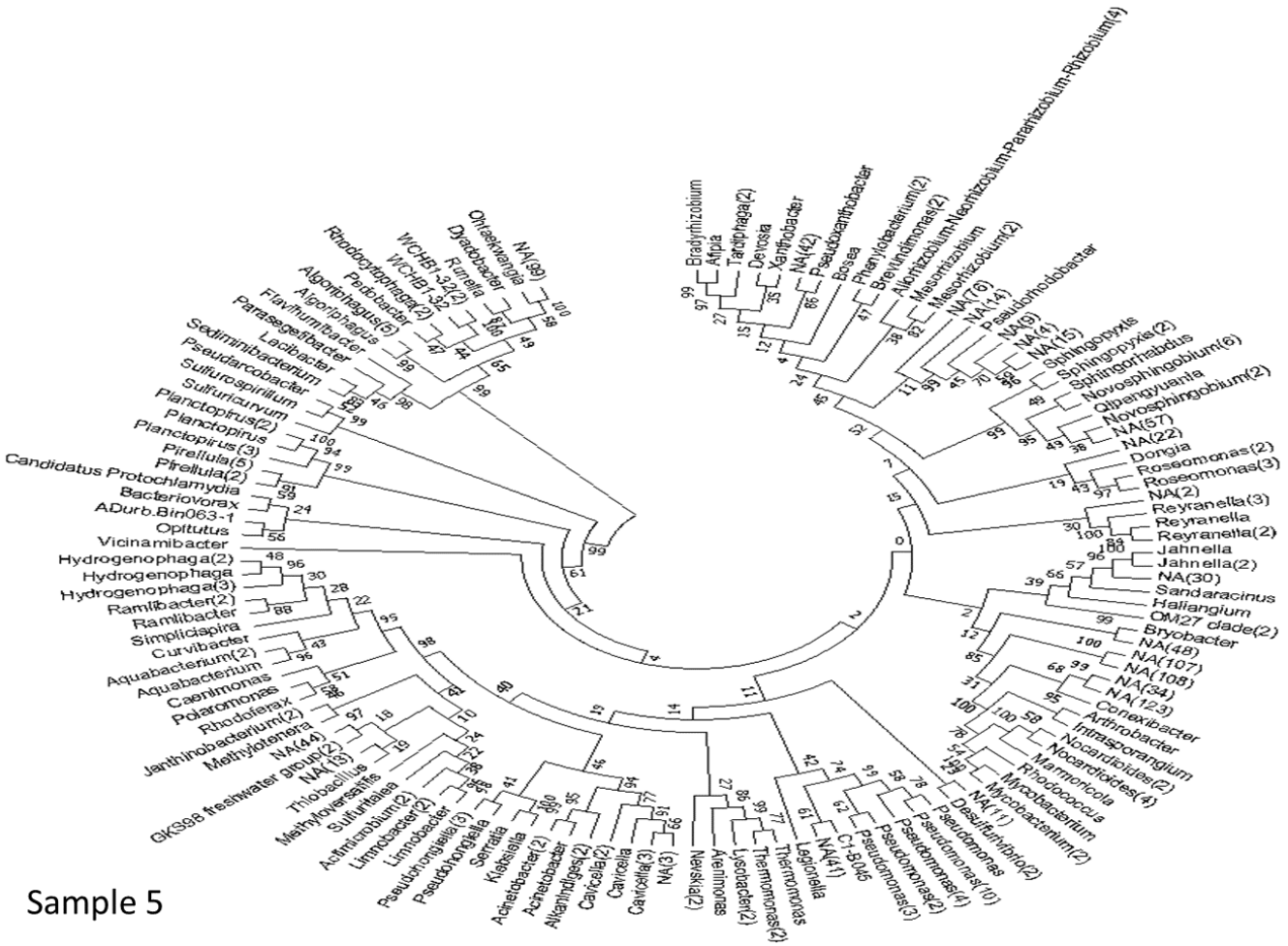

Figure E5: Phylogenetic trees of microbial diversity of six soil samples.

Heat map

At 15 °C

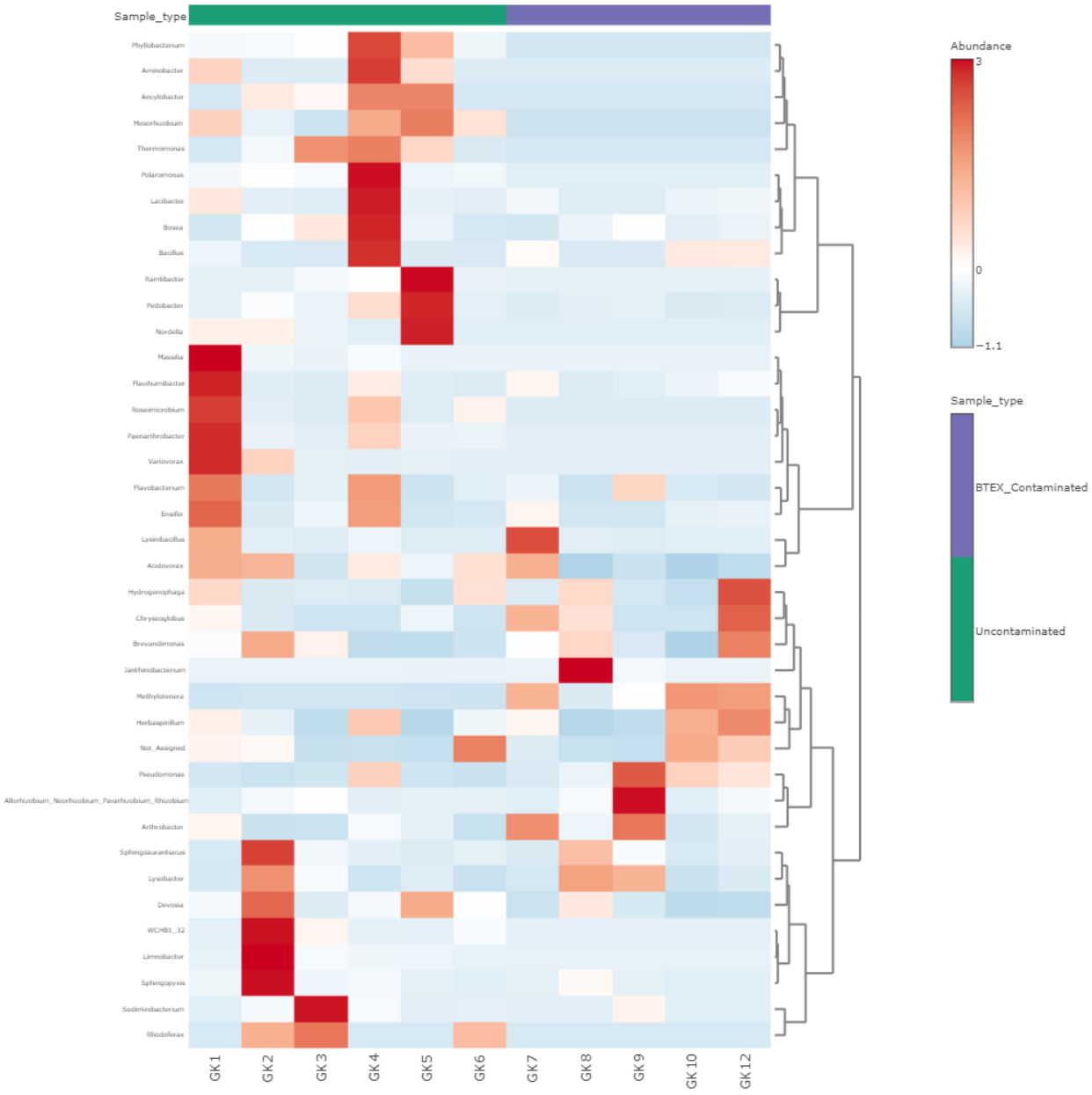

At 28 °C

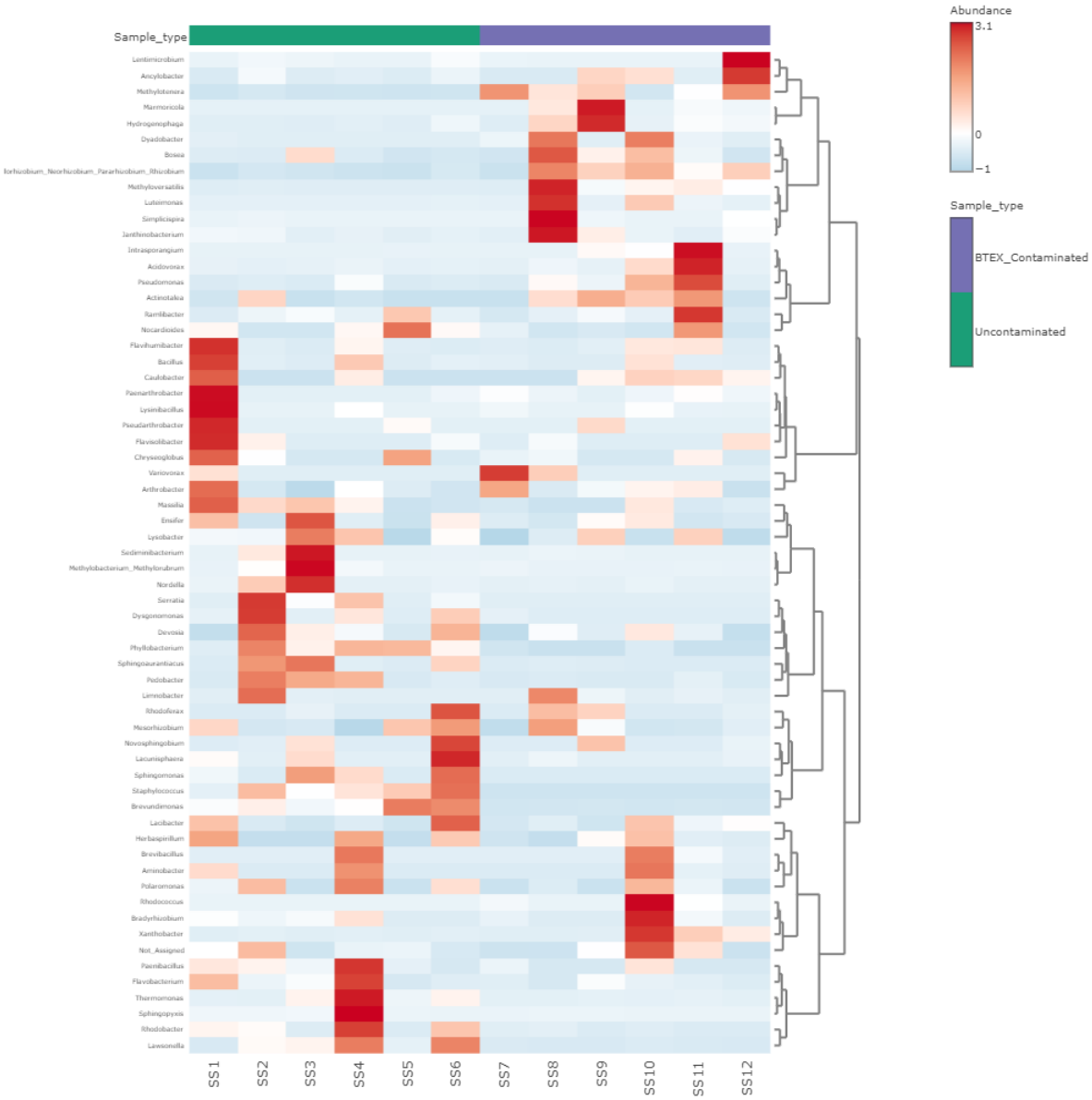
Sample_type
Abundance
3.1
0
−1
Sample_type
BTEX_Contaminated
Uncontaminated
SS1
SS2
SS3
SS4
SS5
SS6
SS7
SS8
SS9
SS10
SS11
SS12

At 40°C

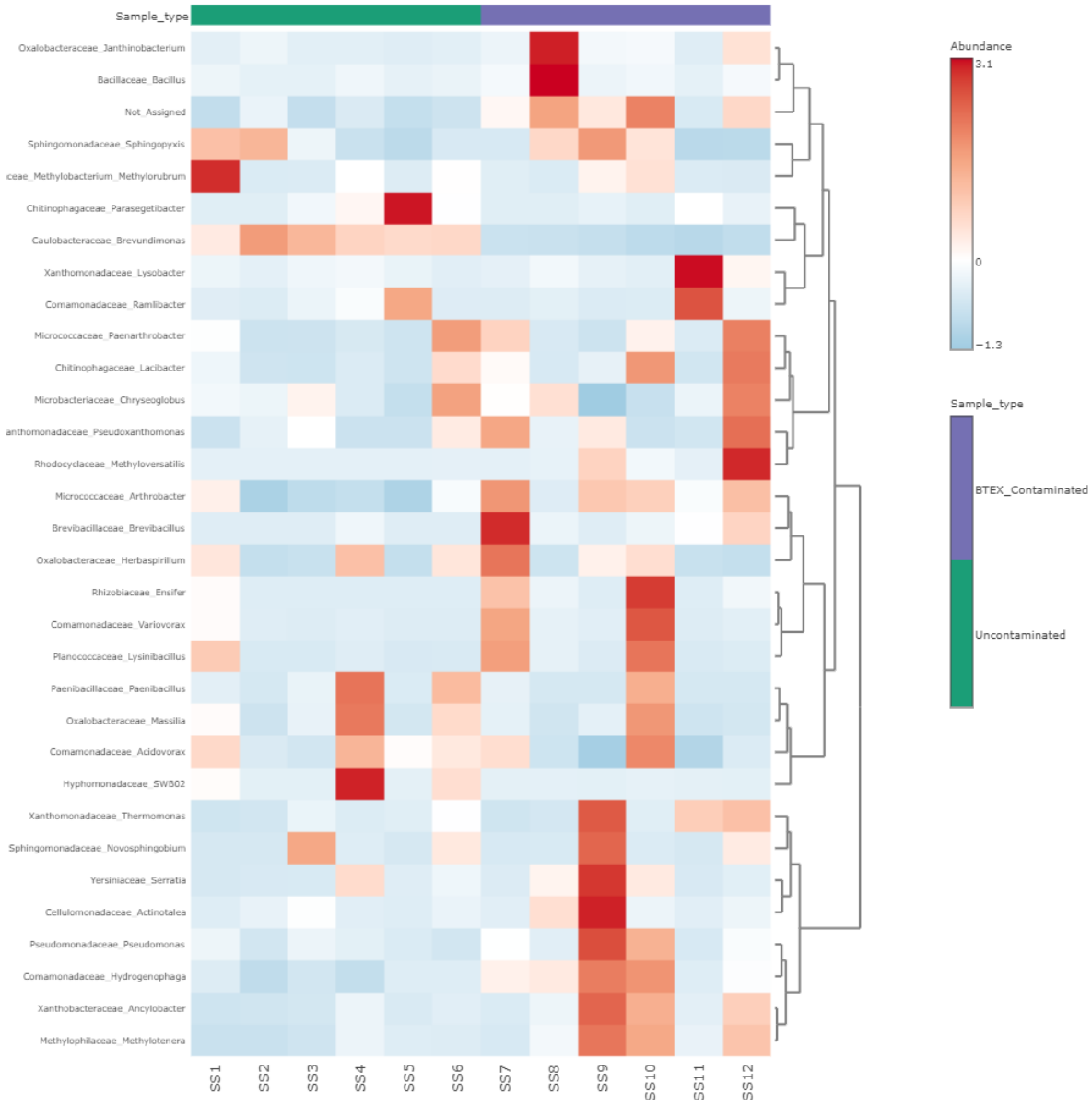

Figure E6: Heat map of bacterial community between contaminated and uncontaminated soil samples at all three temperatures.

Appendix F

(Additional Results, Experimental Hits and Trials)

Additional results

Gram Staining of bacterial isolates

Gram staining is a classical bacterial identification method, based on their cell wall structure. It groups the bacteria into two categories, i.e. Gram Gram-negative (thin peptidoglycan layer) and Gram-positive (thick peptidoglycan layer). Soil isolates were stained with Gram stain and differentiated into Gram-positive and negative based on their colour under the microscope (Figure F1).

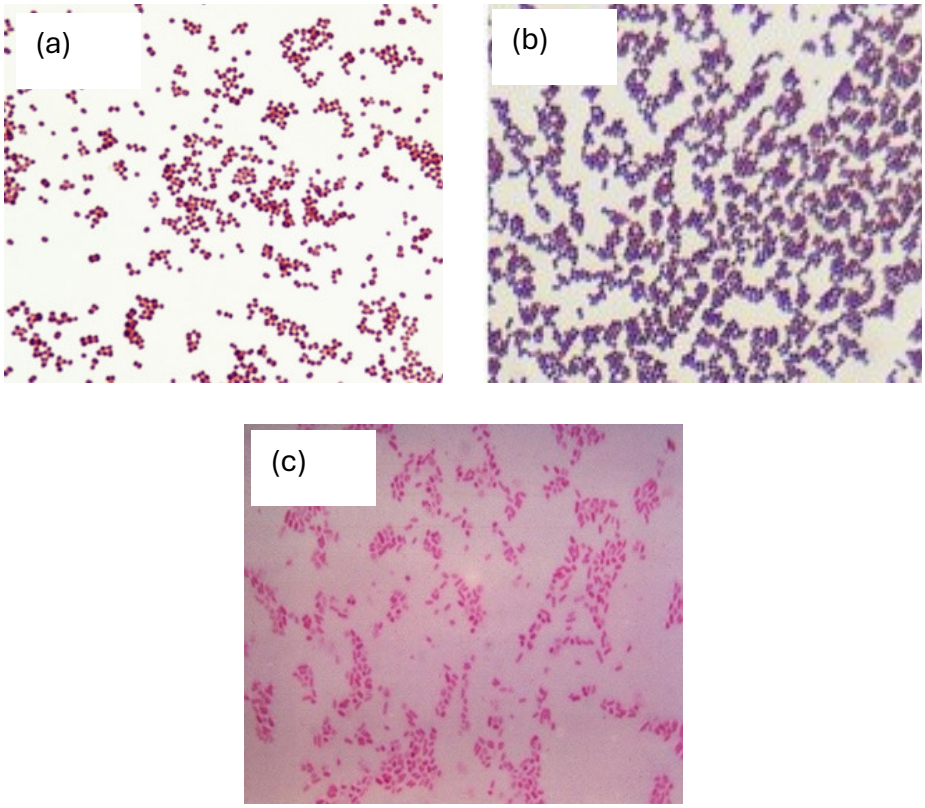

Figure F1: Gram staining of (a) *B. infantis, (b) M. esteraromaticum* and (c) *P. putida*

Growth of isolates in different growth media

To optimize the isolates' growth, MSM was supplemented with (0.2%) glucose and yeast extract. A good growth rate was observed for all isolates in YE media as compared to Glucose media, as illustrated in Figures F2 and F3. YE media showed a shorter lag phase and prolonged stationary phase with higher cell density.

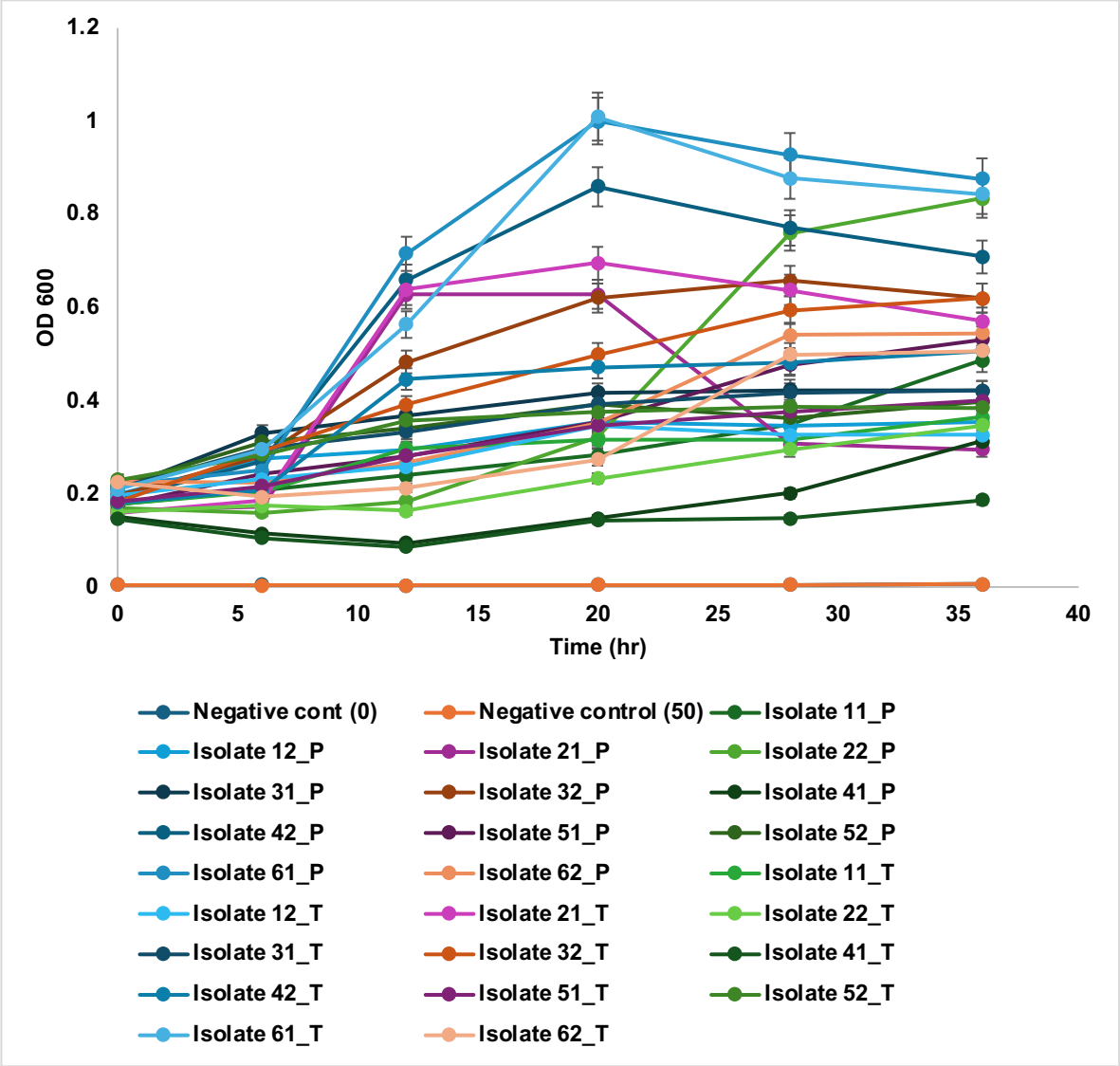

Figure F2: Growth of isolate with respect to time in MSM+G (Glucose) media

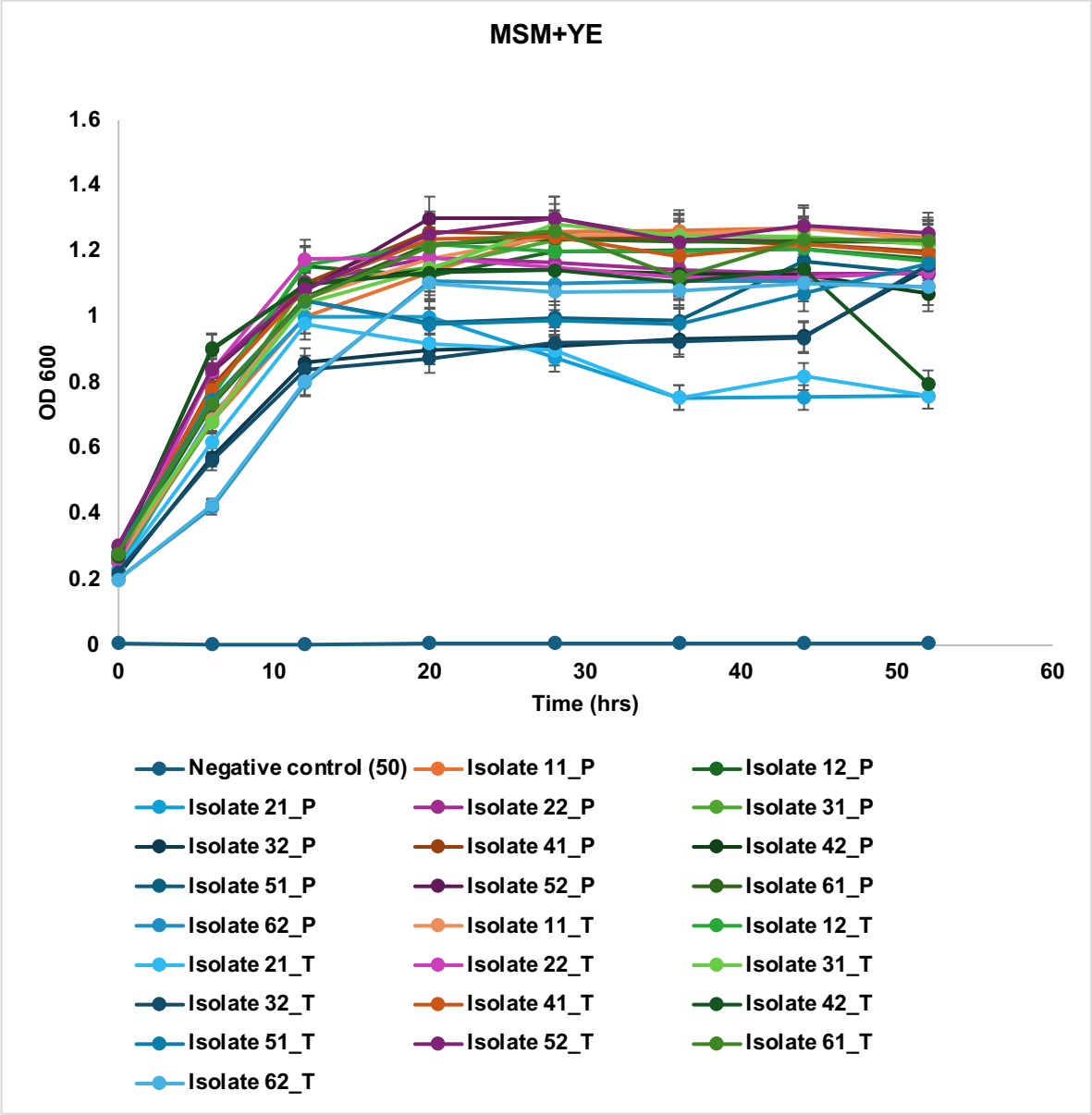

Figure F3: Growth of isolate with respect to time in MSM+YE (Yeast extract) media.

Growth of isolates at different BTEX concentrations

The screening of isolates was performed at five different concentrations of BTEX (100, 200, 400, 500, 1000 mg/L) to determine the tolerance and toxicity. About 70% inhibition of growth was found at 1000 mg/L of BTEX with respect to the control, while at 400 and 500 ppm, the growth of most of the isolates was lower by 10-20% as shown in Figure F4.

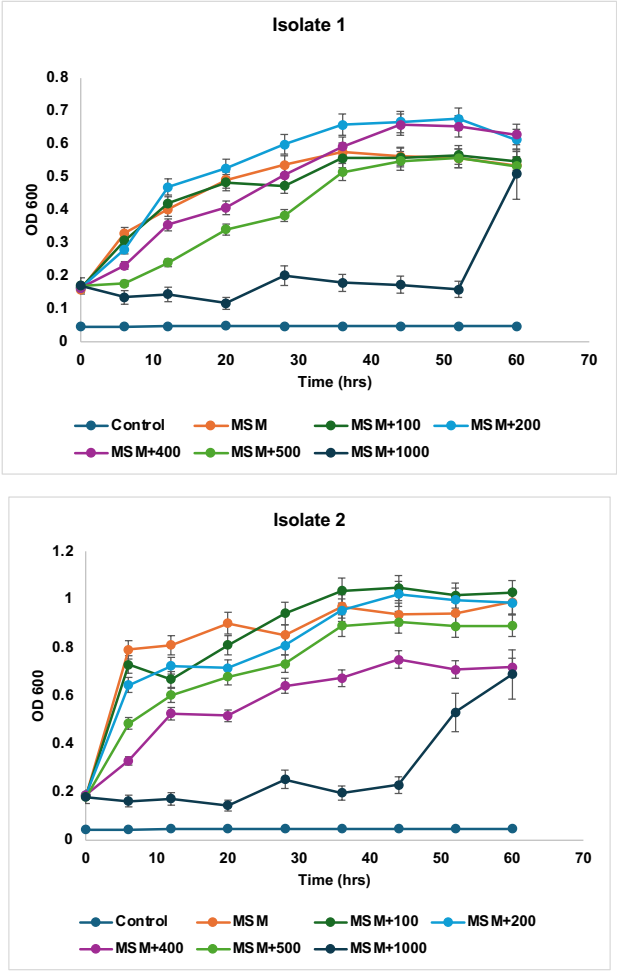

Figure F4: Growth kinetics of two isolates at different concentrations of BTEX in YE media.

Peclet number

Peclet number (Pe) quantifies which mechanism controls contaminant movement**,** which is crucial for understanding BTEX breakthrough patterns. It distinguishes the relative importance of advective transport (movement with flowing water) compared to diffusive transport (molecular spreading)**.** Pe was calculated using the Deff formula:

$$Pe = \frac{UL}{D_{eff}} \qquad \text{(F1)}$$

where U = flow velocity, L = column length and D = diffusion coefficient. Diffusion coefficient was calculated using the Millington-Quirk formula:

$$D_{eff} = D_o \cdot \phi^{4/3} \qquad \text{(F2)}$$

Where, D_o = diffusion coefficient in free water and ϕ= porosity

Table F1: Peclet number for the packed soil columns.

Soil type	ϕ	**D_{eff} (m^2/s)**	**U (m/s)**	**Pe (–)**
Silty loam	0.474	3.70×10^{-10}	3.65×10^{-5}	1.48×10^{4}
Sandy	0.454	3.49×10^{-10}	3.82×10^{-5}	1.64×10^{4}
Coarse sand	0.421	3.16×10^{-10}	4.11×10^{-5}	1.96×10^{4}

The Peclet number was calculated for each soil column using the pore-water velocity (U = q/ ϕ), a column length of 0.15 m and D_o =1×10−9 m^2/s for BTEX in water. Resulting Pe values were on the order of 10^4 as shown in Table F1, indicating strongly advection-dominated transport in all columns.

Preliminary Trials and System Optimization for Soil Columns

1. **Teflon columns:** The initial trials utilized Teflon columns due to their chemical resistance and ease of fabrication (Figure F5). However, BTEX analysis from preliminary injections showed substantial sorption of benzene, toluene, ethylbenzene, and xylenes to the PTFE walls**.** This led to non-recoverable losses (>20–30% in some trials), distorted mass-balance assessments, and inconsistent breakthrough patterns. Because PTFE is moderately permeable to organic vapors and can exhibit hydrophobic partitioning, it was determined that Teflon columns were unsuitable for quantitative BTEX mass-transfer studies.

Figure F5: Teflon columns.

2. **Stainless steel columns in an airtight chamber**

A second design employed stainless steel cylinders with a top opening**,** placed inside an airtight chamber to simultaneously capture volatilized BTEX (Figure F6). This configuration

minimized sorptive losses and provided a chemically inert environment. However, the design presented several limitations, such as non-uniform and loose soil packing, which could not operate as a continuous flow degradation experiment, restricting it to a batch-type and sampling during the experiment was impractical without disturbing the system.

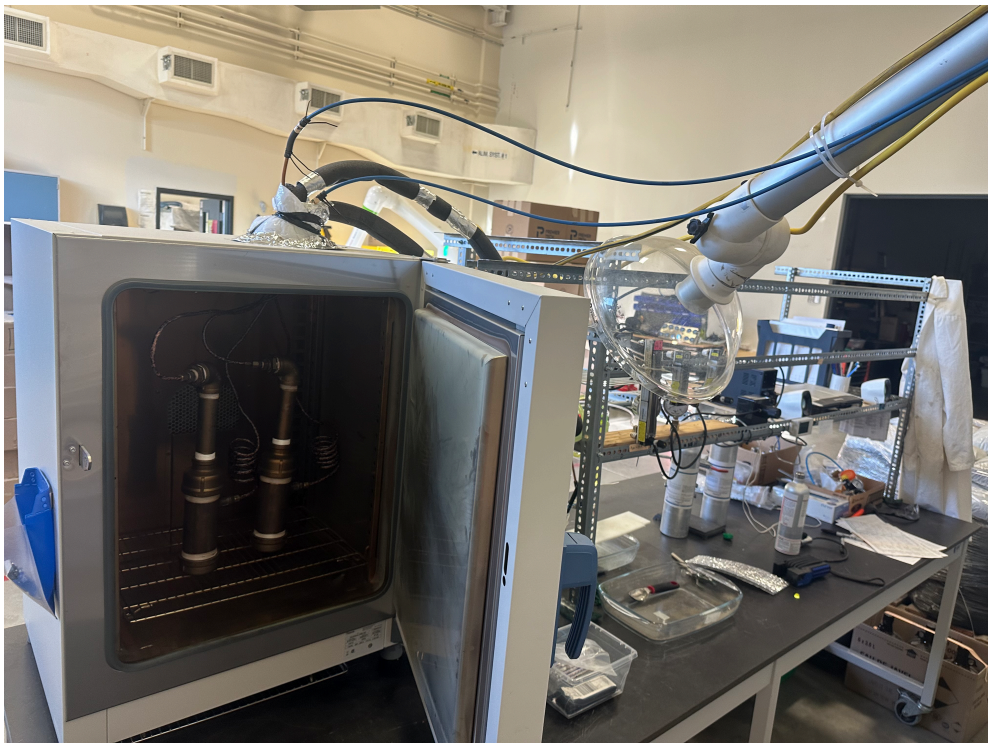

Figure F6: Stainless steel columns in an airtight chamber.

3. **Stainless steel columns with PPE (Polyethylene) tubing – Silty loam soil**

   This configuration involved closed stainless steel columns connected with PPE tubing (Figure F7)**.** Firstly, columns were packed with silty loam soil. While this setup facilitated flow-through operation, significant challenges were encountered during column saturation, such as leakage while saturation of columns due to backpressure produced by very fine-grained silty loam soil.

4. **Stainless steel columns with PPE tubing – Coarse sand**

   To reduce pressure buildup, the same column configuration was used with coarse sand**,** which improved hydraulic conductivity and eliminated leakage issues. This experiment went well and was completed with all cyclic and constant temperatures. However, the results were not

promising when the mass balance of BTEX was performed at the end. >40 % of BTEX was lost in all control and treatment columns. This resulted from PPE tubing, as they exhibited high diffusivity to BTEX. Losses occurred both during injection and during flow, causing severe underestimation of effluent concentrations.

Figure F7: Stainless steel columns with PPE tubing.

5. **Stainless steel columns with stainless steel tubing**

The final and successful configuration employed the same columns used in trial 4, by replacing the tubing and all the inlet and outlet connections with stainless steel to avoid loss during experimentation (Figures F8 and F9). This design eliminated all previous issues, while providing high reproducibility, robust hydraulic control, and chemically inert pathways for BTEX, making it suitable for the geothermal bioremediation study.

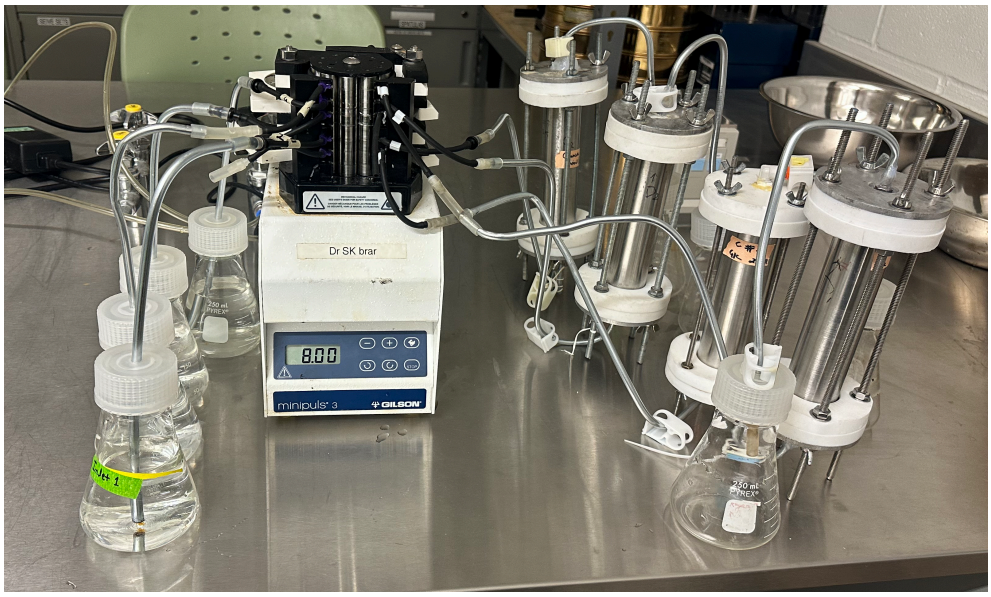

Figure F8: Stainless steel columns with steel tubing during saturation.

Figure F9: Stainless steel columns with steel tubing during sample injection.